

Docket Number 50-346  
License Number NPF-3  
Serial Number 2640  
Attachment 5

**DESIGN AND LICENSING REPORT  
DAVIS-BESSE SPENT FUEL POOL RERACK PROJECT  
HOLTEC INTERNATIONAL**

***NON-PROPRIETARY VERSION***

(313 pages follow)



**HOLTEC**  
INTERNATIONAL

Holtec Center, 555 Lincoln Drive West, Marlton, NJ 08053

Telephone (856) 797-0900

Fax (856) 797-0909

**DESIGN AND LICENSING REPORT  
DAVIS-BESSE SPENT FUEL POOL  
RERACK PROJECT**

for

***FIRST ENERGY***

**HOLTEC PROJECT NO. 80284**

**HOLTEC REPORT HI-981933**

**REPORT CATEGORY: A**

**REPORT CLASS: SAFETY RELATED**

This document version has all proprietary information removed and has replaced those sections, figures, and tables with highlighting and/or notes to designate the removal of such information. This document is to be used only in connection with the performance of work by Holtec International or its designated subcontractors. Reproduction, publication or presentation, in whole or in part, for any other purpose by any party other than the Client is expressly forbidden.

## REVIEW AND CERTIFICATION LOG FOR MULTIPLE AUTHORS

Sheet 1 of 2

REPORT NUMBER: 992329

PROJECT NUMBER: 80284

Document Portion	REVISION 0		REVISION 1		REVISION 2		REVISION 3	
	Author	Reviewer	Author	Reviewer	Author	Reviewer	Author	Reviewer
Chapter 1	Scott Pelet SHP 9-11-00	C. Bullock C.S. 9/13/00	Scott Pelet SHP 11-17-00	C. Bullock C.S. 11/21/00				
Chapter 2	Scott Pelet SHP 9-12-00	C. Bullock C.S. 9/13/00	Scott Pelet SHP 11-17-00	C. Bullock C.S. 11/21/00				
Chapter 3	Scott Pelet SHP 9-12-00	C. Bullock C.S. 9/13/00	Scott Pelet SHP 11-17-00	C. Bullock C.S. 11/21/00				
Chapter 4	Stefan Olson S. ANTON 9-13-00	Scott Pelet SHP 9-13-00	Scott Pelet SHP 11-17-00	C. Bullock C.S. 11/21/00				
Chapter 5	Stefan Olson E. Rasmussen 9/13/00	Scott Pelet SHP 9-13-00	Scott Pelet SHP 11-17-00	C. Bullock C.S. 11/21/00				
Chapter 6	Scott Pelet SHP 9-13-00	C. Bullock C.S. 9/13/00	Scott Pelet SHP 11-17-00	C. Bullock C.S. 11/21/00				
Chapter 7	Scott Pelet SHP 9-12-00	C. Bullock C.S. 9/13/00	Scott Pelet SHP 11-17-00	C. Bullock C.S. 11/21/00				
Chapter 8	Scott Pelet SHP 9-11-00	C. Bullock C.S. 9/13/00	Scott Pelet SHP 11-17-00	C. Bullock C.S. 11/21/00				

This document conforms to the requirements of the Design Specification and the applicable sections of the governing codes. By signing this page, you are confirming that you have filled out the DVC questionnaire stored in Holtec's network directory n:\pdxwin\working\dvc.

Note: Signatures and printed names are required in the review block.

\* A revision of this document will be ordered by the Project Manager and carried out if any of its contents is materially affected during evolution of this project. The determination as to the need for revision will be made by the Project Manager with input from others, as deemed necessary by him.

† Must be Project Manager or his designee.

‡ Distribution: C: Client  
M: Designated Manufacturer  
F: Florida Office

\*\*\* Report Category on the cover page indicates the contractual status of the document as\*\*\*

A=to be submitted to client for approval I=to be submitted to client for information only N=not submitted externally

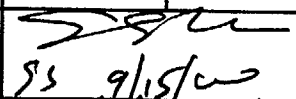
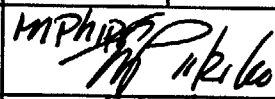
THE REVISION CONTROL OF THIS DOCUMENT IS BY A "SUMMARY OF REVISIONS LOG" PLACED BEFORE THE TEXT OF THE REPORT.

## REVIEW AND CERTIFICATION LOG FOR MULTIPLE AUTHORS

Sheet 2 of 2

REPORT NUMBER: 992329

PROJECT NUMBER: 80284

Document Portion	REVISION 0		REVISION 1		REVISION 2		REVISION 3	
	Author	Reviewer	Author	Reviewer	Author	Reviewer	Author	Reviewer
Chapter 9	Scott Pellet SHP 9-15-00	C. Bullard C.B. 9/13/00	Scott Pellet SHP 11-17-00	C. Bullard C.B. 11/21/00				
Chapter 10	Scott Pellet SHP 9-9-00	C. Bullard C.B. 9/13/00	Scott Pellet SHP 11-17-00	C. Bullard C.B. 11/21/00				
Chapter 11	Scott Pellet SHP 9-9-00	C. Bullard C.B. 9/13/00	Scott Pellet SHP 11-17-00	C. Bullard C.B. 11/21/00				
QA APPROVAL	 SS 9/15/00		 M Phelan 11/21/00					
PROJECT MANAGER†	Scott A. Pellet SHP 9-15-00		Scott A. Pellet SHP 11-21-00					

This document conforms to the requirements of the Design Specification and the applicable sections of the governing codes. By signing this page, you are confirming that you have filled out the DVC questionnaire stored in Holtec's network directory n:\pdxwin\working\dvc.

Note: Signatures and printed names are required in the review block.

\* A revision of this document will be ordered by the Project Manager and carried out if any of its contents is materially affected during evolution of this project. The determination as to the need for revision will be made by the Project Manager with input from others, as deemed necessary by him.

† Must be Project Manager or his designee.

‡ Distribution: C: Client  
 M: Designated Manufacturer  
 F: Florida Office

\*\*\* Report Category on the cover page indicates the contractual status of the document as\*\*\*  
 A=to be submitted to client for approval      I=to be submitted to client for information only      N=not submitted externally



Holtec Center, 555 Lincoln Drive West, Marlton, NJ 08053

Telephone (609) 797- 0900

Fax (609) 797 - 0909

### QA AND ADMINISTRATIVE INFORMATION LOG

(To Be Filled In By the Principal Author of the Document and Placed After the Title Page)

<p>Document No: <b>HI-992329</b></p>	<p>CATEGORY:    <input type="checkbox"/> <b>Generic</b>                            <input checked="" type="checkbox"/> <b>Project Specific</b></p>						
<p>Holtec Project No: <b>80284</b></p>							
<p>In accordance with the Holtec Quality Assurance Manual, and associated Holtec Quality Procedures (HQPs), this document is categorized as a :</p> <table style="width: 100%; border: none;"> <tr> <td style="width: 50%; padding: 5px; vertical-align: top;"> <input type="checkbox"/> <b>Calculation Package *</b> (Per HQP 3.2)         </td> <td style="width: 50%; padding: 5px; vertical-align: top;"> <input checked="" type="checkbox"/> <b>Technical Report (Per HQP 3.2)</b> (Such as a Licensing report)         </td> </tr> <tr> <td style="padding: 5px; vertical-align: top;"> <input type="checkbox"/> <b>Design Criterion Document</b> (Per HQP 3.4)         </td> <td style="padding: 5px; vertical-align: top;"> <input type="checkbox"/> <b>Design Specification</b> (Per HQP 3.4)         </td> </tr> <tr> <td colspan="2" style="padding: 5px;"> <input type="checkbox"/> <b>Other (Specify):</b> _____         </td> </tr> </table>		<input type="checkbox"/> <b>Calculation Package *</b> (Per HQP 3.2)	<input checked="" type="checkbox"/> <b>Technical Report (Per HQP 3.2)</b> (Such as a Licensing report)	<input type="checkbox"/> <b>Design Criterion Document</b> (Per HQP 3.4)	<input type="checkbox"/> <b>Design Specification</b> (Per HQP 3.4)	<input type="checkbox"/> <b>Other (Specify):</b> _____	
<input type="checkbox"/> <b>Calculation Package *</b> (Per HQP 3.2)	<input checked="" type="checkbox"/> <b>Technical Report (Per HQP 3.2)</b> (Such as a Licensing report)						
<input type="checkbox"/> <b>Design Criterion Document</b> (Per HQP 3.4)	<input type="checkbox"/> <b>Design Specification</b> (Per HQP 3.4)						
<input type="checkbox"/> <b>Other (Specify):</b> _____							
<p>The formatting of the contents of this document is in accordance with the instructions of HQP 3.2 or 3.4 except as noted below:</p> <p>_____</p> <p>_____</p> <p>_____</p>							
<p>This document is labelled :</p> <p><input type="checkbox"/> <b>Nonproprietary</b>    <input checked="" type="checkbox"/> <b>Holtec Proprietary</b>    <input type="checkbox"/> <b>Privileged Intellectual Property (PIP)</b></p> <p>Documents labelled Privileged Intellectual Property contains extremely valuable intellectual/commercial property of Holtec International. They can not be released to external organizations or entites without explicit approval of a company corporate officer. The recipient of Holtec's proprietary or Privileged Intellectual Property (PIP) document bears full and undivided responsibility to safeguard it against loss or duplication.</p> <p>* Revisions to the calculation Packages may be made by adding supplements to the document and replacing the "Table of Contents", the "Review and Certification" page and the "Revision Log".</p>							

## SUMMARY OF REVISIONS

Revision 1 contains the following pages:	
COVER PAGE	1 page
REVIEW AND CERTIFICATION LOG	2 pages
QA AND ADMINISTRATIVE INFORMATION LOG	1 page
SUMMARY OF REVISIONS	1 page
TABLE OF CONTENTS	10 pages
1.0 INTRODUCTION	7 pages
2.0 OVERVIEW OF THE PROPOSED CAPACITY EXPANSION	22 pages
3.0 MATERIAL, HEAVY LOAD, AND CONSTRUCTION	23 pages
4.0 CRITICALITY SAFETY EVALUATION	31 pages
-- APPENDIX 4A	25 pages
5.0 THERMAL-HYDRAULIC CONSIDERATIONS	41 pages
6.0 STRUCTURAL/SEISMIC CONSIDERATIONS	57 pages
7.0 FUEL HANDLING AND CONSTRUCTION ACCIDENTS	29 pages
8.0 FUEL POOL STRUCTURE INTEGRITY CONSIDERATIONS	38 pages
9.0 RADIOLOGICAL EVALUATION	8 pages
10.0 INSTALLATION	11 pages
11.0 ENVIRONMENTAL COST/BENEFIT ASSESSMENT	6 pages
TOTAL	313 pages

Revision 1 incorporates client comments.

# TABLE OF CONTENTS

---

1.0	INTRODUCTION.....	1-1
1.1	References .....	1-5
2.0	OVERVIEW OF THE PROPOSED CAPACITY EXPANSION.....	2-1
2.1	Introduction .....	2-1
2.2	Summary of Principal Design Criteria .....	2-2
2.3	Applicable Codes and Standards.....	2-4
2.4	Quality Assurance Program.....	2-10
2.5	Mechanical Design.....	2-10
2.6	Rack Fabrication Methods .....	2-11
2.7	Rack Module Description.....	2-12
3.0	MATERIAL, HEAVY LOAD, AND CONSTRUCTION CONSIDERATIONS .....	3-1
3.1	Introduction .....	3-1
3.2	Structural Materials.....	3-1
3.3	Poison Material (Neutron Absorber).....	3-1
3.3.1	Boral Material Characteristics.....	3-3
3.4	Compatibility with Coolant.....	3-4
3.5	Heavy Load Considerations for the Proposed Re-racking .....	3-4
3.6	Temporary Crane.....	3-10
3.7	References .....	3-13
4.0	CRITICALITY SAFETY EVALUATION .....	4-1
4.1	Design Bases .....	4-1
4.2	Summary of Criticality Analyses .....	4-5
4.2.1	Normal Operating Conditions .....	4-5
4.2.2	Abnormal and Accident Conditions.....	4-8
4.3	Reference Fuel Storage Cells .....	4-9
4.3.1	Reference Fuel Assembly.....	4-9
4.3.2	Fuel Storage Cells .....	4-9
4.4	Analytical Methodology.....	4-10
4.4.1	Reference Design Calculations .....	4-10
4.4.2	Fuel Burnup Calculations and Uncertainties .....	4-11
4.4.3	Effect of Axial Burnup Distribution.....	4-12
4.4.4	Long Term Changes in Reactivity.....	4-13
4.5	Criticality Analyses and Tolerances .....	4-14
4.5.1	Nominal Design Case.....	4-14
4.5.2	Uncertainties Due to Burnup.....	4-14
4.5.3	Uncertainties Due to Tolerances .....	4-14
4.5.4	Eccentric Fuel Positioning .....	4-15
4.5.5	Water-Gap Spacing Between Racks.....	4-15
4.5.6	Water-Gap Spacing Between Racks and Pool Walls.....	4-15
4.6	Abnormal and Accident Conditions.....	4-16

## TABLE OF CONTENTS

4.6.1	Temperature and Water Density Effects .....	4-16
4.6.2	Lateral Rack Movement .....	4-16
4.6.3	Abnormal Location of a Fuel Assembly .....	4-17
4.6.4	Dropped Fuel Assembly .....	4-17
4.7	References .....	4-19
Appendix 4A	“Benchmark Calculations” .....	Total of 25 Pages including 6 figures
4A.1	Introduction and Summary .....	4A-1
4A.2	Effect of Enrichment .....	4A-3
4A.3	Effect of <sup>10</sup> B Loading .....	4A-4
4A.4	Miscellaneous and Minor Parameters .....	4A-5
4A.4.1	Reflector Material and Spacings .....	4A-5
4A.4.2	Fuel Pellet Diameter and Lattice Pitch .....	4A-5
4A.4.3	Soluble Boron Concentration Effects .....	4A-5
4A.5	MOX Fuel .....	4A-6
4A.6	References .....	4A-7
5.0	<b>THERMAL-HYDRAULIC CONSIDERATIONS</b> .....	5-1
5.1	Introduction .....	5-1
5.2	Cooling System Description .....	5-3
5.3	Discharge/Cooling Alignment Scenarios .....	5-4
5.4	Maximum SFP Bulk Temperature Methodology .....	5-8
5.5	Minimum Time-to-Boil and Maximum Boiloff Rate Methodology .....	5-11
5.6	Local Water Temperature Methodology .....	5-12
5.6.1	Local Temperature Evaluation Methodology .....	5-13
5.7	Fuel Rod Cladding Temperature Methodology .....	5-17
5.8	Results and Conclusions .....	5-18
5.8.1	Maximum SFP Bulk Temperatures .....	5-19
5.8.2	Minimum Time-to-Boil and Maximum Boiloff Rate .....	5-20
5.8.3	Local Water and Fuel Cladding Temperatures .....	5-21
5.9	Fuel Handling Area Ventilation (FHAV) .....	5-21
5.10	Transfer Pit .....	5-22
5.10.1	Transfer Pit Bulk Temperature Methodology .....	5-22
5.10.2	Transfer Pit - Gate Closed .....	5-23
5.10.3	Transfer Pit - Gate Open .....	5-24
5.10.4	Transfer Pit - Conclusion .....	5-28
5.11	References .....	5-29
6.0	<b>STRUCTURAL/SEISMIC CONSIDERATIONS</b> .....	6-1
6.1	Introduction .....	6-1
6.2	Overview of Rack Structural Analysis Methodology .....	6-1
6.2.1	Background of Analysis Methodology .....	6-2
6.3	Description of Racks .....	6-5
6.3.1	Fuel Weights .....	6-6
6.4	Synthetic Time-Histories .....	6-6

## TABLE OF CONTENTS

6.5	WPMR Methodology .....	6-7
6.5.1	Model Details for Spent Fuel Racks .....	6-7
6.5.1.1	Assumptions .....	6-7
6.5.1.2	Element Details .....	6-9
6.5.2	Fluid Coupling Effect.....	6-10
6.5.2.1	Multi-Body Fluid Coupling Phenomena .....	6-11
6.5.3	Stiffness Element Details .....	6-12
6.5.4	Coefficients of Friction .....	6-13
6.5.5	Governing Equations of Motion.....	6-14
6.6	Structural Evaluation of Spent Fuel Rack Design.....	6-15
6.6.1	Kinematic and Stress Acceptance Criteria .....	6-15
6.6.2	Stress Limit Evaluations.....	6-16
6.6.3	Dimensionless Stress Factors .....	6-19
6.6.4	Loads and Loading Combinations for Spent Fuel Racks .....	6-20
6.7	Parametric Simulations .....	6-21
6.7.1	Transfer Pit Rack.....	6-22
6.8	Time History Simulation Results .....	6-22
6.8.1	Rack Displacements .....	6-22
6.8.2	Pedestal Vertical Forces .....	6-23
6.8.3	Pedestal Friction Forces .....	6-23
6.8.4	Rack Impact Loads .....	6-23
6.8.4.1	Rack to Rack Impacts.....	6-24
6.8.4.2	Rack to Wall Impacts .....	6-24
6.8.4.3	Fuel to Cell Wall Impact Loads .....	6-24
6.9	Rack Structural Evaluation.....	6-25
6.9.1	Rack Stress Factors .....	6-25
6.9.2	Pedestal Thread Shear Stress .....	6-26
6.9.3	Local Stresses Due to Impacts.....	6-26
6.9.4	Weld Stresses .....	6-27
6.9.5	Bearing Pad Analysis .....	6-29
6.10	Level A Evaluation.....	6-31
6.11	Hydrodynamic Loads on Pool Walls.....	6-31
6.12	Local Stress Considerations .....	6-31
6.12.1	Cell Wall Buckling.....	6-31
6.12.2	Analysis of Welded Joints in the Racks .....	6-32
6.13	References .....	6-33
7.0	<b>FUEL HANDLING AND MECHANICAL ACCIDENTS.....</b>	<b>7-1</b>
7.1	Introduction .....	7-1
7.2	Description of Mechanical Accidents .....	7-1
7.2.1	Shallow Drop Events.....	7-2
7.2.2	Deep Drop Events.....	7-3
7.2.3	Rack Drop Event.....	7-4
7.2.4	Uplift Force Evaluation.....	7-5

## TABLE OF CONTENTS

7.3	Mathematical Model .....	7-5
7.4	Results .....	7-5
7.4.1	Shallow Drop Events Results .....	7-5
7.4.2	Deep Drop Events Results .....	7-6
7.4.3	Rack Drop Event Results .....	7-7
7.4.4	Uplift Force Evaluation .....	7-8
7.5	Closure .....	7-8
7.6	References .....	7-9
8.0	<b>SPENT FUEL POOL AREA STRUCTURE INTEGRITY CONSIDERATIONS .....</b>	<b>8-1</b>
8.1	Introduction .....	8-1
8.2	Description of Spent Fuel Storage Area Structure .....	8-1
8.3	Definition of Individual Loads .....	8-2
8.3.1	Static Loading (Dead and Live Loads) .....	8-2
8.3.2	Thermal Load - $T_o$ , $T_a$ .....	8-3
8.3.3	Seismic Induced Loads - ( $E$ , $E'$ ) .....	8-4
8.4	Analysis Procedures .....	8-5
8.4.1	3-D Finite Element Model .....	8-6
8.4.2	Boundary Conditions .....	8-6
8.4.3	Material Properties .....	8-6
8.4.4	Load Combinations .....	8-7
8.4.4.1	Concrete .....	8-7
8.4.4.2	Steel Struts .....	8-8
8.5	Results of Numerical Analyses and Safety Factor Calculations .....	8-9
8.6	Pool Liner .....	8-11
8.7	Conclusions .....	8-12
8.8	References .....	8-13
9.0	<b>RADIOLOGICAL EVALUATION .....</b>	<b>9-1</b>
9.1	Solid Radwaste .....	9-1
9.2	Liquid Radwaste .....	9-2
9.3	Gaseous Releases .....	9-2
9.4	Personnel Doses .....	9-3
9.5	Anticipated Dose During Rack Installation .....	9-5
10.0	<b>INSTALLATION .....</b>	<b>10-1</b>
10.1	Introduction .....	10-1
10.2	Rack Arrangement .....	10-5
10.3	Pool Obstructions .....	10-5
10.4	SFP Cooling and Purification .....	10-6
10.4.1	SFP Cooling .....	10-6
10.4.2	Purification .....	10-7
10.5	Fuel Shuffling .....	10-7
10.6	Removal and Decontamination of Existing Racks and Associated Structures ..	10-7

## TABLE OF CONTENTS

---

10.7	Installation of New Racks .....	10-8
10.8	Safety, Health Physics, and ALARA Methods.....	10-10
10.8.1	Safety.....	10-10
10.8.2	Health Physics .....	10-10
10.8.3	ALARA .....	10-10
10.9	Radwaste Material Control.....	10-11
11.0	ENVIRONMENTAL COST/BENEFIT ASSESSMENT .....	11-1
11.1	Introduction.....	11-1
11.2	Imperative for SFP Rack Replacement.....	11-1
11.3	Appraisal of Alternative Options .....	11-2
11.3.1	Alternative Option Summary .....	11-4
11.4	Cost Estimate .....	11-5
11.5	Resource Commitment.....	11-5
11.6	Environmental Considerations.....	11-6
11.7	References.....	11-6

## TABLE OF CONTENTS

---

### Tables

2.1.1	Geometric and Physical Data for High Density Racks.....	2-15
2.5.1	Module Data for Spent Fuel Racks .....	2-16
3.3.1	Boral Experience List - PWRs .....	3-14 and 3-15
3.3.2	Boral Experience List - BWRs.....	3-16 and 3-17
3.3.3	1100 Alloy Aluminum Physical Characteristics .....	3-18
3.3.4	Chemical Composition - Aluminum (1100 Alloy) .....	3-19
3.3.5	Chemical Composition and Physical Properties of Boron Carbide .....	3-20
3.5.1	Heavy Load Handling Compliance Matrix (NUREG-0612).....	3-21
4.1.1	Fuel Assembly Specifications .....	4-21
4.2.1	Summary of Criticality Safety Analyses for the MZTR Pattern .....	4-22
4.2.2	Summary of Criticality Safety Analyses for the Checkerboard Pattern .....	4-23
4.2.3	Summary of Criticality Safety Analyses for the Homogeneous Loading Pattern .....	4-24
4.2.4	Reactivity Effects of Abnormal and Accident Conditions.....	4-25
4.5.1	Reactivity Effects of Manufacturing Tolerances.....	4-26
4.6.1	Reactivity Effects of Temperature and Void.....	4-27
4A.1	Summary of Criticality Benchmark Calculations.....	4A-9 thru 4A-13
4A.2	Comparison of MCNP4a and Keno5a Calculated Reactivities for Various Enrichments .....	4A-14
4A.3	MCNP4a Calculated Reactivities for Critical Experiments with Neutron Absorbers .....	4A-15
4A.4	Comparison of MCNP4a and KENO5a Calculated Reactivities for Various <sup>10</sup> B Loadings.....	4A-16
4A.5	Calculations for Critical Experiments with Thick Lead and Steel Reflectors .....	4A-17
4A.6	Calculations for Critical Experiments with Various Soluble Boron Concentrations.....	4A-18
4A.7	Calculations for Critical Experiments with MOX Fuel .....	4A-19
5.3.1	Davis-Besse Historic and Projected Fuel Discharge Schedule .....	5-30
5.4.1	Data for SFP Bulk Temperature Evaluation.....	5-31
5.5.1	Data for Time-to-Boil Evaluation .....	5-32
5.6.1	Data for SFP Local Temperature Evaluation .....	5-33
5.8.1	Results of Transient Temperature Evaluation.....	5-34
5.8.2	Spent Fuel Pool Results of Maximum Local Temperature Evaluations .....	5-35
5.8.3	Decay Heat Loads for Partial Core Discharge Scenarios 1 & 2 .....	5-36
5.8.4	Decay Heat Loads for "Type A" Full Core Discharge Scenarios 3A & 4A.....	5-37
5.8.5	Decay Heat Loads for "Type B" Full Core Discharge Scenarios 3B & 4B.....	5-38
6.2.1	Partial Listing of Fuel Rack Applications Using DYNARACK.....	6-35 through 6-37

## TABLE OF CONTENTS

6.3.1	Rack Material Data (200°F) (ASME - Section II, Part D) .....	6-38
6.4.1	Time-History Statistical Correlation Results .....	6-39
6.5.1	Degrees-of-Freedom.....	6-40
6.9.1	Comparison of Bounding Calculated Loads/Stresses vs. Code Allowable at Impact Locations and at Welds .....	6-41
7.2.1	Material Definition .....	7-10
7.3.1	Impact Weight and Impact Velocity Calculations.....	7-11
7.3.2	Structural and Material Definition of Impactor and Target.....	7-12
8.4.1	Concrete and Reinforcement Properties.....	8-14
8.4.2	Material Properties .....	8-15
8.4.3	Individual Load Cases .....	8-16
8.5.1	Scenario 1 (SFP Full, CP & TP Empty, Struts Installed) Reinforced Concrete Minimum Safety Factors .....	8-18
8.5.1.1	SFP East Wall Above Elevation 561'.....	8-18
8.5.1.2	SFP East Wall Below Elevation 561' .....	8-18
8.5.1.3	SFP West Wall Above Elevation 561' .....	8-19
8.5.1.4	SFP West Wall Below Elevation 561'.....	8-19
8.5.1.5	TP & CP West Wall Above Elevation 561' .....	8-20
8.5.1.6	TP & CP West Wall Below Elevation 561'.....	8-20
8.5.1.7	TP & SFP North Wall Above Elevation 561'.....	8-21
8.5.1.8	TP & SFP North Wall Below Elevation 561'.....	8-21
8.5.1.9	CP & SFP South Wall Above Elevation 561' .....	8-22
8.5.1.10	CP & SFP South Wall Below Elevation 561'.....	8-22
8.5.1.11	CP North Wall.....	8-23
8.5.1.12	Walls Under the SFP Slab.....	8-23
8.5.1.13	SFP Slab.....	8-24
8.5.1.14	TP Slab .....	8-24
8.5.2	Scenario 2 (SFP Full, CP Empty, TP @ 578' Elev, Struts Removed) Reinforced Concrete Minimum Safety Factors.....	8-25
8.5.2.1	SFP East Wall Above Elevation 561'.....	8-25
8.5.2.2	SFP East Wall Below Elevation 561' .....	8-25
8.5.2.3	SFP West Wall Above Elevation 561' .....	8-26
8.5.2.4	SFP West Wall Below Elevation 561'.....	8-26
8.5.2.5	TP West Wall Above Elevation 561' .....	8-27
8.5.2.6	TP West Wall Below Elevation 561'.....	8-27
8.5.2.7	TP & SFP North Wall Above Elevation 561'.....	8-28
8.5.2.8	TP & SFP North Wall Below Elevation 561'.....	8-28
8.5.2.9	CP & SFP South Wall Above Elevation 561' .....	8-29
8.5.2.10	CP & SFP South Wall Below Elevation 561'.....	8-29
8.5.2.11	CP North Wall.....	8-30
8.5.2.12	Walls Under the SFP Slab.....	8-30
8.5.2.13	SFP Slab.....	8-31
8.5.2.14	TP Slab .....	8-31

TABLE OF CONTENTS

---

8.5.3 Scenario 1 (SFP Full, CP & TP Empty, Struts Installed) Steel Strut Minimum Safety Factors ..... 8-32

9.3.1 Average Activity of Weekly SFP Samples ..... 9-7

9.5.1 Estimate of Person-REM Dose During Re-racking ..... 9-8

## TABLE OF CONTENTS

---

### **Figures**

- 1.1 Pool Layout for Davis-Besse Spent Fuel Pool
- 1.2 Rack Temporary Placement Plan in Fuel Transfer Pit
  
- 2.1 Schematic of Typical Davis-Besse Rack Structure
- 2.2 Box Cell Fabricated from Seam Welded Precision Formed Channels
- 2.3 Composite Box Cell Assembly
- 2.4 Typical Array of Storage Cells
- 2.5 Support Pedestal for Holtec PWR Rack
- 2.6 Three PWR Cells in Elevation View
  
- 3.5.1 Auxiliary Building - Spent Fuel Pool Area Plan View
- 3.6.1 Temporary Crane
  
- 4.2.1 Minimum Required Fuel Assembly Burnup as a Function of Nominal Initial Enrichment to Permit Storage in the Spent Fuel Pool or Transfer Pit
- 4.2.2 Examples of a Mixed Zone Three Region Spent Fuel Pool Configuration for the Davis-Besse Nuclear Power Station
- 4.2.3 Examples of a Spent Fuel Pool Configuration for the Davis-Besse Nuclear Power Station including MZTR, Checkerboarding and Homogeneous Loading in Various Combinations
- 4.3.1 Schematic View of a Single Storage Cell in the Spent Fuel Racks for Davis-Besse Nuclear Power Station
  
- 4A.1 MCNP Calculated k-eff Values for Various Values of the Spectral Index
- 4A.2 KENO5a Calculated k-eff Values for Various Values of the Spectral Index
- 4A.3 MCNP Calculated k-eff Values at Various U-235 Enrichments
- 4A.4 KENO5a Calculated k-eff Values at Various U-235 Enrichments
- 4A.5 Comparison of MCNP and KENO5a Calculations for Various Fuel Enrichments
- 4A.6 Comparison of MCNP and KENO5a Calculations for Various Boron-10 Areal Densities
  
- 5.6.1 Two-Dimensional Spent Fuel Pool Geometry Grid
- 5.6.2 Spent Fuel Pool Two Dimensional CFD Model - Temperature
- 5.6.3 Spent Fuel Pool Two Dimensional CFD Model - Velocity Vectors
  
- 6.4.1 Davis-Besse SFP and Cask Pit Time History Accelerogram (X-Direction, SSE)
- 6.4.2 Davis-Besse SFP and Cask Pit Time History Accelerogram (Y-Direction, SSE)
- 6.4.3 Davis-Besse SFP and Cask Pit Time History Accelerogram (Z-Direction, SSE)
- 6.4.4 Davis-Besse SFP and Cask Pit Time History Accelerogram (X-Direction, OBE)
- 6.4.5 Davis-Besse SFP and Cask Pit Time History Accelerogram (Y-Direction, OBE)
- 6.4.6 Davis-Besse SFP and Cask Pit Time History Accelerogram (Z-Direction, OBE)

## TABLE OF CONTENTS

---

- 6.5.1 Schematic of the Dynamic Model of a Single Rack Module Used in DYNARACK
- 6.5.2 Fuel-to-Rack Gap/Impact Elements at Level of Rattling Mass
- 6.5.3 Two Dimensional View of the Spring-Mass Simulation
- 6.5.4 Rack Degrees-of-Freedom with Shear and Bending Springs
- 6.5.5 Rack Periphery Gap/Impact Elements
- 6.9.1 Bearing Pad Analysis Model
- 6.9.2 Bearing Pad Analysis-Concrete Stress
- 6.9.3 Bearing Pad Analysis- Pad Stress
- 6.11.1 Rack Hydrodynamic Pressures
- 6.12.1 Welded Joint in Rack
  
- 7.2.1 Plan View of "Shallow Drop"
- 7.2.2 Plan View of "Deep Drop" Scenario 1
- 7.2.3 Plan View of "Deep Drop" Scenario 2
- 7.4.1 Isometric of "Shallow Drop" Finite Element Model
- 7.4.2 Isometric of Scenario 1 "Shallow Drop" Von Mises Stress
- 7.4.3 Isometric of Scenario 2 "Shallow Drop" Von Mises Stress
- 7.4.4 Isometric View of Over-Pedestal "Deep Drop" Finite Element Model
- 7.4.5 Over-Pedestal "Deep Drop" Pedestal Von Mises Stress
- 7.4.6 Over-Pedestal "Deep Drop" Bearing Pad Von Mises Stress
- 7.4.7 Over-Pedestal "Deep Drop" Liner Von Mises Stress
- 7.4.8 Over-Pedestal "Deep Drop" Concrete Von Mises Stress
- 7.4.9 Plan of On-Center "Deep Drop" Finite Element Model
- 7.4.10 On-Center "Deep Drop" Baseplate Von Mises Stress
- 7.4.11 On-Center "Deep Drop" Baseplate Plastic Strain
- 7.4.12 On-Center "Deep Drop" Baseplate Deformation
- 7.4.13 "Heaviest Rack" Drop; Maximum Von Mises Stress - Liner
- 7.4.14 "Heaviest Rack" Drop; Maximum Von Mises Stress - Concrete
  
- 8.2.1 Plan View of Auxiliary Bldg. Below SFP
- 8.2.2 Sectional View A-A of Auxiliary Building
- 8.2.3 Sectional View B-B of Auxiliary Building
- 8.2.4 Sectional View C-C of Auxiliary Building
- 8.2.5 Sectional View D-D of Auxiliary Building
- 8.4.1 3-D Finite-Element Model

In February of 2000, the NRC approved License Amendment No. 237 (License No. NPF-3) to allow the Davis-Besse Nuclear Power Station (DBNPS) to store up to 289 spent fuel assemblies in the Cask Pit, which is filled with water and connected to the Spent Fuel Pool (SFP). The increased fuel storage capacity was needed as the number of spent fuel assemblies stored in the SFP had increased to the point that all the fuel in the reactor could not be discharged to the SFP. Storage of fuel in the Cask Pit regained full core offload capability, and will maintain it through April of 2006 (end of Fuel Cycle 15). A re-rack of the SFP is required to provide additional increase in storage capacity to allow continued long term operation of the Station. To allow safe access to the existing racks for their removal, the re-racking must take place prior to the refueling outage in April, 2004. This report was prepared to present discussions and results of the design and analyses of the high density racks to be supplied by Holtec International and installed during a re-racking of the SFP.

The Davis-Besse Nuclear Power Station is a single unit pressurized water reactor (PWR) facility located 21 miles east of Toledo near Oak Harbor, Ohio. The Babcock & Wilcox (B&W) Company designed the nuclear steam supply system. The facility, capable of an electrical output of 873 net Megawatts-electric, received its operating license from the NRC in April 1977, and commenced commercial operations in January 1978.

The new storage rack array proposed for the DBNPS Unit 1 SFP is shown in the plan view provided by Figure 1.1. Note that racks N1, N2, N3, and N4 are shown relocated from the temporary Cask Pit rack layout presented in the earlier license amendment discussed above. Two of these racks (N1 and N2) have been fabricated, installed in the Cask Pit, and are currently in use.

Re-racking of the DBNPS SFP will require use of underwater divers. If not installed to maintain full core offload capability, racks N3 and N4 will be installed in the Cask Pit during the re-rack effort. The racks will allow fuel to be moved out of the SFP for diver safety. If additional safety margin is required, any one of the new SFP racks can be temporarily placed in the DBNPS

Transfer Pit, (see Figure 1.2. (The Transfer Pit is filled with water and connected to the SFP.) These racks will be emptied and relocated to the SFP during the latter stages of the SFP re-rack.

With racks in the Cask Pit to support the SFP re-racking, a NUHOMS™ Dry Fuel Storage Module can not be unloaded, as unloading a module requires setting a cask in the Pit. The condition which could lead to unloading a module is based on the module concrete temperature being greater than 350°F for longer than 24 hours [3]. (The module concrete temperature is more limiting than the fuel temperature.) Due to the conservative nature of the limit and the module design (which is completely passive), the exceedance of this limit does not require immediate unloading of the module. The guidance on this condition allows for an evaluation of the detrimental effects of the temperature on the concrete structural strength to determine the need for unloading the module.

The only way to increase the concrete temperature above 350°F is to have all module vents plugged for 40 hours and the outside air temperature greater than 100°F. (The time is based on a module heat load of 24,000 watts. The heat load in the Davis-Besse modules is about one half of this.) To preclude the possibility of reaching the limit and allow time to correct a problem, a daily surveillance is required which verifies, 1) the concrete temperature is less than 260°F, 2) the concrete temperature has changed less than 25°F in the last 24 hours, and 3) the module vents are not plugged. Therefore, the probability of being required to unload a module due to a malfunction of the passive NUHOMS system is remote. If an unloading was determined to be necessary during the re-racking, there would be time to make room in the Spent Fuel Pool for the fuel in the Cask Pit, move the fuel, and remove the Cask Pit racks.

The new Holtec racks are freestanding and self-supporting. The principal construction materials for the new racks are ASME SA-240-Type 304 stainless steel sheet and plate stock, and ASME SA-564-630 (precipitation hardened stainless steel) for the adjustable support spindles. The only non-stainless material utilized in the rack is the neutron absorber material, which is a hot-rolled cermet of aluminum and boron carbide, clad in aluminum (patented product name Boral™).

The new Holtec racks are designed to the stress limits of, and analyzed in accordance with, Section III, Division 1, Subsection NF of the American Society of Mechanical Engineers (ASME) Boiler and Pressure Vessel (B&PV) Code [1]. The material procurement, analysis, and fabrication of the rack modules conform to 10CFR50 Appendix B requirements.

The rack design and analysis methodologies employed in the storage capacity expansion are a direct evolution of previous re-rack license applications. This Design and Licensing Report documents the design and analyses performed to demonstrate that the new Holtec supplied racks meet all governing requirements of the applicable codes and standards. This report also documents that the racks meet the USNRC "OT Position for Review and Acceptance of Spent Fuel Storage and Handling Applications", and the addendum thereto [2].

Sections 2 and 3 of this report provide an abstract of the design and material information on the new racks.

The criticality safety analysis requires that the neutron multiplication factor for the stored fuel array be bounded by the USNRC  $k_{eff}$  limit of 0.95 under assumptions of 95% probability and 95% confidence. The criticality safety analysis provided in Section 4 sets the requirements on the Boral panel length and the amount of  $B^{10}$  per unit area (i.e., loading density) of the Boral panel for the new high density racks.

Thermal-hydraulic considerations require that the fuel cladding will not fail due to excessive temperature, and that the steady state pool bulk temperature will remain within the limits prescribed for the Cask Pit, Transfer Pit, and Spent Fuel Pool to satisfy the structural strength, operational, and regulatory requirements. The thermal-hydraulic analyses carried out in support of this storage expansion effort are described in Section 5.

Rack module structural analysis requires that the primary stresses in the rack module structure will remain below the ASME B&PV Code (Subsection NF) [1] allowables. Demonstrations of seismic and structural adequacy are presented in Section 6.0. The structural qualification also

requires that the subcriticality of the stored fuel will be maintained under all postulated accident scenarios. The structural consequences of these postulated accidents are evaluated and presented in Section 7 of this report.

Section 8 contains the structural analysis to demonstrate the adequacy of the SFP reinforced concrete structure. A synopsis of the geometry of the reinforced concrete structure is also presented in Section 8.

The radiological considerations are documented in Section 9.0. Sections 10, and 11, respectively, discuss the salient considerations in the installation of the new racks, and a cost/benefit and environmental assessment to establish the superiority of the wet storage expansion option.

All computer programs utilized to perform the analyses documented in this Design and Licensing Report are benchmarked and verified. These programs have been utilized by Holtec International in numerous re-rack license applications over the past decade.

The analyses presented herein clearly demonstrate that the rack module arrays possess wide margins of safety in respect to all considerations of safety specified in the OT Position Paper [2], namely, nuclear subcriticality, thermal-hydraulic safety, seismic and structural adequacy, radiological compliance, and mechanical integrity.

1.1 References

- [1] American Society of Mechanical Engineers (ASME), Boiler & Pressure Vessel Code, Section III, 1986 Edition, including up to 1988 addenda, Subsection NF, and Appendices.
- [2] USNRC, "OT Position for Review and Acceptance of Spent Fuel Storage and Handling Applications," April 14, 1978, and Addendum dated January 18, 1979.
- [3] Certificate of Compliance - Standardized NUHOMS-24P, Certificate Number 72-1004, Amendment Number 2.

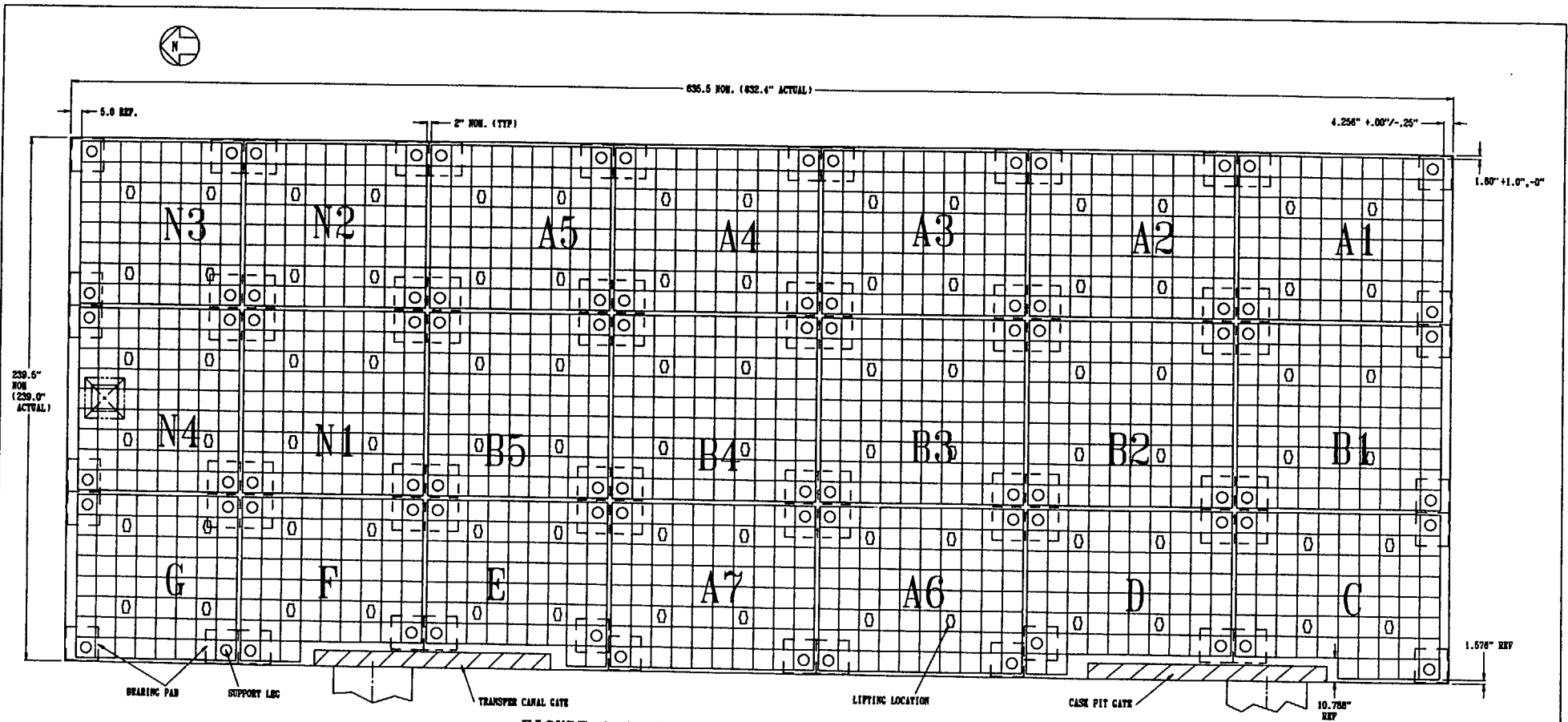
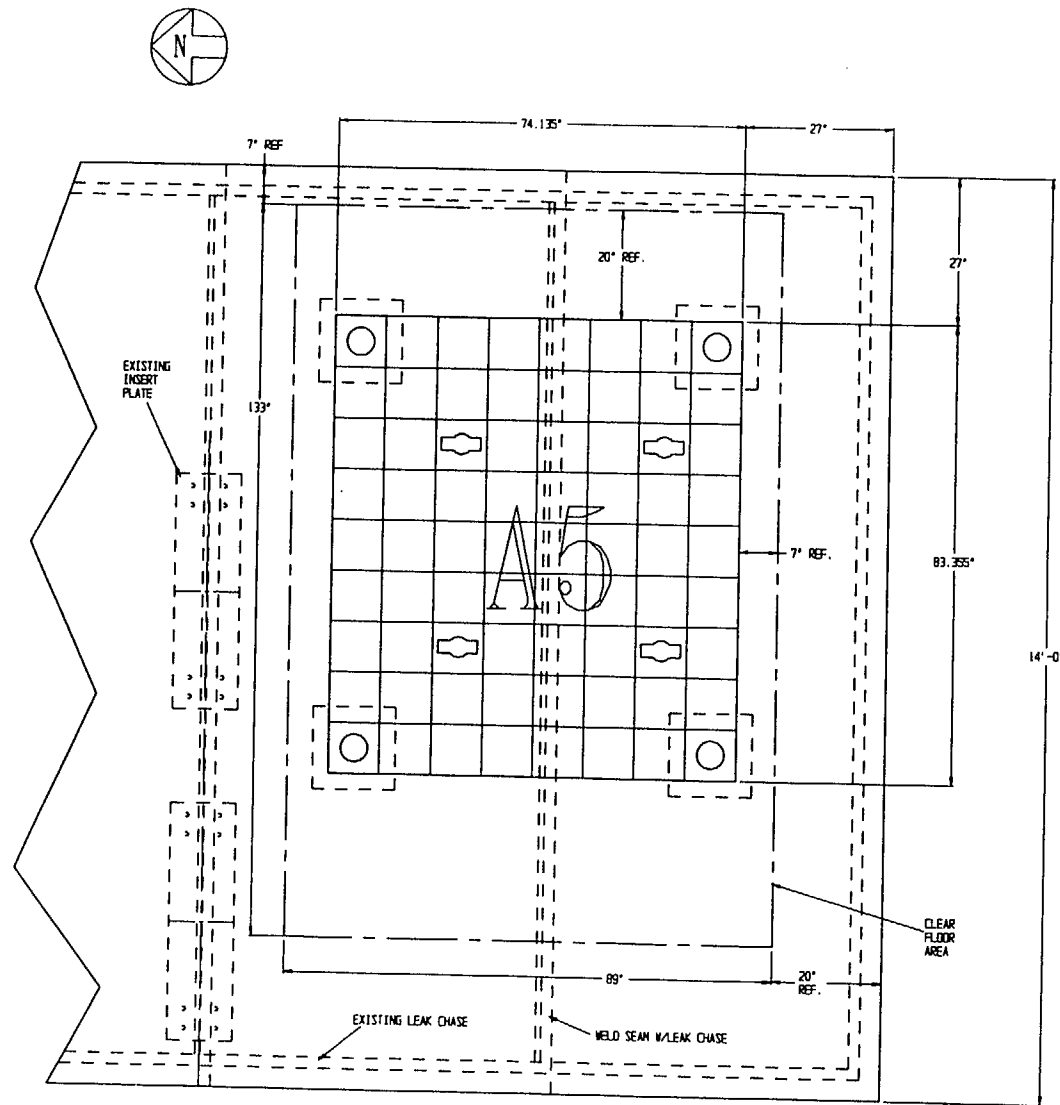


FIGURE 1.1: POOL LAYOUT FOR DAVIS-BESSE SPENT FUEL POOL

HOLTEC PROPRIETARY

HOLTEC REPORT HI-992329

F:\PROJECTS\980284\LICRS-SFP-FIGURE.1.1



**FIGURE 1.2; RACK TEMPORARY PLACEMENT PLAN IN FUEL TRANSFER PIT**

NOTE: RACK A-5 IS USED AS AN EXAMPLE. ANY NEW SFP RACK WHICH DOES NOT EXCEED THE CLEAR FLOOR AREA MAY BE PLACED IN THE TRANSFER PIT. THE RACK MAY BE POSITIONED ANY WHERE WITHIN THE CLEAR FLOOR AREA.

## 2.0 OVERVIEW OF THE PROPOSED CAPACITY EXPANSION

### 2.1 Introduction

Upon completion of the re-racking, the Davis-Besse Nuclear Power Station (DBNPS) Spent Fuel Pool (SFP) will contain 21 rack modules with a total of 1624 fuel storage cells. All modules will be free-standing, and made primarily from Type 304 austenitic stainless steel containing honeycomb storage cells interconnected through longitudinal welds. A panel of Boral™ cermet containing a high areal loading of the Boron-10 ( $B^{10}$ ) isotope provides appropriate neutron attenuation between adjacent storage cells. Figure 2.1 provides a schematic of the typical storage rack module. Data on the cross sectional dimensions, weight, and cell count for each rack module in the SFP are presented in Table 2.1.1.

The SFP will incorporate the Mixed Zone Three Region (MZTR) Storage concept for fuel storage. In the terminology of wet storage technology, the new rack modules will be of the non-flux-trap design and are referred to as Region 2 style racks. The idea of MZTR storage is to establish a multi-region storage configuration in the pool with a rack configuration that is comprised of Region 2 style racks only.

Note: These racks are of the same design as was approved by the NRC for the Cask Pit, (Amendment No. 237, License No. NPF-3).

The baseplates on all rack modules extend out beyond the rack module wall formed by the outside wall of the peripheral cells, such that the contiguous edges of the plates act to set a geometric separation between the facing cells in the adjacent modules. The geometric separation between the adjacent modules created by the baseplate extension serves to establish a "flux trap" space between the modules. In other words, although there is a single panel of neutron absorber between any two fuel assemblies stored in the same module, there are two poison panels with a specified water flux trap between them separating fuel assemblies located in cells in two facing modules. Out of these flux trap locations and peripheral cell locations (cells adjacent to pool walls), a certain number of storage cells can be designated for storing very low burnup or fresh (unburned) fuel. These so-called Region 1 cells are discussed in more detail in Section 4. The remaining storage cells have enrichment/burnup restrictions.

Appropriate restrictions on the enrichment/burnup of the fuel stored in cells designated as Region 2 cells and Region 3 cells are presented in Section 4.

As an alternative to MZTR storage, the plant will also be able to store fuel in a checkerboarding pattern without any enrichment/burnup restrictions. Examples of this type of storage configuration are also discussed in Section 4.

Each new rack module is supported by four pedestals, which are remotely adjustable. Thus, the racks can be made vertical and the top of the racks can easily be made co-planar with each other. The rack module support pedestals are engineered to accommodate minor level variations in the pool floor flatness.

Between the rack module pedestals and the SFP liner is a bearing pad, which serves to diffuse the load imposed by storage racks on the liner and into the reinforced concrete structure of the pool slab.

The overall design of the rack modules is similar to those presently in service in the spent fuel pools at many other nuclear plants, among them Donald C. Cook of American Electric Power, and Connecticut Yankee of Northeast Utilities. Altogether, over 50 thousand storage cells of this design have been provided by Holtec International to various nuclear plants around the world.

## 2.2 Summary of Principal Design Criteria

The key design criteria for the new spent fuel racks are set forth in the USNRC memorandum entitled "OT Position for Review and Acceptance of Spent Fuel Storage and Handling Applications", dated April 14, 1978 as modified by amendment dated January 18, 1979. The individual sections of this report expound on the specific design bases derived from the above-mentioned "OT Position Paper". A brief summary of the design bases for the racks are summarized in the following:

- a. Disposition: All new rack modules are required to be freestanding.

- b. Kinematic Stability: All freestanding modules must be kinematically stable (against tipping or overturning) if a seismic event is imposed on any module.
- c. Structural Compliance: All primary stresses in the rack modules must satisfy the limits postulated in Section III subsection NF of the 1986 ASME B & PV Code.
- d. Thermal-Hydraulic Compliance: The spatial average bulk pool temperature is required to remain under 140°F in the wake of a partial offload, with two SFP Cooling System trains in operation.
- e. Criticality Compliance: Cells designated as Region 1 must be able to store Zirconium (Zircaloy) clad fuel of the maximum reactivity used (or proposed to be used) in the Reactor with up to 5.05 w/o nominal initial enrichment while maintaining the reactivity  $\leq$  0.95. Region 3 cells must be able to store fuel of 5.05 w/o nominal enrichment and 45.00 GWD/MTU burnup or a reactivity equivalent based on lower burnup and enrichment combinations while maintaining the reactivity  $\leq$  0.95. Region 2 cells (barrier fuel) are intended for well burned fuel (5.05 w/o nominal enrichment and 55.00 GWD/MTU burnup or a reactivity equivalent based on lower burnup and enrichment combinations).
- f. Radiological Compliance: The re-racking must not lead to a violation of the off-site dose limits, or adversely affect the area dose environment as set forth in the DBNPS Updated Safety Analysis Report (USAR). The radiological implications of the installation of the new racks also need to be ascertained and deemed to be acceptable.
- g. Spent Fuel Pool Structure: The ability of the reinforced concrete structure to satisfy the load combinations set forth in the DBNPS USAR must be demonstrated.
- h. Liner Integrity: The integrity of the liner under cyclic in-plane loading during a seismic event must be demonstrated.

- i. Bearing Pads: The bearing pad size and thickness must ensure that the pressure on the liner continues to satisfy the American Concrete Institute (ACI) limits during and after a design basis seismic event.
- j. Accident Events: In the event of postulated drop events (uncontrolled lowering of a fuel assembly, for instance), it is necessary to demonstrate that the subcritical geometry of the rack structure is not compromised.
- k. Construction Events: The field construction services required to be carried out for executing the rack installation must be demonstrated to be within the "state of the proven art".

The foregoing design bases are further articulated in Sections 4 through 10 of this licensing report.

### 2.3 Applicable Codes and Standards

The following codes, standards and practices are used as applicable for the design, construction, and assembly of the fuel storage racks. Additional specific references related to detailed analyses are given in each section.

- a. Design Codes
  - (1) American Institute of Steel Construction (AISC) Manual of Steel Construction, 8<sup>th</sup> Edition, 1980.
  - (2) American National Standards Institute (ANSI) N210-1976, "Design Objectives for Light Water Reactor Spent Fuel Storage Facilities at Nuclear Power Stations" (contains guidelines for fuel rack design).
  - (3) ASME B & PV Code Section III, 1986 Edition, up to and including 1988 Addenda; ASME Section VIII, 1986 Edition; ASME Section IX, latest version.
  - (4) American Society for Nondestructive Testing SNT-TC-1A June, 1980 Recommended Practice for Personnel Qualifications and Certification in Non-destructive Testing.

- (5) American Concrete Institute Building Code Requirements for Reinforced Concrete (ACI 318-63).
- (6) Code Requirements for Nuclear Safety Related Concrete Structures, ACI 349-85/ACI 349R-85, and ACI 349.1R-80.
- (7) ASME Y14.5M, Dimensioning and Tolerancing
- (8) ACI Detailing Manual - 1980.
- (9) ASME B & PV Code, Section II-Parts A and C, 1986 Edition up to and including 1988 Addenda.
- (10) ASME B & PV Code NCA3800 - Metallic Material Organization's Quality System Program.

b. Standards of American Society for Testing and Materials (ASTM)

- (1) ASTM E165 - Standard Test Method for Liquid Penetrant Examination.
- (2) ASTM A240 - Standard Specification for Heat-Resisting Chromium and Chromium-Nickel Stainless Steel Plate, Sheet and Strip for Pressure Vessels.
- (3) ASTM A262 - Standard Practices for Detecting Susceptibility to Intergranular Attack in Austenitic Stainless Steel.
- (4) ASTM A276 - Standard Specification for Stainless Steel Bars and Shapes.
- (5) ASTM A479 - Standard Specification for Stainless Steel Bars and Shapes for use in Boilers and other Pressure Vessels.
- (6) ASTM A564 - Standard Specification for Hot-Rolled and Cold-Finished Age-Hardening Stainless Steel Bars and Shapes.
- (7) ASTM C750 - Standard Specification for Nuclear-Grade Boron Carbide Powder.
- (8) ASTM A380 - Standard Practice for Cleaning, Descaling, and Passivation of Stainless Steel Parts, Equipment and Systems.
- (9) ASTM C992 - Standard Specification for Boron-Based Neutron Absorbing Material Systems for Use in Nuclear Spent Fuel Storage Racks.
- (10) ASTM E3 - Standard Practice for Preparation of Metallographic Specimens.

- (11) ASTM E190 - Standard Test Method for Guided Bend Test for Ductility of Welds.

c. Welding Code:

ASME B & PV Code, Section IX - Welding and Brazing Qualifications, latest version.

d. Quality Assurance, Cleanliness, Packaging, Shipping, Receiving, Storage, and Handling

- (1) ANSI N45.2.1 - Cleaning of Fluid Systems and Associated Components during Construction Phase of Nuclear Power Plants - 1973 (R.G. 1.37).
- (2) ANSI N45.2.2 - Packaging, Shipping, Receiving, Storage and Handling of Items for Nuclear Power Plants - 1972 (R.G. 1.38).
- (3) ANSI N45.2.6 - Qualifications of Inspection, Examination, and Testing Personnel for the Construction Phase of Nuclear Power Plants - 1978 (Regulatory Guide 1.58).
- (4) ANSI N45.2.8 - Supplementary Quality Assurance Requirements for Installation, Inspection and Testing of Mechanical Equipment and Systems for the Construction Phase of Nuclear Plants - 1975 (R.G. 1.116).
- (5) ANSI N45.2.11 - Quality Assurance Requirements for the Design of Nuclear Power Plants - 1974 (R.G. 1.64).
- (6) ANSI N45.2.12 - Requirements for Auditing of Quality Assurance Programs for Nuclear Power Plants - 1977 (R.G. 1.144).
- (7) ANSI N45.2.13 - Quality Assurance Requirements for Control of Procurement of Items and Services for Nuclear Power Plants - 1976 (R. G. 1.123).
- (8) ANSI N45.2.23 - Qualification of Quality Assurance Program Audit Personnel for Nuclear Power Plants - 1978 (R.G. 1.146).
- (9) ASME B & PV Code, Section V, Nondestructive Examination, latest version.
- (10) ANSI N16.9-75 - Validation of Calculation Methods for Nuclear Criticality Safety.

e. USNRC Documents

- (1) "OT Position for Review and Acceptance of Spent Fuel Storage and Handling Applications," dated April 14, 1978, and the modifications to this document of January 18, 1979.
- (2) NUREG 0612, "Control of Heavy Loads at Nuclear Power Plants", USNRC, Washington, D.C., July, 1980.

f. Other ANSI Standards (not listed in the preceding)

- (1) ANSI/ANS 8.1 - Nuclear Criticality Safety in Operations with Fissionable Materials Outside Reactors.
- (2) ANSI/ANS 8.17 - Criticality Safety Criteria for the Handling, Storage, and Transportation of LWR Fuel Outside Reactors.
- (3) ANSI N45.2 - Quality Assurance Program Requirements for Nuclear Power Plants - 1977.
- (4) ANSI N45.2.9 - Requirements for Collection, Storage and Maintenance of Quality Assurance Records for Nuclear Power Plants - 1974.
- (5) ANSI N45.2.10 - Quality Assurance Terms and Definitions - 1973.
- (6) ANSI N14.6 - American National Standard for Special Lifting Devices for Shipping Containers Weighing 10,000 pounds (4500 kg) or more for Nuclear Materials - 1978.
- (7) ANSI/ASME N626-3 - Qualification and Duties of Specialized Professional Engineers.

g. Code-of-Federal Regulations (CFR)

- (1) 10CFR20 - Standards for Protection Against Radiation.
- (2) 10CFR21 - Reporting of Defects and Non-compliance.
- (3) 10CFR50 Appendix A - General Design Criteria for Nuclear Power Plants.
- (4) 10CFR50 Appendix B - Quality Assurance Criteria for Nuclear Power Plants and Fuel Reprocessing Plants.
- (5) 10CFR61 - Licensing Requirements for Land Disposal of Radioactive Waste.
- (6) 10CFR71 - Packaging and Transportation of Radioactive Material.

h. Regulatory Guides (RG)

- (1) RG 1.13 - Spent Fuel Storage Facility Design Basis (Revision 2 Proposed).
- (2) RG 1.25 - Assumptions Used for Evaluating the Potential Radiological Consequences of a Fuel Handling Accident in the Fuel Handling and Storage Facility for Boiling and Pressurized Water Reactors, Rev. 0 - March, 1972.
- (3) RG 1.28 - Quality Assurance Program Requirements - Design and Construction, Rev. 2 - February, 1979 (endorses ANSI N45.2).
- (4) RG 1.29 - Seismic Design Classification, Rev. 2 - February, 1976.
- (5) RG 1.31 - Control of Ferrite Content in Stainless Steel Weld Metal.
- (6) RG 1.38 - Quality Assurance Requirements for Packaging, Shipping, Receiving, Storage and Handling of Items for Water-Cooled Nuclear Power Plants, Rev. 2 - May, 1977 (endorses ANSI N45.2.2).
- (7) RG 1.44 - Control of the Use of Sensitized Stainless Steel.
- (8) RG 1.58 - Qualification of Nuclear Power Plant Inspection, Examination, and Testing Personnel, Rev. 1 - September 1980 (endorses ANSI N45.2.6).
- (9) RG 1.61 - Damping Values for Seismic Design of Nuclear Power Plants, Rev. 0, 1973.
- (10) RG 1.64 - Quality Assurance Requirements for the Design of Nuclear Power Plants, Rev. 2 - June, 1976 (endorses ANSI N45.2.11).
- (11) RG 1.71 - Welder Qualifications for Areas of Limited Accessibility.
- (12) RG 1.74 - Quality Assurance Terms and Definitions, Rev. 2 - February, 1974 (endorses ANSI N45.2.10).
- (13) RG 1.85 - Materials Code Case Acceptability - ASME Section III, Division 1.
- (14) RG 1.88 - Collection, Storage and Maintenance of Nuclear Power Plant Quality Assurance Records, Rev. 2 - October, 1976 (endorses ANSI N45.2.9).
- (15) RG 1.92 - Combining Modal Responses and Spatial Components in Seismic Response Analysis, Rev. 1 - February, 1976.

- (16) RG 1.116 - Quality Assurance Requirements for Installation, Inspection and Testing of Mechanical Equipment and Systems, Rev. 0-R - May, 1977 (endorses ANSI N45.2.8-1975)
- (17) RG 1.123 - Quality Assurance Requirements for Control of Procurement of Items and Services for Nuclear Power Plants, Rev. 1 - July, 1977 (endorses ANSI N45.2.13).
- (18) RG 1.124 - Service Limits and Loading Combinations for Class 1 Linear-Type Component Supports, Revision 1, January, 1978.
- (19) RG 1.144 - Auditing of Quality Assurance Programs for Nuclear Power Plants, Rev. 1 - September, 1980 (endorses ANSI N45.2.12-1977)
- (20) RG 3.4 - Nuclear Criticality Safety in Operations with Fissionable Materials at Fuels and Materials Facilities.
- (21) RG 8.8 - Information Relative to Ensuring that Occupational Radiation Exposures at Nuclear Power Stations will be as Low as Reasonably Achievable (ALARA).
- (22) IE Information Notice 83-29 - Fuel Binding Caused by Fuel Rack Deformation.
- (23) RG 8.38 - Control of Access to High and Very High Radiation Areas in Nuclear Power Plants, June, 1993.

i. Branch Technical Position

- (1) CPB 9.1-1 - Criticality in Fuel Storage Facilities.
- (2) APCS 9-2 - Residual Decay Energy for Light-Water Reactors for Long-Term Cooling - November, 1975.

j. American Welding Society (AWS) Standards

- (1) AWS D1.1 - Structural Welding Code - Steel.
- (2) AWS D1.3 - Structure Welding Code - Sheet Steel.
- (3) AWS D9.1 - Sheet Metal Welding Code.
- (4) AWS A2.4 - Standard Symbols for Welding, Brazing and Nondestructive Examination.
- (5) AWS A3.0 - Standard Welding Terms and Definitions.

- (6) AWS A5.12 - Specification for Tungsten and Tungsten Alloy Electrodes for Arc-welding and Cutting
- (7) AWS QC1 - Standard for AWS Certification of Welding Inspectors.

#### 2.4 Quality Assurance Program

The governing quality assurance requirements for fabrication of the spent fuel racks are stated in 10CFR50 Appendix B. Holtec's Nuclear Quality Assurance Program has been reviewed and approved by the DBNPS Nuclear Assurance Department. This program is designed to provide a flexible but highly controlled system for the design, analysis and licensing of customized components in accordance with various codes, specifications, and regulatory requirements.

The manufacturing of the racks will be carried out by Holtec's designated manufacturer, U.S. Tool & Die, Inc. (UST&D). The UST&D Quality Assurance Program enforced on the manufacturer's shop floor shall provide for all controls necessary to fulfill all quality assurance requirements. UST&D has manufactured high-density racks for over 60 nuclear plants around the world. UST&D has been audited by the nuclear industry group Nuclear Procurement Issues Committee (NUPIC), and the Quality Assurance branch of the USNRC Office of Nuclear Material Safety and Safeguards (NMSS) with satisfactory results.

Installation of the racks by Holtec will be controlled by the Holtec Nuclear Quality Assurance Manual and by the DBNPS site-specific requirements.

#### 2.5 Mechanical Design

The rack modules are designed as cellular structures such that each fuel assembly has a square opening with full length lateral support and a flat horizontal-bearing surface. All of the storage locations are constructed with multiple cooling flow holes to ensure that redundant flow paths for the coolant are available. The basic characteristics of the spent fuel rack modules are summarized in Table 2.5.1.

A central objective in the design of the new rack modules is to maximize structural strength while minimizing inertial mass and dynamic response. Accordingly, the rack modules have been designed to simulate multi-flange beam structures resulting in excellent de-tuning characteristics with respect to the applicable seismic events. The next subsection presents an item-by-item description of the rack modules in the context of the fabrication methodology.

## 2.6 Rack Fabrication Methods

The object of this section is to provide a brief description of the rack module construction activities, which enable an independent appraisal of the adequacy of design. The pertinent methods used in manufacturing the high-density storage racks may be stated as follows:

1. The rack modules are fabricated in such a manner that the storage cell surfaces, which would come in contact with the fuel assembly, will be free of harmful chemicals and projections (e.g., weld splatter).
2. The component connection sequence and welding processes are selected to reduce fabrication distortions.
3. The fabrication process involves operational sequences that permit immediate accessibility for verification by the inspection staff.
4. The racks are fabricated per the UST&D Appendix B Quality Assurance Program, which ensures, and documents, that the fabricated rack modules meet all of the requirements of the design and fabrication documents.

## 2.7 Rack Module Description

The composite box assembly, the baseplate, and the support pedestals constitute the principal components of the fuel rack modules. The following description provides details of all of the major rack components.

- i. Composite box cell assembly: The rack module manufacturing begins with fabrication of the "box cell" from ASME SA-240-304 stainless steel. The box cells are fabricated from two precision formed channels by seam welding in a machine equipped with copper chill bars and pneumatic clamps to minimize distortion due to welding heat input. The minimum weld penetration is 80% of the box cell metal gage. This process results in a square cross section box cell, as shown in Figure 2.2. The clear inside nominal dimension of the PWR box cell is 9.0".

Sheathing of ASME SA-240-304 stainless steel is attached to each side of the box cell with the poison material installed in the sheathing cavity. The sheathing design objective calls for securing Boral to the box cell surface. This is accomplished by die forming the internal and external Boral sheathings to provide end flares with smooth edges, as shown in Figure 2.3. The flanges of the sheathing are welded to the box cell using skip welds and spot welds. The sheathings serve to locate and position the poison sheet accurately, and to preclude its movement under seismic conditions. The sheathing also isolates the Boral from the fuel assembly. The square cross section box cell with Boral panels affixed to its external surfaces is referred to as the "composite box cell assembly".

Each box cell has at least two one inch diameter lateral holes punched near its bottom edge to provide auxiliary flow holes. For those box cells located over support legs, four flow holes are required to compensate for the loss of the baseplate flow holes described below.

The composite box cell assemblies are arranged in a checkerboard array and welded edge-to-edge to form an assemblage of storage cell locations, as shown in Figure 2.4.

Austenitic stainless steel corner welds connect the storage box cells to each other. The extent of welding is selected to "detune" the racks from the stipulated seismic input motion. Filler panels and corner angles are welded to the edges of box cells at the outside boundary of the rack to complete the formation of the peripheral cells. The inter-box welding and pitch adjustment is accomplished by small longitudinal connectors. The connectors are sized and placed to ensure that the 9.0" inside cell clear dimension on developed cells is maintained after inclusion of any reductions from the sheathing. This assemblage of box cell assemblies results in a honeycomb structure with axial, flexural and torsional rigidity depending on the extent of intercell welding provided. It can be seen from Figure 2.4 that all four corners of each interior box cell are connected to the contiguous box cells resulting in a well-defined path for "shear flow".

- ii. Baseplate: A 3/4 inch thick baseplate of ASME SA-240-304 provides a continuous horizontal surface for supporting the fuel assemblies. The baseplate has a 5 inch diameter hole in each cell location, except at lift locations. For the four lift locations, the flow holes are a 3.12 inch diameter hole with a coincidental 2.625 inch by 5.125 inch slot to allow insertion and engagement of the lifting rig. The location of all baseplate holes coincide with the cell centerlines. The baseplate is attached to the base of the rack cell assemblage by fillet welds and extends horizontally approximately 1" beyond the periphery of the rack cell assemblage at locations where racks interface. At locations where an outside edge of a rack module is adjacent to a pool wall, the baseplate extension varies between 1/4" and 1".
- iii. The neutron absorber material: As mentioned in the preceding section, Boral is used as the neutron absorber material. Each storage cell side is equipped with one integral Boral sheet (poison material). The Boral extends the entire length of the active fuel.
- iv. Sheathing: As described earlier, the sheathing serves as the locator and retainer of the poison material and isolates the Boral from the fuel assembly.

- v. Support Pedestals: All support pedestals are the adjustable type as shown in Figure 2.5. The 10 inch square top (female threaded) portion is made of austenitic steel material. The bottom (male threaded) part is made of ASME SA-564-630 (17:4 Ph series) stainless steel to avoid galling problems. Each support pedestal is equipped with a readily accessible socket to enable remote leveling of the rack after its placement in the pool. The support pedestals are located at the centerlines of cells to ensure accessibility of the leveling tool through the 5 inch diameter flow hole in the baseplate.

The assembly of the rack modules is carried out by welding the composite box cell assemblies in a vertical fixture with the baseplate serving as the bottom positioner.

A typical elevation view of three adjacent PWR storage cells is shown in Figure 2.6.

TABLE 2.1.1: GEOMETRIC AND PHYSICAL DATA FOR HIGH DENSITY RACKS						
MODULE I.D.	NO. OF CELLS		MODULE ENVELOPE SIZE		WEIGHT (lbs)	NO. OF CELLS PER RACK
	N-S Direction	E-W Direction	N-S	E-W		
N1	9	9	83.355"	83.355"	12,150	81
N2	9	8	83.355"	74.135"	10,800	72
N3	8	8	74.135"	74.135"	9,600	64
N4	8	9	74.135"	83.355"	10,800	72
A1	10	8	92.575"	74.135"	12,600	80
A2	10	8	92.575"	74.135"	12,600	80
A3	10	8	92.575"	74.135"	12,600	80
A4	10	8	92.575"	74.135"	12,600	80
A5	9	8	83.355"	74.135"	10,800	72
A6	10	8	92.575"	74.135"	12,600	80
A7	10	8	92.575"	74.135"	12,600	80
B1	10	9	92.575"	83.355"	14,030	90
B2	10	9	92.575"	83.355"	14,030	90
B3	10	9	92.575"	83.355"	14,030	90
B4	10	9	92.575"	83.355"	14,030	90
B5	9	9	83.355"	83.355"	12,150	81
C	10	8	92.575"	74.135"	12,080	75
D	10	8	92.575"	74.135"	11,590	72
E	9	8	83.355"	74.135"	9,750	65
F	9	8	83.355"	74.135"	9,900	66
G	8	8	74.135"	74.135"	10,300	64

Table 2.5.1

## MODULE DATA FOR SPENT FUEL RACKS \*

Storage cell inside nominal dimension	9.0 in.
Cell pitch	9.22 in.
Storage cell height (above the plate)	161.625 in.
Baseplate hole size (away from pedestal)	5.0 in. **
Baseplate thickness	0.75 in.
Support pedestal height	4.25 in.
Support pedestal type	Remotely adjustable pedestals
Number of support pedestals	4
Number of cell walls containing 1" diameter supplemental flow holes at base for cells located away from pedestals	2
Number of cell walls containing 1" diameter flow holes at base for cells located above pedestals	4
Remote lifting and handling provisions	Yes
Poison material	Boral
Poison length	148 in.
Poison width	7.5 in.

\* All dimensions are nominal values

\*\* Except at lifting locations

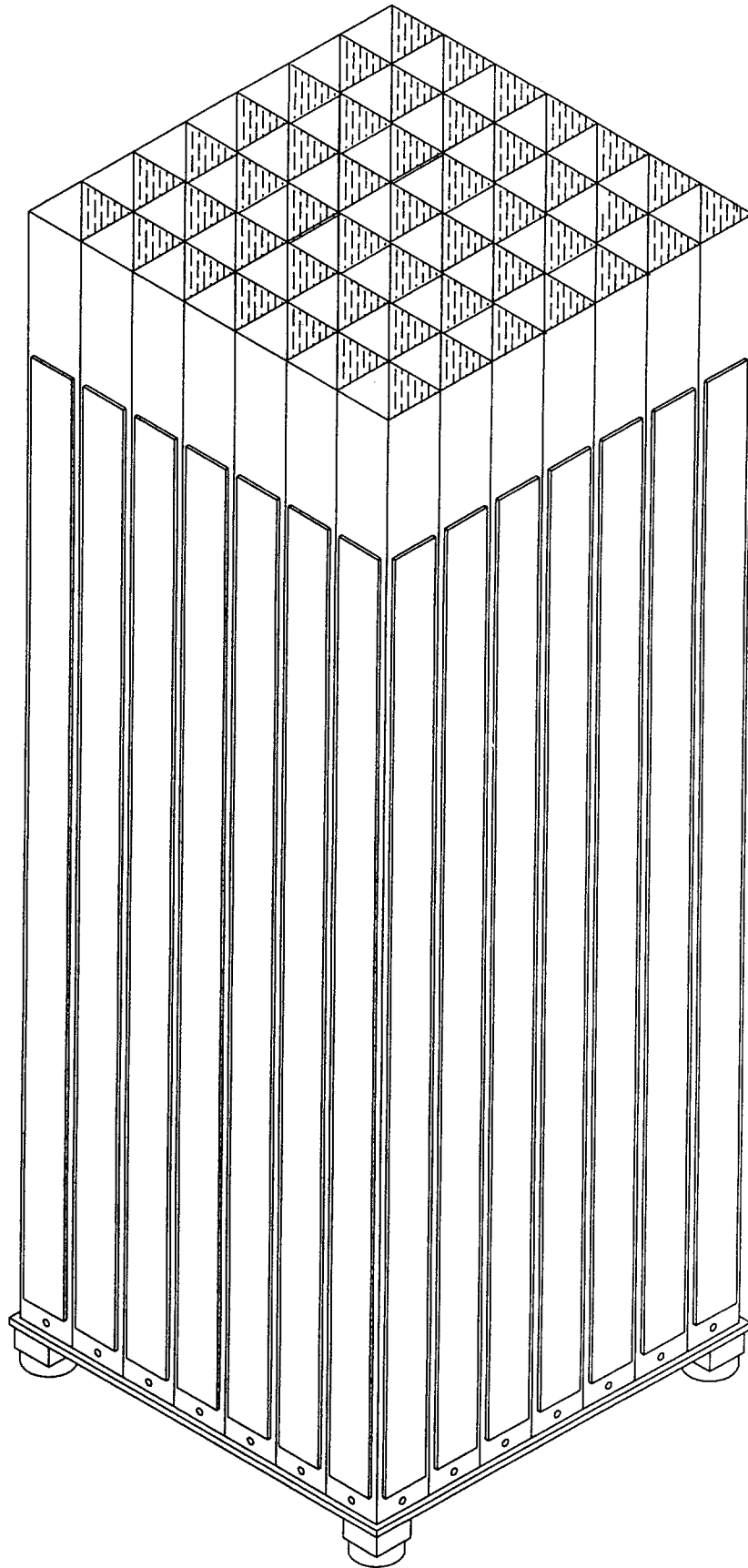
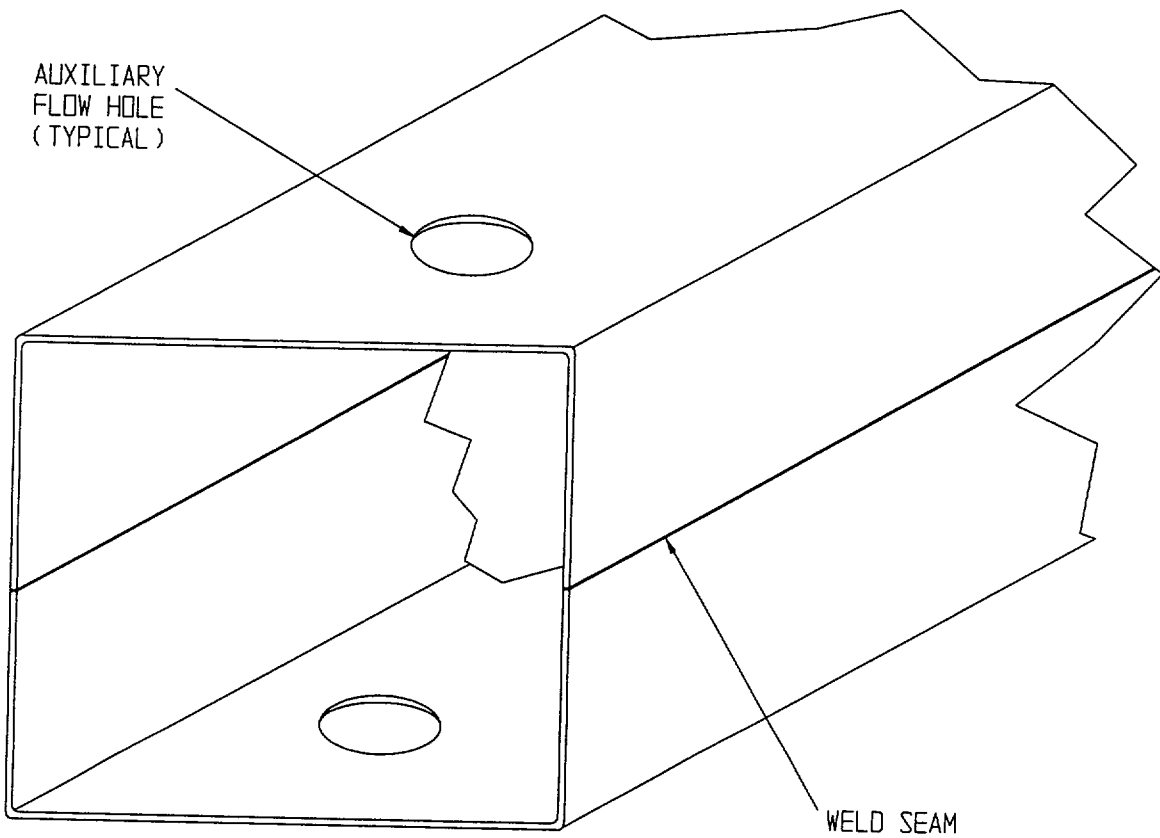


FIGURE 2.1; SCHEMATIC OF TYPICAL DAVIS-BESSE RACK STRUCTURE



**FIGURE 2.2; BOX CELL FABRICATED FROM SEAM WELDED  
PRECISION FORMED CHANNELS**

HI-992329

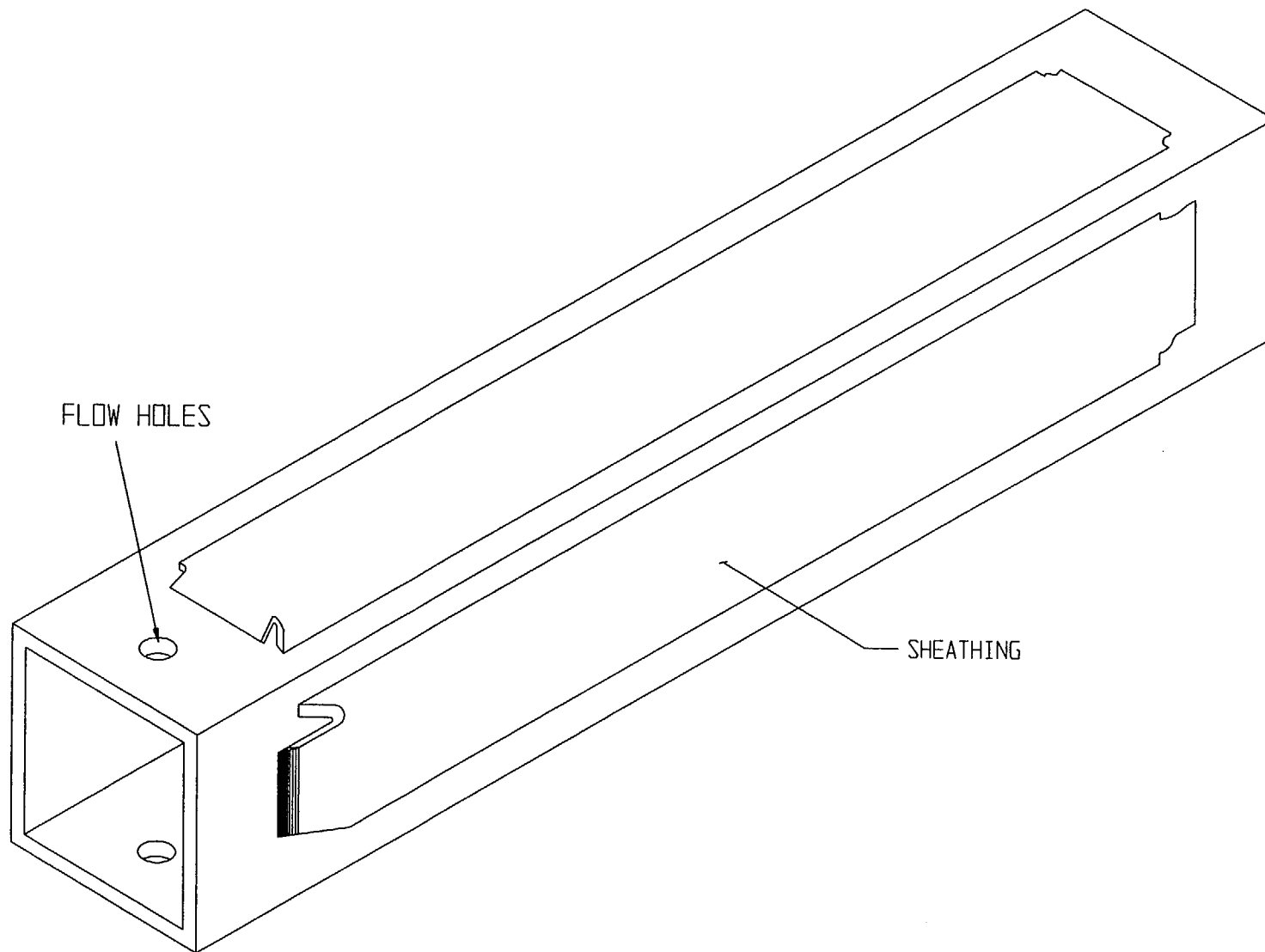


FIGURE 2.3; COMPOSITE BOX CELL ASSEMBLY

HI-992329

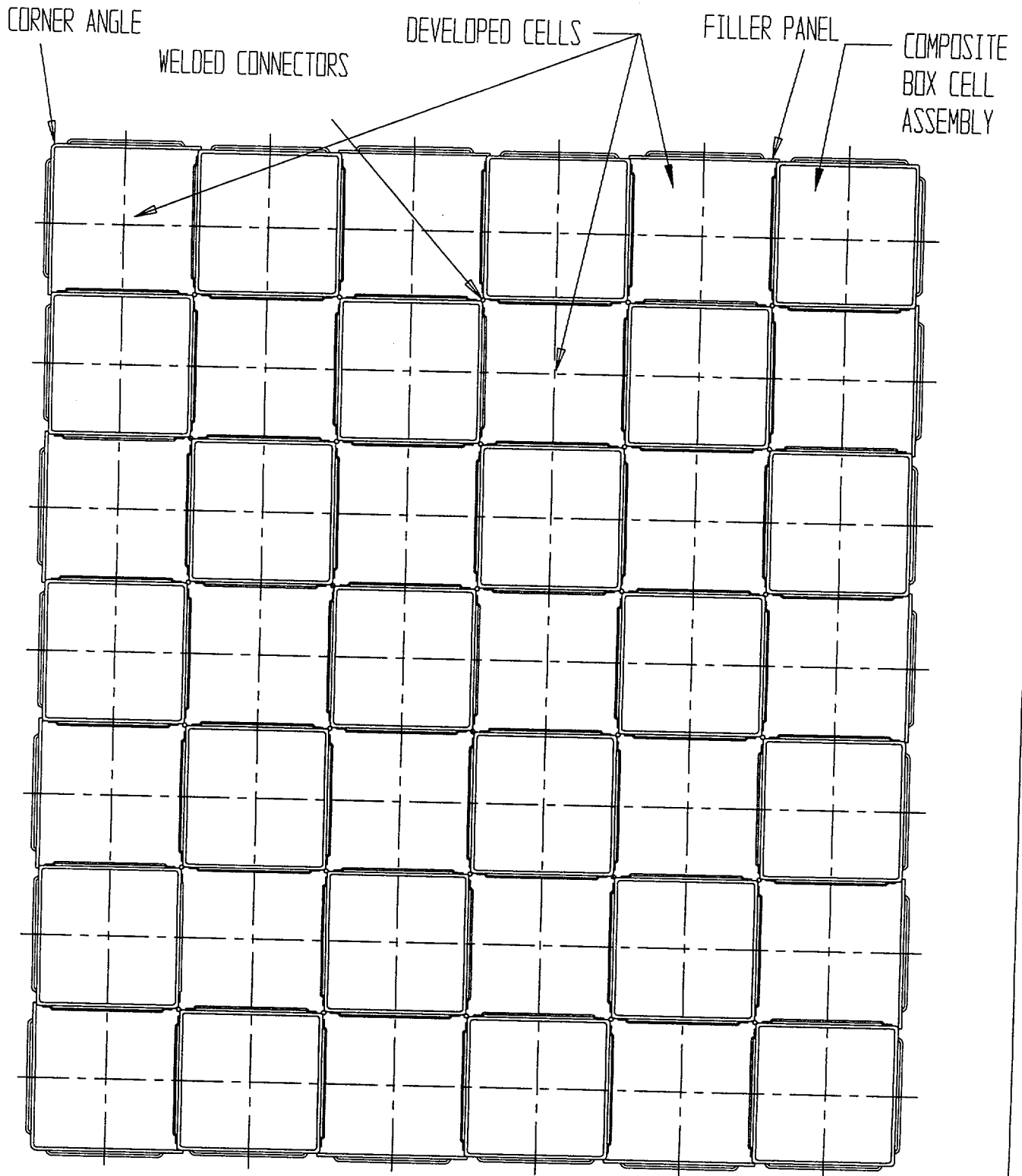


FIGURE 2.4; TYPICAL ARRAY OF STORAGE CELLS  
(NON-FLUX TRAP CONSTRUCTION)

HI-992329

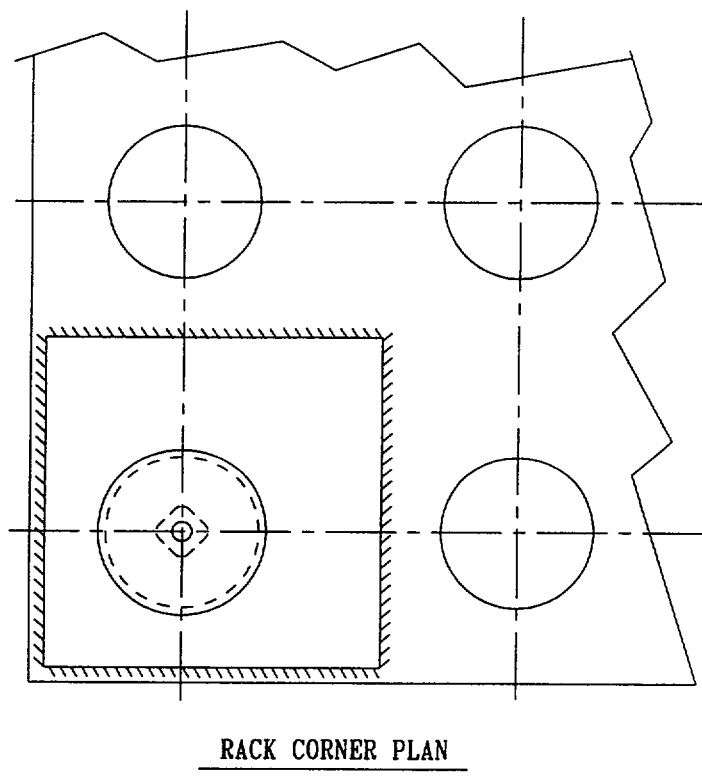
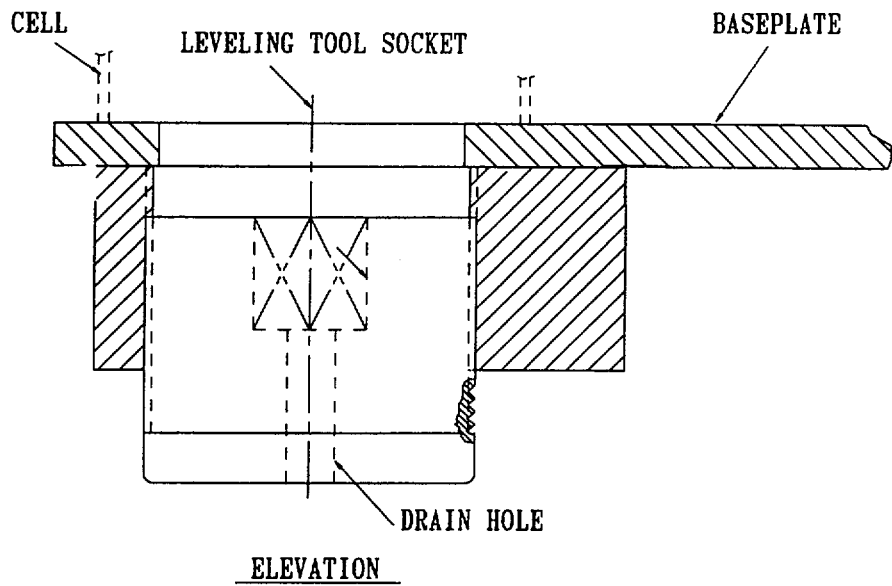


FIGURE 2.5; SUPPORT PEDESTAL FOR HOLTEC PWR RACK

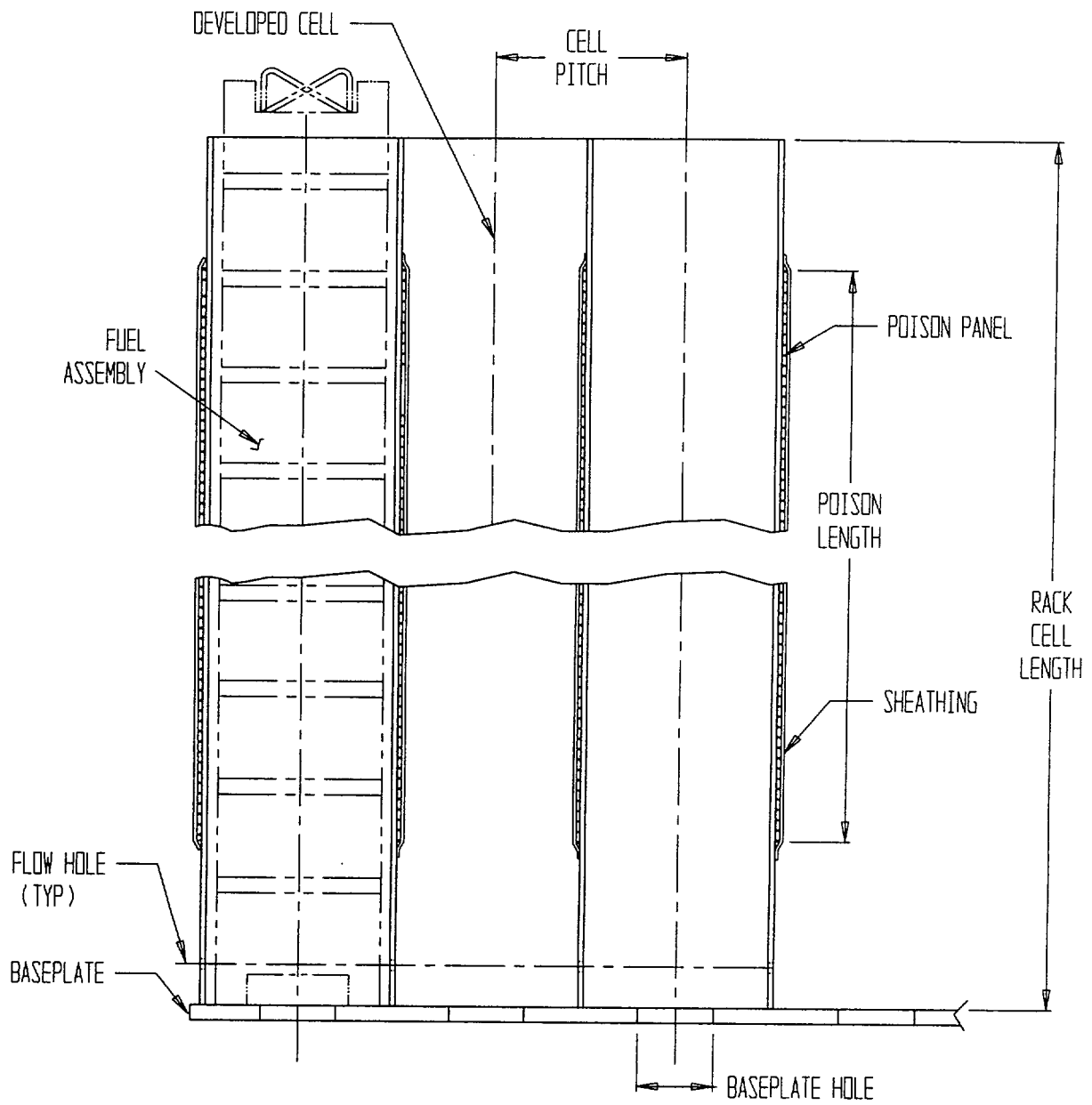


FIGURE 2.6: THREE PWR CELLS IN ELEVATION VIEW

HI992329

### 3.0 MATERIAL, HEAVY LOAD, AND CONSTRUCTION CONSIDERATIONS

#### 3.1 Introduction

Safe storage of nuclear fuel in the Spent Fuel Pool (SFP) requires that the materials utilized in the rack fabrication be of proven durability and compatible with the pool water environment. Likewise, all activities in the rack installations must comply with the provisions of NUREG-0612 [3.1.1] to eliminate the potential for damage to fuel presently stored in the SFP or any safety related equipment. This section provides a synopsis of the considerations with regard to long-term service life and short-term construction safety.

#### 3.2 Structural Materials

The following structural materials are utilized in the fabrication of the new spent fuel racks:

- a. ASME SA-240-304 for all composite box subassembly sheet metal, baseplate and cell connecting bar stock
- b. Internally threaded support pedestals: ASME SA-240-304
- c. Externally threaded spindle for the support pedestal: ASME SA-564-630 precipitation hardened stainless steel (heat treated to 1100°F)
- d. Weld material: ASME Type 308

#### 3.3 Poison Material (Neutron Absorber)

In addition to the structural and non-structural stainless steel material, the racks employ Boral™, a patented product of AAR Manufacturing, as the neutron absorber material. Boral is a hot-rolled cermet of aluminum and boron carbide, clad in aluminum. A brief description of Boral and its pool experience list follows.

Boral is a thermal neutron poison material composed of boron carbide and 1100 alloy aluminum. Boron carbide is a compound having a high boron content in a physically stable and chemically

inert form. The 1100 alloy aluminum is a lightweight metal with high tensile strength, which is protected from corrosion by a highly resistant oxide film. The oxide film is formed by a strongly adhering film of impervious hydrated aluminum oxide, which passivates the surface of the aluminum in the SFP environment. The corrosion layer penetrates the aluminum surface of the Boral only a few microns. There is no net loss of aluminum cladding through the passivation process. The central matrix of the cermet is not affected by corrosion. The two materials, boron carbide and aluminum, are chemically compatible and ideally suited for long-term use in the radiation, thermal and chemical environment of the SFP. Boral has been shown [3.3.1] to be superior to alternative materials previously used as neutron absorbers in storage racks.

Boral has been extensively used in fuel rack applications in recent years. Its use in the spent fuel pools as the neutron absorbing material can be attributed to its proven performance (over 150 pool years of experience) and the following unique characteristics:

- i. The content and placement of boron carbide provides a very high removal cross-section for thermal neutrons.
- ii. Boron carbide, in the form of fine particles, is homogeneously dispersed throughout the central layer of the Boral panels.
- iii. The boron carbide and aluminum materials in Boral do not degrade as a result of long-term exposure to radiation.
- iv. The neutron absorbing central layer of Boral is clad with permanently bonded surfaces of aluminum.
- v. Boral is stable, strong, durable, and corrosion resistant.

Boral is manufactured by AAR Manufacturing under the control and surveillance of Holtec International's Quality Assurance/Quality Control Program that conforms to the requirements of 10CFR50 Appendix B, "Quality Assurance Criteria for Nuclear Power Plants". Holtec

International has been evaluated by the Davis-Besse Nuclear Power Station (DBNPS) Nuclear Assurance Department and is an approved supplier for the design, fabrication and installation of the SFP racks.

As indicated in Tables 3.3.1 and 3.3.2, Boral has been licensed by the USNRC for use in numerous BWR and PWR spent fuel storage racks and has been extensively used in international nuclear installations.

### 3.3.1 Boral Material Characteristics

**Aluminum:** Aluminum is a silvery-white, ductile metallic element. The 1100 alloy aluminum is used extensively in heat exchangers, pressure and storage tanks, chemical equipment, reflectors and sheet metal work.

It has high resistance to corrosion in industrial and marine atmospheres. Aluminum has an atomic number of 13, atomic weight of 26.98, specific gravity of 2.69 and valence of 3. The physical, mechanical and chemical properties of the 1100 alloy aluminum are listed in Tables 3.3.3 and 3.3.4.

The excellent corrosion resistance of the 1100 alloy aluminum is provided by the protective oxide film that quickly develops on its surface from exposure to the atmosphere or water. This film prevents the loss of metal from general corrosion or pitting corrosion.

**Boron Carbide:** The boron carbide contained in Boral is a fine granulated powder that conforms to ASTM C-750-80 nuclear grade Type III. The material conforms to the chemical composition and properties listed in Table 3.3.5.

References [3.3.2], [3.3.3], and [3.3.4] provide further discussion as to the suitability of these materials for use in spent fuel storage module applications.

### 3.4 Compatibility with Coolant

All materials used in the construction of the Holtec racks have been determined to be compatible with the DBNPS Spent Fuel Pool, Cask Pit, and Transfer Pit, and have an established history of in-pool usage. As evidenced in Tables 3.3.1 and 3.3.2, Boral has been successfully used in fuel pools. Austenitic stainless steel (304) is perhaps the most widely used stainless alloy in nuclear power plants.

### 3.5 Heavy Load Considerations for the Proposed Re-racking

The Spent Fuel Cask Crane (SFCC) will be used for removal of the existing racks, and the installation of the new storage racks in the SFP, and installation and removal of the Cask Pit cover. Due to the limited travel of the SFCC, a temporary crane (see section 3.6) will be required for the removal and installation of the racks. The SFCC is subject to the requirements of NUREG-0612, "Control of Heavy Loads at Nuclear Power Plants". Safe handling of heavy loads by the SFCC will be ensured by following the defense in depth approach guidelines of NUREG 0612:

- Defined safe load paths in accordance with approved procedures
- Supervision of heavy load lifts by designated individuals
- Crane operator training and qualification that satisfies the requirements of ANSI/ASME B30.2-1976 [3.5.1]
- Use of lifting devices (slings) that are selected, inspected and maintained in accordance with ANSI B30.9-1971 [3.5.2]
- Inspection, testing and maintenance of cranes in accordance with ANSI/ASME B30.2-1976
- Ensuring the design of the SFCC is equivalent to the requirements of CMAA-70 [3.5.3] and ANSI/ASME B30.2-1976
- Reliability of special lifting devices by application of design safety margins, and periodic inspection and examinations using approved procedures

- Use of a cover to protect the fuel assemblies stored temporarily in the Cask Pit or Transfer Pit during movement of heavy loads over the stored fuel.

The following are some of the salient features which make lifting heavy loads during the re-racking a safe evolution:

a. Safe Load Paths and Procedures

The Cask Pit, which will contain fuel during most of the re-racking, is located west of the SFP, between the Auxiliary Building Train Bay/Loading Area and the SFP, (see Figure 3.5-1). During re-racking the load path of some racks will transverse the Cask Pit. Therefore, a Cask Pit cover shall be used to protect the fuel in the Cask Pit. The cover will be designed to ASME B & PV Code, Division 1, Subsection NF. The cover will be qualified to withstand the drop of the heaviest rack, including rigging, from an appropriate height. The height that heavy loads may travel over the Cask Pit cover will be administratively controlled by procedures.

The Cask Pit cover is a heavy load. The activities associated with its installation and removal will be administratively controlled by procedures to meet the requirements of NUREG-0612.

Safe load paths will be identified for moving the remaining heavy loads in the Fuel Building. Safe load paths will maximize the benefits of strategic fuel shuffles that allow for the greatest distance between a heavy load and stored fuel.

Note: All fuel movements to support the re-racking will utilize the fuel handling bridge, and be controlled per the normal DBNPS fuel movement procedures.

All heavy loads are lifted in such a manner that the C.G. of the lift point is aligned with the C.G. of the load being lifted. Turnbuckles rather than slings are utilized to "fine tune" the verticality of the new rack being lifted.

Movement of heavy loads will be conducted in accordance with written procedures, which will be reviewed and approved by DBNPS.

b. Supervision of Lifts

Procedures used during the removal/installation of the SFP racks and the Cask Pit cover require supervision of heavy load lifts by a designated individual who is responsible for ensuring procedure compliance and safe lifting practices.

c. Crane Operator Training

All crew members involved in the use of the lifting and upending equipment will be given training by Holtec International using a videotape-aided instruction course which has been utilized in previous re-rack operations.

d. Lifting Devices Design and Reliability

The SFCC is comprised of a main hook rated for 140 tons as well as an auxiliary hook rated for 20 tons. A temporary hoist with an appropriate capacity will be attached to the SFCC hook to be used to prevent submergence of the hook.

The following table determines the maximum lift weight during rack installation.

Item	Weight (lbs)
Rack	14,030 (maximum)
Lift Rig	1,000
Rigging	500
Temporary hoist	2,000
Total Lift	17,530

It is clear, based on the heaviest rack weight to be lifted, that the heaviest load being lifted is well below the rating of the SFCC hooks. The temporary hoist to be used in conjunction with the SFCC hook will be selected to provide an adequate load capacity and comply with NUREG-0612.

Remotely engaging lift rigs, meeting all requirements of NUREG-0612 as a single failure proof design, will be used to lift the new rack modules. Dual load paths are built into the design of the lift rig via four independent load paths. There are four separate eye pads as well as four separate lifting rods. The design of the lift rig allows for the failure of one load path while maintaining a 5:1 safety factor in each of the remaining load paths. Therefore, the lift rig complies with the duality feature called for in Section 5.1.6 (3a) of NUREG 0612.

The rig has the following attributes:

- The traction rod is designed to prevent loss of its engagement with the rig in the locked position. Moreover, the locked configuration can be directly verified from above the pool water without the aid of an underwater camera.
- The stress analysis of the rig is carried out and the primary stress limits postulated in ANSI N14.6 [3.5.4] are met.
- The rig is load tested with 300% of the maximum weight to be lifted. The test weight is maintained in the air for 10 minutes. All critical weld joints are liquid penetrant examined to establish the soundness of all critical joints.

The existing racks are made up of a rack structure which contains individual fuel storage cells. These racks are not free standing. There are seismic braces which are attached to the rack structure and extend out to the pool walls, (but are not attached to the wall). Prior to lifting the existing racks from the SFP, the individual storage cells will be removed from the rack structure. Then, as

necessary, any rack-to-wall seismic braces will be removed. Finally the rack structure will be lifted from the pool after being cut into appropriate parts. The rack material will be lifted with slings. The weight of a cell is approximately 270 lbs. A complete rack structure, including all seismic braces, weighs approximately 9,600 lbs. Standard rigging will be used for the removal of all pieces. NUREG-0612 shall govern all picks involving the removal of components that make up the existing rack array. The rigging utilized to install and remove the Cask Pit cover shall meet the requirements of NUREG-0612.

e. Crane Maintenance

The SFCC is maintained functional per the DBNPS preventative maintenance procedures.

The proposed heavy loads compliance will be in accordance with the guidelines of NUREG-0612, which calls for measures to "provide an adequate defense-in-depth for handling of heavy loads near spent fuel...". The NUREG-0612 guidelines cite four major causes of load handling accidents, namely

- i. operator errors
- ii. rigging failure
- iii. lack of adequate inspection
- iv. inadequate procedures

The racking program ensures maximum emphasis on mitigating the potential load drop accidents by implementing measures to eliminate shortcomings in all aspects of the operation including the four aforementioned areas. A summary of the measures specifically planned to deal with the major causes is provided below.

Operator errors: As mentioned above, comprehensive training will be provided to the installation crew. All training shall be in compliance with ANSI B30.2.

Rigging failure: The lifting device designed for handling and installation of the new racks has redundancies in the lift legs and lift eyes such that there are four independent load members in the new rack lift rig. Failure of any one load bearing member would not result in uncontrolled swing of the load, or lead to uncontrolled lowering of the load. The rig complies with all provisions of ANSI 14.6-1978, including compliance with the primary stress criteria, load testing at 300% of maximum lift load, and dye examination of critical welds.

The new rack lift rig design is similar to the rigs used in the initial racking or the re-rack of numerous other plants, such as Hope Creek, Millstone Unit 1, Indian Point Unit Two, Ulchin II, Laguna Verde, J.A. FitzPatrick, and Three Mile Island Unit 1.

The slings used to remove the parts of the existing racks will be selected, inspected, and maintained in accordance with ANSI B30.9-1971 [3.5.2].

Lack of adequate inspection: The designer of the racks has developed a set of inspection points that have been proven to eliminate any incidence of rework or erroneous installation in numerous prior re-rack projects. Surveys and measurements are performed on the storage racks prior to and subsequent to placement into the pools to ensure that the as-built dimensions and installed locations are acceptable. Measurements of the pool and floor elevations are also performed to determine actual pool configuration and to allow height adjustments of the pedestals prior to rack installation. These inspections minimize rack manipulation during placement into the pool.

Inadequate procedures: Procedures will be developed to address operations pertaining to rack removal and installation. These procedures will include, but not limited to, mobilization, rack handling, upending, lifting, installation, verticality, alignment, dummy gage testing, site safety, and ALARA compliance. The procedures will be the successors of the procedures successfully implemented in previous projects.

Table 3.5.1 provides a synopsis of the requirements delineated in NUREG-0612, and its intended compliance.

### 3.6 Temporary Crane

Due to the limited travel of the SFCC, a temporary crane (Figure 3.6-1) is required. As necessary, this crane will position existing racks for removal by the SFCC, and complete final positioning of the new racks after being placed in the SFP by the SFCC. All racks will be submerged when moved by this crane. The crane uses the existing rails of the fuel bridge, thereby spanning the SFP, Cask Pit, and Transfer Pit. The Temporary Crane will be moved along the rails by the fuel bridge.

Note: The Temporary Crane will not be used to move fuel.

The Temporary Crane is designed using CMAA-70 and the AISC manual and meets the intent of NUREG 0612 through a defense-in-depth approach. This is justified through the operational and equipment conditions listed below:

- Short Lift Height

The Temporary Crane lifts the racks only several inches above the pool floor to move them horizontally. The Temporary Crane does not lift any heavy loads out of the pool or over any safety related equipment.

- Rack Drop Analyzed

A rack drop from 46 feet above the pool floor was analyzed, which showed that catastrophic damage leading to rapid loss of pool water does not occur. A potential rack drop from the Temporary Crane with a lift height of only several inches would have substantially reduced consequences.

- Separation Between Load and Fuel

The operational procedures ensure a sufficient horizontal distance between load and fuel.

- Steps Proceduralized

The operation of the Temporary Crane is fully proceduralized which ensures that the operation stays within the limits outlined here. All steps are planned well ahead of occurrence to ensure adherence to a logical sequence.

- Trained Personnel

The crane is operated by trained personnel only.

- Crane Fabrication

The crane is manufactured as safety related equipment and load tested to 120% of the maximum lifted load.

- Hoist rating meets NUREG 0612

The effects of a seismic event on the Temporary Crane was evaluated.

- Deformation

Analysis shows no yielding during a seismic event. If a local failure of the Temporary Crane is postulated, the overall deformation of the crane is limited to the lift height of the load of only several inches. This precludes a global failure. Therefore, the drop of the entire crane into the pool is not a credible event.

- Tipover

Due to the crane geometry, a potential tipover is not possible in the east-west direction. For all scenarios evaluated, the crane has been shown to remain stable in the north-south direction. Therefore, tipover of the crane is not a credible event.

The Temporary Crane will be placed on/removed from the fuel bridge rails a number of times during re-racking. Safe handling of this heavy load by the SFCC will be ensured by the

structural design of the crane, and by following the NUREG defense-in-depth guidelines specified in Section 3.5,

### 3.7 References

- [3.1.1] NUREG-0612, "Control of Heavy Loads at Nuclear Power Plants," July 1980.
- [3.3.1] "Nuclear Engineering International," July 1997 issue, pp 20-23.
- [3.3.2] "Spent Fuel Storage Module Corrosion Report," Brooks & Perkins Report 554, June 1, 1977.
- [3.3.3] "Suitability of Brooks & Perkins Spent Fuel Storage Module for Use in PWR Storage Pools," Brooks & Perkins Report 578, July 7, 1978.
- [3.3.4] "Boral Neutron Absorbing/Shielding Material - Product Performance Report," Brooks & Perkins Report 624, July 20, 1982.
- [3.5.1] ANSI/ASME B30.2, "Overhead and Gantry Cranes, (Top Running Bridge, Single or Multiple Girder, Top Running Trolley Hoist)," American Society of Mechanical Engineers, 1976.
- [3.5.2] ANSI B30.9, "Safety Standards for Slings," 1971.
- [3.5.3] CMMA Specification 70, "Electrical Overhead Traveling Cranes," Crane Manufacturers Association of America, Inc., 1983.
- [3.5.4] ANSI N14.6-1978, Standard for Special Lifting Devices for Shipping Containers Weighing 10000 Pounds or more for Nuclear Materials," American National Standard Institute, Inc., 1978.
- [3.5.5] ANSI/ASME B30.20, "Below-the-Hook Lifting Devices," American Society of Mechanical Engineers, 1993.

Table 3.3.1

## BORAL EXPERIENCE LIST - PWRs

Plant	Utility	Docket No.	Mfg. Year
Maine Yankee	Maine Yankee Atomic Power	50-309	1977
Donald C. Cook	Indiana & Michigan Electric	50-315/316	1979
Sequoyah 1,2	Tennessee Valley Authority	50-327/328	1979
Salem 1,2	Public Service Electric & Gas	50-272/311	1980
Zion 1,2	Commonwealth Edison	50-295/304	1980
Bellefonte 1, 2	Tennessee Valley Authority	50-438/439	1981
Yankee Rowe	Yankee Atomic Power	50-29	1964/1983
Gosgen	Kernkraftwerk Gosgen-Daniken AG (Switzerland)		1984
Koeberg 1,2	ESCOM (South Africa)		1985
Beznau 1,2	Nordostschweizerische Kraftwerke AG (Switzerland)		1985
12 various Plants	Electricite de France (France)	--	1986
Indian Point 3	NY Power Authority	50-286	1987
Byron 1,2	Commonwealth Edison	50-454/455	1988
Braidwood 1,2	Commonwealth Edison	50-456/457	1988
Yankee Rowe	Yankee Atomic Power	50-29	1988
Three Mile Island I	GPU Nuclear	50-289	1990
Sequoyah (rerack)	Tennessee Valley Authority	50-327	1992
Donald C. Cook (rerack)	American Electric Power	50-315/316	1992
Beaver Valley Unit 1	Duquesne Light Company	50-334	1993
Fort Calhoun	Omaha Public Power District	50-285	1993

Table 3.3.1			
BORAL EXPERIENCE LIST - PWRs			
Plant	Utility	Docket No.	Mfg. Year
Zion 1 & 2 (rerack)	Commonwealth Edison	50-295/304	1993
Salem Units 1 & 2 (rerack)	Public Gas and Electric Company	50-272/311	1995
Ulchin Unit 1	Korea Electric Power Company (Korea)	--	1995
Haddam Neck	Connecticut Yankee Atomic Power Company	50-213	1996
Ulchin Unit 2	Korea Electric Power Company (Korea)	--	1996
Kori-4	Korea Electric Power Company (Korea)	--	1996
Yonggwang 1,2	Korea Electric Power Company (Korea)	--	1996
Sizewell B	Nuclear Electric, plc (United Kingdom)	--	1997
Angra 1	Furnas Centrais-Elétricas SA (Brazil)	--	1997
Vogtle 2	Southern Nuclear	50-424	1997
Waterford 3	Entergy Operations	50-382	1997
Callaway	Union Electric	50-483	1997
Wolf Creek	Wolf Creek Nuclear Operating Corp.	50-482	1999
Davis Besse (added racks)	First Energy	50-346	1999
Millstone 3	Northeast Utilities	50-423	2000
Byron	Commonwealth Edison	50-455	2000

Table 3.3.2

## BORAL EXPERIENCE LIST - BWRs

Plant	Utility	Docket No.	Mfg. Year
Cooper	Nebraska Public Power	50-298	1979
J.A. FitzPatrick	NY Power Authority	50-333	1978
Duane Arnold	Iowa Electric Light & Power	50-331	1979
Browns Ferry 1,2,3	Tennessee Valley Authority	50-259/260/296	1980
Brunswick 1,2	Carolina Power & Light	50-324/325	1981
Clinton	Illinois Power	50-461/462	1981
Dresden 2,3	Commonwealth Edison	50-237/249	1981
E.I. Hatch 1,2	Georgia Power	50-321/366	1981
Hope Creek	Public Service Electric & Gas	50-354/355	1985
Humboldt Bay	Pacific Gas & Electric Company	50-133	1985
LaCrosse	Dairyland Power	50-409	1976
Limerick 1,2	Philadelphia Electric Company	50-352/353	1980
Monticello	Northern States Power	50-263	1978
Peachbottom 2,3	Philadelphia Electric	50-277/278	1980
Perry 1,2	Cleveland Electric Illuminating	50-440/441	1979
Pilgrim	Boston Edison Company	50-293	1978
Susquehanna 1,2	Pennsylvania Power & Light	50-387,388	1979
Vermont Yankee	Vermont Yankee Atomic Power	50-271	1978/1986
Hope Creek	Public Service Electric & Gas	50-354/355	1989
Harris Pool 'B' †	Carolina Power & Light	50-401	1991
Duane Arnold	Iowa Electric Light & Power	50-331	1993
Pilgrim	Boston Edison Company	50-293	1993
LaSalle 1	Commonwealth Edison	50-373	1992

Table 3.3.2

## BORAL EXPERIENCE LIST - BWRs

Plant	Utility	Docket No.	Mfg. Year
Millstone Unit 1	Northeast Utilities	50-245	1989
James A. FitzPatrick	NY Power Authority	50-333	1990
Hope Creek	Public Service Electric & Gas Company	50-354	1991
Duane Arnold Energy Center	Iowa Electric Power Company	50-331	1994
Limerick Units 1,2	PECO Energy	50-352/50-353	1994
Harris Pool 'B' †	Carolina Power & Light Company	50-401	1996
Chinshan 1,2	Taiwan Power Company (Taiwan)	--	1986
Kuosheng 1,2	Taiwan Power Company (Taiwan)	--	1991
Laguna Verde 1,2	Comision Federal de Electricidad (Mexico)	--	1991
Harris Pool 'B' †	Carolina Power & Light Company	50-401	1996
James A. FitzPatrick	NY Power Authority	50-333	1998
Chin Shan 1,2	Taiwan Power Company (Taiwan)	--	1999
Nine Mile 1	Nine Mile Power Corp.	50-220	1999
Oyster Creek	GPU Nuclear	50-219	2000
Hatch 2	Southern Nuclear	50-366	2000

† Fabricated racks for storage of spent fuel transhipped from Brunswick.

Table 3.3.3

1100 ALLOY ALUMINUM PHYSICAL CHARACTERISTICS	
Density	0.098 lb/in <sup>3</sup> 2.713 g/cm <sup>3</sup>
Melting Range	1190°F - 1215°F 643° - 657°C
Thermal Conductivity (77°F)	128 BTU/hr/ft <sup>2</sup> /F/ft 0.53 cal/sec/cm <sup>2</sup> /°C/cm
Coefficient of Thermal Expansion (68°F - 212°F)	13.1 x 10 <sup>-6</sup> in/in-°F 23.6 x 10 <sup>-6</sup> cm/cm-°C
Specific Heat (221°F)	0.22 BTU/lb/°F 0.23 cal/g/°C
Modulus of Elasticity	10 x 10 <sup>6</sup> psi
Tensile Strength (75°F)	13,000 psi (annealed) 18,000 psi (as rolled)
Yield Strength (75°F)	5,000 psi (annealed) 17,000 psi (as rolled)
Elongation (75°F)	35-45% (annealed) 9-20% (as rolled)
Hardness (Brinell)	23 (annealed) 32 (as rolled)
Annealing Temperature	650°F 343°C

Table 3.3.4 CHEMICAL COMPOSITION - ALUMINUM (1100 ALLOY)	
99.00% min.	Aluminum
1.00% max.	Silicone and Iron
0.05-0.20% max.	Copper
0.05% max.	Manganese
0.10% max.	Zinc
0.15% max.	Other

Table 3.3.5

**CHEMICAL COMPOSITION AND PHYSICAL PROPERTIES  
OF BORON CARBIDE**

CHEMICAL COMPOSITION (WEIGHT PERCENT)	
Total boron	70.0 min.
B <sup>10</sup> isotopic content in natural boron	18.0
Boric oxide	3.0 max.
Iron	2.0 max.
Total boron plus total carbon	94.0 min.
PHYSICAL PROPERTIES	
Chemical formula	B <sub>4</sub> C
Boron content (weight percent)	78.28%
Carbon content (weight percent)	21.72%
Crystal structure	rhombohedral
Density	0.0907 lb/in <sup>3</sup> 2.51 g/cm <sup>3</sup>
Melting Point	4442°F 2450°C
Boiling Point	6332°F 3500°C
Boral Loading (minimum grams B <sup>10</sup> per cm <sup>2</sup> )	0.030

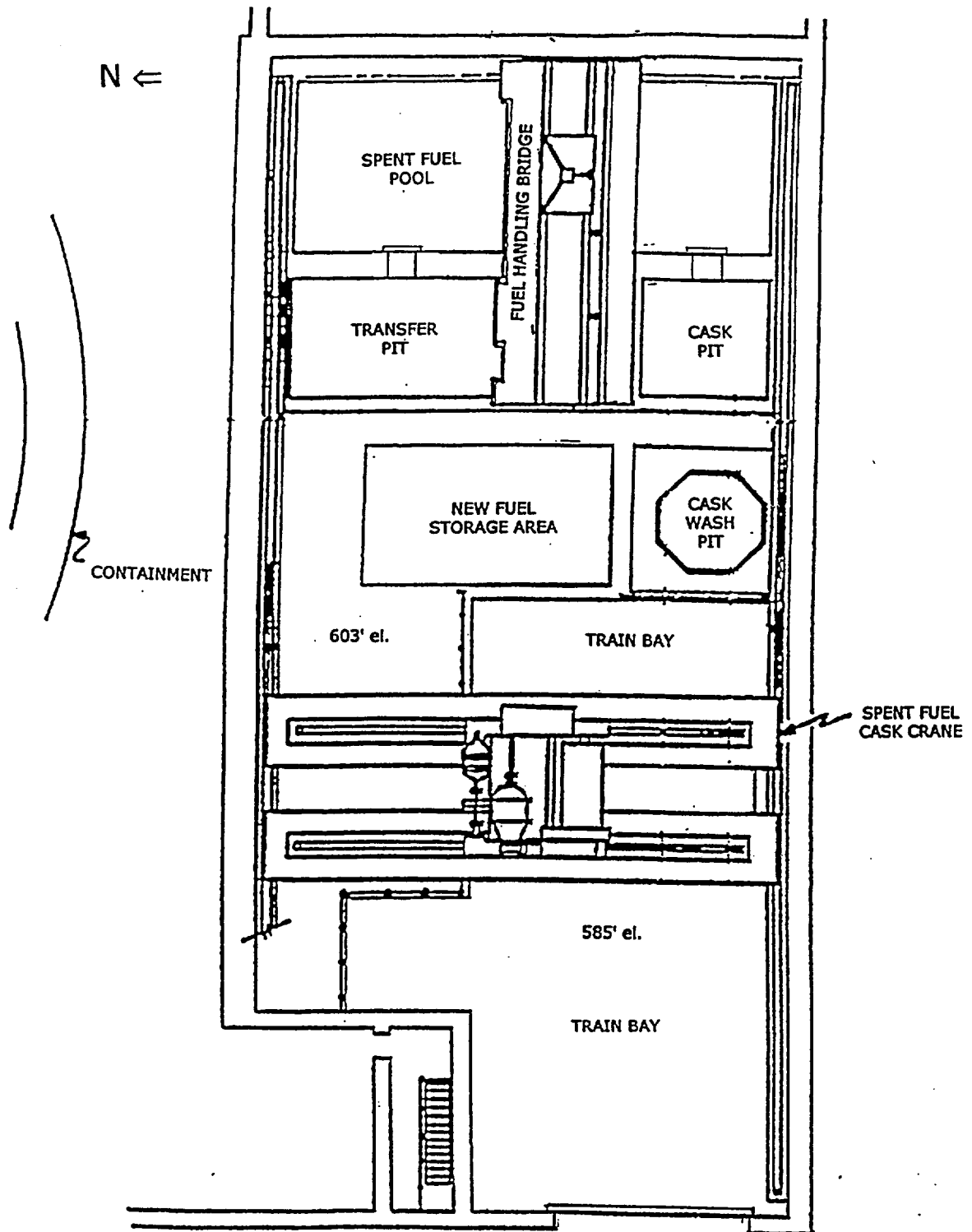
Table 3.5.1

HEAVY LOAD HANDLING COMPLIANCE MATRIX (NUREG-0612)

Criterion	Compliance
1. Are safe load paths defined for the movement of heavy loads to minimize the potential of impact, if dropped, on irradiated fuel?	Yes
2. Will procedures be developed to cover: identification of required equipment, inspection and acceptance criteria required before movement of load, steps and proper sequence for handling the load, defining the safe load paths, and special precautions?	Yes
3. Will crane operators be trained and qualified?	Yes
4. Will special lifting devices meet the guidelines of ANSI 14.6-1978?	Yes
5. Will non-custom lifting devices be installed and used in accordance with ANSI B30.20 [3.5.5], 1993?	Yes
6. Will the cranes be inspected and tested prior to use in rack installation?	Yes
7. Does the crane meet the intent of ANSI B30.2-1976 and CMMA-70?	Yes

Figure 3.5.1

Auxiliary Building – Spent Fuel Pool Area Plan View



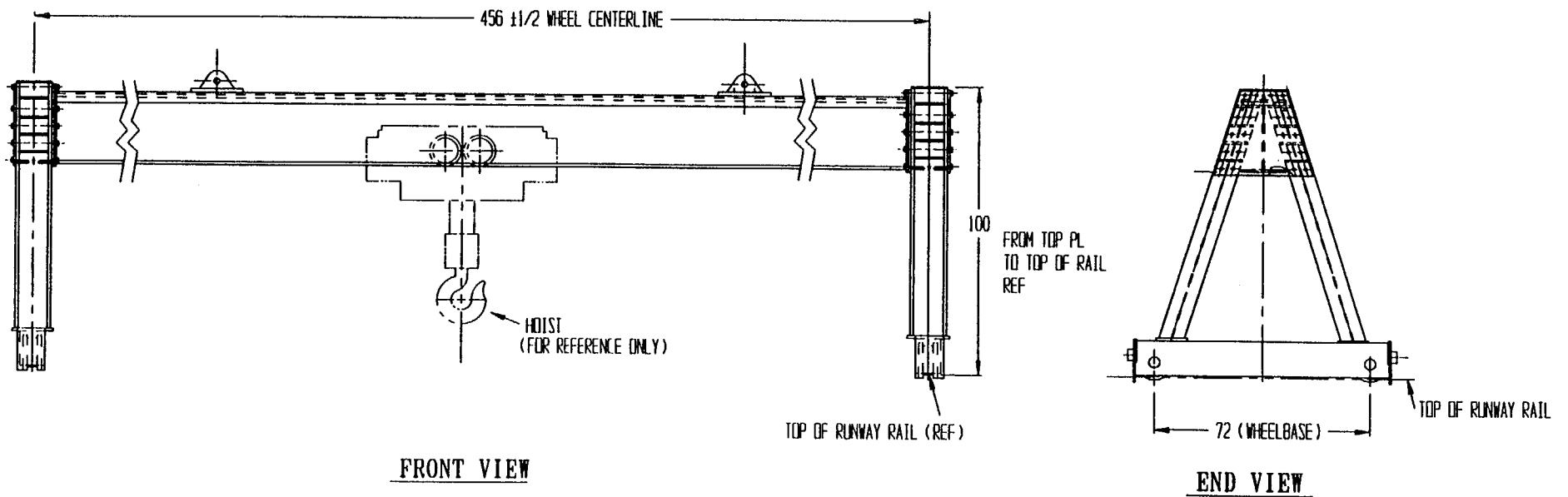


FIGURE 3.6.1; TEMPORARY CRANE

## 4.0 CRITICALITY SAFETY EVALUATION

### 4.1 DESIGN BASES

The high density spent fuel storage racks in the Spent Fuel Pool (SFP) at the Davis-Besse Nuclear Power Station are designed to assure that the effective neutron multiplication factor,  $k_{eff}$ , is equal to or less than 0.95 with the racks fully loaded with fuel of the highest anticipated reactivity, and flooded with un-borated water.

The racks are qualified for storage of fuel in the following storage patterns:

- Mixed Zone Three Region (MZTR), where fresh or low burnup assemblies (identified as Region 1 assemblies) are separated from each other and from intermediate burnup fuel assemblies (identified as Region 3 assemblies) by barrier fuel assemblies with high burnup (identified as Region 2 assemblies).
- Checkerboard (CB) Pattern of empty cells, or cells with non-fuel bearing components, and cells with fresh or low burnup assemblies (Region 1).
- Homogeneous Loading (HL) of intermediate burnup fuel assemblies (Region 3).

Note: Region 2 assemblies correspond to Category A in Technical Specification Figure 3.9-3.  
Region 3 assemblies correspond to Category B in Technical Specification Figure 3.9-3.  
Region 1 assemblies correspond to Category C in Technical Specification Figure 3.9-3.

For Region 2 and Region 3 assemblies, a minimum burnup is required, which is a function of the initial enrichment.

The temporary placement of fuel in a single rack in the Transfer Pit during rack installation, is bounded by the analyses for the SFP.

Including all applicable uncertainties, the maximum  $k_{eff}$  is shown to be less than 0.95 with a 95% probability at a 95% confidence level [4.1.1]. Reactivity effects of abnormal and accident

conditions have also been evaluated to assure that under credible abnormal and accident conditions, the reactivity will not exceed 0.95, with credit for soluble boron in the pool water.

Applicable codes, standards, and regulations or pertinent sections thereof, include the following:

- *Code of Federal Regulations*, Title 10, Part 50, Appendix A, General Design Criterion 62, Prevention of Criticality in Fuel Storage and Handling.
- USNRC Standard Review Plan, NUREG-0800, Section 9.1.2, Spent Fuel Storage, Rev. 3 - July 1981.
- USNRC letter of April 14, 1978, to all Power Reactor Licensees - OT Position for Review and Acceptance of Spent Fuel Storage and Handling Applications, including modification letter dated January 18, 1979.
- L.I. Kopp, "Guidance on the Regulatory Requirements for Criticality Analysis of Fuel Storage at Light-Water Reactor Power Plants," June 1998.
- USNRC Regulatory Guide 1.13, Spent Fuel Storage Facility Design Basis, Rev. 2 (proposed), December 1981.
- ANSI ANS-8.17-1984, Criticality Safety Criteria for the Handling, Storage and Transportation of LWR Fuel Outside Reactors.

USNRC guidelines [4.1.2] and the applicable ANSI standards specify that the maximum effective multiplication factor,  $k_{\text{eff}}$ , including bias, uncertainties, and calculational statistics, shall be less than or equal to 0.95, with 95% probability at the 95% confidence level. In the present criticality safety evaluation of the storage racks, the design basis limit was selected to be 0.95.

To ensure that the true reactivity will always be less than the calculated reactivity, the following conservative assumptions were made:

- Moderator is un-borated water at a temperature of 20°C. The effect of the temperature reduction to 4 °C (corresponding to the maximum reactivity) is included as an additional uncertainty in the calculations.

- The racks are assumed to be fully loaded with the most reactive fuel which complies with the burnup versus initial enrichment curve for the new racks, with no credit for control rods or burnable poison.
- Soluble poison (boron) is conservatively assumed to be completely lost from the spent fuel pool water (design accident condition).
- Neutron absorption in minor structural members is neglected. (i.e., The spacer grids and anything outside the active fuel region, such as end fittings, are replaced by water.)
- The effective multiplication factor of an infinite radial array of storage cells or storage racks containing fuel assemblies is used, except for the assessment of peripheral effects and certain abnormal/accident conditions where neutron leakage is inherent.
- In-core depletion calculations assumed conservative operating conditions: highest fuel and moderator temperature (1300 °F and 610 °F, respectively), a conservative allowance for the soluble boron concentrations (1000 ppm), and burnable poison (4.0 wt% B<sub>4</sub>C) rods present in each guide tube (removed at 35 GWD/MTU). These conditions produce Plutonium in excess of normal operating conditions.
- No axial blankets were assumed to be present in the fuel rods, i.e., the entire active length was assumed to have the same enrichment.

The spent fuel storage racks are designed to accommodate B&W 15x15 Mark B fuel assemblies characterized by the dimensions listed in Table 4.1.1. The fuel specifications in Table 4.1.1 allow for variations in the cladding thickness, and thus, calculations were performed to identify the assembly type with the highest reactivity. The results show that for fresh assemblies with an initial enrichment of 2.55 wt% <sup>235</sup>U or more, assembly type C has the highest reactivity. However, for assemblies with a burnup of 35 GWD/mtU or more, assembly type B is the

bounding assembly. Between these limits there is a transition area, where the bounding assembly is either type B or C. Consequently, all Monte Carlo calculations use assembly type C for the fresh (Region 1) assembly, and assembly type B for the irradiated (Region 2 and Region 3) assemblies.

The water in the Spent Fuel Pool normally contains soluble boron, which would result in a large sub-criticality margin under actual operating conditions. However, the NRC guidelines, based upon the accident condition in which all soluble poison is assumed to have been lost, specify that the limiting  $k_{\text{eff}}$  of 0.95 for normal storage be evaluated for the accident condition that assumes the loss of soluble boron. The double contingency principle of ANSI N16.1-1975 and of the April 1978 NRC letter allows credit for soluble boron under other abnormal or accident conditions, since only a single independent accident need be considered at one time. Consequences of abnormal and accident conditions have also been evaluated, where "abnormal" refers to conditions which may reasonably be expected to occur during the lifetime of the plant, and "accident" refers to conditions which are not expected to occur but nevertheless must be protected against.

## 4.2 SUMMARY OF CRITICALITY ANALYSES

### 4.2.1 Normal Operating Conditions

Calculations have been performed to qualify the racks for storage of fuel assemblies in three different loading patterns:

- Mixed Zone Three Region (MZTR), where fresh or low burnup assemblies (Region 1) are separated from each other and from intermediate burnup fuel assemblies (Region 3) by barrier fuel assemblies with high burnup (Region 2).
- Checkerboard Pattern of empty cells, or cells with non-fuel bearing components, and cells with fresh or low burnup assemblies (Region 1).
- Homogeneous Loading of intermediate burnup fuel assemblies (Region 3).

The three regions are defined as follows:

- Region 1: Maximum nominal initial enrichment of 5.05 wt%  $^{235}\text{U}$ , no burnup required.
- Region 2: Maximum nominal initial enrichment of 5.05 wt%  $^{235}\text{U}$  and a minimum burnup of 55 GWD/mtU. For nominal initial enrichments lower than 5.05 wt%  $^{235}\text{U}$ , the minimum (limiting) burnup can be determined from Figure 4.2.1.
- Region 3: Maximum nominal initial enrichment of 5.05 wt%  $^{235}\text{U}$  and a minimum burnup of 45 GWD/mtU. For nominal initial enrichments lower than 5.05 wt%  $^{235}\text{U}$ , the minimum (limiting) burnup can be determined from Figure 4.2.1.

The bounding case is the MZTR pattern for a rack at the center of the pool. The criticality analyses for this case are summarized in Table 4.2.1, and demonstrate that for the burnup-

enrichment combinations shown in Figure 4.2.1, the maximum  $k_{\text{eff}}$  is less than 0.95. The criticality analyses for the Checkerboard and Homogeneous Loading cases are summarized in Tables 4.2.2 and 4.2.3, respectively.

Typical loading configurations are shown in Figures 4.2.2 and 4.2.3. Other configurations can be used as long as the following requirements are fulfilled.

For the MZTR Pattern:

- Region 1 fuel is only permitted in the outer row of each rack.
- In the outer row of the pool, i.e. cells facing the pool wall, Region 1 fuel assemblies must be separated by at least 1 (one) Region 2 assembly.
- In cells on the outer rack rows not facing the pool wall, Region 1 fuel assemblies must be separated by at least 2 (two) Region 2 assemblies or a rack to rack gap.
- In cells on the outer rack rows not facing the pool wall, Region 1 fuel assemblies must not be placed on the corner of a rack.
- Region 1 fuel assemblies must be separated from Region 3 Fuel assemblies by at least one Region 2 assembly.
- A Region 1 assembly can be replaced by a Region 2 or a Region 3 assembly.
- Empty cells are less reactive than Region 1, 2, or 3 assemblies.
- A Region 3 assembly can be replaced by a Region 2 assembly.

- If an outer row/column of a rack is empty, or contains non-fuel bearing components, the requirements listed above apply to the next row/column, i.e., the first row/column containing fuel.

For interfaces between patterns (see Figure 4.2.2):

Different loading patterns can be used in different racks without restriction, as long as each rack contains only one loading pattern. It is also permissible to use different patterns within one rack, with the following restrictions:

- Only 2 patterns per rack, divided by a straight horizontal or vertical line (see Figure 4.2.3).
- Region 1 fuel assemblies must not be placed directly next to each other.
- Region 1 fuel assemblies in a MZTR pattern must be separated from Region 3 assemblies by at least 2 (two) Region 2 assemblies along the side of the rack. This configuration is shown in Figure 4.2.3 in a rack on the east side of the pool. Note: As shown in Figure 4.2.3, this requirement is not applicable to MZTR/Checkerboard pattern interface.

Due to the increased neutron leakage of a single rack compared to a rack in the SFP, the reactivity of a single rack is below the reactivity of a rack in the SFP with the same loading pattern. Based on this, the analyses for the new SFP racks are bounding for a single rack in the Transfer Pit. Therefore, using the same loading patterns and requirements listed above, it is also permissible to place a single loaded rack into the Transfer Pit.

The burnup criteria identified in Figure 4.2.1 for acceptable storage will be implemented by appropriate administrative procedures.

#### 4.2.2 Abnormal and Accident Conditions

The effects on reactivity of credible abnormal and accident conditions are discussed in Section 4.6 and summarized in Table 4.2.4. Administrative procedures, to assure the presence of soluble poison during fuel handling operations, preclude the possibility of the simultaneous occurrence of two independent accident conditions.

Assuring the presence of soluble poison during fuel handling operations will preclude the possibility of the simultaneous occurrence of the two independent accident conditions. The largest reactivity increase would occur if a fresh fuel assembly of 5.05 wt%  $^{235}\text{U}$  enrichment were to be inadvertently loaded into a cell with the remainder of the rack loaded in a checkerboard pattern. Under these accident conditions, credit for the presence of soluble poison is permitted by the NRC guidelines <sup>†</sup>. Calculations were performed to demonstrate that 630 ppm soluble boron is adequate to assure a  $k_{\text{eff}}$  of 0.945 is not exceeded.

---

<sup>†</sup> Double contingency principle of ANSI N16.1-1975, as specified in the April 14, 1978 NRC letter (section 1.2) and implied in the proposed revision to Reg. Guide 1.13 (Section 1.4, Appendix A).

## 4.3 REFERENCE FUEL STORAGE CELLS

### 4.3.1 Reference Fuel Assembly

The design basis fuel assembly, illustrated in Figure 4.3.1, is the B&W 15x15 Mark B assembly.

### 4.3.2 Fuel Storage Cells

Figure 4.3.1 shows a spent fuel storage cell containing a B&W 15x15 Mark B assembly. The storage cells are composed of stainless steel walls with a single fixed neutron absorber panel, Boral, (held in place by a 0.035 inch stainless steel sheathing) centered on each side in a 0.11 inch channel. Stainless steel boxes are arranged in an alternating pattern such that the connection of the box corners form storage cells between those of the stainless steel boxes. These cells are located on a lattice spacing of  $9.22 \pm 0.005$  inches. The  $0.075 \pm 0.005$  inch thick steel walls define a storage cell which has a 9.0 inches nominal inside dimension. The Boral absorber has a thickness of  $0.101 \pm 0.005$  inches and a nominal B-10 areal density of  $0.0324 \text{ g/cm}^2$  (minimum of  $0.0277 \text{ g/cm}^2$ ). The Boral absorber panels are  $7.5 \pm 0.005$  inches in width and  $148 \pm 0.005$  inches in length. Boral panels are installed on all exterior walls facing other racks, as well as, non-fueled regions, i.e., the Spent Fuel Pool walls. The minimum gap between neighboring racks is 2.0 inches, as assured by the base plate extensions. The nominal rack to pool wall gaps are between 1.688 inches and 5.0 inches. In the calculational models, a conservative rack to wall gap size of 1.0 inches is used instead for all sides of the pool. The baseplate extension of the racks on the sides facing the pool wall is a minimum of 0.25 inches. A possible reduction of the gap size to 0.25 inch is addressed in the accident analyses.

## 4.4 ANALYTICAL METHODOLOGY

### 4.4.1 Reference Design Calculations

The principal method for criticality analysis of the high density storage racks is the three-dimensional Monte Carlo code MCNP4a [4.4.1]. MCNP4a is a continuous energy three-dimensional Monte Carlo code developed at the Los Alamos National Laboratory. MCNP4a calculations used continuous energy cross-section data based on ENDF/B-V, as distributed with the code. Independent verification calculations were performed with KENO5a [4.4.2], which is a three-dimensional multi-group Monte Carlo code developed at the Oak Ridge National Laboratory. The KENO5a calculations used the 238-group cross-section library, which is based on ENDF/B-V data and is distributed as part of the SCALE-4.3 package [4.4.3], coupled with the NITAWL-II program [4.4.4], which adjusts the uranium-238 cross sections to compensate for resonance self-shielding effects. Benchmark calculations, presented in Appendix A, indicate a bias of 0.0009 with an uncertainty of  $\pm 0.0011$  for MCNP4a and  $0.0030 \pm 0.0012$  for KENO5a, both evaluated at the 95% probability, 95% confidence level [4.1.1].

Fuel depletion analyses during core operation were performed with CASMO-4, a two-dimensional multi-group transport theory code based on capture probabilities [4.4.5 - 4.4.7]. Restarting the CASMO-4 calculations in the storage rack geometry at 4 °C yields the two-dimensional infinite multiplication factor ( $k_{inf}$ ) for the storage rack. Parallel calculations with CASMO-4 for the storage rack at various enrichments enable a reactivity equivalent enrichment (fresh fuel) to be determined that provides the same reactivity in the rack as the depleted fuel. CASMO-4 was also used to determine the small reactivity uncertainties (differential calculations) of manufacturing tolerances.

In the geometric models used for the calculations, each fuel rod and its cladding were described explicitly. Boundaries of geometric models not facing the pool walls are modeled as reflecting boundaries, which has the effect of creating an infinite radial array of storage cells or racks. Pool walls are modeled as 4 ft thick concrete slabs. Monte Carlo calculations inherently include a statistical uncertainty due to the random nature of neutron tracking. To minimize the statistical

uncertainty of the MCNP4a and KENO5a calculated reactivities and to assure convergence, a minimum of 2 million neutron histories were accumulated in each calculation.

#### 4.4.2 Fuel Burnup Calculations and Uncertainties

CASMO-4 was used for burnup calculations in the hot operating condition. CASMO-4 has been extensively benchmarked [4.4.6, 4.4.7] against cold, clean, critical experiments (including plutonium-bearing fuel), Monte Carlo calculations, reactor operations, and heavy element concentrations in irradiated fuel.

In the CASMO-4 geometric models, each fuel rod and its cladding were described explicitly and reflective boundary conditions were used between storage cells. These boundary conditions have the effect of creating an infinite array of storage cells.

Conservative assumptions of moderator and fuel temperatures and the average operating soluble boron concentration, along with the presence of burnable poison rods, were used to assure the highest plutonium production and hence conservatively high values of reactivity during burnup. Since critical experiment data with spent fuel is not available for determining the uncertainty in depletion calculations, an allowance for uncertainty in reactivity was assigned based upon other considerations [4.1.2]. Assuming the uncertainty in depletion calculations is less than 5% of the total reactivity decrement, an uncertainty in reactivity <sup>†</sup> for calculations containing irradiated fuel assemblies was assigned. This allowance for burnup uncertainty was included in determination of the acceptable burnup versus enrichment combinations.

---

<sup>†</sup> The majority of the uncertainty in depletion calculations derives from uncertainties in fuel and moderator temperatures and the effect of reactivity control methods (e.g., soluble Boron). For depletion calculations, bounding values of these operating parameters were assumed to assure conservative results in the analyses.

#### 4.4.3 Effect of Axial Burnup Distribution

Initially, fuel loaded into a reactor will burn with a slightly skewed cosine power distribution. As burnup progresses, the burnup distribution tends to flatten, becoming more highly burned in the central region than in the upper and lower regions. At high burnup, the more reactive fuel near the ends of the fuel assembly (less than average burnup) occurs in regions of high neutron leakage. Consequently, it is expected that over most of the burnup history, fuel assemblies with distributed burnups will exhibit a slightly lower reactivity than that calculated for the uniform average burnup. As burnup progresses, the distribution, to some extent, tends to be self-regulating as controlled by the axial power distribution, precluding the existence of large regions of significantly reduced burnup.

Among others, Turner [4.4.8] has provided generic analytic results of the axial burnup effect based upon calculated and measured axial burnup distributions. These analyses confirm the minor and generally negative reactivity effect of the axially distributed burnups at values less than about 27 GWD/mtU with small positive reactivity effects at higher burnup values. FirstEnergy determined a bounding axial power distribution for the criticality analyses of the new racks. The distribution was developed by incorporating the most reactive top and bottom regions from all Davis-Besse spent fuel assemblies, (including assemblies with only one cycle burnup). More over, the distribution includes the effect of partially inserted control rods. Therefore, bounding distribution is not typical on any fuel assembly and is very conservative. Burnup-equivalent enrichments were determined with CASMO-4 for each of 24 equally spaced axial zones and used in three-dimensional Monte Carlo calculations. Results of these calculations, therefore, inherently include the effect of the axial distribution in burnup. Comparison of these results to results of calculations with uniform axial burnup allows the reactivity effect of the axial burnup distribution to be quantified. The results show that using a distributed axial burnup distribution as opposed to an average burnup distribution results in a higher  $k_{eff}$  for the homogeneous loading of Region 3 fuel. However, for the MZTR loading patterns, the axial burnup distribution results in a slight decrease of  $k_{eff}$  as compared to and average burnup distribution. This is due to the fresh fuel assemblies in the

MZTR pattern, which have a dominating influence on the reactivity. A positive reactivity bias (or penalty) is therefore only applied to the homogeneous loading case and is included in the calculation of the maximum  $k_{\text{eff}}$  values.

#### 4.4.4 Long-Term Changes in Reactivity

At reactor shutdown, the reactivity of the fuel initially decreases due to the growth of Xe-135. Subsequently, the Xenon decays and the reactivity increases to a maximum at several hundred hours when the Xenon is gone. Therefore, for conservatism, the Xe is set to zero in the calculations to assure maximum reactivity. During the next 50 years, the reactivity continuously decreases due primarily to Pu-241 decay and Am-241 growth. No credit is taken for this long-term decrease in reactivity other than to indicate additional and increasing conservatism in the design criticality analysis.

## 4.5 CRITICALITY ANALYSES AND TOLERANCES

### 4.5.1 Nominal Design Cases

For the three different loading patterns in the Spent Fuel Pool, the criticality safety analyses are summarized in Tables 4.2.1 to 4.2.3. These data confirm that the maximum reactivity remains conservatively less than the regulatory limit ( $k_{\text{eff}}$  of 0.95). Independent calculations with the KENO5a code provide confirmation of the validity of the reference MCNP4a calculations.

### 4.5.2 Uncertainties Due to Burnup

Since critical experiment data with spent fuel is not available for determining the uncertainty in burnup-dependent reactivity calculations, an allowance for uncertainty in reactivity was assigned based upon other considerations. In accordance with USNRC guidelines [4.1.2], the uncertainty values are calculated as 5% of the difference in reactivity between the respective Reference case and the case with fresh assemblies in each cell of a rack. The allowance is statistically combined with the other reactivity allowances in the determination of the maximum  $k_{\text{eff}}$ . Considering the conservative assumptions employed for the depletion calculations, the allowance is considered to be very conservative.

### 4.5.3 Uncertainties Due to Tolerances

The reactivity effects of manufacturing tolerances are tabulated, along with the actual tolerances, in Table 4.5.1. To determine the  $\Delta k$  associated with a specific manufacturing tolerance, the reference  $k_{\text{inf}}$  was compared to the  $k_{\text{inf}}$  from a calculation with the tolerance included. All of the positive  $\Delta k$  values from the various tolerances are statistically combined (square root of the sum of the squares) to determine the final reactivity uncertainty allowance for manufacturing tolerances. All of the individual reactivity allowances shown in Table 4.5.1 were conservatively calculated for assembly type C at 60 MWD/kgU. The allowances were also evaluated at lower

burnups and for the other assembly types and were found to be less than the reactivity allowances shown in Table 4.5.1.

#### 4.5.4 Eccentric Fuel Positioning

The fuel assembly is assumed to be normally located in the center of the storage rack cell. However, calculations were also made with the fuel assemblies assumed to be in the corner of the storage rack cell (four-assembly cluster at closest approach). These calculations indicated that the reactivity effect is small and negative. Therefore, the reference case in which the fuel assemblies are centered is controlling and no uncertainty for eccentricity is necessary.

#### 4.5.5 Water-Gap Spacing Between Racks

The minimum water-gap between racks, which is 2.0 inches between neighboring racks, constitutes a neutron flux-trap for the storage cells of facing racks. The racks are constructed with the base plates extending beyond the edge of the cells which assures that the minimum spacing between storage racks is maintained under all credible conditions.

#### 4.5.6 Water-Gap Spacing Between Racks and Pool Walls

For the reference calculations, a gap size between racks and pool walls of 1.0 inches is used, which is smaller than the smallest gap on any side of the pool. The baseplate extension of the racks on the sides facing the pool walls is a minimum of 0.25 inches. A possible reduction of the gap size to 0.25 inch is addressed in the accident analyses.

## 4.6 ABNORMAL AND ACCIDENT CONDITIONS

### 4.6.1 Temperature and Water Density Effects

The temperature and void coefficients of reactivity in the Spent Fuel Pool are negative. Temperature effects on reactivity have been calculated (CASMO-4) and the results are shown in Table 4.6.1. In addition, the introduction of voids in the water internal to the storage cell (to simulate boiling) decreased reactivity, as shown in Table 4.6.1.

With soluble boron present, the temperature coefficients of reactivity would differ from those listed in Table 4.6.1. However, the reactivities would also be substantially lower at all temperatures with soluble boron present. The data in Table 4.6.1 is pertinent to the higher-reactivity unborated case.

Since the Monte Carlo codes, MCNP4a and KENO5a, cannot handle temperature dependence, all MCNP4a and KENO5a reference calculations were performed at 20°C and a positive temperature correction factor (the value of  $\Delta k$  between CASMO-4 calculations at 20°C and 4°C) was added to the uncertainties.

### 4.6.2 Lateral Rack Movement

Lateral motion of the storage racks under seismic conditions could potentially alter the spacing between racks. For the rack to rack gaps, the minimum gap size is 2.0 inches, as limited by the base plate extensions. This minimum gap size has been used in the analyses, which are therefore bounding. For the rack to pool wall gaps, the calculations assume a 1.0 inch gap, whereas the minimum gap size, as limited by the base plate extension, is 0.25 inch. For the potential reduction in the rack to pool wall gap under seismic conditions, credit is taken from the soluble boron in the pool water. Calculations demonstrate that a soluble boron concentration of 55 ppm is adequate to assure  $k_{\text{eff}}$  does not exceed .945.

#### 4.6.3 Abnormal Location of a Fuel Assembly

The misloading of a fresh un-irradiated fuel assembly could, in the absence of soluble poison, result in exceeding the regulatory limit ( $k_{\text{eff}}$  of 0.95). This could possibly occur if a fresh fuel assembly of the highest permissible enrichment (5.05 wt%) were to be inadvertently misloaded into one of the storage cells intended for burned fuel, or in an empty cells between other fresh assemblies in the checkerboard pattern. Soluble boron in the Spent Fuel Pool water, for which credit is permitted under these accident conditions, would assure that the reactivity is maintained substantially less than the design limitation. Calculations were performed to demonstrate that a soluble boron concentration of 630 ppm is more than adequate to assure  $k_{\text{eff}}$  does not exceed .945.

In addition, the mislocation of a fresh unirradiated fuel assembly could, in the absence of soluble poison, result in exceeding the regulatory limit ( $k_{\text{eff}}$  of 0.95). This could possibly occur if a fresh fuel assembly of the highest permissible enrichment (5.05 wt%) were to be accidentally mislocated outside of a storage rack adjacent to other fuel assemblies. The worst case would be an assembly mislocated in a corner formed by three storage racks. Calculations were performed for this condition to demonstrate that a soluble boron concentration of 450 ppm is adequate to assure  $k_{\text{eff}}$  does not exceed .945.

#### 4.6.4 Dropped Fuel Assembly

For the case in which a fuel assembly is assumed to be dropped on top of a rack and comes to rest horizontally, there will be a minimum separation distance from the active fuel in the rack of more than 12 inches. At this separation distance, the effect on reactivity is insignificant.

It is also possible to vertically drop an assembly into a location occupied by another assembly. Such a vertical impact would at most cause a small compression of the stored assembly. The distance between the active fuel regions of both assemblies will be sufficient to ensure no neutron interaction between the two assemblies. In addition, the Boron in the water will add to the subcritical condition.

Structural analysis has shown that dropping an assembly into an unoccupied cell could result in a localized deformation of the baseplate of the rack. The resultant effect would be the lowering of a single fuel assembly by the amount of the deformation. This could potentially result in the active fuel height of that assembly no longer being completely covered by the Boral. The immediate eight surrounding fuel cells could also be affected. However, the amount of deformation for these cells would be considerably less. Structural analysis has shown that the amount of localized deformation will not exceed four inches. The reactivity consequence of this situation was investigated. Two configurations were analyzed, both based on the MZTR reference case. The first configuration assumes that a single fresh assembly is lowered by 4 inches. The second configuration assumes that a total of 9 assemblies (a 3 by 3 section) including one fresh assembly is lowered by 4 inches. The calculations demonstrate that a soluble boron concentration of 55 ppm is adequate to assure  $k_{\text{eff}}$  does not exceed .945.

The above described evaluation was also used to evaluate how criticality would be affected by a drop of a fuel assembly on to a storage cell. (An empty cell was selected to maximize penetration into the cell.) From the top of the rack to the top of the Boral is 4.75 inches and the above evaluation allows 4 inches of Boral deformation. Therefore, cell deformation of up to 8.75 inches is acceptable. The impacted cell and the immediately surrounding cells (less than 9) were deformed to a maximum depth of 5 inches. Based on the above described evaluation, a boron concentration of 55 ppm is adequate to assure  $k_{\text{eff}}$  does not exceed .945.

## 4.7 REFERENCES

- [4.1.1] M. G. Natrella, Experimental Statistics, National Bureau of Standards Handbook 91, August 1963.
- [4.1.2] L.I. Kopp, "Guidance on the Regulatory Requirements for Criticality Analysis of Fuel Storage at Light-Water Reactor Power Plants," June 1998.
- [4.4.1] J.F. Briesmeister, Editor, "MCNP - A General Monte Carlo N-Particle Transport Code, Version 4A," LA-12625, Los Alamos National Laboratory (1993).
- [4.4.2] L.M. Petrie and N.F. Landers, "KENO Va - An Improved Monte Carlo Criticality Program with Supergrouping," Volume 2, Section F11 from "SCALE: A Modular System for Performing Standardized Computer Analysis for Licensing Evaluation" NUREG/CR-0200, Rev. 4, January 1990.
- [4.4.3] "SCALE 4.3: A Modular System for Performing Standardized Computer Analysis for Licensing Evaluation For Workstations and Personal Computers, Volume 0," CCC-545, ORNL-RSICC, Oak Ridge National Laboratory (1995).
- [4.4.4] N.M. Greene, L.M. Petrie and R.M. Westfall, "NITAWL-II: Scale System Module for Performing Shielding and Working Library Production," Volume 1, Section F1 from "SCALE: A Modular System for Performing Standardized Computer Analysis for Licensing Evaluation" NUREG/CR-0200, Rev. 4, January 1990.
- [4.4.5] M. Edenius, K. Ekberg, B.H. Forssen, and D. Knott, "CASMO-4 A Fuel Assembly Burnup Program User's Manual," Studsvik/SOA-95/1, Studsvik of America (1995).
- [4.4.6] D. Knott, "CASMO-4 Benchmark Against Critical Experiments," Studsvik/SOA-94/13 (proprietary), Studsvik of America (1995).

- [4.4.7] D. Knott, "CASMO-4 Benchmark Against MCNP," Studsvik/SOA-94/12 (proprietary), Studsvik of America (1995).
- [4.4.8] S.E. Turner, "Uncertainty Analysis - Burnup Distributions", presented at the DOE/SANDIA Technical Meeting on Fuel Burnup Credit, Special Session, ANS/ENS Conference, Washington, D.C., November 2, 1988.

Table 4.1.1  
Fuel Assembly Specifications

<b>Fuel Rod Data</b>			
Fuel Type	A	B	C
Fuel pellet outside diameter, in.	0.370	0.3735	0.3615
Cladding thickness, in.	0.0265	0.0250	0.0240
Cladding outside diameter, in.	0.430	0.430	0.416
Cladding inside diameter, in.	0.377	0.380	0.368
Cladding material	Zr-4		
Pellet density, g/cc	10.522		
Maximum enrichment, wt% <sup>235</sup> U	5.05		
<b>Fuel Assembly Data</b>			
Fuel rod array	15x15		
Number of fuel rods	208		
Fuel rod pitch, in.	0.568		
Number of guide tubes	16		
Guide tube outside diameter, in.	0.530		
Guide tube inside diameter, in.	0.498		
Instrument tube outside diameter, in.	0.493		
Instrument tube inside diameter, in.	0.441		
Active fuel Length, in.	145		

Table 4.2.1

## Summary of the Criticality Safety Analyses for the MZTR Pattern

Design Basis Burnup at 5.05 wt% <sup>235</sup> U	
Region 1	0 MWD/kgU
Region 2	55 MWD/kgU
Region 3	45 MWD/kgU
Uncertainties	
Bias Uncertainty (95%/95%)	± 0.0011
Calculational Statistics <sup>†</sup> (95%/95%)	± 0.0009
Depletion Uncertainty	± 0.0135
Fuel Eccentricity	Negative
Manufacturing Tolerances	± 0.0056
Temperature Correction to 4°C (39°F)	+ 0.0024
Statistical Combination of Uncertainties <sup>††</sup>	± 0.0149
Reference $k_{eff}$ (MCNP4a)	0.9312
Total Uncertainty (above)	0.0149
Axial Burnup Distribution	Negative
Calculational Bias (see Appendix B)	0.0009
<b>Maximum <math>k_{eff}</math></b>	<b>0.9470<sup>†††</sup></b>
<b>Regulatory Limiting <math>k_{eff}</math></b>	<b>0.9500</b>

<sup>†</sup> The value used for the MCNP4a (or KENO5a) statistical uncertainty is 1.84 times the estimated standard deviation. Each final k value calculated by MCNP4a (or KENO5a) is the result of averaging a minimum of 200 cycle k values, and thus, is based on a minimum sample size of 200. The K multiplier, for a one-sided statistical tolerance with 95% probability at the 95% confidence level, corresponding to a sample size of 200, is 1.84 [6].

<sup>††</sup> Square root of the sum of the squares.

<sup>†††</sup> KENO5a verification calculation resulted in a maximum  $k_{eff}$  of 0.9457.

Table 4.2.2

## Summary of the Criticality Safety Analyses for the Checkerboard Pattern

Design Basis Burnup at 5.05 wt% <sup>235</sup> U	
Region 1	0 MWD/kgU
Uncertainties	
Bias Uncertainty (95%/95%)	± 0.0011
Calculational Statistics <sup>†</sup> (95%/95%)	± 0.0011
Depletion Uncertainty	Not Applicable
Fuel Eccentricity	Negative
Manufacturing Tolerances	± 0.0056
Temperature Correction to 4°C (39°F)	+ 0.0024
Statistical Combination of Uncertainties <sup>††</sup>	± 0.0063
Reference $k_{\text{eff}}$ (MCNP4a)	0.9252
Total Uncertainty (above)	0.0063
Axial Burnup Distribution	Negative
Calculational Bias (see Appendix B)	0.0009
<b>Maximum <math>k_{\text{eff}}</math></b>	<b>0.9324<sup>†††</sup></b>
<b>Regulatory Limiting <math>k_{\text{eff}}</math></b>	<b>0.9500</b>

<sup>†</sup> The value used for the MCNP4a (or KENO5a) statistical uncertainty is 1.84 times the estimated standard deviation. Each final  $k$  value calculated by MCNP4a (or KENO5a) is the result of averaging a minimum of 200 cycle  $k$  values, and thus, is based on a minimum sample size of 200. The  $K$  multiplier, for a one-sided statistical tolerance with 95% probability at the 95% confidence level, corresponding to a sample size of 200, is 1.84 [6].

<sup>††</sup> Square root of the sum of the squares.

<sup>†††</sup> KENO5a verification calculation resulted in a maximum  $k_{\text{eff}}$  of 0.9307.

Table 4.2.3

## Summary of the Criticality Safety Analyses for the Homogeneous Loading Pattern

Design Basis Burnup at 5.05 wt% <sup>235</sup> U	
Region 3	45 MWD/kgU
Uncertainties	
Bias Uncertainty (95%/95%)	± 0.0011
Calculational Statistics <sup>†</sup> (95%/95%)	± 0.0008
Depletion Uncertainty	+ 0.0154
Fuel Eccentricity	Negative
Manufacturing Tolerances	± 0.0056
Temperature Correction to 4°C (39°F)	+ 0.0024
Statistical Combination of Uncertainties <sup>††</sup>	± 0.0166
Reference $k_{\text{eff}}$ (MCNP4a)	0.8927
Total Uncertainty (above)	0.0166
Axial Burnup Distribution	0.0256
Calculational Bias (see Appendix B)	0.0009
<b>Maximum <math>k_{\text{eff}}</math></b>	<b>0.9358<sup>†††</sup></b>
<b>Regulatory Limiting <math>k_{\text{eff}}</math></b>	<b>0.9500</b>

<sup>†</sup> The value used for the MCNP4a (or KENO5a) statistical uncertainty is 1.84 times the estimated standard deviation. Each final  $k$  value calculated by MCNP4a (or KENO5a) is the result of averaging a minimum of 200 cycle  $k$  values, and thus, is based on a minimum sample size of 200. The K multiplier, for a one-sided statistical tolerance with 95% probability at the 95% confidence level, corresponding to a sample size of 200, is 1.84 [6].

<sup>††</sup> Square root of the sum of the squares.

<sup>†††</sup> KENO5a verification calculation resulted in a maximum  $k_{\text{eff}}$  of 0.9352.

Table 4.2.4  
 Reactivity Effects of Abnormal and Accident Conditions

Abnormal/Accident Conditions	Reactivity Effect
Temperature Increase (above 4°C)	Negative (Table 4.6.1)
Void (boiling)	Negative (Table 4.6.1)
Assembly Drop (on top of rack)	Negligible
Lateral Rack Movement	Positive - controlled by less than 55 ppm soluble boron
Misplacement or Mislocation of a Fresh Fuel Assembly	Positive - controlled by less than 630 ppm soluble boron

Table 4.5.1  
Reactivity Effects of Manufacturing Tolerances

Tolerance	Reactivity Effect, $\Delta k$
Minimum Boron loading (0.0312 g/cm <sup>2</sup> , 0.0324 g/cm <sup>2</sup> nominal)	0.0025
Minimum Boron width (0.73", 7.5" nominal)	0.0008
Minimum Cell Pitch (9.14", 9.22" nominal)	0.0008
Maximum Box wall thickness (0.075" max., 0.075" nominal)	0.0003
UO <sub>2</sub> Density tolerance (10.722 g/cm <sup>3</sup> , 10.522 g/cm <sup>3</sup> nominal)	0.0038
Enrichment tolerance (0.05 wt% <sup>235</sup> U)	0.0031
Total (statistical sum)	0.0056

Table 4.6.1  
Reactivity Effects of Temperature and Void

Temperature	Reactivity Effect, $\Delta k$
4°C (39°F)	reference
20°C (68°F)	-0.0024
60°C (140°F)	-0.0094
120°C (248°F)	-0.0221
120°C w/ 10% void	-0.0450

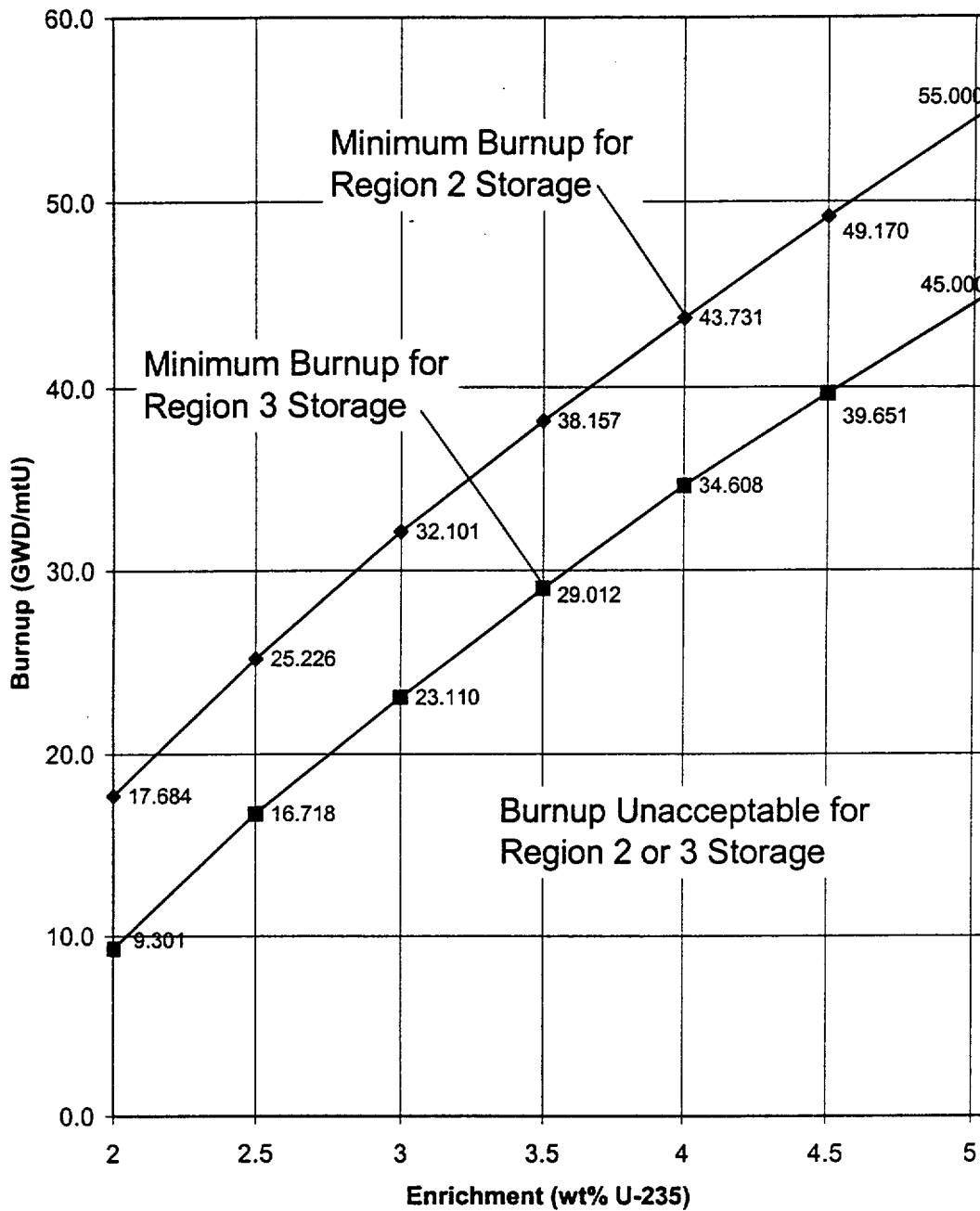
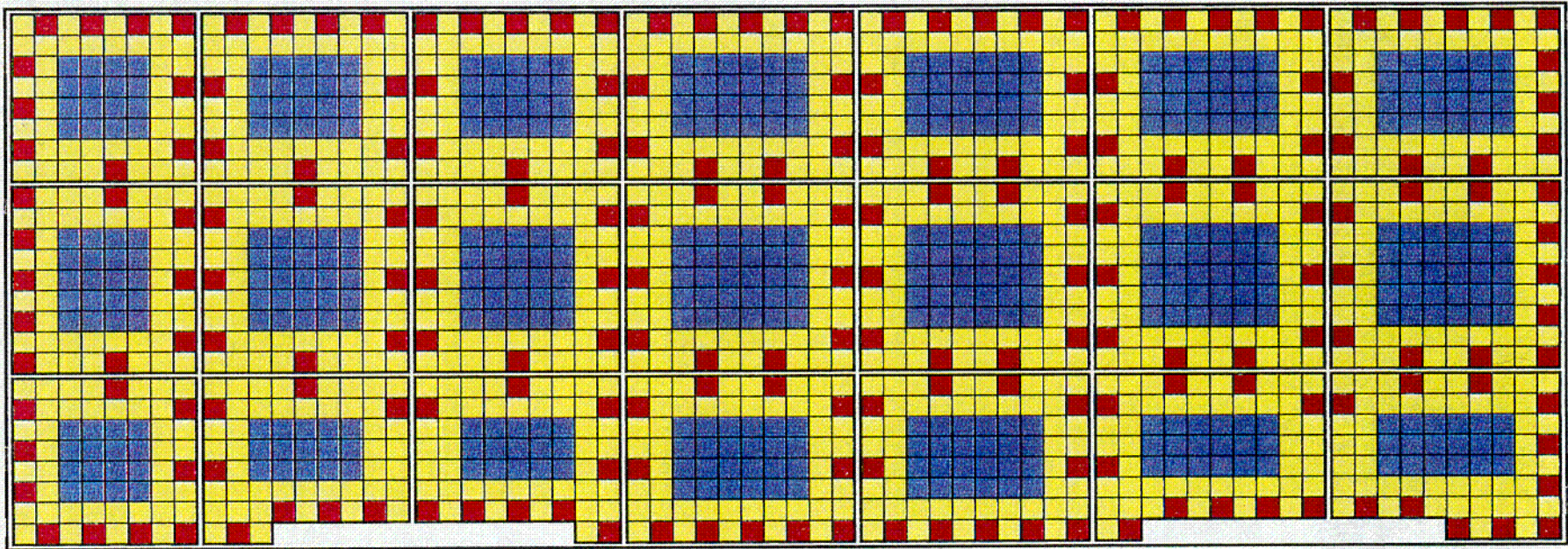


Figure 4.2.1 Minimum Required Fuel Assembly Burnup as a Function of Nominal Initial Enrichment to Permit Storage in the Spent Fuel Pool.

Fuel assemblies with enrichments less than 2.0 wt% <sup>235</sup>U will conservatively be required to meet the burnup requirements of 2.0 wt% <sup>235</sup>U assemblies.

N ←

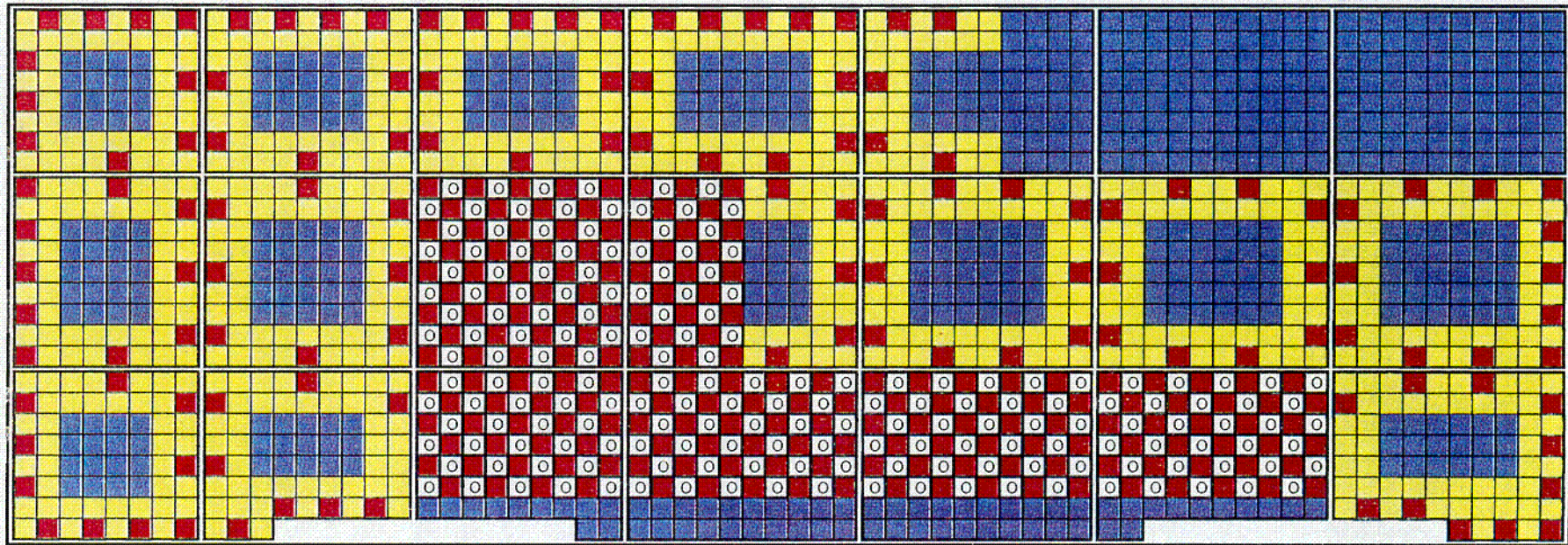


- Region 1 (Fresh or Low Burnup)- Category C in Technical Specification Figure 3.9-3.
- Region 2 (High Burnup)- Category A in Technical Specification Figure 3.9-3.
- Region 3 (Intermediate Burnup)- Category B in Technical Specification Figure 3.9-3.

Figure 4.2.2 Example of a MZTR Spent Fuel Pool Configuration for the Davis-Besse Nuclear Power Station

C-1

N ←



-  Region 1 (Fresh or Low Burnup) - Category C in Technical Specification Figure 3.9-3.
-  Region 2 (High Burnup) - Category A in Technical Specification Figure 3.9-3.
-  Region 3 (Intermediate Burnup) - Category B in Technical Specification Figure 3.9-3.
-  Empty Cells or Non-Fuel Bearing Components

Figure 4.2.3 : Example of a Spent Fuel Pool Configuration for the Davis-Besse Nuclear Power Station including MZTR, Checkerboarding and Homogeneous Loading in various combinations

L-12

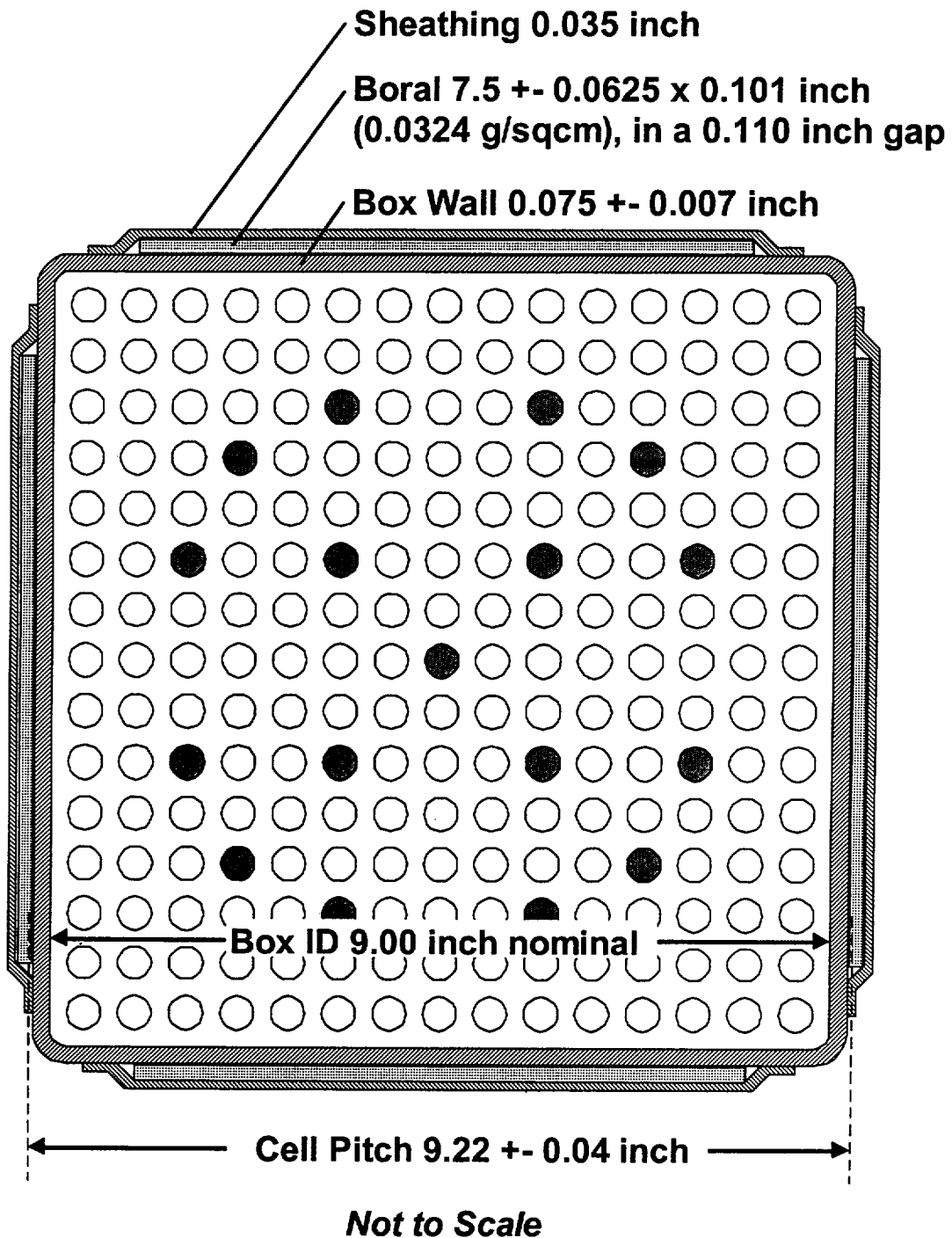


Figure 4.3.1 Schematic View of a Single Storage Cell in the Spent Fuel Racks for Davis-Besse Nuclear Power Station

## APPENDIX 4A: BENCHMARK CALCULATIONS

### 4A.1 INTRODUCTION AND SUMMARY

Benchmark calculations have been made on selected critical experiments, chosen, in so far as possible, to bound the range of variables in the rack designs. Two independent methods of analysis were used, differing in cross section libraries and in the treatment of the cross sections. MCNP4a [4A.1] is a continuous energy Monte Carlo code and KENO5a [4A.2] uses group-dependent cross sections. For the KENO5a analyses reported here, the 238-group library was chosen, processed through the NITAWL-II [4A.2] program to create a working library and to account for resonance self-shielding in uranium-238 (Nordheim integral treatment). The 238 group library was chosen to avoid or minimize the errors<sup>†</sup> (trends) that have been reported (e.g., [4A.3 through 4A.5]) for calculations with collapsed cross section sets.

In rack designs, the three most significant parameters affecting criticality are (1) the fuel enrichment, (2) the <sup>10</sup>B loading in the neutron absorber, and (3) the lattice spacing (or water-gap thickness if a flux-trap design is used). Other parameters, within the normal range of rack and fuel designs, have a smaller effect, but are also included in the analyses.

Table 4A.1 summarizes results of the benchmark calculations for all cases selected and analyzed, as referenced in the table. The effect of the major variables are discussed in subsequent sections below. It is important to note that there is obviously considerable overlap in parameters since it is not possible to vary a single parameter and maintain criticality; some other parameter or parameters must be concurrently varied to maintain criticality.

One possible way of representing the data is through a spectrum index that incorporates all of the variations in parameters. KENO5a computes and prints the "energy of the average lethargy causing fission" (EALF). In MCNP4a, by utilizing the tally option with the identical 238-group energy structure as in KENO5a, the number of fissions in each group may be collected and the EALF determined (post-processing).

---

<sup>†</sup> Small but observable trends (errors) have been reported for calculations with the 27-group and 44-group collapsed libraries. These errors are probably due to the use of a single collapsing spectrum when the spectrum should be different for the various cases analyzed, as evidenced by the spectrum indices.

Figures 4A.1 and 4A.2 show the calculated  $k_{eff}$  for the benchmark critical experiments as a function of the EALF for MCNP4a and KENO5a, respectively (UO<sub>2</sub> fuel only). The scatter in the data (even for comparatively minor variation in critical parameters) represents experimental error<sup>†</sup> in performing the critical experiments within each laboratory, as well as between the various testing laboratories. The B&W critical experiments show a larger experimental error than the PNL criticals. This would be expected since the B&W criticals encompass a greater range of critical parameters than the PNL criticals.

Linear regression analysis of the data in Figures 4A.1 and 4A.2 show that there are no trends, as evidenced by very low values of the correlation coefficient (0.13 for MCNP4a and 0.21 for KENO5a). The total bias (systematic error, or mean of the deviation from a  $k_{eff}$  of exactly 1.000) for the two methods of analysis are shown in the table below.

Calculational Bias of MCNP4a and KENO5a	
MCNP4a	0.0009±0.0011
KENO5a	0.0030±0.0012

The bias and standard error of the bias were derived directly from the calculated  $k_{eff}$  values in Table 4A.1 using the following equations<sup>††</sup>, with the standard error multiplied by the one-sided K-factor for 95% probability at the 95% confidence level from NBS Handbook 91 [4A.18] (for the number of cases analyzed, the K-factor is ~2.05 or slightly more than 2).

$$\bar{k} = \frac{1}{n} \sum_i^n k_i \quad (4A.1)$$

---

† A classical example of experimental error is the corrected enrichment in the PNL experiments, first as an addendum to the initial report and, secondly, by revised values in subsequent reports for the same fuel rods.

†† These equations may be found in any standard text on statistics, for example, reference [4A.6] (or the MCNP4a manual) and is the same methodology used in MCNP4a and in KENO5a.

$$\sigma_{\bar{k}}^2 = \frac{\sum_{i=1}^n k_i^2 - (\sum_{i=1}^n k_i)^2 / n}{n(n-1)} \quad (4A.2)$$

$$Bias = (1 - \bar{k}) \pm K \sigma_{\bar{k}} \quad (4A.3)$$

where  $k_i$  are the calculated reactivities of  $n$  critical experiments;  $\sigma_{\bar{k}}$  is the unbiased estimator of the standard deviation of the mean (also called the standard error of the bias (mean));  $K$  is the one-sided multiplier for 95% probability at the 95% confidence level (NBS Handbook 91 [4A.18]).

Formula 4.A.3 is based on the methodology of the National Bureau of Standards (now NIST) and is used to calculate the values presented on page 4.A-2. The first portion of the equation,  $(1 - \bar{k})$ , is the actual bias which is added to the MCNP4a and KENO5a results. The second term,  $K\sigma_{\bar{k}}$ , is the uncertainty or standard error associated with the bias. The  $K$  values used were obtained from the National Bureau of Standards Handbook 91 and are for one-sided statistical tolerance limits for 95% probability at the 95% confidence level. The actual  $K$  values for the 56 critical experiments evaluated with MCNP4a and the 53 critical experiments evaluated with KENO5a are 2.04 and 2.05, respectively.

The bias values are used to evaluate the maximum  $k_{eff}$  values for the rack designs. KENO5a has a slightly larger systematic error than MCNP4a, but both result in greater precision than published data [4A.3 through 4A.5] would indicate for collapsed cross section sets in KENO5a (SCALE) calculations.

#### 4A.2 Effect of Enrichment

The benchmark critical experiments include those with enrichments ranging from 2.46 w/o to 5.74 w/o and therefore span the enrichment range for rack designs. Figures 4A.3 and 4A.4 show the calculated  $k_{eff}$  values (Table 4A.1) as a function of the fuel enrichment reported for the critical experiments. Linear regression analyses for these data confirms that there are no trends, as indicated by low values of the correlation coefficients (0.03 for MCNP4a and 0.38 for KENO5a). Thus, there are no corrections to the bias for the various

enrichments.

As further confirmation of the absence of any trends with enrichment, a typical configuration was calculated with both MCNP4a and KENO5a for various enrichments. The cross-comparison of calculations with codes of comparable sophistication is suggested in Reg. Guide 3.41. Results of this comparison, shown in Table 4A.2 and Figure 4A.5, confirm no significant difference in the calculated values of  $k_{\text{eff}}$  for the two independent codes as evidenced by the 45° slope of the curve. Since it is very unlikely that two independent methods of analysis would be subject to the same error, this comparison is considered confirmation of the absence of an enrichment effect (trend) in the bias.

#### 4A.3 Effect of $^{10}\text{B}$ Loading

Several laboratories have performed critical experiments with a variety of thin absorber panels similar to the Boral panels in the rack designs. Of these critical experiments, those performed by B&W are the most representative of the rack designs. PNL has also made some measurements with absorber plates, but, with one exception (a flux-trap experiment), the reactivity worth of the absorbers in the PNL tests is very low and any significant errors that might exist in the treatment of strong thin absorbers could not be revealed.

Table 4A.3 lists the subset of experiments using thin neutron absorbers (from Table 4A.1) and shows the reactivity worth ( $\Delta k$ ) of the absorber.<sup>†</sup>

No trends with reactivity worth of the absorber are evident, although based on the calculations shown in Table 4A.3, some of the B&W critical experiments seem to have unusually large experimental errors. B&W made an effort to report some of their experimental errors. Other laboratories did not evaluate their experimental errors.

To further confirm the absence of a significant trend with  $^{10}\text{B}$  concentration in the absorber, a cross-comparison was made with MCNP4a and KENO5a (as suggested in Reg. Guide 3.41). Results are shown in Figure 4A.6 and Table 4A.4 for a typical geometry. These data substantiate the absence of any error (trend) in either of the two codes for the conditions analyzed (data points fall on a 45° line, within an expected 95% probability limit).

---

<sup>†</sup> The reactivity worth of the absorber panels was determined by repeating the calculation with the absorber analytically removed and calculating the incremental ( $\Delta k$ ) change in reactivity due to the absorber.

#### 4A.4 Miscellaneous and Minor Parameters

##### 4A.4.1 Reflector Material and Spacings

PNL has performed a number of critical experiments with thick steel and lead reflectors.<sup>†</sup> Analysis of these critical experiments are listed in Table 4A.5 (subset of data in Table 4A.1). There appears to be a small tendency toward overprediction of  $k_{\text{eff}}$  at the lower spacing, although there are an insufficient number of data points in each series to allow a quantitative determination of any trends. The tendency toward overprediction at close spacing means that the rack calculations may be slightly more conservative than otherwise.

##### 4A.4.2 Fuel Pellet Diameter and Lattice Pitch

The critical experiments selected for analysis cover a range of fuel pellet diameters from 0.311 to 0.444 inches, and lattice spacings from 0.476 to 1.00 inches. In the rack designs, the fuel pellet diameters range from 0.303 to 0.3805 inches O.D. (0.496 to 0.580 inch lattice spacing) for PWR fuel and from 0.3224 to 0.494 inches O.D. (0.488 to 0.740 inch lattice spacing) for BWR fuel. Thus, the critical experiments analyzed provide a reasonable representation of power reactor fuel. Based on the data in Table 4A.1, there does not appear to be any observable trend with either fuel pellet diameter or lattice pitch, at least over the range of the critical experiments applicable to rack designs.

##### 4A.4.3 Soluble Boron Concentration Effects

Various soluble boron concentrations were used in the B&W series of critical experiments and in one PNL experiment, with boron concentrations ranging up to 2550 ppm. Results of MCNP4a (and one KENO5a) calculations are shown in Table 4A.6. Analyses of the very high boron concentration experiments (> 1300 ppm) show a tendency to slightly overpredict reactivity for the three experiments exceeding 1300 ppm. In turn, this would suggest that the evaluation of the racks with higher soluble boron concentrations could be slightly conservative.

---

<sup>†</sup> Parallel experiments with a depleted uranium reflector were also performed but not included in the present analysis since they are not pertinent to the Holtec rack design.

#### 4A.5 MOX Fuel

The number of critical experiments with  $\text{PuO}_2$  bearing fuel (MOX) is more limited than for  $\text{UO}_2$  fuel. However, a number of MOX critical experiments have been analyzed and the results are shown in Table 4A.7. Results of these analyses are generally above a  $k_{\text{eff}}$  of 1.00, indicating that when Pu is present, both MCNP4a and KENO5a overpredict the reactivity. This may indicate that calculation for MOX fuel will be expected to be conservative, especially with MCNP4a. It may be noted that for the larger lattice spacings, the KENO5a calculated reactivities are below 1.00, suggesting that a small trend may exist with KENO5a. It is also possible that the overprediction in  $k_{\text{eff}}$  for both codes may be due to a small inadequacy in the determination of the Pu-241 decay and Am-241 growth. This possibility is supported by the consistency in calculated  $k_{\text{eff}}$  over a wide range of the spectral index (energy of the average lethargy causing fission).

References

- [4A.1] J.F. Briesmeister, Ed., "MCNP4a - A General Monte Carlo N-Particle Transport Code, Version 4A; Los Alamos National Laboratory, LA-12625-M (1993).
- [4A.2] SCALE 4.3, "A Modular Code System for Performing Standardized Computer Analyses for Licensing Evaluation", NUREG-0200 (ORNL-NUREG-CSD-2/U2/R5, Revision 5, Oak Ridge National Laboratory, September 1995.
- [4A.3] M.D. DeHart and S.M. Bowman, "Validation of the SCALE Broad Structure 44-G Group ENDF/B-Y Cross-Section Library for Use in Criticality Safety Analyses", NUREG/CR-6102 (ORNL/TM-12460) Oak Ridge National Laboratory, September 1994.
- [4A.4] W.C. Jordan et al., "Validation of KENO.V.a", CSD/TM-238, Martin Marietta Energy Systems, Inc., Oak Ridge National Laboratory, December 1986.
- [4A.5] O.W. Hermann et al., "Validation of the Scale System for PWR Spent Fuel Isotopic Composition Analysis", ORNL-TM-12667, Oak Ridge National Laboratory, undated.
- [4A.6] R.J. Larsen and M.L. Marx, An Introduction to Mathematical Statistics and its Applications, Prentice-Hall, 1986.
- [4A.7] M.N. Baldwin et al., Critical Experiments Supporting Close Proximity Water Storage of Power Reactor Fuel, BAW-1484-7, Babcock and Wilcox Company, July 1979.
- [4A.8] G.S. Hoovier et al., Critical Experiments Supporting Underwater Storage of Tightly Packed Configurations of Spent Fuel Pins, BAW-1645-4, Babcock & Wilcox Company, November 1991.
- [4A.9] L.W. Newman et al., Urania Gadolinia: Nuclear Model Development and Critical Experiment Benchmark, BAW-1810, Babcock and Wilcox Company, April 1984.

- [4A.10] J.C. Manaranche et al., "Dissolution and Storage Experimental Program with 4.75 w/o Enriched Uranium-Oxide Rods," Trans. Am. Nucl. Soc. 33: 362-364 (1979).
- [4A.11] S.R. Bierman and E.D. Clayton, Criticality Experiments with Subcritical Clusters of 2.35 w/o and 4.31 w/o <sup>235</sup>U Enriched UO<sub>2</sub> Rods in Water with Steel Reflecting Walls, PNL-3602, Battelle Pacific Northwest Laboratory, April 1981.
- [4A.12] S.R. Bierman et al., Criticality Experiments with Subcritical Clusters of 2.35 w/o and 4.31 w/o <sup>235</sup>U Enriched UO<sub>2</sub> Rods in Water with Uranium or Lead Reflecting Walls, PNL-3926, Battelle Pacific Northwest Laboratory, December, 1981.
- [4A.13] S.R. Bierman et al., Critical Separation Between Subcritical Clusters of 4.31 w/o <sup>235</sup>U Enriched UO<sub>2</sub> Rods in Water with Fixed Neutron Poisons, PNL-2615, Battelle Pacific Northwest Laboratory, October 1977.
- [4A.14] S.R. Bierman, Criticality Experiments with Neutron Flux Traps Containing Voids, PNL-7167, Battelle Pacific Northwest Laboratory, April 1990.
- [4A.15] B.M. Durst et al., Critical Experiments with 4.31 wt % <sup>235</sup>U Enriched UO<sub>2</sub> Rods in Highly Borated Water Lattices, PNL-4267, Battelle Pacific Northwest Laboratory, August 1982.
- [4A.16] S.R. Bierman, Criticality Experiments with Fast Test Reactor Fuel Pins in Organic Moderator, PNL-5803, Battelle Pacific Northwest Laboratory, December 1981.
- [4A.17] E.G. Taylor et al., Saxton Plutonium Program Critical Experiments for the Saxton Partial Plutonium Core, WCAP-3385-54, Westinghouse Electric Corp., Atomic Power Division, December 1965.
- [4A.18] M.G. Natrella, Experimental Statistics, National Bureau of Standards, Handbook 91, August 1963.

**Table 4A.1**  
**Summary of Criticality Benchmark Calculations**

Reference	Identification	Enrich.	Calculated $k_{eff}$		EALF <sup>†</sup> (eV)		
			MCNP4a	KENO5a	MCNP4a	KENO5a	
1	B&W-1484 (4A.7)	Core I	2.46	0.9964 ± 0.0010	0.9898 ± 0.0006	0.1759	0.1753
2	B&W-1484 (4A.7)	Core II	2.46	1.0008 ± 0.0011	1.0015 ± 0.0005	0.2553	0.2446
3	B&W-1484 (4A.7)	Core III	2.46	1.0010 ± 0.0012	1.0005 ± 0.0005	0.1999	0.1939
4	B&W-1484 (4A.7)	Core IX	2.46	0.9956 ± 0.0012	0.9901 ± 0.0006	0.1422	0.1426
5	B&W-1484 (4A.7)	Core X	2.46	0.9980 ± 0.0014	0.9922 ± 0.0006	0.1513	0.1499
6	B&W-1484 (4A.7)	Core XI	2.46	0.9978 ± 0.0012	1.0005 ± 0.0005	0.2031	0.1947
7	B&W-1484 (4A.7)	Core XII	2.46	0.9988 ± 0.0011	0.9978 ± 0.0006	0.1718	0.1662
8	B&W-1484 (4A.7)	Core XIII	2.46	1.0020 ± 0.0010	0.9952 ± 0.0006	0.1988	0.1965
9	B&W-1484 (4A.7)	Core XIV	2.46	0.9953 ± 0.0011	0.9928 ± 0.0006	0.2022	0.1986
10	B&W-1484 (4A.7)	Core XV **	2.46	0.9910 ± 0.0011	0.9909 ± 0.0006	0.2092	0.2014
11	B&W-1484 (4A.7)	Core XVI **	2.46	0.9935 ± 0.0010	0.9889 ± 0.0006	0.1757	0.1713
12	B&W-1484 (4A.7)	Core XVII	2.46	0.9962 ± 0.0012	0.9942 ± 0.0005	0.2083	0.2021
13	B&W-1484 (4A.7)	Core XVIII	2.46	1.0036 ± 0.0012	0.9931 ± 0.0006	0.1705	0.1708

**Table 4A.1**  
**Summary of Criticality Benchmark Calculations**

Reference	Identification	Enrich.	Calculated $k_{eff}$		EALF <sup>†</sup> (eV)		
			MCNP4a	KENO5a	MCNP4a	KENO5a	
14	B&W-1484 (4A.7)	Core XIX	2.46	0.9961 ± 0.0012	0.9971 ± 0.0005	0.2103	0.2011
15	B&W-1484 (4A.7)	Core XX	2.46	1.0008 ± 0.0011	0.9932 ± 0.0006	0.1724	0.1701
16	B&W-1484 (4A.7)	Core XXI	2.46	0.9994 ± 0.0010	0.9918 ± 0.0006	0.1544	0.1536
17	B&W-1645 (4A.8)	S-type Fuel, w/886 ppm B	2.46	0.9970 ± 0.0010	0.9924 ± 0.0006	1.4475	1.4680
18	B&W-1645 (4A.8)	S-type Fuel, w/746 ppm B	2.46	0.9990 ± 0.0010	0.9913 ± 0.0006	1.5463	1.5660
19	B&W-1645 (4A.8)	SO-type Fuel, w/1156 ppm B	2.46	0.9972 ± 0.0009	0.9949 ± 0.0005	0.4241	0.4331
20	B&W-1810 (4A.9)	Case 1 1337 ppm B	2.46	1.0023 ± 0.0010	NC	0.1531	NC
21	B&W-1810 (4A.9)	Case 12 1899 ppm B	2.46/4.02	1.0060 ± 0.0009	NC	0.4493	NC
22	French (4A.10)	Water Moderator 0 gap	4.75	0.9966 ± 0.0013	NC	0.2172	NC
23	French (4A.10)	Water Moderator 2.5 cm gap	4.75	0.9952 ± 0.0012	NC	0.1778	NC
24	French (4A.10)	Water Moderator 5 cm gap	4.75	0.9943 ± 0.0010	NC	0.1677	NC
25	French (4A.10)	Water Moderator 10 cm gap	4.75	0.9979 ± 0.0010	NC	0.1736	NC
26	PNL-3602 (4A.11)	Steel Reflector, 0 separation	2.35	NC	1.0004 ± 0.0006	NC	0.1018

**Table 4A.1**  
**Summary of Criticality Benchmark Calculations**

Reference	Identification	Enrich.	Calculated $k_{eff}$		EALF <sup>†</sup> (eV)		
			MCNP4a	KENO5a	MCNP4a	KENO5a	
27	PNL-3602 (4A.11)	Steel Reflector, 1.321 cm sepn.	2.35	0.9980 ± 0.0009	0.9992 ± 0.0006	0.1000	0.0909
28	PNL-3602 (4A.11)	Steel Reflector, 2.616 cm sepn	2.35	0.9968 ± 0.0009	0.9964 ± 0.0006	0.0981	0.0975
29	PNL-3602 (4A.11)	Steel Reflector, 3.912 cm sepn.	2.35	0.9974 ± 0.0010	0.9980 ± 0.0006	0.0976	0.0970
30	PNL-3602 (4A.11)	Steel Reflector, infinite sepn.	2.35	0.9962 ± 0.0008	0.9939 ± 0.0006	0.0973	0.0968
31	PNL-3602 (4A.11)	Steel Reflector, 0 cm sepn.	4.306	NC	1.0003 ± 0.0007	NC	0.3282
32	PNL-3602 (4A.11)	Steel Reflector, 1.321 cm sepn.	4.306	0.9997 ± 0.0010	1.0012 ± 0.0007	0.3016	0.3039
33	PNL-3602 (4A.11)	Steel Reflector, 2.616 cm sepn.	4.306	0.9994 ± 0.0012	0.9974 ± 0.0007	0.2911	0.2927
34	PNL-3602 (4A.11)	Steel Reflector, 5.405 cm sepn.	4.306	0.9969 ± 0.0011	0.9951 ± 0.0007	0.2828	0.2860
35	PNL-3602 (4A.11)	Steel Reflector, Infinite sepn. <sup>††</sup>	4.306	0.9910 ± 0.0020	0.9947 ± 0.0007	0.2851	0.2864
36	PNL-3602 (4A.11)	Steel Reflector, with Boral Sheets	4.306	0.9941 ± 0.0011	0.9970 ± 0.0007	0.3135	0.3150
37	PNL-3926 (4A.12)	Lead Reflector, 0 cm sepn.	4.306	NC	1.0003 ± 0.0007	NC	0.3159
38	PNL-3926 (4A.12)	Lead Reflector, 0.55 cm sepn.	4.306	1.0025 ± 0.0011	0.9997 ± 0.0007	0.3030	0.3044
39	PNL-3926 (4A.12)	Lead Reflector, 1.956 cm sepn.	4.306	1.0000 ± 0.0012	0.9985 ± 0.0007	0.2883	0.2930

**Table 4A.1**  
**Summary of Criticality Benchmark Calculations**

Reference	Identification	Enrich.	Calculated $k_{eff}$		EALF <sup>†</sup> (eV)		
			MCNP4a	KENO5a	MCNP4a	KENO5a	
40	PNL-3926 (4A.12)	Lead Reflector, 5.405 cm sepn.	4.306	0.9971 ± 0.0012	0.9946 ± 0.0007	0.2831	0.2854
41	PNL-2615 (4A.13)	Experiment 004/032 - no absorber	4.306	0.9925 ± 0.0012	0.9950 ± 0.0007	0.1155	0.1159
42	PNL-2615 (4A.13)	Experiment 030 - Zr plates	4.306	NC	0.9971 ± 0.0007	NC	0.1154
43	PNL-2615 (4A.13)	Experiment 013 - Steel plates	4.306	NC	0.9965 ± 0.0007	NC	0.1164
44	PNL-2615 (4A.13)	Experiment 014 - Steel plates	4.306	NC	0.9972 ± 0.0007	NC	0.1164
45	PNL-2615 (4A.13)	Exp. 009 1.05% Boron-Steel plates	4.306	0.9982 ± 0.0010	0.9981 ± 0.0007	0.1172	0.1162
46	PNL-2615 (4A.13)	Exp. 012 1.62% Boron-Steel plates	4.306	0.9996 ± 0.0012	0.9982 ± 0.0007	0.1161	0.1173
47	PNL-2615 (4A.13)	Exp. 031 - Boral plates	4.306	0.9994 ± 0.0012	0.9969 ± 0.0007	0.1165	0.1171
48	PNL-7167 (4A.14)	Experiment 214R - with flux trap	4.306	0.9991 ± 0.0011	0.9956 ± 0.0007	0.3722	0.3812
49	PNL-7167 (4A.14)	Experiment 214V3 - with flux trap	4.306	0.9969 ± 0.0011	0.9963 ± 0.0007	0.3742	0.3826
50	PNL-4267 (4A.15)	Case 173 - 0 ppm B	4.306	0.9974 ± 0.0012	NC	0.2893	NC
51	PNL-4267 (4A.15)	Case 177 - 2550 ppm B	4.306	1.0057 ± 0.0010	NC	0.5509	NC
52	PNL-5803 (4A.16)	MOX Fuel - Type 3.2 Exp. 21	20% Pu	1.0041 ± 0.0011	1.0046 ± 0.0006	0.9171	0.8868

**Table 4A.1**  
**Summary of Criticality Benchmark Calculations**

Reference	Identification	Enrich.	Calculated $k_{eff}$		EALF <sup>†</sup> (eV)		
			MCNP4a	KENO5a	MCNP4a	KENO5a	
53	PNL-5803 (4A.16)	MOX Fuel - Type 3.2 Exp. 43	20% Pu	1.0058 ± 0.0012	1.0036 ± 0.0006	0.2968	0.2944
54	PNL-5803 (4A.16)	MOX Fuel - Type 3.2 Exp. 13	20% Pu	1.0083 ± 0.0011	0.9989 ± 0.0006	0.1665	0.1706
55	PNL-5803 (4A.16)	MOX Fuel - Type 3.2 Exp. 32	20% Pu	1.0079 ± 0.0011	0.9966 ± 0.0006	0.1139	0.1165
56	WCAP-3385 (4A.17)	Saxton Case 52 PuO <sub>2</sub> 0.52" pitch	6.6% Pu	0.9996 ± 0.0011	1.0005 ± 0.0006	0.8665	0.8417
57	WCAP-3385 (4A.17)	Saxton Case 52 U 0.52" pitch	5.74	1.0000 ± 0.0010	0.9956 ± 0.0007	0.4476	0.4580
58	WCAP-3385 (4A.17)	Saxton Case 56 PuO <sub>2</sub> 0.56" pitch	6.6% Pu	1.0036 ± 0.0011	1.0047 ± 0.0006	0.5289	0.5197
59	WCAP-3385 (4A.17)	Saxton Case 56 borated PuO <sub>2</sub>	6.6% Pu	1.0008 ± 0.0010	NC	0.6389	NC
60	WCAP-3385 (4A.17)	Saxton Case 56 U 0.56" pitch	5.74	0.9994 ± 0.0011	0.9967 ± 0.0007	0.2923	0.2954
61	WCAP-3385 (4A.17)	Saxton Case 79 PuO <sub>2</sub> 0.79" pitch	6.6% Pu	1.0063 ± 0.0011	1.0133 ± 0.0006	0.1520	0.1555
62	WCAP-3385 (4A.17)	Saxton Case 79 U 0.79" pitch	5.74	1.0039 ± 0.0011	1.0008 ± 0.0006	0.1036	0.1047

Notes: NC stands for not calculated.

<sup>†</sup> EALF is the energy of the average lethargy causing fission.

<sup>††</sup> These experimental results appear to be statistical outliers ( $> 3\sigma$ ) suggesting the possibility of unusually large experimental error. Although they could justifiably be excluded, for conservatism, they were retained in determining the calculational basis.

Table 4A.2

COMPARISON OF MCNP4a AND KENO5a CALCULATED REACTIVITIES<sup>†</sup>  
FOR VARIOUS ENRICHMENTS

Enrichment	Calculated $k_{\text{eff}} \pm 1\sigma$	
	MCNP4a	KENO5a
3.0	0.8465 $\pm$ 0.0011	0.8478 $\pm$ 0.0004
3.5	0.8820 $\pm$ 0.0011	0.8841 $\pm$ 0.0004
3.75	0.9019 $\pm$ 0.0011	0.8987 $\pm$ 0.0004
4.0	0.9132 $\pm$ 0.0010	0.9140 $\pm$ 0.0004
4.2	0.9276 $\pm$ 0.0011	0.9237 $\pm$ 0.0004
4.5	0.9400 $\pm$ 0.0011	0.9388 $\pm$ 0.0004

---

<sup>†</sup> Based on the GE 8x8R fuel assembly.

Table 4A.3

**MCNP4a CALCULATED REACTIVITIES FOR  
CRITICAL EXPERIMENTS WITH NEUTRON ABSORBERS**

Ref.	Experiment		$\Delta k$ Worth of Absorber	MCNP4a Calculated $k_{eff}$	EALF <sup>†</sup> (eV)
4A.13	PNL-2615	Boral Sheet	0.0139	0.9994 ± 0.0012	0.1165
4A.7	B&W-1484	Core XX	0.0165	1.0008 ± 0.0011	0.1724
4A.13	PNL-2615	1.62% Boron-steel	0.0165	0.9996 ± 0.0012	0.1161
4A.7	B&W-1484	Core XIX	0.0202	0.9961 ± 0.0012	0.2103
4A.7	B&W-1484	Core XXI	0.0243	0.9994 ± 0.0010	0.1544
4A.7	B&W-1484	Core XVII	0.0519	0.9962 ± 0.0012	0.2083
4A.11	PNL-3602	Boral Sheet	0.0708	0.9941 ± 0.0011	0.3135
4A.7	B&W-1484	Core XV	0.0786	0.9910 ± 0.0011	0.2092
4A.7	B&W-1484	Core XVI	0.0845	0.9935 ± 0.0010	0.1757
4A.7	B&W-1484	Core XIV	0.1575	0.9953 ± 0.0011	0.2022
4A.7	B&W-1484	Core XIII	0.1738	1.0020 ± 0.0011	0.1988
4A.14	PNL-7167	Expt 214R flux trap	0.1931	0.9991 ± 0.0011	0.3722

<sup>†</sup>EALF is the energy of the average lethargy causing fission.

Table 4A.4

COMPARISON OF MCNP4a AND KENO5a  
CALCULATED REACTIVITIES<sup>†</sup> FOR VARIOUS <sup>10</sup>B LOADINGS

<sup>10</sup> B, g/cm <sup>2</sup>	Calculated $k_{\text{eff}} \pm 1\sigma$	
	MCNP4a	KENO5a
0.005	1.0381 ± 0.0012	1.0340 ± 0.0004
0.010	0.9960 ± 0.0010	0.9941 ± 0.0004
0.015	0.9727 ± 0.0009	0.9713 ± 0.0004
0.020	0.9541 ± 0.0012	0.9560 ± 0.0004
0.025	0.9433 ± 0.0011	0.9428 ± 0.0004
0.03	0.9325 ± 0.0011	0.9338 ± 0.0004
0.035	0.9234 ± 0.0011	0.9251 ± 0.0004
0.04	0.9173 ± 0.0011	0.9179 ± 0.0004

<sup>†</sup> Based on a 4.5% enriched GE 8x8R fuel assembly.

Table 4A.5

CALCULATIONS FOR CRITICAL EXPERIMENTS WITH  
THICK LEAD AND STEEL REFLECTORS<sup>†</sup>

Ref.	Case	E, wt%	Separation, cm	MCNP4a $k_{eff}$	KENO5a $k_{eff}$
4A.11	Steel Reflector	2.35	1.321	$0.9980 \pm 0.0009$	$0.9992 \pm 0.0006$
		2.35	2.616	$0.9968 \pm 0.0009$	$0.9964 \pm 0.0006$
		2.35	3.912	$0.9974 \pm 0.0010$	$0.9980 \pm 0.0006$
		2.35	$\infty$	$0.9962 \pm 0.0008$	$0.9939 \pm 0.0006$
4A.11	Steel Reflector	4.306	1.321	$0.9997 \pm 0.0010$	$1.0012 \pm 0.0007$
		4.306	2.616	$0.9994 \pm 0.0012$	$0.9974 \pm 0.0007$
		4.306	3.405	$0.9969 \pm 0.0011$	$0.9951 \pm 0.0007$
		4.306	$\infty$	$0.9910 \pm 0.0020$	$0.9947 \pm 0.0007$
4A.12	Lead Reflector	4.306	0.55	$1.0025 \pm 0.0011$	$0.9997 \pm 0.0007$
		4.306	1.956	$1.0000 \pm 0.0012$	$0.9985 \pm 0.0007$
		4.306	5.405	$0.9971 \pm 0.0012$	$0.9946 \pm 0.0007$

<sup>†</sup> Arranged in order of increasing reflector-fuel spacing.

Table 4A.6

CALCULATIONS FOR CRITICAL EXPERIMENTS WITH VARIOUS SOLUBLE BORON CONCENTRATIONS

Reference	Experiment	Boron Concentration, ppm	Calculated $k_{eff}$	
			MCNP4a	KENO5a
4A.15	PNL-4267	0	$0.9974 \pm 0.0012$	-
4A.8	B&W-1645	886	$0.9970 \pm 0.0010$	$0.9924 \pm 0.0006$
4A.9	B&W-1810	1337	$1.0023 \pm 0.0010$	-
4A.9	B&W-1810	1899	$1.0060 \pm 0.0009$	-
4A.15	PNL-4267	2550	$1.0057 \pm 0.0010$	-

Table 4A.7

## CALCULATIONS FOR CRITICAL EXPERIMENTS WITH MOX FUEL

Reference	Case <sup>†</sup>	MCNP4a		KENO5a	
		$k_{\text{eff}}$	EALF <sup>††</sup>	$k_{\text{eff}}$	EALF <sup>11</sup>
PNL-5803 [4A.16]	MOX Fuel - Exp. No. 21	1.0041±0.0011	0.9171	1.0046±0.0006	0.8868
	MOX Fuel - Exp. No. 43	1.0058±0.0012	0.2968	1.0036±0.0006	0.2944
	MOX Fuel - Exp. No. 13	1.0083±0.0011	0.1665	0.9989±0.0006	0.1706
	MOX Fuel - Exp. No. 32	1.0079±0.0011	0.1139	0.9966±0.0006	0.1165
WCAP-3385-54 [4A.17]	Saxton @ 0.52" pitch	0.9996±0.0011	0.8665	1.0005±0.0006	0.8417
	Saxton @ 0.56" pitch	1.0036±0.0011	0.5289	1.0047±0.0006	0.5197
	Saxton @ 0.56" pitch borated	1.0008±0.0010	0.6389	NC	NC
	Saxton @ 0.79" pitch	1.0063±0.0011	0.1520	1.0133±0.0006	0.1555

Note: NC stands for not calculated

<sup>†</sup> Arranged in order of increasing lattice spacing.

<sup>††</sup> EALF is the energy of the average lethargy causing fission.

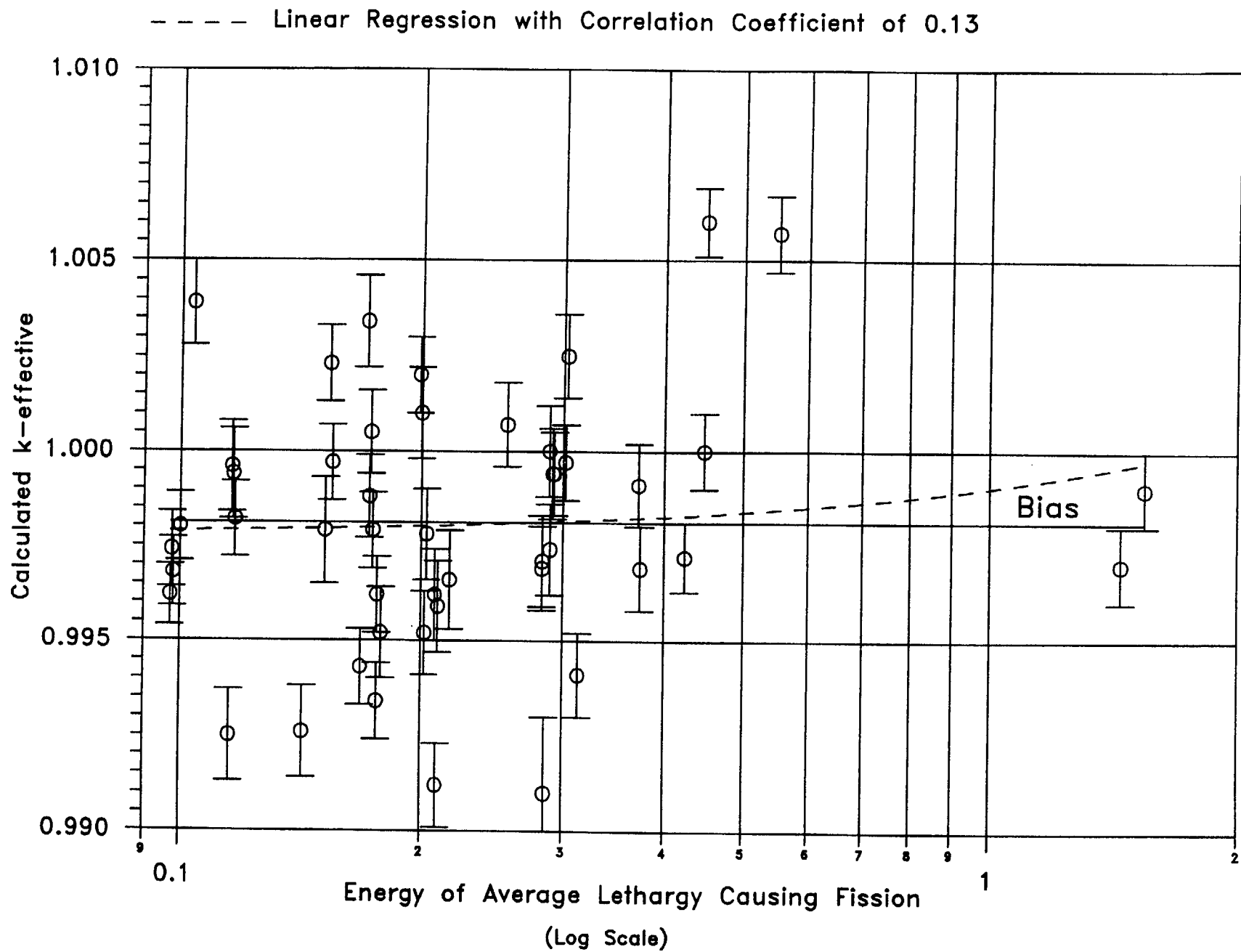
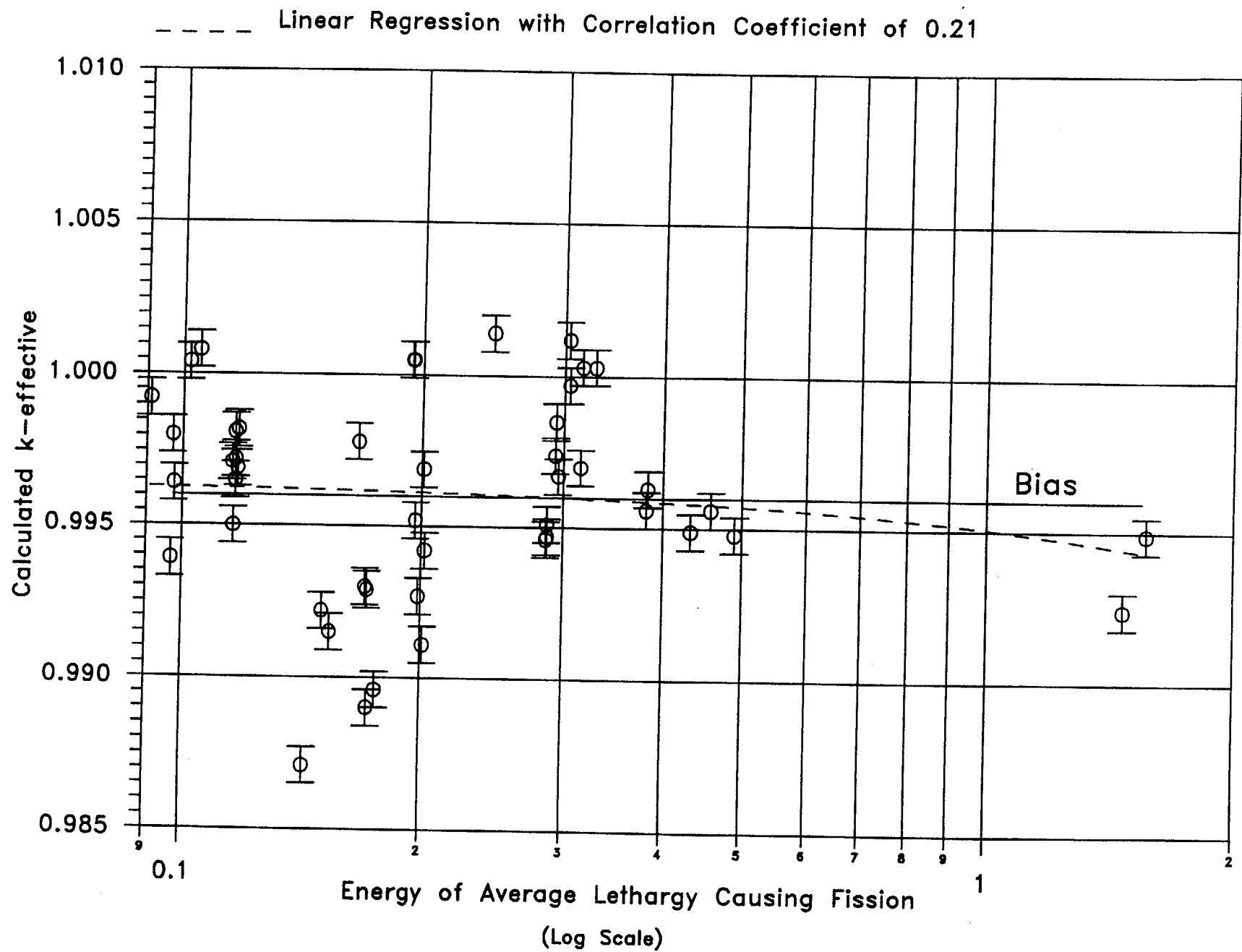


FIGURE 4A.1 MCNP CALCULATED  $k$ -eff VALUES for VARIOUS VALUES OF THE SPECTRAL INDEX



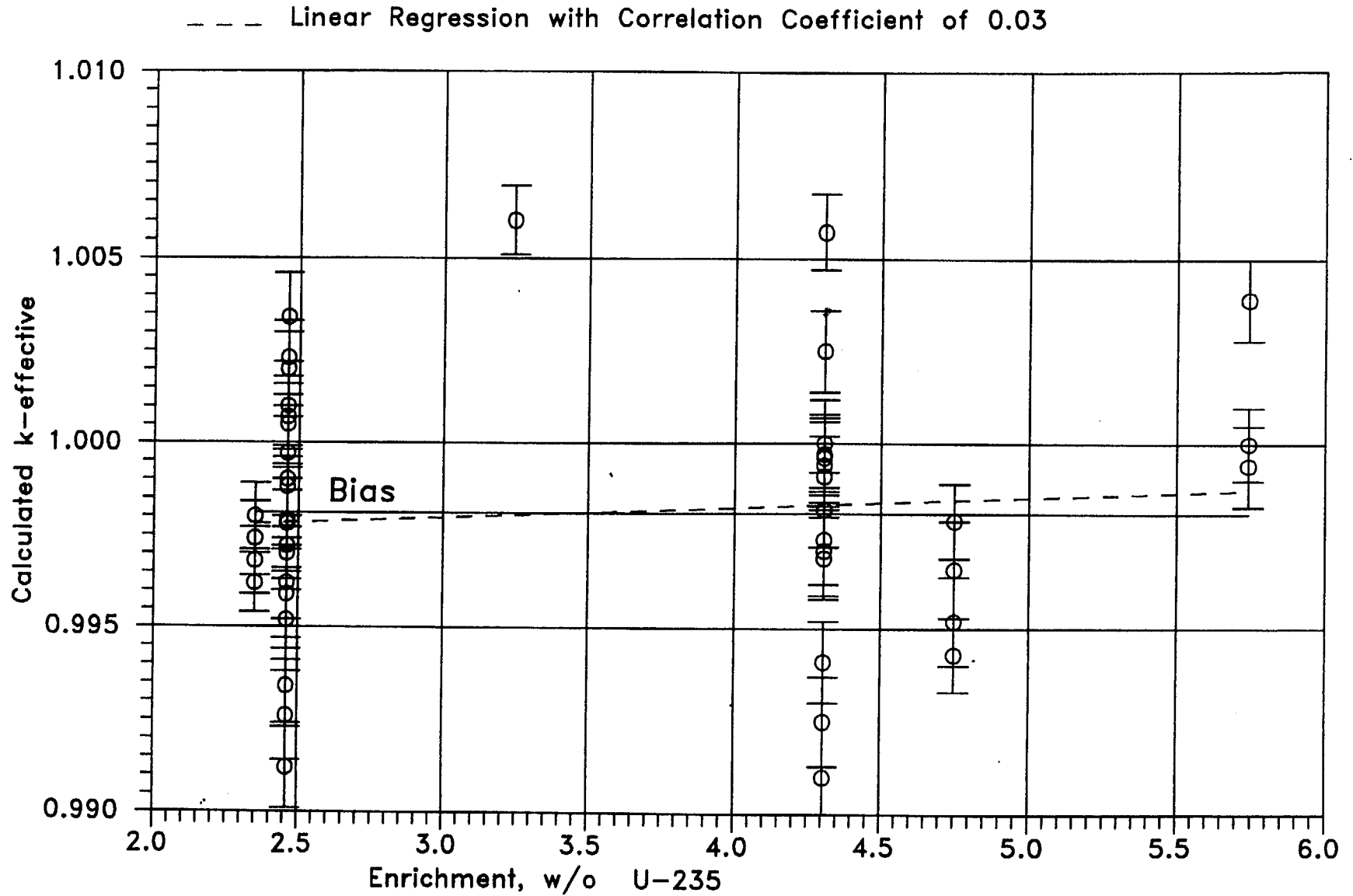


FIGURE 4A.3 MCNP CALCULATED  $k$ -eff VALUES AT VARIOUS U-235 ENRICHMENTS

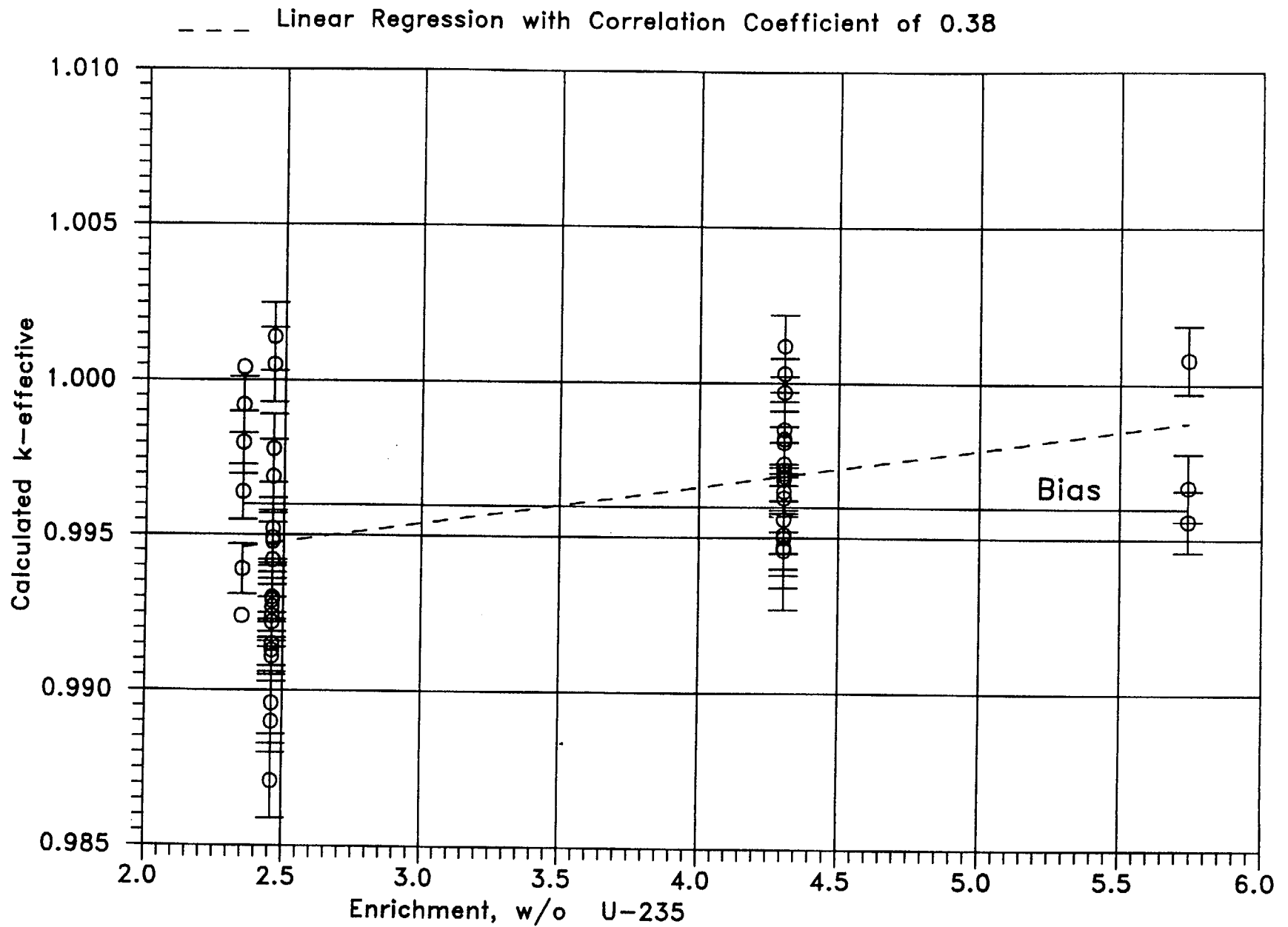


FIGURE 4A.4 KENO CALCULATED k-eff VALUES  
AT VARIOUS U-235 ENRICHMENTS

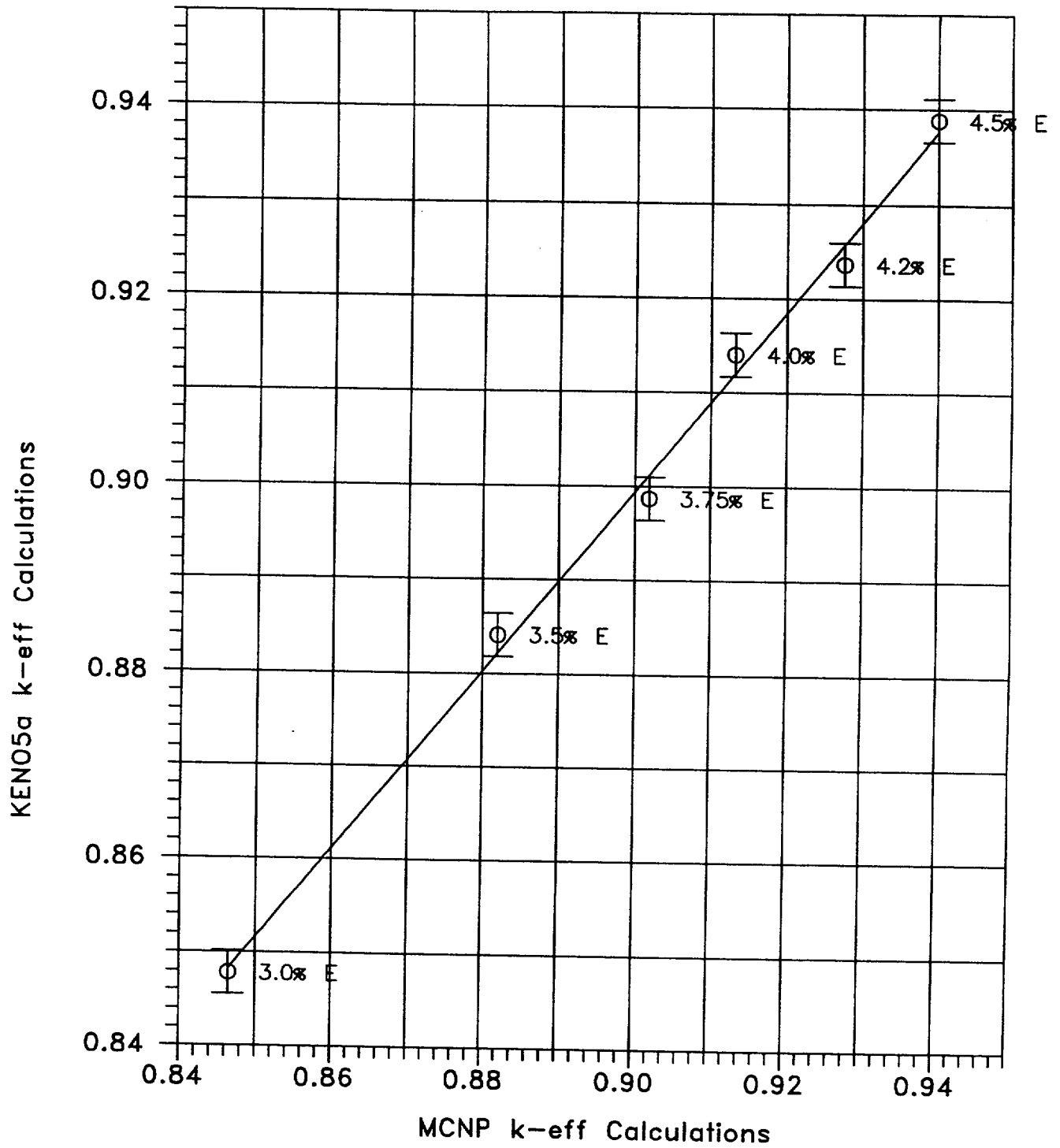


FIGURE 4A.5 COMPARISON OF MCNP AND KENO5A CALCULATIONS FOR VARIOUS FUEL ENRICHMENTS

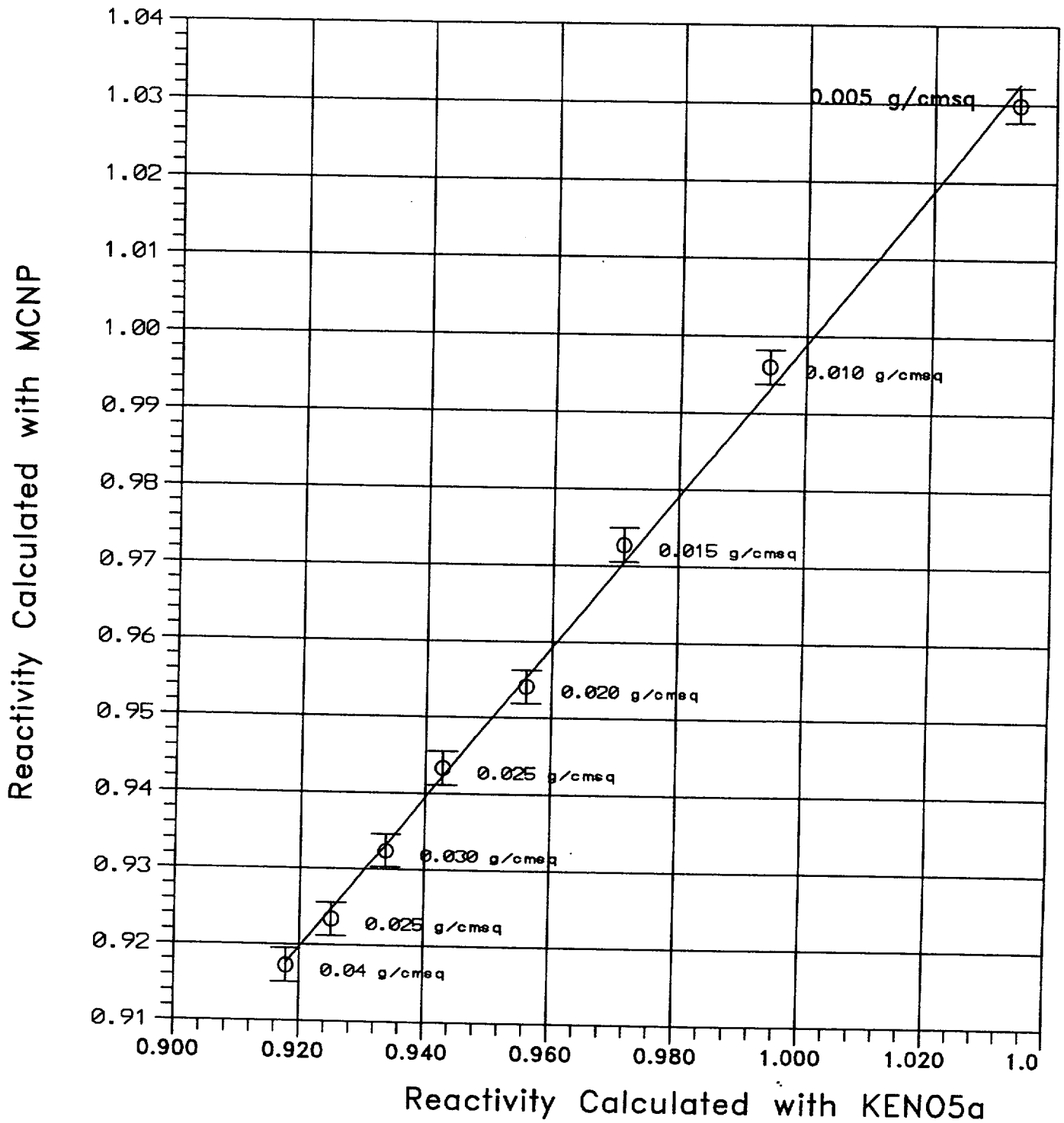


FIGURE 4A.6 COMPARISON OF MCNP AND KENO5a CALCULATIONS FOR VARIOUS BORON-10 AREAL DENSITIES

## 5.0 THERMAL-HYDRAULIC CONSIDERATIONS

### 5.1 Introduction

This chapter provides a summary of the methods, models, analyses, and numerical results of the thermal hydraulic evaluations performed to justify installation of high density fuel storage racks in the Davis-Besse Nuclear Power Station (DBNPS) Unit 1 Spent Fuel Pool (SFP). These evaluations demonstrate compliance to the provisions of Section III of the USNRC "OT Position Paper for Review and Acceptance of Spent Fuel Storage and Handling Applications," dated April 14, 1978. Evaluations were performed for the Spent Fuel Pool Cooling System (SFPCS), Decay Heat Removal System (DHRS), SFP, and Transfer Pit.

The Transfer Pit is a normally flooded pit which is separated from the SFP by a 3 feet thick wall. A 3 feet wide slot in the wall connects the Transfer Pit to the SFP. There is a gate which can be installed in the slot to allow draining the Pit with out lowering the level in the SFP. If required for underwater diver safety during the re-racking process, a single rack will be placed in the Transfer Pit for temporary fuel storage.

As part of the decision making process to re-rack the Spent Fuel Pool (SFP) a thermal-hydraulic analysis was completed for the SFP, which assumed the SFP was completely re-racked with high density racks. The results of this analysis were used as a conservative starting point for thermal-hydraulic analysis which justified the use of the Cask Pit for fuel storage - LAR 98-0007, NRC approval 2/29/00 (docket 50-346). Therefore, the heat loads resulting from re-racking the SFP will not affect the results of the Cask Pit thermal-hydraulic analysis. The following SFP thermal-hydraulic information is the same as was submitted in LAR 98-0007 with the following exceptions, a) the Cask Pit information has been removed, b) section 5.10 has been added to address the temporary placement of fuel in the Transfer Pit, c) clarifying words have been added to address NRC comments on LAR 98-007, and d) the maximum heat generation rate for a single fuel assembly in the SFP or Transfer Pit has been specified.

The DBNPS is requesting approval to; 1) replace all existing spent fuel storage racks in the DBNPS SFP, 2) allow temporary storage of fuel in the Transfer Pit during the reracking, and 3) relocate the Cask Pit and Transfer Pit racks to the SFP. This re-racking will increase the total fuel storage capacity of the SFP to 1624 fuel assemblies, from the currently licensed capacity of 1024 (735 in SFP and 289 in Cask Pit). The increased spent fuel storage capacity would be accompanied by an increase in the decay heat load. The ability of the existing DBNPS cooling systems to safely remove the additional decay heat from the SFP must be demonstrated.

The thermal hydraulic qualification analyses for the SFP and Transfer Pit were performed to show that fuel stored in these areas will be adequately cooled and the temperature of the structures will be appropriately limited. The analyses can be further described as follows:

- i. An evaluation of the maximum SFP bulk temperature for the predicted DBNPS fuel discharge schedule was performed. This analysis was performed to establish that maximum bulk coolant temperature limits and SFP structural temperature limits would not be exceeded.
- ii. An evaluation of loss-of-forced cooling scenarios in the SFP was completed to establish the minimum time to perform corrective actions to prevent boiling and maximum makeup water requirements.
- iii. The maximum fuel rod cladding temperature for fuel stored in the SFP was determined to establish that boiling at any location around the fuel is not possible. This evaluation was based conservatively on the maximum local water temperature in the SFP and the water-to-clad temperature difference for the hottest fuel assembly in the hottest location in the SFP.
- iv. With the maximum bulk temperature conservatively limited to 140°F with the SFP-to-Transfer Pit gate closed, the maximum Transfer Pit heat load was determined based only

on the passive heat losses off the top of the Pit water to the building atmosphere. (This maximum heat load is conservatively used as a limit with the gate open.) Evaluations were also completed for the Transfer Pit to address, a) structural temperature, b) required makeup, c) boiling based on the hottest fuel assemblies in the SFP, and d) operation with the gate open.

The following sections present plant system descriptions, analysis assumptions, a synopsis of the analysis methods employed, and the final results.

## 5.2 Cooling Systems Description

A complete description of the Spent Fuel Pool Cooling System (SFPCS) is found in the DBNPS USAR, Section 9.1.3. The SFPCS is designed to remove decay heat from the fuel stored in the SFP. The SFPCS at the DBNPS consists of two half system capacity recirculating pumps, two half system capacity heat exchangers, the associated valves and piping. The SFPCS pumps are horizontal, centrifugal units with a rated capacity of 1,100 gpm. The SFPCS heat exchangers are shell and tube units. The cold cooling water shell side flow is supplied from the plant Component Cooling Water (CCW) system. SFP water is pumped through the heat exchange tube side. The SFPCS heat exchanger design performance is listed below.

Heat Transferred:	5.25×10 <sup>6</sup> Btu/hr
Shell Side Flow Rate:	650 gpm
Shell Side Inlet Temperature:	95°F
Shell Side Outlet Temperature:	111.2°F
Tube Side Flow Rate:	1000 gpm
Tube Side Inlet Temperature:	120°F
Tube Side Outlet Temperature:	109.5°F

The Decay Heat Removal System (DHRS), described in the DBNPS USAR Section 9.3.5, serves as the Seismic Class I backup cooling system to the SFPCS. The DHRS consists of two

recirculating pumps and two heat exchangers. The DHRS is permanently connected to the SFPCS via a 10-inch line. Two normally closed gate valves provide isolation between the DHRS and the SFPCS. The DHRS pumps are single-stage, centrifugal units with a rated capacity of 3,000 gpm. The DHRS heat exchangers, which are also cooled by the CCW system, are shell and tube units with the following design performance:

Heat Transferred:  $26.9 \times 10^6$  Btu/hr  
SFP Water Flow Rate: 3000 gpm  
SFP Water Inlet Temperature: 140°F  
CCW Flow Rate: 6000 gpm  
CCW Inlet Temperature: 95°F

Loss of water from the SFP is unlikely since the SFP and piping within the SFP are Seismic Class I. Makeup water is readily available. The DHRS is permanently connected to the Class I boundary of the SFP. This system can provide borated make up water to the SFP from the Borated Water Storage Tank. SFP makeup water is also available from the Seismic Class II Demineralized Water Storage Tank or Clean Waste Receiver Tank.

### 5.3 Discharge/Cooling Alignment Scenarios

The DBNPS operating requirements with respect to core offloads are based on the shutdown risk program described in procedure NG-DB-00116, "Outage Nuclear Safety Control." With the core not fully offloaded, one SFP cooling train is required to be functional if a Decay Heat Removal (DHR) train is available for SFP cooling. Both SFP cooling trains are required to be functional if neither DHR train is available for SFP cooling. With the core fully offloaded, both SFP cooling trains are required to be functional and one DHR train is required to be functional for SFP cooling. The DHR train may be temporarily removed from functional status to support other outage evolutions, provided specific provisions are enacted to ensure that the DHR train remains readily available to support SFP cooling.

A SFP water temperature indicator is provided in the control room. The indicator reading is logged by the control room operator once per 8 hours. A log maximum of 120 °F is provided to alert the operator that additional attention is warranted should the SFP water temperature reach that range. Spent Fuel Pool temperature indication is also available via the plant computer.

A SFP high temperature annunciator alarm is provided in the control room, with a setpoint of 125°F. Upon receipt of the alarm, alarm procedure DB-OP-02003, "ECCS Alarm Panel 3 Annunciators," directs the operator to; 1) check for SFP high temperature by observing the control room SFP temperature indicator or computer point, 2) check that the SFP heat exchanger outlet temperatures are less than 100 °F, 3) verify adequate component cooling water (CCW) flow rate to each SFP heat exchanger if SFP heat exchanger outlet temperature is greater than 100 °F, 4) take appropriate actions if CCW flow rate is not adequate, and 5) raise cooling capacity by starting a second SFP pump if only one SFP pump is running. If the SFP cooling system has been lost or is not sufficient to maintain SFP water temperature below 125°F, the alarm procedure directs the operator to utilize the Decay Heat Removal (DHR) system.

If a DHR train being utilized for SFP cooling is lost, and no DHR train can be aligned to provide SFP cooling, abnormal procedure DB-OP-02527, "Loss of Decay Heat Removal," instructs the operator to place both trains of SFP cooling in service. In the event the SFP temperature reaches 125°F, the procedure further directs the operator to evacuate the SFP area and place the Emergency Ventilation System in service on the SFP area. With the SFP area evacuated, fuel handling in the SFP area would not occur.

A total of six reactor core discharge/cooling scenarios were postulated. These scenarios are:

Scenario	Discharge Type	Cooling System Alignment
1	Partial Core (2 years at power)*	2 SFPCS Pumps and Heat Exchangers
2	Partial Core (2 years at power)*	1 SFPCS Pump and Heat Exchanger
3A	Type A Full Core (65 days at power)**	2 SFPCS Pumps and Heat Exchangers
3B	Type B Full Core (2 years at power)***	2 SFPCS Pumps and Heat Exchangers
4A	Type A Full Core (65 days at power)**	1 DHRS Train
4B	Type B Full Core (2 years at power)***	1 DHRS Train

- \* Discharge of 72 fuel assemblies which had been at power for 2 years, following a refueling outage 2 years earlier that discharged 72 assemblies which had been at power for 2 years.
- \*\* Discharge of 177 fuel assemblies which had been at power for 65 days, following a refueling outage 65 days earlier that discharged 72 assemblies which had been at power for 2 years.
- \*\*\* Discharge of 177 fuel assemblies which had been at power for 2 years, following a refueling outage 2 years earlier that discharged 72 assemblies which had been at power for 2 years.

Scenarios 2, 3A and 3B correspond to cooling alignment combinations which are not typically used for the specified discharge type. These scenarios are included to demonstrate the bulk temperature will remain below boiling even under extreme circumstances. Time-to-boil, boiloff rate, and local temperature analyses are performed for the most limiting (i.e., highest bulk temperature and decay heat flux) of the full core discharge Scenarios 4A and 4B.

The partial core discharge scenarios (Scenarios 1 and 2) are based on 72 assemblies discharged into the SFP which already contains 1609 previously discharged assemblies. This analyzed

stored fuel inventory (1681) conservatively exceeds the maximum expected inventory of 1624. The minimum decay time of the previously discharged fuel assemblies for these scenarios is 2 years. (Table 5.8.3 shows the decay heat load for each fuel batch.)

The "Type A" full core discharge scenarios are based on 177 assemblies discharged into the SFP which already contains 1537 previously discharged assemblies. This analyzed fuel inventory (1714) conservatively exceeds the maximum expected inventory of 1624. This full core discharge takes place after 65 days of full power operation since the last partial core discharge. The minimum decay time of the previously discharged fuel assemblies for these scenarios is 65 days. (Table 5.8.4 shows the decay heat load for each fuel batch.)

The "Type B" full core discharge scenarios are based on 177 assemblies discharged into an SFP which already contains 1537 previously discharged assemblies. This analyzed fuel inventory (1714) conservatively exceeds the maximum expected inventory of 1624. This full core discharge takes place after 2 years of full power operation since the last partial core discharge. The minimum decay time of the previously discharged fuel assemblies for these scenarios is 2 years. (Table 5.8.5 shows the decay heat load for each fuel batch.)

Table 5.3.1 presents the historic and projected fuel discharge schedule used to determine the decay heat loads for these analyses.

In all scenarios, the cooling water which removes heat from the SFPCS and DHRS heat exchangers is assumed to be at its design maximum temperature and design basis flow rate.

#### 5.4 Maximum SFP Bulk Temperature Methodology

This section presents the methodology for calculating the maximum SFP bulk temperatures for the scenarios presented in the preceding section. The following conservative assumptions are applied in the maximum SFP bulk temperature calculations:

- The decay heat load is based on a discharge schedule with bounding projected fuel parameters.
- The minimum initial enrichment for projected discharged batches is used for previously discharged fuel decay heat calculations.
- The thermal capacity of the SFP is based on the net SFP water volume only, with the SFP at the Technical Specification minimum level. The considerable energy storage capability of the fuel racks, fuel assemblies, and SFP structure is neglected.
- The cooling effects of evaporation heat losses and all other passive heat removal mechanisms (i.e., conduction through walls and slab) are neglected.

The transient thermal response of the SFP and the attendant cooling systems is governed by a first-order, ordinary differential equation. The governing differential equation can be written by utilizing conservation of energy as:

$$C \frac{dT}{d\tau} = Q(\tau) - Q_{HX}(T) - Q_{EV}(T)$$

where:

C = Pool thermal capacity, Btu/°F

T = Pool bulk temperature, °F

$\tau$  = Time after reactor shutdown, hr

$Q(\tau)$  = Time varying decay heat generation rate, Btu/hr

$Q_{HX}(T)$  = Temperature dependent SFPCS or DHRS heat rejection rate, Btu/hr

$Q_{EV}(T)$  = Temperature dependent passive SFP heat loss to the environment,  
Btu/hr

$Q_{HX}(T)$  is a function of the SFP temperature and the cooling water flow rate and temperature can be written in terms of the temperature effectiveness ( $p$ ) as follows:

$$Q_{HX}(T) = W_t C_t p (T - t_i)$$

where:

$W_t$  = CCW water flow rate, lb/hr

$C_t$  = CCW water specific heat capacity, Btu/(lb×°F)

$p$  = SFPCS or DHRS heat exchanger temperature effectiveness

$T$  = SFP bulk pool water temperature, °F

$t_i$  = CCW water inlet temperature, °F

The temperature effectiveness, a measure of the heat transfer efficiency of the SFPCS or DHRS heat exchangers, is defined as:

$$p = \frac{t_o - t_i}{T - t_i}$$

where  $t_o$  is the CCW outlet temperature (°F) and all other terms are as defined above.

$Q_{EV}(T)$  is a nonlinear function of the SFP temperature and ambient temperature. This term is conservatively neglected in the maximum SFP bulk temperature calculations. However, a discussion of this term is provided for understanding of the conservatism applied to this calculation.

The differential equation that defines the transient thermal response of the SFP is solved numerically. The decay heat load from previously discharged fuel assemblies is calculated using Holtec's QA validated LONGOR program [5.4.3]. This program incorporates the ORIGEN2 isotope generation and depletion code [5.4.4] to perform the decay heat calculations. The transient decay heat loads and SFP bulk temperatures are calculated using Holtec's QA validated BULKTEM program [5.4.5], which also incorporates the ORIGEN2 code. The maximum SFP bulk temperature is extracted from the results of the transient evaluations. The major input values for this analysis are summarized in Table 5.4.1.

## 5.5 Minimum Time-to-Boil and Maximum Boiloff Rate Methodology

This section presents the methodology for calculating the minimum time-to-boil and corresponding maximum boiloff rate for the scenarios presented in Section 5.3.

The following conservatisms are applied in the SFP time-to-boil and boiloff rate calculations:

- The SFP bulk temperature and decay heat generation rates are assumed to be the calculated maximum bulk temperature and the coincident decay heat generation rates. Maximizing the initial temperature and utilizing the coincident decay heat generation rates will conservatively minimize the time-to-boil.
- The thermal capacity of the SFP is based on the net water volume only. The considerable energy storage capability of the fuel racks, fuel assemblies, and SFP structure is neglected.
- Heat losses through the SFP walls and slab are neglected.
- In calculating the SFP passive heat losses, the building housing the SFP fuel pool is assumed to have a conservative ambient air temperature of 110°F and 100% relative humidity. These conditions yield a conservative time-reducing SFP thermal capacity while minimizing the credit for evaporative and other passive heat losses.

The governing enthalpy balance equation for this condition, subject to these conservative assumptions, can be written as:

$$C(\tau) \frac{dT}{d\tau} = Q(\tau + \tau_0) - Q_{EV}(T)$$

where  $C(\tau)$  is the time-reducing thermal capacity,  $\tau$  is the time after cooling is lost (hr) and  $\tau_0$  is the loss of cooling time after shutdown (hr). The other terms of this equation are defined in Section 5.4, including a discussion of  $Q_{EV}(T)$ . Temperature dependent passive heat losses from the SFP surface are accounted for in this analysis.

This differential equation is solved using a numerical solution technique to obtain the bulk SFP temperature as a function of time. This analysis is performed using Holtec's QA validated TBOIL program [5.5.1]. This program utilizes the highly conservative correlations of ASB 9-2 [5.5.2] to perform the decay heat calculations, thereby imparting even more conservatism to the results. The major input values for this analysis are summarized in Table 5.5.1.

## 5.6 Local Water Temperature Methodology

This section summarizes the methodology for evaluating the maximum local water temperature for the SFP. A conservative evaluation for a bounding amalgam of conditions is performed. The result of this evaluation is a bounding temperature difference between the maximum local water temperature and the SFP bulk pool temperature. The maximum temperature difference is added to the maximum bulk SFP temperature to determine the maximum local temperature in the SFP. The maximum SFP local temperature is determined to ensure the SFPCS and DHRS heat removal capacity is acceptable to remove the additional heat of the fuel.

In order to determine the maximum local water temperature, a series of conservative assumptions are made. The most important of these assumptions are:

- With a full core discharged into the SFP racks, approximately equidistant from the coolant water inlet and outlet, the remaining cells in the SFP are postulated to be occupied with previously discharged fuel.
- The hottest fuel assemblies have a radial peak of 1.64 and an axial peak of 1.52.

- The hottest assemblies, located together in the SFP, are assumed to be located in pedestal cells of the racks. These cells have a reduced water entrance area, caused by the pedestal blocking the baseplate hole, and a correspondingly increased hydraulic resistance.
- No downcomer flow is assumed to exist between the rack modules.
- All rack cells are conservatively assumed to be 50% blocked at the cell outlet to account for drop accidents resulting in damage to the upper end of the cells.
- The hydraulic resistance parameters for the rack cells, permeability and inertial resistance, are worsened by 15% and 25%, respectively.

#### 5.6.1 Local Temperature Evaluation Methodology

The inlet piping that returns cooled water from the SFPCS terminates above the level of the fuel racks. It is not apparent from heuristic reasoning alone that the cooled water delivered to the SFP would not bypass the hot fuel racks and exit through the outlet piping. To demonstrate adequate cooling of hot fuel in the SFP, it is therefore necessary to rigorously quantify the velocity field in the SFP created by the interaction of buoyancy driven flows and water injection. A Computational Fluid Dynamics (CFD) analysis for this demonstration is required. The objective of this study is to demonstrate that the principal thermal-hydraulic criterion of ensuring local subcooled conditions in the SFP is met for all postulated fuel discharge/cooling alignment scenarios. The local thermal-hydraulic analysis is performed such that partial cell blockage and slight fuel assembly variations are bounded. An outline of the CFD approach is described in the following.

There are several significant geometric and thermal-hydraulic features of the DBNPS SFP that need to be considered for a rigorous CFD analysis. From a fluid flow modeling standpoint, there are two regions to be considered. One region is the free-fluid region above the racks in the SFP

where the classical Navier-Stokes equations are solved with turbulence effects included. The other region is the heat generating fuel assemblies located in the spent fuel racks located near the bottom of the SFP. In this region, water flow is directed vertically upwards due to buoyancy forces through relatively small flow channels formed by the Babcock and Wilcox (B&W) 15x15 fuel assembly rod arrays in each rack cell. This region was modeled as a porous solid region in which the classical Darcy's Law, given below, governs fluid flow:

$$\frac{\partial P}{\partial X_i} = -\frac{\mu}{K(i)} V_i - C \rho |V_i| \frac{V_i}{2g}$$

where:

$\partial P/\partial X_i$ =Pressure gradient in the 'i' direction, psi/ft

$\mu$ =Fluid viscosity, lbxsec/ft<sup>2</sup>

$K(i)$ =Permeability in the 'i' direction, ft<sup>2</sup>

$V_i$ =Fluid velocity in the 'd' direction, ft/sec

$C$ =Inertial resistance factor, 1/ft

$\rho$ =Fluid density, lb/ft<sup>3</sup>

$g$ =Gravitational acceleration, ft/sec<sup>2</sup>

The permeability and inertial resistance parameters for the rack cells loaded with B&W 15x15 fuel were determined based on friction factor correlations for the laminar flow conditions typically encountered due to the low buoyancy induced velocities and the small size of the flow channels.

The DBNPS SFP geometry required an adequate portrayal of large scale and small scale features, spatially distributed heat sources in the spent fuel racks, and water inlet/outlet configuration. Relatively cooler bulk SFP water normally flows down between the fuel rack outline and SFP wall liner clearance known as the downcomer. Near the bottom of the racks, the flow turns from a vertical to horizontal direction into the bottom plenum supplying cooling water to the rack

cells. Heated water issuing out of the top of the racks mixes with the SFP free-fluid region water. An adequate modeling of these features on the CFD program involves meshing the large scale SFP free fluid region and small scale downcomer and bottom plenum regions with sufficient number of computational cells to capture the bulk and local features of the flow field.

The distributed heat sources in the SFP racks are modeled by identifying distinct heat generation zones considering full-core discharge, bounding peak effects, and presence of background decay heat from previous discharges. Three heat generating zones were modeled. The first zone contains the heat generated by fuel from previous discharges and the second and third zones contain the decay heat generated by fuel from a bounding full-core-discharge scenario. The two full core discharge zones are differentiated by one zone with higher than average decay heat generation and the other with lower than average decay heat generation. This is a conservative model, since all of the fuel with higher than average decay heat is placed in a contiguous area. A uniformly distributed heat generation rate was applied throughout each distinct zone.

The CFD analysis was performed on the FLUENT [5.6.4] fluid flow and heat transfer modeling program. The FLUENT code enables buoyancy flow and turbulence effects to be included in the CFD analysis. Turbulence effects are modeled by relating time-varying Reynolds' Stresses to the mean bulk flow quantities with the  $k$ - $\epsilon$  turbulence model. The  $k$ - $\epsilon$  model is appropriate for the DBNPS CFD analysis. The  $k$ - $\epsilon$  turbulence model is a time-tested, general-purpose turbulence model. This model has been demonstrated to give good results for the majority of turbulent fluid flow phenomena.

Rigorous modeling of fluid flow problems requires a solution to the classical Navier-Stokes equations of fluid motion [5.6.1]. The governing equations (in modified form for turbulent flows with buoyancy effects included) are written as:

$$\frac{\partial \rho_o u_i}{\partial t} + \frac{\partial \rho_o \langle u'_i u'_j \rangle}{\partial x_i} = \frac{\partial}{\partial x_j} \left[ \mu \left( \frac{\partial u_i}{\partial x_j} + \frac{\partial u_j}{\partial x_i} \right) \right] - \frac{\partial p}{\partial x_i} - (\rho - \rho_o) g_i + \frac{\partial \rho_o \langle u'_i u'_j \rangle}{\partial x_j}$$

where :

$\rho_o$  = Fluid density at temperature  $T_o$ , lb/ft<sup>3</sup>

$u_i$  = Time averaged velocity in the 'i' direction

$\rho \langle u'_i u'_j \rangle$  = Time-averaged Reynolds stresses derived from  $u'_i$  and  $u'_j$

$u_i$  = Turbulence induced fluctuating velocity component in the 'i' direction

$\mu$  = Fluid viscosity

$g_i$  = Gravitational acceleration in the 'i' direction

$x_i$  = Cartesian coordinate 'i' direction

The Reynolds stress tensor is expressed in terms of the mean flow quantities by defining a turbulent viscosity  $F_t$  and a turbulent velocity scale  $k^{1/2}$  as shown below [5.6.2]:

$$\rho \langle u'_i u'_j \rangle = 2/3 \rho (k^{1/2})^2 \delta_{ij} - \mu_t \left[ \frac{\partial u_i}{\partial x_j} + \frac{\partial u_j}{\partial x_i} \right]$$

The procedure to obtain the turbulent viscosity and velocity length scales involves a solution of two additional transport equations for kinetic energy (k) and rate of energy dissipation ( $\epsilon$ ). This methodology, known as the k- $\epsilon$  model for turbulent flows, is described by Launder and Spalding [5.6.3].

Some of the major input values for this analysis are summarized in Table 5.6.1. A view of the assembled CFD model for the SFP is presented in Figure 5.6.1. Figures 5.6.2 and 5.6.3 present temperature contours and velocity vectors, respectively, in the SFP model.

## 5.7 Fuel Rod Cladding Temperature Methodology

This section summarizes the method to calculate the temperature of the fuel rod cladding. Similar to the local water temperature calculation methodology presented in the preceding section, this evaluation is performed for a single, bounding scenario. The maximum temperature difference between the fuel cladding and the local water temperature is calculated for the hottest fuel assembly in the SFP.

The maximum specific power of a fuel assembly ( $q_A$ ) can be given by:

$$q_A = q F_{xy}$$

where:

$F_{xy}$  = Radial peaking factor

$q$  = Average fuel assembly specific power, Btu/hr

The peaking factors are given in Table 5.6.1. The maximum temperature rise of SFP water is computed for the most disadvantageously located fuel assembly, which is defined as that assembly which is subject to the highest local SFP water temperature and has the highest decay heat generation rate. Having determined the maximum local water temperature in the SFP, it is possible to determine the maximum fuel cladding temperature. A fuel rod can produce  $F_z$  times the average heat emission rate over a small length, where  $F_z$  is the axial rod peaking factor. The axial heat distribution in a rod is generally a maximum in the central region, and tapers off at its two extremities. Thus, peak cladding heat flux over an infinitesimal area is given by the equation:

$$q_c = \frac{q F_{xy} F_z}{A_c}$$

where  $A_c$  is the total cladding external heat transfer area in the active fuel length region.

Within each fuel assembly sub-channel, water is continuously heated by the cladding as it moves axially upwards from bottom to top under laminar flow conditions. Rohsenow and Hartnett [5.7.1] report a Nusselt-number based heat transfer correlation for laminar flow in a heated channel. The film temperature driving force ( $\Delta T_f$ ) at the peak cladding flux location is calculated as follows:

$$h_f \frac{D_h}{K_w} = Nu$$

$$\Delta T_f = \frac{q_c}{h_f}$$

where:

$h_f$  = Fluid film heat transfer coefficient, Btu/(hr×ft<sup>2</sup>×°F)

$D_h$  = Sub-channel hydraulic diameter, ft

$K_w$  = Water thermal conductivity, Btu/(hr×ft×°F)

$Nu$  is the Nusselt number for laminar flow heat transfer

In order to introduce some additional conservatism in the analysis, we assume that the fuel cladding has a crud deposit resistance  $R_c$  (equal to 0.0005 ft<sup>2</sup>-hr-°F/Btu) that covers the entire surface. Thus, including the temperature drop across the crud resistance, the cladding to water local temperature difference ( $\Delta T_c$ ) is given by:

$$\Delta T_c = \Delta T_f + R_c \times q_c$$

## 5.8 Results and Conclusions

This section contains results from the analyses performed for the postulated discharge scenarios.

Based on the discharge scenarios and the assumed peaking factors in section 5.6, the maximum total heat generation rate of a single fuel assembly discharged to the SFP is 80,209 watts

(273,870 Btu/hr). The maximum heat generation rate per square foot of assembly heat transfer surface is 445 watts/sq. ft (1520 Btu/hr-sq. ft).

### 5.8.1 Maximum SFP Bulk Temperatures

For the discharge/cooling scenarios postulated in Section 5.3, the maximum calculated SFP bulk temperatures are summarized in Table 5.8.1. Table 5.8.1 also reports the decay heat loads for each scenario coincident with the peak bulk temperatures and the time after reactor shutdown that the peak temperature is reached. The maximum decay heat load -  $30.15 \times 10^6$  Btu/hr - occurred in scenario 3A prior to reaching the peak bulk temperature. Scenarios 3A and 4A evaluate an unplanned discharge occurring 65 days after a planned refueling. For these two scenarios, the reported time is the time after the second (unplanned) reactor shutdown. Tables 5.8.3 through 5.8.5 present decay heat loads, per discharge batch, for partial core discharge scenarios (Table 5.8.3), Type A full-core discharges (Table 5.8.4) and Type B full-core discharges (Table 5.8.5).

For Scenarios 1, 4A, and 4B, SFP bulk temperatures must remain within the limits of the American Concrete Institute (ACI) Code Requirements for Nuclear Safety Related Concrete Structures ACI-349, to protect the integrity of the SFP structure. The ACI Code permits long-term temperatures of up to 150°F and short-term temperature excursions in localized areas (e.g., skin effects) up to 350°F. As discussed in Section 5.3, Scenarios 2, 3A, and 3B are considered non-typical operation conditions and are only compared to the bulk boiling temperature of 212°F.

The results presented in Table 5.8.1 demonstrate that calculated bulk temperatures for the first four scenarios listed remain below their respective allowable limits. The calculated peak bulk temperatures for Scenarios 4A and 4B exceed the 150°F concrete temperature limit for long term normal operating conditions by less than 1.5°F. In both scenarios, the SFP bulk temperature will remain above 150°F for less than 28 hours. The effect of this bulk SFP temperature condition is

evaluated and determined to be acceptable in the structural evaluations in Chapter 8. Given the conservatism assumptions incorporated into the calculations, actual SFP bulk temperatures will be lower than the calculated values reported in Table 5.8.1. Therefore, it can be concluded that both the SFP bulk water and the SFP structure temperatures can be maintained at acceptable levels by the existing cooling systems.

### 5.8.2 Minimum Time-to-Boil and Maximum Boiloff Rate

For discharge/cooling Scenarios 1 and 4A, the calculated time-to-boil and maximum boiloff rates are summarized in Table 5.8.1. These results show that, in the extremely unlikely event of a complete failure of both the SFPCS and DHRS, there would be at least 3.78 hours available for corrective actions prior to the onset of boiling. The maximum water boiloff rate is less than 70 gpm. The DHRS is permanently connected to the Seismic Class I boundary of the SFP. By already-proceduralized valve line-ups, the DHRS can provide borated makeup water to the SFP from the Borated Water Storage Tank, (by pumped or gravity-fill methods). SFP makeup water is also available from the Seismic Class II Demineralized Water Storage Tank or the Clean Waste Receiver Tank. Therefore, it can be concluded that sufficient time for remedial actions is available and that makeup capacity will exceed the makeup demand.

In the unlikely event the establishment of makeup to the SFP was delayed following a loss-of-forced-cooling event, approximately 25 hours of boiling would be required to reduce SFP level from the Technical Specification minimum level of 23 feet above the top of fuel assemblies seated in the storage racks, to the level corresponding to 9-1/2 feet above the top of fuel stored in the racks, given a SFP plan area of approximately 1057 ft<sup>2</sup>, and assuming a constant boil-off rate of 70 gpm. A minimum of 9-1/2 feet of borated water above the top of active fuel stored in the racks will ensure adequate biological shielding. In summary, 25 hours provides operators with more than sufficient time to intervene with available means to maintain or restore the SFP water level.

### 5.8.3 Local Water and Fuel Cladding Temperatures

The CFD study has analyzed a bounding local thermal-hydraulic scenario. In this scenario, a bounding full-core discharge is considered in which the 177 assemblies are located in the SFP, approximately equidistant from the water inlet and outlet, while the balance of the rack cells are postulated to be occupied by fuel from previous discharges. The difference between the peak local temperature and the coincident SFP bulk temperature was conservatively calculated to be 42.75°F (Table 5.8.2, row B).

The peak fuel cladding temperature is determined for the hottest location in the SFP as obtained from the CFD model for the DBNPS SFP. The maximum calculated temperature difference between the fuel cladding and the local water ( $\Delta T_c$ ) was calculated to be 36.10°F (Table 5.8.2, row D). This calculated cladding  $\Delta T_c$  is applied, along with the maximum temperature difference between the local water temperature and the SFP bulk temperature, to the calculated maximum SFP bulk temperature (Scenarios 4A and 4B) of approximately 151.50°F. This yields a conservatively bounding 194.25°F maximum local water temperature and a conservatively bounding 230.35°F peak cladding temperature (Table 5.8.2, rows C and E). These conservative bounding maximum local temperatures are less than the 239°F local boiling temperature at the top of the racks. Therefore, it can be concluded that boiling does not occur anywhere within the DBNPS SFP.

### 5.9 Fuel Handling Area Ventilation (FHAV)

An evaluation of the Fuel Handling Area Ventilation (FHAV) system was performed. This evaluation was performed for the full core discharge scenario 4A, which provides the greatest heat load burden to the FHAV system. Using the design inlet air parameters from the DBNPS USAR, the maximum calculated building temperature is 103°F. The relative humidity was calculated to increase by less than 25 percent relative humidity. Therefore, it is concluded that

the additional burden on the FHAV system, as a result of the peak heat loads from the SFP, is within the design capability of the FHAV system.

## 5.10 Transfer Pit

### 5.10.1 Transfer Pit Bulk Temperature Methodology

The Transfer Pit is connected to the Spent Fuel Pool (SFP) by a three foot wide gate. There is no direct, forced cooling of the Transfer Pit. A Computational Fluid Dynamics (CFD) thermal-hydraulic analysis was completed for the Cask Pit, which is also connected to the SFP by a similar three foot wide gate and also has no forced cooling. This CFD analysis concluded there is adequate buoyancy driven flow through the gate to appropriately cool 289 fuel assemblies having a total heat output of 252,200 watts. (Storage of fuel in the Cask Pit was approved per LAR 98-0007, Docket 50-346, on 2/29/00.) Even though the same would be true for the Transfer Pit, the maximum heat load of the Pit was determined assuming a closed gate, with only passive heat losses to the building environment off the water surface. Additionally, for this analysis, the bulk temperature was conservatively limited to 140°F.

The passive heat losses include the effects of natural convection, thermal radiation, and mass diffusion. The formulation for these losses is as follows:

[REDACTED]

The evaporation water loss rate is calculated by dividing the mass diffusion term in the passive heat loss equation given above by the latent heat of vaporization of water. The major inputs for this analysis are summarized below.

<b>Data for Transfer Pit Bulk Temperature</b>	
Transfer Pit Length	431.5 inches
Transfer Pit Width	167.5 inches
Building Ambient Temperature	569.67°K (=110+459.67)
Maximum Bulk Temperature	599.67 °R (=140+459.67)
Emissivity of Water	0.96 @100°F
Building Relative Humidity	100%

### 5.10.2 Transfer Pit - Gate Closed

Based on the methodology presented in section 5.10.1, to maintain the Transfer Pit bulk temperature at 140°F with the Transfer Pit-to-SFP gate closed, the maximum heat load was determined to be 88,110 watts (300,806 <sup>Btu</sup>/<sub>hr</sub>). The corresponding evaporation rate is 0.542 gpm. With the bulk temperature limited to 140°F by the allowed maximum heat load, the American Concrete Institute (ACI) long term limit of 150°F for Nuclear Safety Related Concrete Structures (ACI-349) is not exceeded. In addition, there will be no bulk boiling.

At an evaporation rate of 0.542 gpm, it would take greater than 5 days to lower the level of the Transfer Pit from the normal operating level to the Technical Specification action level. Borated water may be added to the Transfer Pit from the Borated Water Storage Tank (BWST) by gravity fill or via the BWST Transfer Pump. Therefore, it can be concluded that sufficient time for remedial actions is available, and that makeup capacity will exceed the makeup demand.

The following table conservatively determines the Transfer Pit maximum local temperatures by starting with the maximum bulk temperature of 140°F, and adding the local temperature differences calculated for the hottest location in the SFP, (see section 5.8.3).

<b>Transfer Pit - Gate Closed Bounding Local Temperature Evaluation</b>		
A	Maximum Bulk Transfer Pit Temperature	140.00°F
B	SFP Bulk-to-Local Water Temperature Difference	42.75°F
C	Transfer Pit Maximum Local Water Temperature [A + B]	182.75°F
D	SFP Fuel Local Water-to-Cladding Temperature Difference	36.10°F
E	Transfer Pit Maximum Fuel Cladding Temperature [C + D]	218.85°F

The conservative bounding maximum local water and fuel cladding temperatures are less than the 239°F boiling temperature at the top of the racks. Therefore, it can be concluded that boiling will not take place anywhere in the Transfer Pit when the gate is installed.

### 5.10.3 Transfer Pit - Gate Open

The Transfer Pit is connected to the SFP by a three foot wide gate. There is no direct, forced cooling of the Transfer Pit. A Computational Fluid Dynamics (CFD) thermal-hydraulic analysis

was completed for the Cask Pit, which is also connected to the SFP by a three foot wide gate and has no forced cooling. This CFD analysis concluded there is adequate buoyancy driven flow through the gate to appropriately cool 289 fuel assemblies having a total heat output of 252,200 watts. (Storage of fuel in the Cask Pit was approved per LAR 98-0007, Docket 50-346, on 2/29/00.) Based on the results of the Cask Pit analysis it could be concluded the Transfer Pit, (which is a physically similar structure to the Cask Pit), with 88,110 watts of heat would be cooled by buoyancy flow through the open Cask Pit-to-SFP gate.

To further evaluate the Transfer Pit with the gate to the SFP open, the following conservative assumptions were made:

- i) The SFP bulk temperature for each offload/cooling scenario is at its maximum for assuming the SFP is completely re-racked and each cell contains a spent fuel assembly (per the Table 5.3.1 fuel discharge schedule). This is conservative because, a) the rack used in the Transfer Pit will be placed in the SFP as part of the re-racking process, b) the re-racking is to take place when there is approximately 700 discharged spent fuel assemblies rather than the approximately 1700 for which the SFP bulk temperatures were calculated, and c) the re-racking will take place approximately one year after the last refueling, but the maximum SFP bulk temperatures were determined from the highest heat loading immediately after a refueling.
- ii) The Transfer Pit bulk temperature will reach equilibrium at 4°F above the SFP bulk temperature. This 4°F temperature increase was calculated for the Cask Pit which has a maximum heat load of 252,200 watts, as compared to the Transfer Pit maximum heat load of 88,110 watts.
- iii) The bulk-to-local water and the local water-to-fuel cladding temperature differences are the same as determined for the hottest location in the SFP. Per section 5.8.3, this hottest

location is in the middle of a group of the hottest fuel assemblies recently discharged from the reactor. Based on the heat load restriction for the Transfer Pit of 88,110 watts, only one of the hottest assemblies can be placed in the Transfer Pit.

With no fuel in the Transfer Pit and the Transfer Pit-to-SFP gate open, the Pit and SFP bulk temperatures will be the same. Based on assumptions i) and ii) above, with fuel in the Transfer Pit, the following table represents equilibrium Pit bulk temperatures.

<b>Transfer Pit - Gate Open Bounding Bulk Temperatures</b>			
<b>Scenario</b>	<b>Discharge Type</b>	<b>Cooling System Alignment</b>	<b>Bulk Temperature (°F)</b>
1	Partial Core (2 years at power)*	2 SFPCS Pumps and Heat Exchangers	136.98
2	Partial Core (2 years at power)*	1 SFPCS Pump and Heat Exchanger	173.32
3A	Type A Full Core (65 days at power)**	2 SFPCS Pumps and Heat Exchangers	169.87
3B	Type B Full Core (2 years at power)***	2 SFPCS Pumps and Heat Exchangers	168.90
4A	Type A Full Core (65 days at power)**	1 DHRS Train	155.42
4B	Type B Full Core (2 years at power)***	1 DHRS Train	154.67

\* Discharge of 72 fuel assemblies which had been at power for 2 years, following a refueling outage 2 years earlier that discharged 72 assemblies which had been at power for 2 years.

\*\* Discharge of 177 fuel assemblies which had been at power for 65 days, following a refueling outage 65 days earlier that discharged 72 assemblies which had been at power for 2 years.

\*\*\* Discharge of 177 fuel assemblies which had been at power for 2 years, following a refueling outage 2 years earlier that discharged 72 assemblies which had been at power for 2 years.

For Scenarios 1, 4A, and 4B, to protect the integrity of the Transfer Pit structure, the Pit bulk temperatures must remain within the limits of the American Concrete Institute (ACI) Code Requirements for Nuclear Safety Related Concrete Structures (ACI-349). The ACI Code permits long-term temperatures of up to 150°F, and short-term temperature excursions in localized areas (e.g., skin effects) up to 350°F. As discussed in Section 5.3, Scenarios 2, 3A, and 3B are considered non-typical operating conditions and are only compared to the bulk boiling temperature of 212°F.

The results presented in the above table demonstrate the calculated bulk temperatures of the first four scenarios listed remain below their respective allowable limits. The calculated peak bulk temperatures for Scenarios 4A and 4B exceed the 150°F concrete temperature limit for long term operating conditions by less than 5.5°F. In both scenarios, the Transfer Pit bulk temperature will remain above 150°F for approximately 60 hours. The effect of this Transfer Pit bulk temperature condition is evaluated and determined to be acceptable in the structural evaluations of Chapter 8. Given the conservative assumptions incorporated into the evaluations, actual Transfer Pit bulk temperatures will be lower than reported in the above table. Therefore, it can be concluded both the Transfer Pit bulk water and the Pit structure temperatures will be maintained at acceptable levels with the Transfer Pit-to-SFP gate open.

As explained on assumption i) above, the fuel in the Transfer Pit does not constitute an addition to the analyzed heat load for the cooling systems. Therefore, with the gate open and the extra volume of the Transfer Pit, the time-to-boil specified in Table 5.8.1 for the SFP will be conservative. (The maximum boiloff rate would remain the same.) Based on this, the acceptance of the SFP time-to-boil and the boiloff rate (see section 5.8.2) is not effected by the Transfer Pit containing fuel and the Transfer Pit-to-SFP gate being open.

The following table conservatively determines the Transfer Pit maximum local temperatures by starting with the maximum bulk temperature of 155.42°F (Scenario 4A), and adding the local temperature differences calculated for the hottest location in the SFP, (see section 5.8.3).

<b>Transfer Pit - Gate Open Bounding Local Temperature Evaluation</b>		
A	Maximum Bulk Transfer Pit Temperature	155.42°F
B	SFP Bulk-to-Local Water Temperature Difference	42.75°F
C	Transfer Pit Maximum Local Water Temperature [A + B]	198.17°F
D	SFP Fuel Local Water-to-Cladding Temperature Difference	36.10°F
E	Transfer Pit Maximum Fuel Cladding Temperature [C + D]	234.27°F

The conservative bounding maximum local water and fuel cladding temperatures are less than the 239°F boiling temperature at the top of the racks. Therefore, it can be concluded that boiling will not take place anywhere in the Transfer Pit when the gate is open.

#### 5.10.4 Transfer Pit - Conclusion

Fuel may be stored in the Transfer Pit with the Transfer Pit-to-SFP gate closed or open. The analysis limits the Transfer Pit heat load to 88,110 watts. The same fuel which is allowed to be stored in the SFP can be stored in the Transfer Pit.

## 5.11 References

- [5.4.1] "Heat Loss to the Ambient from Spent Fuel Pools: Correlation of Theory with Experiment", Holtec Report HI-90477, Rev. 0, April 3, 1990.
- [5.4.2] "An Improved Correlation for Evaporation from Spent Fuel Pools", Holtec Report HI-971664, Rev. 0.
- [5.4.3] "QA Documentation for LONGOR v1.0," Holtec Report HI-951390, Revision 0.
- [5.4.4] Croff, A.G., "ORIGEN2 - A Revised and Updated Version of the Oak Ridge Isotope Generation and Depletion Code," ORNL-5621, Oak Ridge National Laboratory, 1980.
- [5.4.5] "QA Documentation for BULKTEM v3.0," Holtec Report HI-951391, Revision 1.
- [5.5.1] "QA Validation for TBOIL v1.6," Holtec Report HI-92832, Revision 2.
- [5.5.2] USNRC Branch Technical Position ASB 9-2, "Residual Decay Energy for Light Water Reactors for Long Term Cooling," Revision 2, July 1981.
- [5.6.1] Batchelor, G.K., "An Introduction to Fluid Dynamics", Cambridge University Press, 1967.
- [5.6.2] Hinze, J.O., "Turbulence", McGraw Hill Publishing Co., New York, NY, 1975.
- [5.6.3] Launder, B.E., and Spalding, D.B., "Lectures in Mathematical Models of Turbulence", Academic Press, London, 1972.
- [5.6.4] "QA Documentation and Validation of the FLUENT Version 4.32 CFD Analysis Program", Holtec Report HI-961444, Revision 0.
- [5.7.1] Rohsenow, N.M., and Hartnett, J.P., "Handbook of Heat Transfer", McGraw Hill Book Company, New York, 1973.

**Table 5.3.1**

**Davis-Besse Historic and Projected Fuel Discharge Schedule**

Number of Assemblies	Discharge Date (Month & Year)	Average Burnup (MWd/MTU)	<sup>235</sup> U Enrichment (wt%)	Uranium Weight (kgU)
53	March 1982	23888	2.48	472.16
85	July 1983	26996	2.67	472.21
65	September 1984	28153	2.64	471.06
65	March 1988	34190	3.00	468.75
60	January 1990	31142	3.02	468.21
59	August 1991	36254	3.18	468.25
61	March 1993	38046	3.15	467.85
65	October 1994	41039	3.45	468.37
74	April 1996	42948	3.71	467.88
77	April 1998	46492	3.90	467.89
77	March 2000	49491	4.32	467.93
73	March 2002	51134	4.43	467.83
73	March 2004	52972	4.20	479.86
73	March 2006	55782	3.99	489.51
73	March 2008	55783	3.99	489.51
72	March 2010	55881	4.00	489.80
72	March 2012	55881	4.00	489.80
72	March 2014	55881	4.00	489.80
72	March 2016	55881	4.00	489.80
72	March 2018	55881	4.00	489.80
72	March 2020	55881	4.00	489.80
72	March 2022	55881	4.00	489.80
72	March 2024	55881	4.00	489.80

Note: In performing calculations, the listed burnup values are increased by 2% to include uncertainties in the reactor thermal power.

<b>TABLE 5.4.1</b>	
<b>DATA FOR SFP BULK TEMPERATURE EVALUATION</b>	
Reactor Thermal Power	2827.5 MWt
Reactor Core Size	177 assemblies
SFPCS HX Coolant Flow Rate	650 gpm
SFPCS HX Coolant Temperature	95°F
DHRS HX Coolant Flow Rate	6000 gpm
DHRS HX Coolant Temperature	95°F
Minimum In-Core Hold Time	150 hours
Fuel Assembly Discharge Rate	4 per hour
Spent Fuel Pool Length (N-S)	635.5 inches
Spent Fuel Pool Length (E-W)	239.5 inches
Spent Fuel Pool Depth	36.86 feet
SFPCS HX Design Conditions	
Coolant Inlet Temperature	95°F
Coolant Outlet Temperature	111.2°F
SFP Water Inlet Temperature	120°F
DHRS HX Design Conditions	
Coolant Inlet Temperature	95°F
SFP Water Inlet Temperature	140°F
Coolant Flow Rate	6000 gpm
Heat Removal Rate	26.9×10 <sup>6</sup> Btu/hr
Bounding Fuel Assembly Weight	1682 pounds

<b>TABLE 5.5.1</b>	
<b>DATA FOR TIME-TO-BOIL EVALUATION</b>	
Spent Fuel Pool Length (N-S)	635.5 inches
Spent Fuel Pool Length (E-W)	239.5 inches
Spent Fuel Pool Depth	36.9 feet
Total Rack Weight	268,000 lb
Bounding Fuel Assembly Weight	1682 pounds
SFP Building Ambient Temperature	110°F
Emissivity of Water	0.96
SFP Net Water Volume	31,580 ft <sup>3</sup>

<b>TABLE 5.6.1</b>	
<b>DATA FOR SFP LOCAL TEMPERATURE EVALUATION</b>	
Bounding Assembly Weight	1682 pounds
Radial Peaking Factor	1.64
Axial Peaking Factor	1.52
Maximum Number of Fuel Assemblies Assumed for Analysis	1714
Cooled Water Flow Rate	3000 gpm
Type of fuel assembly	Babcock and Wilcox 15×15
Fuel Rod Outer Diameter	0.430 inches max. 0.416 inches min.
Rack Cell Inner Dimension	9.0 inches
Active Fuel Length	145 inches
Number of Rods per Assembly*	225 rods
Rack Cell Length	161 5/8 inches
Bottom Plenum Height	6 inches

\* Note: Fuel assembly is modeled as a square array with all locations containing fuel rods for permeability determinations. 208 fuel rods are used for heat transfer calculations.

**TABLE 5.8.1**  
**Results of Transient Temperature Evaluations**

Scenario	Discharge Type	Coolant System Alignment	Bulk Temperature			Minimum Time to Boil (hrs)	Maximum Boil-off Rate (gpm)
			Maximum Bulk Temperature (°F)	Coincident Decay Heat Load (Btu/hr)	Time After Reactor Shutdown (hrs)		
1	Partial Core - 2 yrs at Full Power <sup>#</sup>	2 SFPCS Pumps and Heat Exchangers	132.98	15.89x10 <sup>6</sup>	183	10.42	34.45
2	Partial Core - 2 yrs at Full Power <sup>#</sup>	1 SFP Pump and Heat Exchanger	169.32	15.55x10 <sup>6</sup>	197	N/A**	N/A**
3A <sup>+</sup>	Full Core - 65 days at Full Power <sup>##</sup>	2 SFPCS Pumps and Heat Exchangers	165.87	29.66x10 <sup>6</sup>	205*	N/A**	N/A**
3B	Full Core - 2 yrs at Full Power <sup>###</sup>	2 SFPCS Pumps and Heat Exchangers	164.90	29.28x10 <sup>6</sup>	205	N/A**	N/A**
4A	Full Core - 65 days at Full Power <sup>##</sup>	1 DHRS Train	151.42	29.75x10 <sup>6</sup>	203*	3.78	69.57
4B	Full Core - 2 yrs at Full Power <sup>###</sup>	1 DHRS Train	150.67	29.38x10 <sup>6</sup>	203	N/A**	N/A**

\*Time for these scenarios, which evaluate an unplanned reactor shutdown 65 days after a planned refueling (which discharged 72 fuel assemblies), is measured from the start of the unplanned shutdown.

\*\*As discussed in Section 5.3, boiling evaluations are not performed for Scenarios 2, 3A, and 3B as they are non-typical operating lineups. Boiling evaluations are performed for Scenario 1 and the most limiting of Scenarios 4A and 4B (highest bulk temperature and decay heat flux).

<sup>#</sup> Discharge of 72 assemblies which had been at power 2 yrs., following a refueling outage 2 years earlier that discharged 72 assemblies which had been at power 2yrs.

<sup>##</sup> Discharge of 177 assemblies which had been at power 65 days, following a refueling outage 65 days earlier that discharged 72 assemblies which had been at power 2yrs.

<sup>###</sup> Discharge of 177 assemblies which had been at power 65 days, following a refueling outage 2 years earlier that discharged of 72 assemblies which had been at power 2yrs.

<sup>+</sup>The maximum heat load - 30.15x10<sup>6</sup> - occurred in Scenario 3A prior to reaching the maximum bulk temperature.

**TABLE 5.8.2**  
**SPENT FUEL POOL**  
**RESULTS OF MAXIMUM LOCAL TEMPERATURE EVALUATIONS**

A	Bounding SFP Bulk Temperature	151.50°F
B	Bulk to Local Water Temperature Difference	42.75°F
C	Maximum Local Water Temperature [A+B]	194.25°F
D	Fuel Cladding to Water Temperature Difference	36.10°F
E	Maximum Fuel Cladding Temperature [C+D]	230.35°F

**TABLE 5.8.3**

**DECAY HEAT LOADS FOR PARTIAL CORE DISCHARGE SCENARIOS 1 & 2**

Discharge Batch	# of Assemblies ( ) = Cumulative	Discharge Date	Decay Heat (Btu/hr)
1	53	March 1982	40,099.32
2	85 (138)	July 1983	72,152.89
3	65 (203)	September 84	58,636.24
4	65 (268)	March 1988	73,822.39
5	60 (328)	January 1990	63,242.48
6	59 (387)	August 1991	74,574.05
7	61 (448)	March 1993	83,601.08
8	65 (513)	October 1994	98,356.98
9	74 (587)	April 1996	119,350.40
10	77 (664)	April 1998	140,176.60
11	77 (741)	March 2000	153,592.60
12	73 (814)	March 2002	156,539.30
13	73 (887)	March 2004	176,943.80
14	73 (960)	March 2006	204,284.60
15	73 (1033)	March 2008	213,309.70
16	72 (1105)	March 2010	220,983.70
17	72 (1177)	March 2012	232,538.40
18	72 (1249)	March 2014	246,620.70
19	72 (1321)	March 2016	265,758.20
20	72 (1393)	March 2018	295,367.10
21	72 (1465)	March 2020	351,335.20
22	72 (1537)	March 2022	489,991.60
23	72 (1609)	March 2024	960,605.10
24*	72 (1681)	March 2026	11,097,101.03 10,759,077.75

\* Note: Decay heat loads coincident with maximum bulk temperature reported for Scenario 1 (first value) and Scenario 2 (second value).

**TABLE 5.8.4****DECAY HEAT LOADS FOR "TYPE A" FULL CORE DISCHARGE  
SCENARIOS 3A & 4A**

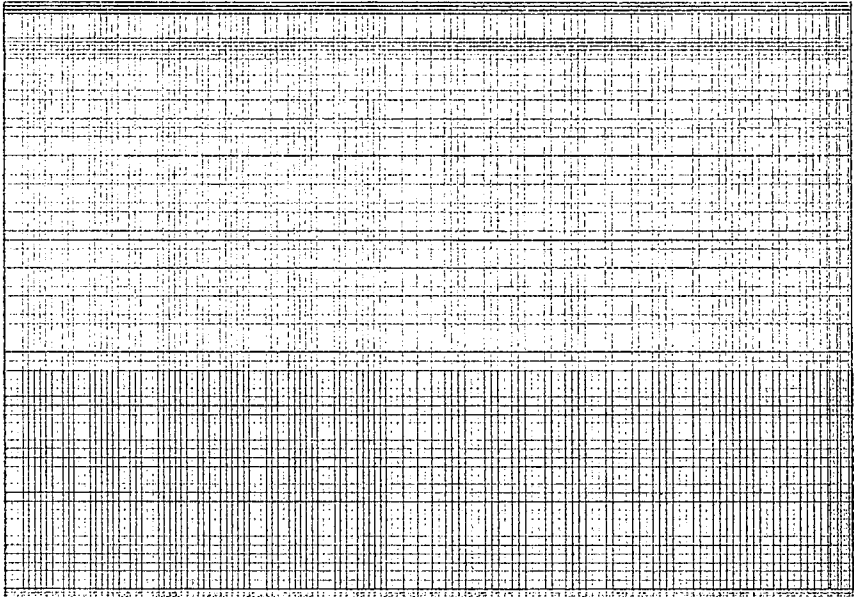
Discharge Batch	# of Assemblies ( ) = Cumulative	Discharge Date	Decay Heat (Btu/hr)
1	53	March 1982	42,328.48
2	85 (138)	July 1983	76,331.10
3	65 (203)	September 84	62,084.82
4	65 (268)	March 1988	78,512.34
5	60 (328)	January 1990	67,259.85
6	59 (387)	August 1991	79,533.70
7	61 (448)	March 1993	89,318.64
8	65 (513)	October 1994	105,360.20
9	74 (587)	April 1996	128,094.90
10	77 (664)	April 1998	150,874.30
11	77 (741)	March 2000	165,643.90
12	73 (814)	March 2002	169,360.80
13	73 (887)	March 2004	192,247.10
14	73 (960)	March 2006	223,432.40
15	73 (1033)	March 2008	235,140.70
16	72 (1105)	March 2010	246,620.70
17	72 (1177)	March 2012	265,758.20
18	72 (1249)	March 2014	295,367.10
19	72 (1321)	March 2016	351,335.20
20	72 (1393)	March 2018	489,991.60
21	72 (1465)	March 2020	960,605.10
22	72 (1537)	March 2022	4,242,958.51
23*	177 (1714)	May 2020	20,938,393.61 21,035,277.29

\* Note: Decay heat loads coincident with maximum bulk temperature reported for Scenario 3A (first value) and Scenario 4A (second value).

**TABLE 5.8.5****DECAY HEAT LOADS FOR "TYPE B" FULL CORE DISCHARGE  
SCENARIOS 3B & 4B**

Discharge Batch	# of Assemblies ( ) = Cumulative	Discharge Date	Decay Heat (Btu/hr)
1	53	March 1982	41,192.54
2	85 (138)	July 1983	74,194.04
3	65 (203)	September 84	60,329.18
4	65 (268)	March 1988	76,120.57
5	60 (328)	January 1990	65,208.01
6	59 (387)	August 1991	76,987.87
7	61 (448)	March 1993	86,396.55
8	65 (513)	October 1994	101,754.70
9	74 (587)	April 1996	123,604.50
10	77 (664)	April 1998	145,341.00
11	77 (741)	March 2000	159,372.30
12	73 (814)	March 2002	162,716.90
13	73 (887)	March 2004	184,236.80
14	73 (960)	March 2006	213,309.70
15	73 (1033)	March 2008	223,432.40
16	72 (1105)	March 2010	232,538.40
17	72 (1177)	March 2012	246,620.70
18	72 (1249)	March 2014	265,758.20
19	72 (1321)	March 2016	295,367.10
20	72 (1393)	March 2018	351,335.20
21	72 (1465)	March 2020	489,991.60
22	72 (1537)	March 2022	960,605.10
23*	177 (1714)	March 2024	24,641,247.20 24,743,019.99

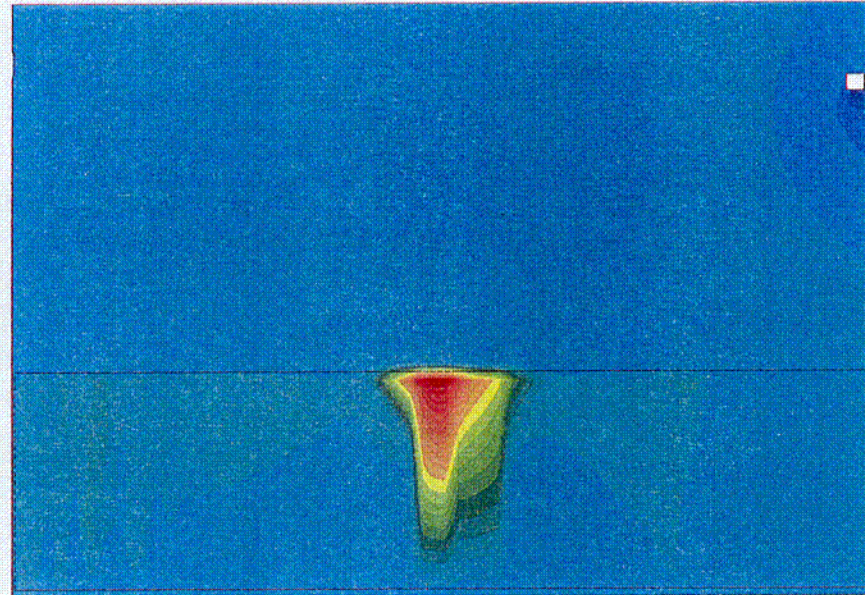
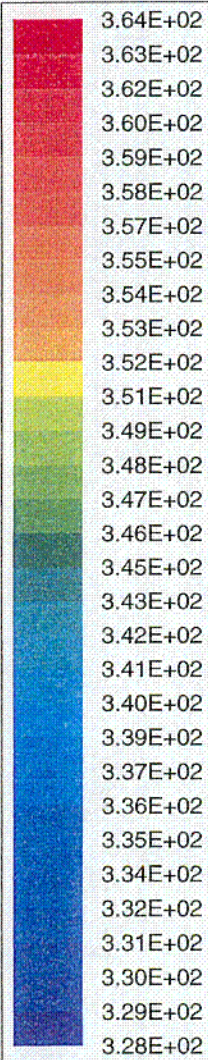
\* Note: Decay heat loads coincident with maximum bulk temperature reported for Scenario 3B (first value) and Scenario 4B (second value).



Grid ( 148 X 79 )

Mar 08 1999  
Fluent 4.48  
Fluent Inc.

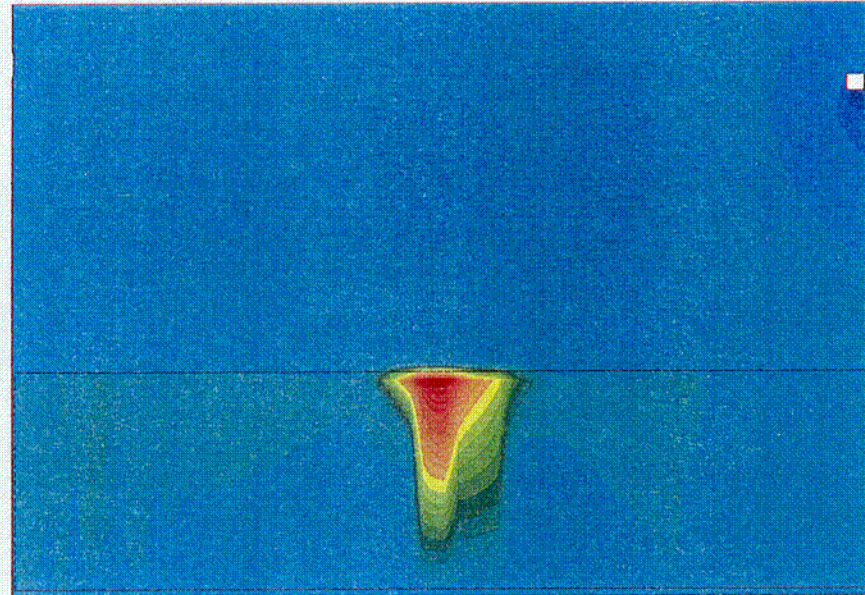
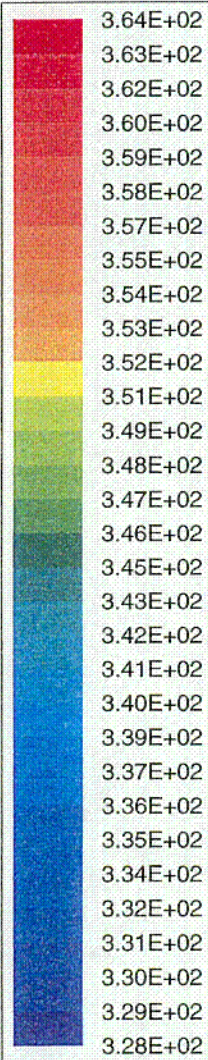
FIGURE 5.6.1: Two-Dimensional Spent Fuel Pool Geometry Grid



DAVIS-BESSE SPENT FUEL POOL TWO-DIMENSIONAL CFD MODEL  
 Temperature (K)  
 Max = 3.639E+02 Min = 3.276E+02

Mar 08 1999  
 Fluent 4.48  
 Fluent Inc.

FIGURE 5.6.2: Two-Dimensional Spent Fuel Pool Model - Temperature Contours



DAVIS-BESSE SPENT FUEL POOL TWO-DIMENSIONAL CFD MODEL

Temperature (K)

Max = 3.639E+02 Min = 3.276E+02

Mar 08 1999

Fluent 4.48

Fluent Inc.

FIGURE 5.6.2: Two-Dimensional Spent Fuel Pool Model - Temperature Contours

## 6.0 STRUCTURAL/SEISMIC CONSIDERATIONS

### 6.1 Introduction

This section considers the structural adequacy of the new Spent Fuel Pool (SFP) maximum density spent fuel racks under all loadings postulated for normal, seismic, and accident conditions at the Davis-Besse Nuclear Power Station (DBNPS). The module layout for the Davis-Besse Spent Fuel Pool (SFP) is illustrated in Figure 1.1, along with the X and Y coordinate axes used to identify displacement orientation.

The analyses, undertaken to confirm the structural integrity of the racks, are performed in compliance with the USNRC Standard Review Plan [6.1.1] and the OT Position Paper [6.1.2]. An abstract of the methodology, modeling assumptions, key results, and summary of the parametric evaluation is presented. Delineation of the relevant criteria is discussed in the text associated with each analysis.

### 6.2 Overview of Rack Structural Analysis Methodology

The response of a free-standing rack module to seismic inputs is highly nonlinear and involves a complex combination of motions (sliding, rocking, twisting, and turning), resulting in impacts and friction effects. Some of the unique attributes of the rack dynamic behavior include a large fraction of the total structural mass in a confined rattling motion, friction support of rack pedestals against lateral motion, and large fluid coupling effects due to deep submergence and independent motion of closely spaced adjacent structures.

Linear methods, such as modal analysis and response spectrum techniques, cannot accurately simulate the structural response of such a highly nonlinear structure to seismic excitation. An accurate simulation is obtained only by direct integration of the nonlinear equations of motion with the three pool slab acceleration time-histories applied as the forcing functions acting simultaneously.

Whole Pool Multi-Rack (WPMR) analysis is the vehicle utilized in this project to simulate the dynamic behavior of the complex storage rack structures. The following sections provide the basis for this selection and discussion on the development of the methodology.

### 6.2.1 Background of Analysis Methodology

Reliable assessment of the stress field and kinematic behavior of the rack modules calls for a conservative dynamic model incorporating all *key attributes* of the actual structure. This means that the model must feature the ability to execute the concurrent motion forms compatible with the free-standing installation of the modules.

The model must possess the capability to effect momentum transfers which occur due to rattling of fuel assemblies inside storage cells and the capability to simulate lift-off and subsequent impact of support pedestals with the pool liner (or bearing pad). The contribution of the water mass in the interstitial spaces around the rack modules and within the storage cells must be modeled in an accurate manner, since erring in quantification of fluid coupling on either side of the actual value is no guarantee of conservatism.

The Coulomb friction coefficient at the pedestal-to-pool liner (or bearing pad) interface may lie in a rather wide range and a conservative value of friction cannot be prescribed *a priori*. In fact, a perusal of results of rack dynamic analyses in numerous docket (Table 6.2.1) indicates that an upper bound value of the coefficient of friction often maximizes the computed rack displacements as well as the equivalent elastostatic stresses.

In short, there are a large number of parameters with potential influence on the rack kinematics. The comprehensive structural evaluation must deal with all of these without sacrificing conservatism.

The three-dimensional single rack dynamic model introduced by Holtec International in the Enrico Fermi Unit 2 rack project (ca. 1980) and used in some 50 rerack projects since that time (Table 6.2.1) addresses most of the above mentioned array of parameters. The details of this methodology are also published in the permanent literature [6.2.1]. Despite the versatility of the 3-D seismic model, the accuracy of the single rack simulations has been suspect due to one key

element; namely, hydrodynamic participation of water around the racks. During dynamic rack motion, hydraulic energy is either drawn from or added to the moving rack, modifying its submerged motion in a significant manner. Therefore, the dynamics of one rack affects the motion of all others in the pool.

A dynamic simulation, which treats only one rack, or a small grouping of racks, is intrinsically inadequate to predict the motion of rack modules with any quantifiable level of accuracy. Three-dimensional Whole Pool Multi-Rack analyses carried out on several previous plants demonstrate that single rack simulations under predict rack displacement during seismic responses [6.2.2].

Briefly, the 3-D rack model dynamic simulation, involving one or more spent fuel racks, handles the array of variables as follows:

Interface Coefficient of Friction Parametric runs are made with upper bound and lower bound values of the coefficient of friction. The limiting values are based on experimental data which have been found to be bounded by the values 0.2 and 0.8. Simulations are also performed with the array of pedestals having randomly chosen coefficients of friction in a Gaussian distribution with a mean of 0.5 and lower and upper limits of 0.2 and 0.8, respectively. In the fuel rack simulations, the Coulomb friction interface between rack support pedestal and liner is simulated by piecewise linear (friction) elements. These elements function only when the pedestal is physically in contact with the pool liner.

Rack Beam Behavior Rack elasticity, relative to the rack base, is included in the model by introducing linear springs to represent the elastic bending action, twisting, and extensions.

Impact Phenomena Compression-only gap elements are used to provide for opening and closing of interfaces such as the pedestal-to-bearing pad interface, and the fuel assembly-to-cell wall interface. These interface gaps are modeled using nonlinear spring elements. The term "nonlinear spring" is a generic term used to denote the mathematical representation of the condition where a restoring force is not linearly proportional to displacement.

Fuel Loading Scenarios The fuel assemblies are conservatively assumed to rattle in unison which obviously exaggerates the contribution of impact against the cell wall.

Fluid Coupling Holtec International extended Fritz's classical two-body fluid coupling model to multiple bodies and utilized it to perform the first two-dimensional multi-rack analysis (Diablo Canyon, ca. 1987). Subsequently, laboratory experiments were conducted to validate the multi-rack fluid coupling theory. This technology was incorporated in the computer code DYNARACK [6.2.4] which handles simultaneous simulation of all racks in the pool as a Whole Pool Multi-Rack 3-D analysis. This development was first utilized in Chinshan, Oyster Creek, and Shearon Harris plants [6.2.1, 6.2.3] and, subsequently, in numerous other rerack projects. The WPMR analyses have corroborated the accuracy of the single rack 3-D solutions in predicting the maximum structural stresses, and also serve to improve predictions of rack kinematics.

For closely spaced racks, demonstration of kinematic compliance is verified by including all modules in one comprehensive simulation using a WPMR model. In WPMR analysis, all rack modules are modeled simultaneously and the coupling effect due to this multi-body motion is included in the analysis. Due to the superiority of this technique in predicting the dynamic behavior of closely spaced submerged storage racks, the Whole Pool Multi-Rack analysis methodology is used for this project.

### 6.3 Description of Racks

The new high density storage racks are analyzed for installation as follows:

#### **RACK WEIGHT DATA**

Model #/Module I.D.	Cells/Module	Array Size	Empty Rack † Dry Weight (lbs)
1/N3	64	8x8	9,600
2/N2	72	9x8	10,800
3/A5	72	9x8	10,800
4/A4	80	10x8	12,600
5/A3	80	10x8	12,600
6/A2	80	10x8	12,600
7/A1	80	10x8	12,600
8/N4	72	8x9	10,800
9/N1	81	9x9	12,150
10/B5	81	9x9	12,150
11/B4	90	10x9	14,030
12/B3	90	10x9	14,030
13/B2	90	10x9	14,030
14/B1	90	10x9	14,030
15/G	64	8x8	10,300
16/F	66	9x8	9,900
17/E	65	9x8	9,750
18/A7	80	10x8	12,600
19/A6	80	10x8	12,600
20/D	72	10x8	11,590
21/C	75	10x8	12,080

For the purpose of modeling, the racks are numbered, 1 through 21. Rack #1 is module N3 in the northeast corner of the pool. The numbering progresses north to south, so that module A1, in the southeast corner is Rack #7 and module C in the southwest corner is Rack #21.

Rack material is defined in Table 6.3.1.

---

† The rack weights listed above represent the values used in the rack seismic/structural analyses. All of these values are conservative (approximately 7 lbs/cell). Racks N1, N2, N3, and N4, contain slightly less conservatism.

The cartesian coordinate system utilized within the rack dynamic model has the following nomenclature:

- x = Horizontal axis along plant North
- y = Horizontal axis along plant West
- z = Vertical axis upward from the rack base

### 6.3.1 Fuel Weights

For the dynamic rack simulations, the dry fuel weight is conservatively taken to be 1682 lbs. The actual fuel assembly weight is 1550 lbs. The higher fuel weight value of 1682 lbs is used to account for control components being stored along with fuel assemblies. Therefore, the analyses conservatively consider control components to be stored along with an assembly at every location.

### 6.4 Synthetic Time-Histories

The synthetic time-histories in three orthogonal directions (N-S, E-W, and vertical) are generated in accordance with the provisions of SRP [6.1.1], Section 3.7.1. In order to prepare an acceptable set of acceleration time-histories, Holtec International's proprietary code GENEQ [6.4.1] is utilized.

A preferred criterion for the synthetic time-histories in SRP 3.7.1 calls for both the response spectrum and the power spectral density corresponding to the generated acceleration time-history to envelope their target (design basis) counterparts with only finite enveloping infractions. The time-histories for the pools have been generated to satisfy this preferred criterion. The seismic files also satisfy the requirements of statistical independence mandated by SRP 3.7.1.

Figures 6.4.1 through 6.4.3 provide plots of the time-history accelerograms which were generated over a 20 second duration for the SSE event. Figures 6.4.4 through 6.4.6 provide plots of the time-history accelerograms which were generated over a 20 second duration for the OBE event. These artificial time-histories are used in all non-linear dynamic simulations of the racks.

Results of the correlation function of the three time-histories are given in Table 6.4.1. Absolute values of the correlation coefficients are shown to be less than 0.15, indicating that the desired statistical independence of the three data sets has been met.

## 6.5 WPMR Methodology

Recognizing that the analytical work effort must deal with both stress and displacement criteria, the sequence of model development and analysis steps that are undertaken are summarized in the following:

- a. Prepare 3-D dynamic models suitable for a time-history analysis of the new maximum density racks. These models include the assemblage of all rack modules in each pool. Include all fluid coupling interactions and mechanical coupling appropriate to performing an accurate non-linear simulation. This 3-D simulation is referred to as a Whole Pool Multi-Rack model.
- b. Perform 3-D dynamic analyses on various physical conditions (such as coefficient of friction and extent of cells containing fuel assemblies). Archive appropriate displacement and load outputs from the dynamic model for post-processing.
- c. Perform stress analysis of high stress areas for the limiting case of all the rack dynamic analyses. Demonstrate compliance with ASME Code Section III, Subsection NF limits on stress and displacement.

### 6.5.1 Model Details for Spent Fuel Racks

The dynamic modeling of the rack structure is prepared with special consideration of all nonlinearities and parametric variations. Particulars of modeling details and assumptions for the Whole Pool Multi-Rack analysis of racks are given in the following:

#### 6.5.1.1 Assumptions

- a. The fuel rack structure motion is captured by modeling the rack as a 12 degree-of-freedom structure. Movement of the rack cross-section at any height is described by six degrees-of-freedom of the rack base and six degrees-of-freedom at the rack top. In this manner, the response of the module, relative to the base-plate, is

captured in the dynamic analyses once suitable springs are introduced to couple the rack degrees-of-freedom and simulate rack stiffness.

- b. Rattling fuel assemblies within the rack are modeled by five lumped masses located at  $H$ ,  $.75H$ ,  $.5H$ ,  $.25H$ , and at the rack base ( $H$  is the rack height measured above the base-plate). Each lumped fuel mass has two horizontal displacement degrees-of-freedom. Vertical motion of the fuel assembly mass is assumed equal to rack vertical motion at the base-plate level. The centroid of each fuel assembly mass can be located off-center, relative to the rack structure centroid at that level, to simulate a partially loaded rack.
- c. Seismic motion of a fuel rack is characterized by random rattling of fuel assemblies in their individual storage locations. All fuel assemblies are assumed to move in-phase within a rack. This exaggerates computed dynamic loading on the rack structure and, therefore, yields conservative results.
- d. Fluid coupling between the rack and fuel assemblies, and between the rack and wall, is simulated by appropriate inertial coupling in the system kinetic energy. Inclusion of these effects uses the methods of [6.5.2, 6.5.3] for rack/assembly coupling and for rack-to-rack coupling.
- e. Fluid damping and form drag are conservatively neglected.
- f. Sloshing is found to be negligible at the top of the rack and is, therefore, neglected in the analysis of the rack.
- g. Potential impacts between the cell walls of the new racks and the contained fuel assemblies are accounted for by appropriate compression-only gap elements between masses involved. The possible incidence of rack-to-wall or rack-to-rack impact is simulated by gap elements at the top and bottom of the rack in two horizontal directions. Bottom gap elements are located at the base-plate elevation. The initial gaps reflect the presence of baseplate extensions, and the rack stiffnesses are chosen to simulate local structural detail.
- h. Pedestals are modeled by gap elements in the vertical direction and as "rigid links" for transferring horizontal stress. Each pedestal support is linked to the pool liner (or bearing pad) by two friction springs. The spring rate for the friction springs includes any lateral elasticity of the stub pedestals. Local pedestal vertical spring stiffness accounts for floor elasticity and for local rack elasticity just above the pedestal.
- i. Rattling of fuel assemblies inside the storage locations causes the gap between fuel assemblies and cell wall to change from a maximum of twice the nominal gap to a theoretical zero gap. Fluid coupling coefficients are based on the nominal gap in order to provide a conservative measure of fluid resistance to gap closure.

- j. The model for the rack is considered supported, at the base level, on four pedestals modeled as non-linear compression only gap spring elements and eight piecewise linear friction spring elements. These elements are properly located with respect to the centerline of the rack beam, and allow for arbitrary rocking and sliding motions.

#### 6.5.1.2 Element Details

Figure 6.5.1 shows a schematic of the dynamic model of a single rack. The schematic depicts many of the characteristics of the model including all of the degrees-of-freedom and some of the spring restraint elements.

Table 6.5.1 provides a complete listing of each of the 22 degrees-of-freedom for a rack model. Six translational and six rotational degrees-of-freedom (three of each type on each end) describe the motion of the rack structure. Rattling fuel mass motions (shown at nodes 1\*, 2\*, 3\*, 4\*, and 5\* in Figure 6.5.1) are described by ten horizontal translational degrees-of-freedom (two at each of the five fuel masses). The vertical fuel mass motion is assumed (and modeled) to be the same as that of the rack baseplate.

Figure 6.5.2 depicts the fuel to rack impact springs (used to develop potential impact loads between the fuel assembly mass and rack cell inner walls) in a schematic isometric. Only one of the five fuel masses is shown in this figure. Four compression only springs, acting in the horizontal direction, are provided at each fuel mass.

Figure 6.5.3 provides a 2-D schematic elevation of the storage rack model, discussed in more detail in Section 6.5.3. This view shows the vertical location of the five storage masses and some of the support pedestal spring members.

Figure 6.5.4 shows the modeling technique and degrees-of-freedom associated with rack elasticity. In each bending plane a shear and bending spring simulate elastic effects [6.5.4].

Linear elastic springs coupling rack vertical and torsional degrees-of-freedom are also included in the model.

Figure 6.5.5 depicts the inter-rack impact springs (used to develop potential impact loads between racks or between rack and wall).

### 6.5.2 Fluid Coupling Effect

In its simplest form, the so-called "fluid coupling effect" [6.5.2, 6.5.3] can be explained by considering the proximate motion of two bodies under water. If one body (mass  $m_1$ ) vibrates adjacent to a second body (mass  $m_2$ ), and both bodies are submerged in frictionless fluid, then Newton's equations of motion for the two bodies are:

$$(m_1 + M_{11}) \ddot{X}_1 + M_{12} \ddot{X}_2 = \text{applied forces on mass } m_1 + O(X_1^2)$$

$$M_{21} \ddot{X}_1 + (m_2 + M_{22}) \ddot{X}_2 = \text{applied forces on mass } m_2 + O(X_2^2)$$

$\ddot{X}_1$ , and  $\ddot{X}_2$  denote absolute accelerations of masses  $m_1$  and  $m_2$ , respectively, and the notation  $O(X^2)$  denotes nonlinear terms.

$M_{11}$ ,  $M_{12}$ ,  $M_{21}$ , and  $M_{22}$  are fluid coupling coefficients which depend on body shape, relative disposition, etc. Fritz [6.5.3] gives data for  $M_{ij}$  for various body shapes and arrangements. The fluid adds mass to the body ( $M_{11}$  to mass  $m_1$ ), and an inertial force proportional to acceleration of the adjacent body (mass  $m_2$ ). Thus, acceleration of one body affects the force field on another. This force field is a function of inter-body gap, reaching large values for small gaps. Lateral motion of a fuel assembly inside a storage location encounters this effect. For example, fluid coupling behavior will be experienced between nodes 2 and 2\* in Figure 6.5.1. The rack analysis also contains inertial fluid coupling terms, which model the effect of fluid in the gaps between adjacent racks.

Terms modeling the effects of fluid flowing between adjacent racks in a single rack analysis suffer from the inaccuracies described earlier. These terms are usually computed assuming that all racks adjacent to the rack being analyzed are vibrating in-phase or 180° out of phase. The WPMR analyses do not require any assumptions with regard to phase.

Rack-to-rack gap elements have initial gaps set to 100% of the physical gap between the racks or between outermost racks and the adjacent pool walls.

#### 6.5.2.1 Multi-Body Fluid Coupling Phenomena

During the seismic event, all racks in the pool are subject to the input excitation simultaneously. The motion of each free-standing module would be autonomous and independent of others as long as they did not impact each other and no water were present in the pool. While the scenario of inter-rack impact is not a common occurrence and depends on rack spacing, the effect of water (the so-called fluid coupling effect) is a universal factor. As noted in Ref. [6.5.2, 6.5.4], the fluid forces can reach rather large values in closely spaced rack geometries. It is, therefore, essential that the contribution of the fluid forces be included in a comprehensive manner. This is possible only if all racks in the pool are *allowed* to execute 3-D motion in the mathematical model. For this reason, single rack or even multi-rack models involving only a portion of the racks in the pool, are inherently inaccurate. The Whole Pool Multi-Rack model removes this intrinsic limitation of the rack dynamic models by simulating the 3-D motion of all modules simultaneously. The fluid coupling effect, therefore, encompasses interaction between *every* set of racks in the pool, i.e., the motion of one rack produces fluid forces on all other racks and on the pool walls. Stated more formally, both near-field and far-field fluid coupling effects are included in the analysis.

The derivation of the fluid coupling matrix [6.5.5] relies on the classical inviscid fluid mechanics principles, namely the principle of continuity and Kelvin's recirculation theorem. While the

derivation of the fluid coupling matrix is based on no artificial construct, it has been nevertheless verified by an extensive set of shake table experiments [6.5.5].

### 6.5.3 Stiffness Element Details

Three element types are used in the rack models. Type 1 are linear elastic elements used to represent the beam-like behavior of the integrated rack cell matrix. Type 2 elements are the piece-wise linear friction springs used to develop the appropriate forces between the rack pedestals and the supporting bearing pads. Type 3 elements are non-linear gap elements, which model gap closures and subsequent impact loadings i.e., between fuel assemblies and the storage cell inner walls, and rack outer periphery spaces.

If the simulation model is restricted to two dimensions (one horizontal motion plus one vertical motion, for example), for the purposes of model clarification only, then Figure 6.5.3 describes the configuration. This simpler model is used to elaborate on the various stiffness modeling elements.

Type 3 gap elements modeling impacts between fuel assemblies and racks have local stiffness  $K_i$  in Figure 6.5.3. Support pedestal spring rates  $K_s$  are modeled by type 3 gap elements. Local compliance of the concrete floor is included in  $K_s$ . The type 2 friction elements are shown in Figure 6.5.3 as  $K_f$ . The spring elements depicted in Figure 6.5.4 represent type 1 elements.

Friction at support/liner interface is modeled by the piecewise linear friction springs with suitably large stiffness  $K_f$  up to the limiting lateral load  $\mu N$ , where  $N$  is the current compression load at the interface between support and liner. At every time-step during transient analysis, the current value of  $N$  (either zero if the pedestal has lifted off the liner, or a compressive finite value) is computed.

The gap element  $K_s$ , modeling the effective compression stiffness of the structure in the vicinity of the support, includes stiffness of the pedestal, local stiffness of the underlying pool slab, and local stiffness of the rack cellular structure above the pedestal.

The previous discussion is limited to a 2-D model solely for simplicity. Actual analyses incorporate 3-D motions.

#### 6.5.4 Coefficients of Friction

To eliminate the last significant element of uncertainty in rack dynamic analyses, multiple simulations are performed to adjust the friction coefficient ascribed to the support pedestal/pool bearing pad interface. These friction coefficients are chosen consistent with the two bounding extremes from Rabinowicz's data [6.5.1]. Simulations are also performed by imposing intermediate value friction coefficients developed by a random number generator with Gaussian normal distribution characteristics. The assigned values are then held constant during the entire simulation in order to obtain reproducible results.<sup>†</sup> Thus, in this manner, the WPMR analysis results are brought closer to the realistic structural conditions.

The coefficient of friction ( $\mu$ ) between the pedestal supports and the pool floor is indeterminate. According to Rabinowicz [6.5.1], results of 199 tests performed on austenitic stainless steel plates submerged in water show a mean value of  $\mu$  to be 0.503 with standard deviation of 0.125. Upper and lower bounds (based on twice standard deviation) are 0.753 and 0.253, respectively. Analyses are therefore performed for coefficient of friction values of 0.2 (lower limit) and for 0.8 (upper limit), and for random friction values clustered about a mean of 0.5. The bounding values of  $\mu = 0.2$  and 0.8 have been found to envelope the upper limit of module response in previous rerack projects.

---

<sup>†</sup> It is noted that DYNARACK has the capability to change the coefficient of friction at any pedestal at each instant of contact based on a random reading of the computer clock cycle. However, exercising this option would yield results that could not be reproduced. Therefore, the random choice of coefficients is made only once per run.

### 6.5.5 Governing Equations of Motion

Using the structural model discussed in the foregoing, equations of motion corresponding to each degree-of-freedom are obtained using Lagrange's Formulation [6.5.4]. The system kinetic energy includes contributions from solid structures and from trapped and surrounding fluid. The final system of equations obtained have the matrix form:

$$[M] \left[ \frac{d^2 q}{d t^2} \right] = [Q] + [G]$$

where:

- [M] - total mass matrix (including structural and fluid mass contributions). The size of this matrix will be  $22n \times 22n$  for a WPMR analysis ( $n$  = number of racks in the model).
- q - the nodal displacement vector relative to the pool slab displacement (the term with q indicates the second derivative with respect to time, i.e., acceleration)
- [G] - a vector dependent on the given ground acceleration
- [Q] - a vector dependent on the spring forces (linear and nonlinear) and the coupling between degrees-of-freedom

The above column vectors have length  $22n$ . The equations can be rewritten as follows:

$$\left[ \frac{d^2 q}{d t^2} \right] = [M]^{-1} [Q] + [M]^{-1} [G]$$

This equation set is mass uncoupled, displacement coupled at each instant in time. The numerical solution uses a central difference scheme built into the proprietary computer program DYNARACK [6.2.4].

## 6.6 Structural Evaluation of Spent Fuel Rack Design

### 6.6.1 Kinematic and Stress Acceptance Criteria

There are two sets of criteria to be satisfied by the rack modules:

#### a. Kinematic Criteria

An isolated fuel rack situated in the middle of the storage cavity is most vulnerable to overturning because such a rack would be hydrodynamically uncoupled from any adjacent structures. Therefore, to assess the margin against overturning, a single rack module is evaluated. According to Ref [6.1.1 and 6.1.2], the minimum required safety margins under the OBE and SSE events are 1.5 and 1.1, respectively. The maximum rotations of the rack (about the two principal axes) are obtained from a post processing of the rack time history response output. The ratio of the rotation required to produce incipient tipping in either principal plane to the actual maximum rotation in that plane from the time history solution is the margin of safety. All ratios available for the OBE and SSE events should be greater than 1.5 and 1.1, respectively to satisfy the regulatory acceptance criteria. However, to be conservative, the worst case displacements from the SSE simulations must ensure a safety factor of 1.5.

#### b. Stress Limit Criteria

Stress limits must not be exceeded under the postulated load combinations provided herein.

## 6.6.2 Stress Limit Evaluations

The stress limits presented below apply to the rack structure and are derived from the ASME Code, Section III, Subsection NF [6.6.1]. Parameters and terminology are in accordance with the ASME Code. Material properties are obtained from the ASME Code Appendices [6.6.2], and are listed in Table 6.3.1.

### (i) Normal and Upset Conditions (Level A or Level B)

- a. Allowable stress in tension on a net section is:

$$F_t = 0.6 S_y$$

Where,  $S_y$  = yield stress at temperature, and  $F_t$  is equivalent to primary membrane stress.

- b. Allowable stress in shear on a net section is:

$$F_v = .4 S_y$$

- c. Allowable stress in compression on a net section is:

$$F_a = S_y \left( .47 - \frac{k l}{444 r} \right)$$

where  $kl/r$  for the main rack body is based on the full height and cross section of the honeycomb region and does not exceed 120 for all sections.

$l$  = unsupported length of component

$k$  = length coefficient which gives influence of boundary conditions. The following values are appropriate for the described end conditions:

1 (simple support both ends)

2 (cantilever beam)

½ (clamped at both ends)

$r$  = radius of gyration of component

- d. Maximum allowable bending stress at the outermost fiber of a net section, due to flexure about one plane of symmetry is:

$$F_b = 0.60 S_y \quad (\text{equivalent to primary bending})$$

- e. Combined bending and compression on a net section satisfies:

$$\frac{f_a}{F_a} + \frac{C_{mx} f_{bx}}{D_x F_{bx}} + \frac{C_{my} f_{by}}{D_y F_{by}} < 1$$

where:

$f_a$  = Direct compressive stress in the section

$f_{bx}$  = Maximum bending stress along x-axis

$f_{by}$  = Maximum bending stress along y-axis

$C_{mx}$  = 0.85

$C_{my}$  = 0.85

$D_x$  =  $1 - (f_a/F'_{ex})$

$D_y$  =  $1 - (f_a/F'_{ey})$

$F'_{ex,ey}$  =  $(\pi^2 E)/(2.15 (kl/r)_{x,y}^2)$

$E$  = Young's Modulus

and subscripts x,y reflect the particular bending plane.

- f. Combined flexure and compression (or tension) on a net section:

$$\frac{f_a}{0.6 S_y} + \frac{f_{bx}}{F_{bx}} + \frac{f_{by}}{F_{by}} < 1.0$$

The above requirements are to be met for both direct tension or compression.

- g. Welds

Allowable maximum shear stress on the net section of a weld is given by:

$$F_w = 0.3 S_u$$

where  $S_u$  is the weld material ultimate strength at temperature. For fillet weld legs in contact with base metal, the shear stress on the gross section is limited to  $0.4S_y$ , where  $S_y$  is the base material yield strength at temperature.

(ii) Level D Service Limits

Section F-1334 (ASME Section III, Appendix F [6.6.2]), states that limits for the Level D condition are the smaller of 2 or  $1.167S_u/S_y$  times the corresponding limits for the Level A condition if  $S_u > 1.2S_y$ , or 1.4 if  $S_u$  less than or equal  $1.2S_y$  except for requirements specifically listed below.  $S_u, S_y$  are the ultimate strength and yield strength at the specified rack design temperature. Examination of material properties for 304 stainless demonstrates that 1.2 times the yield strength is less than the ultimate strength.

Exceptions to the above general multiplier are the following:

- a) Stresses in shear shall not exceed the lesser of  $0.72S_y$  or  $0.42S_u$ . In the case of the Austenitic Stainless material used here,  $0.72S_y$  governs.
- b) Axial Compression Loads shall be limited to  $2/3$  of the calculated buckling load.
- c) Combined Axial Compression and Bending - The equations for Level A conditions shall apply except that:

$F_a = 0.667 \times \text{Buckling Load} / \text{Gross Section Area}$ ,  
and the terms  $F'_{ex}$  and  $F'_{ey}$  may be increased by the factor 1.65.

- d) For welds, the Level D allowable maximum weld stress is not specified in Appendix F of the ASME Code. An appropriate limit for weld throat stress is conservatively set here as:

$$F_w = (0.3 S_u) \times \text{factor}$$

where:

$$\text{factor} = (\text{Level D shear stress limit}) / (\text{Level A shear stress limit})$$

### 6.6.3 Dimensionless Stress Factors

For convenience, the stress results are presented in dimensionless form. Dimensionless stress factors are defined as the ratio of the actual developed stress to the specified limiting value. The limiting value of each stress factor is 1.0. The stress factors reported here include adjustments for ASME Code Section III, Subsection NF slenderness ratio requirements. Stress factors reported are:

$R_1$  = Ratio of direct tensile or compressive stress on a net section to its allowable value  
(note pedestals only resist compression)

$R_2$  = Ratio of gross shear on a net section in the x-direction to its allowable value

$R_3$  = Ratio of maximum x-axis bending stress to its allowable value for the section

$R_4$  = Ratio of maximum y-axis bending stress to its allowable value for the section

$R_5$  = Combined flexure and compressive factor (as defined in the foregoing)

$R_6$  = Combined flexure and tension (or compression) factor (as defined in the foregoing)

$R_7$  = Ratio of gross shear on a net section in the y-direction to its allowable value

#### 6.6.4 Loads and Loading Combinations for Spent Fuel Racks

The applicable loads and their combinations, which must be considered in the seismic analysis of rack modules, are excerpted from the OT Position [6.1.2] and SRP, Section 3.8.4 [6.1.1]. The load combinations considered are identified below:

Loading Combination	Service Level
$D + L$ $D + L + T_o$ $D + L + T_o + E$	Level A
$D + L + T_a + E$ $D + L + T_o + P_f$	Level B
$D + L + T_a + E'$ $D + L + T_o + F_d$	Level D  The functional capability of the fuel racks must be demonstrated.

Where:

- D = Dead weight-induced loads (including fuel assembly weight)
- L = Live Load (not applicable for the fuel rack, since there are no moving objects in the rack load path)
- $P_f$  = Upward force on the racks caused by postulated stuck fuel assembly
- $F_d$  = Impact force from accidental drop of the heaviest load from the maximum possible height.
- E = Operating Basis Earthquake (OBE)
- $E'$  = Safe Shutdown Earthquake (SSE)
- $T_o$  = Differential temperature induced loads (normal operating or shutdown condition based on the most critical transient or steady state condition)
- $T_a$  = Differential temperature induced loads (the highest temperature associated with the postulated abnormal design conditions)

$T_a$  and  $T_o$  produce local thermal stresses. The worst thermal stress field in a fuel rack is obtained when an isolated storage location has a fuel assembly generating heat at maximum postulated rate and surrounding storage locations contain no fuel. Heated water makes unobstructed contact with the inside of the storage walls, thereby producing maximum possible temperature difference between adjacent cells. Secondary stresses produced are limited to the body of the rack; that is, support pedestals do not experience secondary (thermal) stresses.

### 6.7 Parametric Simulations

The following table presents a complete listing of the simulations discussed herein:

LIST OF RACK SIMULATIONS				
<u>Case</u>	<u>Model</u>	<u>Load Case</u>	<u>COF</u>	<u>Event</u>
1	WPMR	All Racks Fully Loaded	0.2	SSE
2	WPMR	All Racks Fully Loaded	0.8	SSE
3	WPMR	All Racks Fully Loaded	Random	SSE
4	WPMR	All Racks Fully Loaded	0.2	OBE
5	WPMR	All Racks Fully Loaded	0.8	OBE
6	WPMR	All Racks Fully Loaded	Random	OBE
7	Single Rack	Module D Fully Loaded	0.8	SSE
8	Single Rack	Module D Half Loaded (E-W)	0.8	SSE
9	Single Rack	Module D Half Loaded (N-S)	0.8	SSE
10	Single Rack	Module D Half Loaded (Diag)	0.8	SSE
11	Single Rack	Module D Nearly Empty	0.8	SSE
12	Single Rack	Module B4 Fully Loaded	0.8	SSE

where:

Random = Gaussian distribution with a mean of 0.5 Coefficient of friction (upper and lower limits of 0.8 and 0.2).

### 6.7.1 Transfer Pit Rack

There is an additional configuration represented by the possibility of temporarily installing a rack in the transfer pit. The results from the single rack evaluations included in the gamut of simulations listed above bound any single rack to be installed in the transfer pit. The single rack simulations included above represent the heaviest and highest aspect (length/width plan dimension) ratio racks. These two rack attributes are expected to control in the behavior of single (uncoupled) racks in seismic analyses. Therefore, the predicted dynamic behavior and corresponding displacements and stresses of the single rack to be installed in the transfer pit will be bounded by the analyses listed above.

## 6.8 Time History Simulation Results

The results from the DYNARACK runs may be seen in the raw data output files. However, due to the huge quantity of output data, a post-processor is used to scan for worst case conditions and develop the stress factors discussed in subsection 6.6.3. Further reduction in this bulk of information is provided in this section by extracting the worst case values from the parameters of interest; namely displacements, support pedestal forces, impact loads, and stress factors. This section also summarizes other analyses performed to develop and evaluate structural member stresses which are not determined by the post processor.

### 6.8.1 Rack Displacements

The maximum rack displacements are obtained from the time histories of the motion of the upper and lower four corners of each rack in each of the simulations. The maximum absolute value of displacement in the two horizontal directions, relative to the pool slab, is reported for each rack, at the top and bottom corners. The maximum displacement in either direction, is 0.337" from module D during simulation 1 of the WPMR analyses and 0.430" from simulation 7 of the single rack analysis, which was performed for module D. To assess the safety margin against rack overturning for the new racks, an evaluation is performed considering the maximum rack displacement value of 0.43" obtained from case 7. The safety factor against overturning is shown to be 111, which far exceeds the acceptance criteria of 1.5. It is to be noted that case 12, a

single rack run for module B4, one of the heaviest racks in the pool, had a displacement of only 0.308". This confirms that the simulations for module D (the rack with the highest aspect ratio) control over the heaviest rack.

The existing racks are currently installed with seismic braces to the walls of the Spent Fuel Pool. These braces must be removed in order to disassemble and remove the existing racks. Dynamic analyses were performed for the existing racks to establish kinematic stability in the unlikely scenario that a seismic event occurs during reracking. The model consisted of a single rack with no fluid coupling to adjacent surfaces. The maximum displacements were determined to be less than 1 degree, which is much less than the rotation required for overturning. Thus, the existing racks are kinematically stable in the interim reracking configuration.

#### 6.8.2 Pedestal Vertical Forces

The maximum vertical pedestal force obtained in the WPMR simulations was 107,000 lbf for module B-1, one of the four heaviest racks, in both simulations 2 and 3. The maximum vertical pedestal force obtained in the single rack simulations was 122,000 lbf for module B-4 in simulation 12.

#### 6.8.3 Pedestal Friction Forces

The maximum interface shear force value in any direction bounding all pedestals in the WPMR simulations is 27,500 lbf for module A2 in case 3. From the single rack runs, a maximum shear force of 26,300 lbf was calculated for case 10, which was run for module D.

#### 6.8.4 Rack Impact Loads

A freestanding rack, by definition, is a structure subject to potential impacts during a seismic event. Impacts arise from rattling of the fuel assemblies in the storage rack locations and, in some instances, from localized impacts between the racks, or between a peripheral rack and the pool wall. The following sections discuss the bounding values of these impact loads.

#### 6.8.4.1 Rack to Rack Impacts

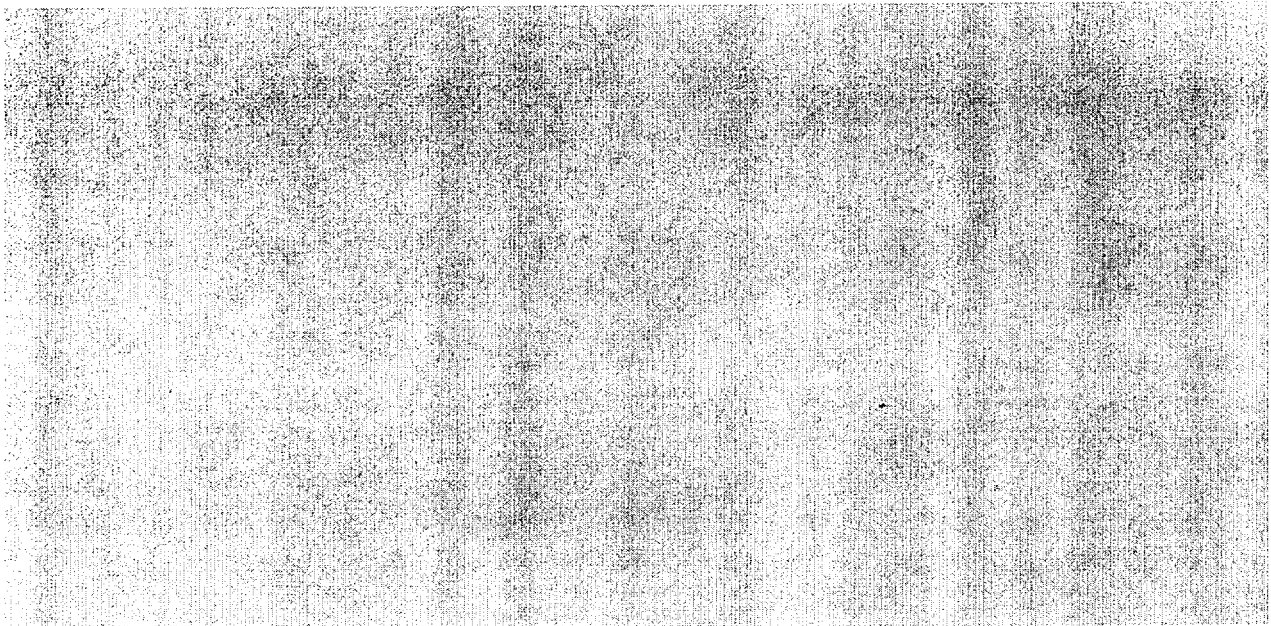
Gap elements track the potential for impacts between any rack and the pool walls. The results for each simulation have been scanned for non-zero values. The simulation results show that no gap element between any rack and any portion of the pool walls and between any two rack tops closes. The tabular results do show some contact forces develop between rack-to-rack at the baseplate elevation during the simulations. Baseplate gaps are initially set to zero, so impact loads (contact forces) are expected. The maximum contact load of 9858 lbf occurred in simulation no. 1 at a localized rack bottom location).

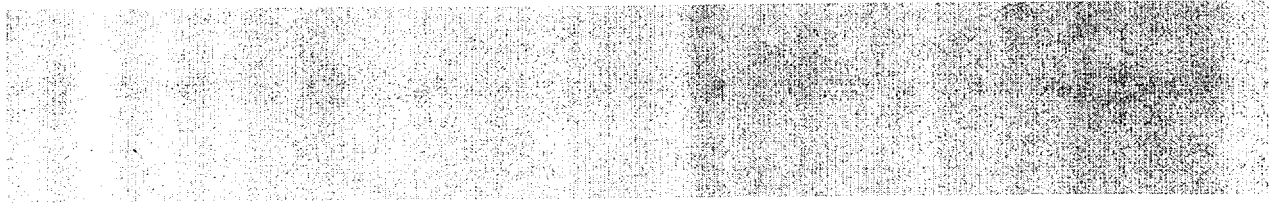
#### 6.8.4.2 Rack to Wall Impacts

The storage racks do not impact the pool walls under any simulation.

#### 6.8.4.3 Fuel to Cell Wall Impact Loads

A review of all simulations performed allows determination of the maximum instantaneous impact load between fuel assembly and fuel cell wall at any modeled impact site. The maximum fuel/cell wall impact load is 517 lbf for module E in case 1. The cell wall integrity under this instantaneous impact load has been evaluated and shown to remain intact with no permanent damage.





## 6.9 Rack Structural Evaluation

### 6.9.1 Rack Stress Factors

The time history results from the DYNARACK solver provide the pedestal normal and lateral interface forces, which may be converted to the limiting bending moment and shear force at the bottom baseplate-pedestal interface. In particular, maximum values for the previously defined stress factors are determined for every pedestal in the array of racks. With this information available, the structural integrity of the pedestal can be assessed and reported. The net section maximum (in time) bending moments and shear forces can also be determined at the bottom baseplate-rack cellular structure interface for each spent fuel rack in the pool. Using these forces and moments, the maximum stress in the limiting rack cell (box) can be evaluated.

The stress factor results for male and female pedestals, and for the entire spent fuel rack cellular cross section just above the bottom casting has been determined. These factors are reported for every rack in each simulation, and for each pedestal in every rack. These locations are the most heavily loaded net sections in the structure so that satisfaction of the stress factor criteria at these locations ensures that the overall structural criteria set forth in Section 6.6 are met.

An evaluation of the stress factors for all of the simulations performed, leads to the conclusion that all stress factors, as defined in Section 6.6.3, are less than the mandated limit of 1.0 for all of the load cases examined. From all of the simulations, the bounding stress factor was found to be 0.298 for the OBE simulations 4 thru 6, which all occurred in module A7. The maximum calculated SSE stress factor was 0.216 for case 12 (module B4). All these stress factors are for cell wall stresses, since these control over the pedestal stress factors. The values for all other

defined stress factors are archived and show that the requirements of Section 6.6 are indeed satisfied for the load levels considered for every limiting location in every rack in the array.

### 6.9.2 Pedestal Thread Shear Stress

The maximum engagement thread stresses under faulted conditions for every pedestal for every rack in the pool from all the simulations run was 5178 psi for the single rack run of case number 12. This maximum stress is less than the Level A allowable stress of  $0.4 * F_y = 0.4(25,000) = 10,000$  psi.

### 6.9.3 Local Stresses Due to Impacts

Impact loads at the pedestal base (discussed in subsection 6.8.2) produce stresses in the pedestal for which explicit stress limits are prescribed in the Code. However, impact loads on the cellular region of the racks, as discussed in subsection 6.8.4.3 above, produce stresses which attenuate rapidly away from the loaded region. This behavior is characteristic of secondary stresses.

Even though limits on secondary stresses are not prescribed in the Code for class 3 NF structures, evaluations must be made to ensure that the localized impacts do not lead to plastic deformations in the storage cells which affect the sub-criticality of the stored fuel array.

#### a. Impact Loading Between Fuel Assembly and Cell Wall

Local cell wall integrity is conservatively estimated from peak impact loads. Plastic analysis is used to obtain the limiting impact load which would lead to gross permanent deformation. As shown in Table 6.9.1, the limiting impact load (of 3,031 lbf, including a safety factor of 2.0) is much greater than the highest calculated impact load value (of 517 lbf, see subsection 6.8.4.3) obtained from any of the rack analyses. Therefore, fuel impacts do not represent a significant concern with respect to fuel rack cell deformation.

#### b. Impacts Between Adjacent Racks

As may be seen from subsection 6.8.4.1, the bottom of the storage racks will impact each other at a few locations during seismic events. Since the loading is presented edge-on to

the 3/4" baseplate membrane, the distributed stresses after local deformation will be negligible. The impact loading will be distributed over a large area (a significant portion of the entire minimum baseplate length of about 74 inches by its 3/4 inch thickness). The resulting compressive stress from the highest impact load of 9858 lbs distributed over 55 sq. inches is only 180 psi, which is negligible. This is a conservative computation, since the simulation assumes a local impact site. Therefore, any deformation will not affect the configuration of the stored fuel.

#### 6.9.4 Weld Stresses

Weld locations subjected to significant seismic loading are at the bottom of the rack at the baseplate-to-cell connection, at the top of the pedestal support at the baseplate connection, and at cell-to-cell connections. Bounding values of resultant loads are used to qualify the connections.

##### a. Baseplate-to-Rack Cell Welds

For Level A or B conditions, Ref. [6.6.1] permits an allowable weld stress of  $\tau = .3 S_u = 21300$  psi. As stated in subsection 6.6.2, the allowable may be increased for Level D by an amplification factor which is equal to 1.8 ( $= .72S_y/.4S_y$ ). The allowable stress increase factor of 1.8 greatly exceeds the ratio of maximum SSE to OBE stresses. Therefore, Level B becomes the governing condition.

Weld dimensionless stress factors are produced through the use of a simple conversion (ratio) factor applied to the corresponding stress factor in the adjacent rack material. The ratio 2.20 is developed from the differences in material thickness and length versus weld throat dimension and length:

$$RATIO = \text{[REDACTED]}$$

The highest predicted weld stress for OBE is calculated from the highest R6 value (see subsection 6.9.1) as follows:

$$R6 * [(0.6) Fy] * \text{RATIO} = 0.298 * [0.6 * 25000] * 2.2 = 9,834 \text{ psi}$$

This value is less than the Level A allowable weld stress value, which is 21,300.

Therefore, all weld stresses between the baseplate and cell wall base are acceptable.

b. Baseplate-to-Pedestal Welds

The weld between baseplate and support pedestal is checked using finite element analysis to determine that the maximum stress is 4,232 psi under a Level D event. This calculated stress value is well below the OBE allowable of 21,300 psi which is conservative.

c. Cell-to-Cell Welds

Cell-to-cell connections are by a series of connecting welds along the cell height. Stresses in storage cell to cell welds develop due to fuel assembly impacts with the cell wall. These weld stresses are conservatively calculated by assuming that fuel assemblies in adjacent cells are moving out of phase with one another so that impact loads in two adjacent cells are in opposite directions; this tends to separate the two cells from each other at the weld.

Table 6.9.1 gives results for the maximum allowable load that can be transferred by these welds based on the available weld area. An upper bound on the load required to be transferred is also given in Table 6.9.1 and is much lower than the allowable load. This upper bound value is very conservatively obtained by applying the bounding rack-to-fuel impact load from any simulation in two orthogonal directions simultaneously, and multiplying the result by 2 to account for the simultaneous impact of two assemblies. An equilibrium analysis at the connection then yields the upper bound load to be transferred.

It is seen from the results in Table 6.9.1 that the calculated load is well below the allowable.

The cell-to-cell welds are also subjected to shear resulting from the "shear flow" behavior associated with beam action. Shear flow tends to delaminate the cell boxes and will be maximized near the center of the rack near the baseplate. An evaluation is performed based on the rack dimensionless stress factors R2 and R7 discussed above. It is seen from the results in Table 6.9.1 that the weld stress is determined to be 5,075 psi, which is less than the allowable of 10,000 psi.

#### 6.9.5 Bearing Pad Analysis

To protect the pool slab from highly localized dynamic loadings, bearing pads are placed between the pedestal base and the slab. Fuel rack pedestals impact on these bearing pads during a seismic event and pedestal loading is transferred to the liner. Bearing pad dimensions are set to ensure that the average pressure on the slab surface due to a static load plus a dynamic impact load does not exceed the American Concrete Institute, ACI-349 [6.9.1] limit on bearing pressures. Section 10.17 of [6.9.2] gives the design bearing strength as

$$f_b = \phi (.85 f'_c) \epsilon$$

where  $\phi = .7$  and  $f'_c$  is the specified concrete strength for the spent fuel pool.  $\epsilon = 1$  except when the supporting surface is wider on all sides than the loaded area. In that case,  $\epsilon = (A_2/A_1)^{.5}$ , but not more than 2.  $A_1$  is the actual loaded area, and  $A_2$  is an area greater than  $A_1$  and is defined in [6.9.2]. Using a value of  $\epsilon > 1$  includes credit for the confining effect of the surrounding concrete. It is noted that this criterion is in conformance with the ultimate strength primary design methodology of the American Concrete Institute in use since 1971. For the DBNPS,  $f'_c = 4,000$  psi and the allowable static bearing pressure is  $f_b = 4,760$  psi, assuming full concrete confinement. The allowable bearing pressure computed above is conservatively computed by taking  $\epsilon=1$  to account for lack of total concrete confinement in the leak chase region. Thus, the

maximum allowable concrete bearing pressure is 2,380 psi. The acceptance criterion for the bearing pad is to show that this primarily compressive component remains in the elastic range.

The analyses are performed with ANSYS using finite element models, which place a bearing pad and rack pedestal directly above a leak chase location, and in areas of existing liner hold down plate obstructions. The liner hold down plates are approximately 1" in height above the liner. These configurations are selected with the intent of bounding all other possible bearing pad/pool floor interfaces. The liner plate is conservatively neglected in order to maximize bearing pad and concrete stresses. The analysis applies the maximum vertical pedestal load from results for all pedestals scanned from the time-history solutions from all simulations. The maximum vertical pedestal load is taken to be 122,000 lbs.

The bearing pads in the SFP will be 2" thick, except in areas of liner hold down plate interferences, where the pad will be 1" thick with approximately 1" thick shims surrounding the interfering plates. The bearing pads in the TP will be 1.5" thick. Bearing pad models were prepared to evaluate all possible configurations. All bearing pads will be made from austenitic stainless steel plate stock. Figure 6.9.1 provides an isometric of the controlling ANSYS finite element model (leak chase condition). The model permits the bearing pad to deform and lose contact with the liner, if the conditions of elastostatics so dictate. Figure 6.9.1 shows the bearing pad and underlying leak chase located within the supporting concrete. The slab is modeled as an elastic foundation. Figure 6.9.2 shows the pressure profile in the underlying concrete computed by the ANSYS analysis.

The average pressure at the pad to liner interface is computed and compared against the above-mentioned limit. Calculations show that the average pressure at the slab / liner interface is 1,360 psi, which is well below the allowable value of 2,380 psi, providing a factor of safety of 1.75. The stress distribution in the bearing pad is also evaluated, with the results shown in Figure 6.9.3. The peak bending stress in the bearing pad under the maximum vertical load is 24,170 psi. The material yield strength of 25,000 psi at 200°F provides an allowable stress of 1.2 Sy (i.e.,

30,000 psi) producing a factor of safety against yield of about 1.24. Therefore, the bearing pad design devised for the DBNPS SFP is deemed appropriate for the prescribed loadings.

#### 6.10 Level A Evaluation

The Level A condition is not a governing condition for spent fuel racks since the general level of loading is far less than Level B loading. Additionally, the material stresses computed for the Level B loadings were compared against Level A allowables. This practice ensures Level A conditions are always bounded by level B conditions.

#### 6.11 Hydrodynamic Loads on Pool Walls

The hydrodynamic pressures that develop between adjacent racks and the pool walls can be developed from the archived results produced by the WPMR analysis. The time dependent pressures are determined for the rack that resulted in the maximum displacement. The pressure plots on the four walls of the SFP at the time of maximum (in absolute value) instantaneous hydrodynamic pressure for the SSE event are shown in Figure 6.11.1.

#### 6.12 Local Stress Considerations

This section presents the results of evaluations for the possibility of cell wall buckling and the secondary stresses produced by temperature effects.

##### 6.12.1 Cell Wall Buckling

The allowable local buckling stresses in the fuel cell walls are obtained by using classical plate buckling analysis. The evaluation for cell wall buckling is based on the applied stress being uniform along the entire length of the cell wall. In the actual fuel rack, the compressive stress comes from consideration of overall bending of the rack structures during a seismic event, and as such is negligible at the rack top, and maximum at the rack bottom.

The critical buckling stress is determined to be 10,117 psi. The computed compressive stress in the cell wall, based on the R5 stress factor, is 3,825 psi. Therefore, there is more than a 1.5 margin of safety against local cell wall buckling.

#### 6.12.2 Analysis of Welded Joints in the Racks

Cell-to-cell welded joints are examined under the loading conditions arising from thermal effects due to an isolated hot cell in this subsection. This secondary stress condition is evaluated alone and not combined with primary stresses from other load conditions.

A thermal gradient between cells will develop when an isolated storage location contains a fuel assembly emitting maximum postulated heat, while the surrounding locations are empty. We can obtain a conservative estimate of weld stresses along the length of an isolated hot cell by considering a beam strip uniformly heated by the thermal gradient, and restrained from growth along one long edge. This thermal gradient is based on the results of the thermal-hydraulic evaluations, which show that the difference between the local cell maximum temperatures and the bulk temperature in the pool is 42.75°F. The analyzed configuration is shown in Figure 6.12.1.

Using shear beam theory, an estimate of the maximum value of the average shear stress in the strip is given as  $\tau_{\max} = 11,778$  psi. Since this is a secondary thermal stress, we use all allowable shear stress criteria for faulted conditions ( $0.42 * S_u = 29,820$  psi) as a guide to indicate that the maximum shear is acceptable. The margin of safety against cell wall shear failure due to cell wall growth is 2.5 for the worst case hot cell conditions.

## 6.13 References

- [6.1.1] USNRC NUREG-0800, Standard Review Plan, June 1987.
- [6.1.2] (USNRC Office of Technology) "OT Position for Review and Acceptance of Spent Fuel Storage and Handling Applications", dated April 14, 1978, and January 18, 1979 amendment thereto.
- [6.2.1] Soler, A.I. and Singh, K.P., "Seismic Responses of Free Standing Fuel Rack Constructions to 3-D Motions", Nuclear Engineering and Design, Vol. 80, pp. 315-329 (1984).
- [6.2.2] Soler, A.I. and Singh, K.P., "Some Results from Simultaneous Seismic Simulations of All Racks in a Fuel Pool", INNEM Spent Fuel Management Seminar X, January, 1993.
- [6.2.3] Singh, K.P. and Soler, A.I., "Seismic Qualification of Free Standing Nuclear Fuel Storage Racks - the Chin Shan Experience, Nuclear Engineering International, UK (March 1991).
- [6.2.4] Holtec Proprietary Report HI-961465 - WPMR Analysis User Manual for Pre&Post Processors & Solver, August, 1997.
- [6.4.1] Holtec Proprietary Report HI-89364 - Verification and User's Manual for Computer Code GENEQ, January, 1990.
- [6.5.1] Rabinowicz, E., "Friction Coefficients of Water Lubricated Stainless Steels for a Spent Fuel Rack Facility," MIT, a report for Boston Edison Company, 1976.
- [6.5.2] Singh, K.P. and Soler, A.I., "Dynamic Coupling in a Closely Spaced Two-Body System Vibrating in Liquid Medium: The Case of Fuel Racks," 3rd International Conference on Nuclear Power Safety, Keswick, England, May 1982.
- [6.5.3] Fritz, R.J., "The Effects of Liquids on the Dynamic Motions of Immersed Solids," Journal of Engineering for Industry, Trans. of the ASME, February 1972, pp 167-172.

- [6.5.4] Levy, S. and Wilkinson, J.P.D., "The Component Element Method in Dynamics with Application to Earthquake and Vehicle Engineering," McGraw Hill, 1976.
- [6.5.5] Paul, B., "Fluid Coupling in Fuel Racks: Correlation of Theory and Experiment", (Proprietary), NUSCO/Holtec Report HI-88243.
- [6.6.1] ASME Boiler & Pressure Vessel Code, Section III, Subsection NF, 1989 Edition.
- [6.6.2] ASME Boiler & Pressure Vessel Code, Section III, Appendices, 1989 Edition.
- [6.8.1] Chun, R., Witte, M. and Schwartz, M., "Dynamic Impact Effects on Spent Fuel Assemblies," UCID-21246, Lawrence Livermore National Laboratory, October 1987.
- [6.9.1] ACI 349-85, Code Requirements for Nuclear Safety Related Concrete Structures, American Concrete Institute, Detroit, Michigan, 1985.
- [6.9.2] ACI 318-95, Building Code requirements for Structural Concrete," American Concrete Institute, Detroit, Michigan, 1995.

Table 6.2.1

PARTIAL LISTING OF FUEL RACK APPLICATIONS USING DYNARACK		
PLANT	DOCKET NUMBER(s)	YEAR
Enrico Fermi Unit 2	USNRC 50-341	1980
Quad Cities 1 & 2	USNRC 50-254, 50-265	1981
Rancho Seco	USNRC 50-312	1982
Grand Gulf Unit 1	USNRC 50-416	1984
Oyster Creek	USNRC 50-219	1984
Pilgrim	USNRC 50-293	1985
V.C. Summer	USNRC 50-395	1984
Diablo Canyon Units 1 & 2	USNRC 50-275, 50-323	1986
Byron Units 1 & 2	USNRC 50-454, 50-455	1987
Braidwood Units 1 & 2	USNRC 50-456, 50-457	1987
Vogtle Unit 2	USNRC 50-425	1988
St. Lucie Unit 1	USNRC 50-335	1987
Millstone Point Unit 1	USNRC 50-245	1989
Chinshan	Taiwan Power	1988
D.C. Cook Units 1 & 2	USNRC 50-315, 50-316	1992
Indian Point Unit 2	USNRC 50-247	1990
Three Mile Island Unit 1	USNRC 50-289	1991
James A. FitzPatrick	USNRC 50-333	1990
Shearon Harris Unit 2	USNRC 50-401	1991
Hope Creek	USNRC 50-354	1990
Kuosheng Units 1 & 2	Taiwan Power Company	1990

Table 6.2.1

## PARTIAL LISTING OF FUEL RACK APPLICATIONS USING DYNARACK

PLANT	DOCKET NUMBER(s)	YEAR
Ulchin Unit 2	Korea Electric Power Co.	1990
Laguna Verde Units 1 & 2	Comision Federal de Electricidad	1991
Zion Station Units 1 & 2	USNRC 50-295, 50-304	1992
Sequoyah	USNRC 50-327, 50-328	1992
LaSalle Unit 1	USNRC 50-373	1992
Duane Arnold Energy Center	USNRC 50-331	1992
Fort Calhoun	USNRC 50-285	1992
Nine Mile Point Unit 1	USNRC 50-220	1993
Beaver Valley Unit 1	USNRC 50-334	1992
Salem Units 1 & 2	USNRC 50-272, 50-311	1993
Limerick	USNRC 50-352, 50-353	1994
Ulchin Unit 1	KINS	1995
Yonggwang Units 1 & 2	KINS	1996
Kori-4	KINS	1996
Connecticut Yankee	USNRC 50-213	1996
Angra Unit 1	Brazil	1996
Sizewell B	United Kingdom	1996
Waterford 3	USNRC 50-382	1997
J.A. Fitzpatrick	USNRC 50-333	1998
Callaway	USNRC 50-483	1998
Nine Mile Unit 1	USNRC 50-220	1998

Table 6.2.1

## PARTIAL LISTING OF FUEL RACK APPLICATIONS USING DYNARACK

PLANT	DOCKET NUMBER(s)	YEAR
Chin Shan	Taiwan Power Company	1998
Vermont Yankee	USNRC 50-271	1998
Millstone 3	USNRC 50-423	1998
Byron/Braidwood	USNRC 50-454, 50-455, 50-567, 50-457	1999
Wolf Creek	USNRC 50-482	1999
Plant Hatch Units 1 & 2	USNRC 50-321, 50-366	1999
Harris Pools C and D	USNRC 50-401	1999

Table 6.3.1 RACK MATERIAL DATA (200°F) (ASME - Section II, Part D)			
Stainless Steel Material	Young's Modulus E (psi)	Yield Strength S <sub>y</sub> (psi)	Ultimate Strength S <sub>u</sub> (psi)
SA240, Type 304 (cell boxes)	27.6 x 10 <sup>6</sup>	25,000	71,000
SUPPORT MATERIAL DATA (200°F)			
SA240, Type 304 (upper part of support feet)	27.6 x 10 <sup>6</sup>	25,000	71,000
SA-564-630 (lower part of support feet; age hardened at 1100°F)	28.5 x 10 <sup>6</sup>	106,300	140,000

Table 6.4.1 TIME-HISTORY STATISTICAL CORRELATION RESULTS	
OBE	
Data1 to Data2	0.057
Data1 to Data3	0.008
Data2 to Data3	-0.002
SSE	
Data1 to Data2	0.064
Data1 to Data3	0.006
Data2 to Data3	-0.004

Data1 corresponds to the time-history acceleration values along the X axis (South)

Data2 corresponds to the time-history acceleration values along the Y axis (East)

Data3 corresponds to the time-history acceleration values along the Z axis (Vertical)

Table 6.5.1

Degrees-of-freedom

<u>LOCATION (Node)</u>	<u>DISPLACEMENT</u>			<u>ROTATION</u>		
	$U_x$	$U_y$	$U_z$	$\theta_x$	$\theta_y$	$\theta_z$
1	$p_1$	$p_2$	$p_3$	$q_4$	$q_5$	$q_6$
2	$p_7$	$p_8$	$p_9$	$q_{10}$	$q_{11}$	$q_{12}$
Node 1 is assumed to be attached to the rack at the bottom most point. Node 2 is assumed to be attached to the rack at the top most point. Refer to Figure 6.5.1 for node identification.						
2*	$p_{13}$	$p_{14}$				
3*	$p_{15}$	$p_{16}$				
4*	$p_{17}$	$p_{18}$				
5*	$p_{19}$	$p_{20}$				
1*	$p_{21}$	$p_{22}$				
where the relative displacement variables $q_i$ are defined as:  $p_i = q_i(t) + U_x(t) \quad i = 1,7,13,15,17,19,21$ $= q_i(t) + U_y(t) \quad i = 2,8,14,16,18,20,22$ $= q_i(t) + U_z(t) \quad i = 3,9$ $= q_i(t) \quad i = 4,5,6,10,11,12$ $p_i$ denotes absolute displacement (or rotation) with respect to inertial space $q_i$ denotes relative displacement (or rotation) with respect to the floor slab  * denotes fuel mass nodes $U(t)$ are the three known earthquake displacements						

Table 6.9.1 COMPARISON OF BOUNDING CALCULATED LOADS/STRESSES VS. CODE ALLOWABLES AT IMPACT LOCATIONS AND AT WELDS		
Item/Location	SSE	
	Calculated	Allowable <sup>†</sup>
Fuel assembly/cell wall impact, lbf.	517	3,031 <sup>††</sup>
Rack/baseplate weld, psi	9,834	21,300
Female pedestal/baseplate weld, psi	4,232	21,300
Cell/cell welds, psi, based on impact loads	2,298 <sup>†††</sup>	10,000
Cell/cell welds, psi, based on shear flow	5,075 <sup>†††</sup>	10,000

<sup>†</sup> Note that Level A condition allowables were conservatively applied against SSE loads.

<sup>††</sup> Based on the limit load for a cell wall. The allowable load on the fuel assembly itself may be less than this value (see discussion in Section 6.8.4.3), but will be greater than 517 lbs.

<sup>†††</sup> Based on the base metal stresses adjacent to weld placements resulting from the maximum shear flow developed between two adjacent cells.

Figure 6.4.1; Davls-Besse SFP and Cask Plt  
Time History Accelerogram  
X direction Bounding SSE Spectra (2% Dampng)

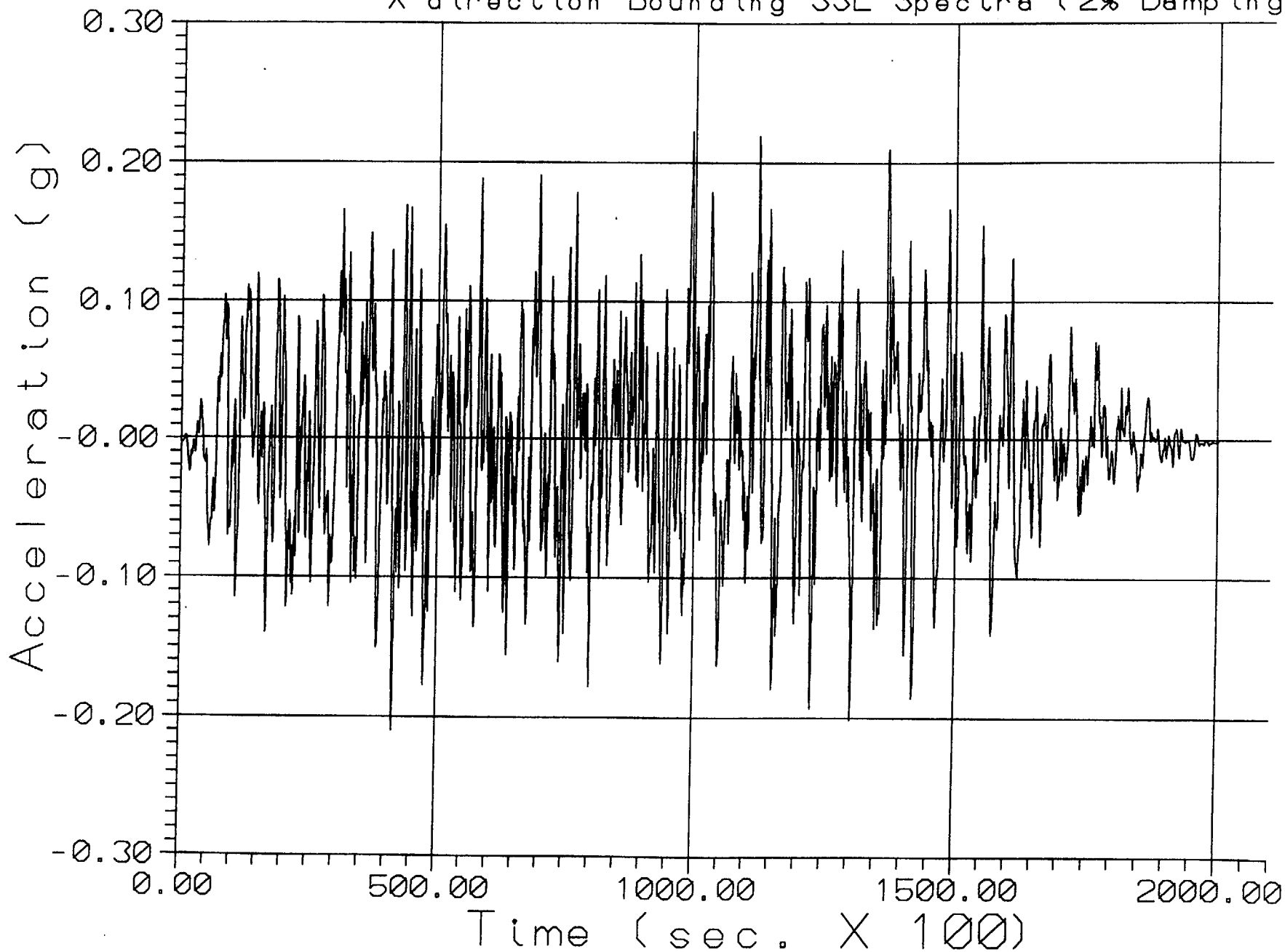


Figure 6.4.2; Davits-Besse SFP and Cask Plt  
Time History Accelerogram  
Y direction Bounding SSE Spectra (2% Damping)

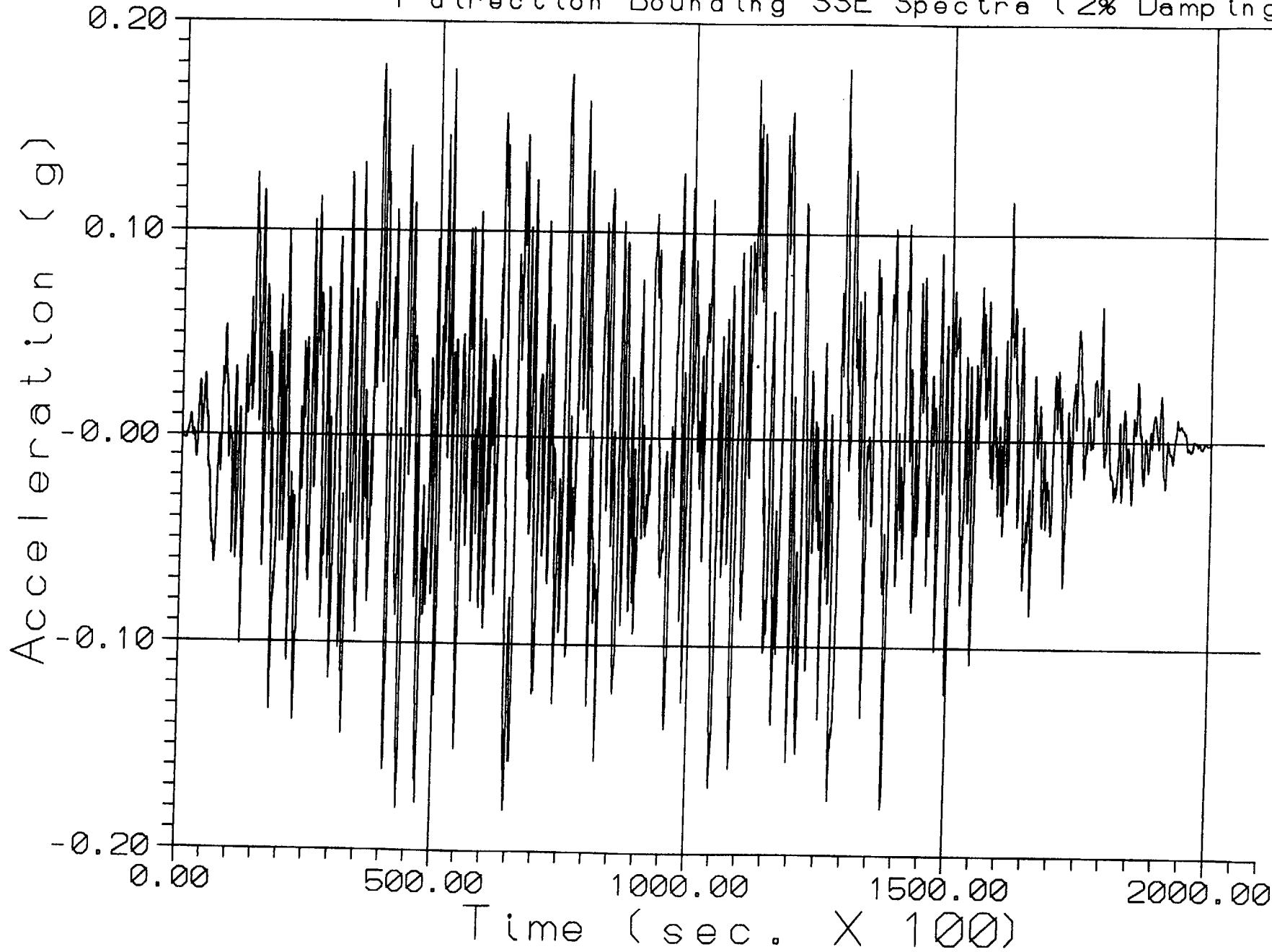


Figure 6.4.3: Davits-Besse SFP and Cask P1t  
Time History Accelerogram  
Z direction Bounding SSE Spectra (2% Damping)

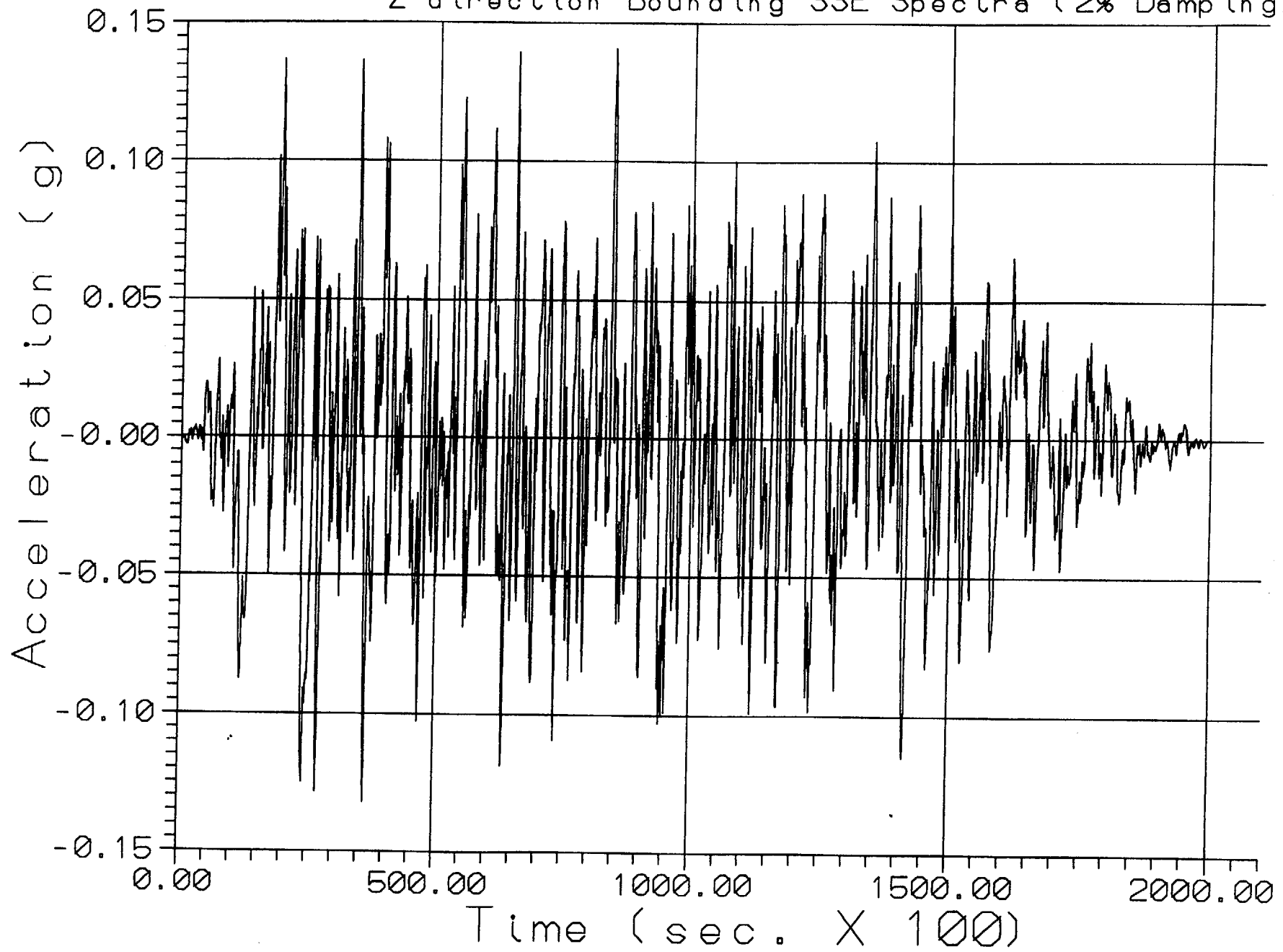


Figure 6.4.4; Davis-Besse SFP and Cask Pit  
Time History Accelerogram  
X direction Bounding OBE Spectra (2% Damping)

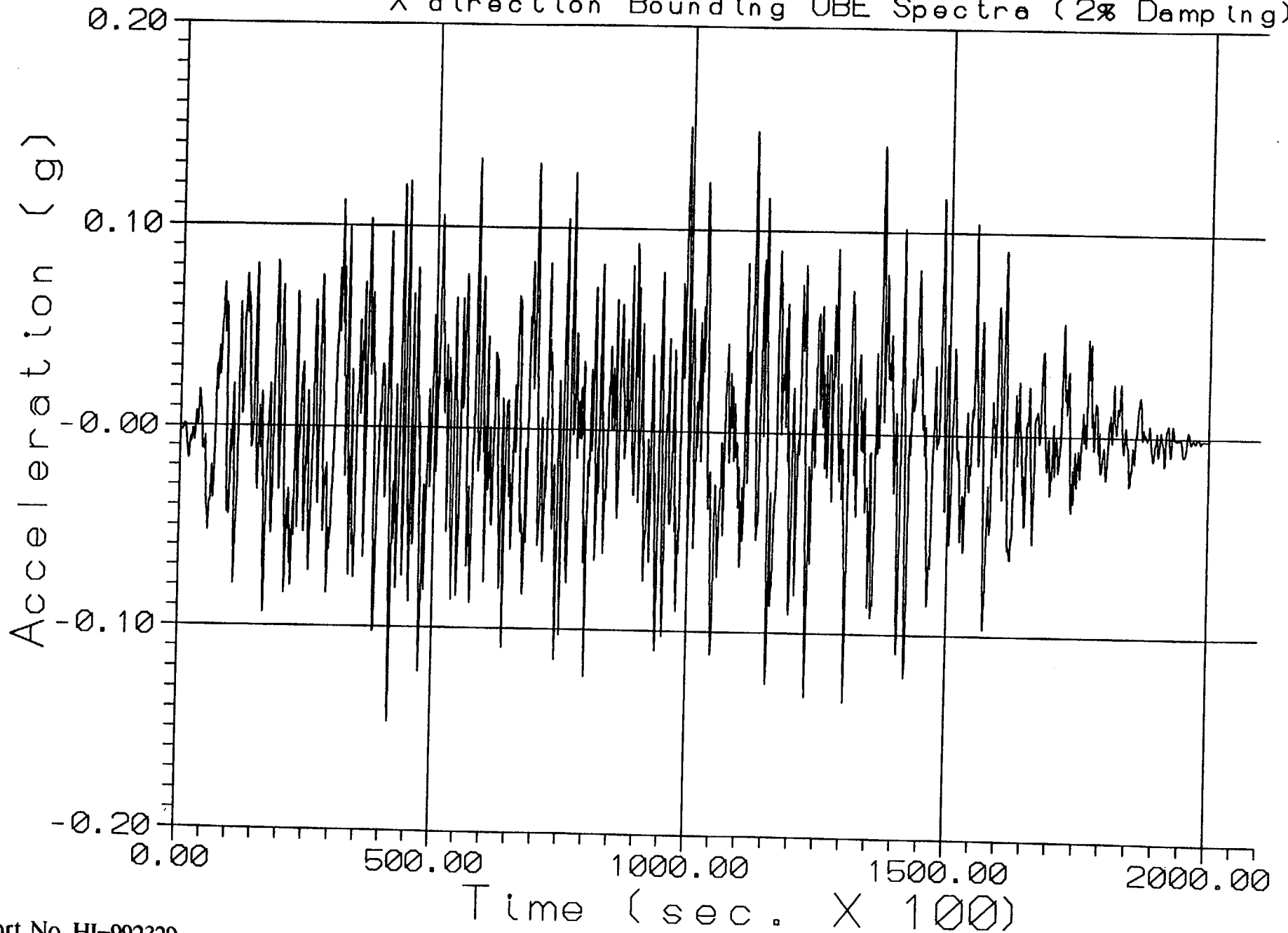


Figure 6.4.5: Davits-Besse SFP and Cask Plt  
Time History Accelerogram  
Y direction Bounding OBE Spectra (2% Damping)

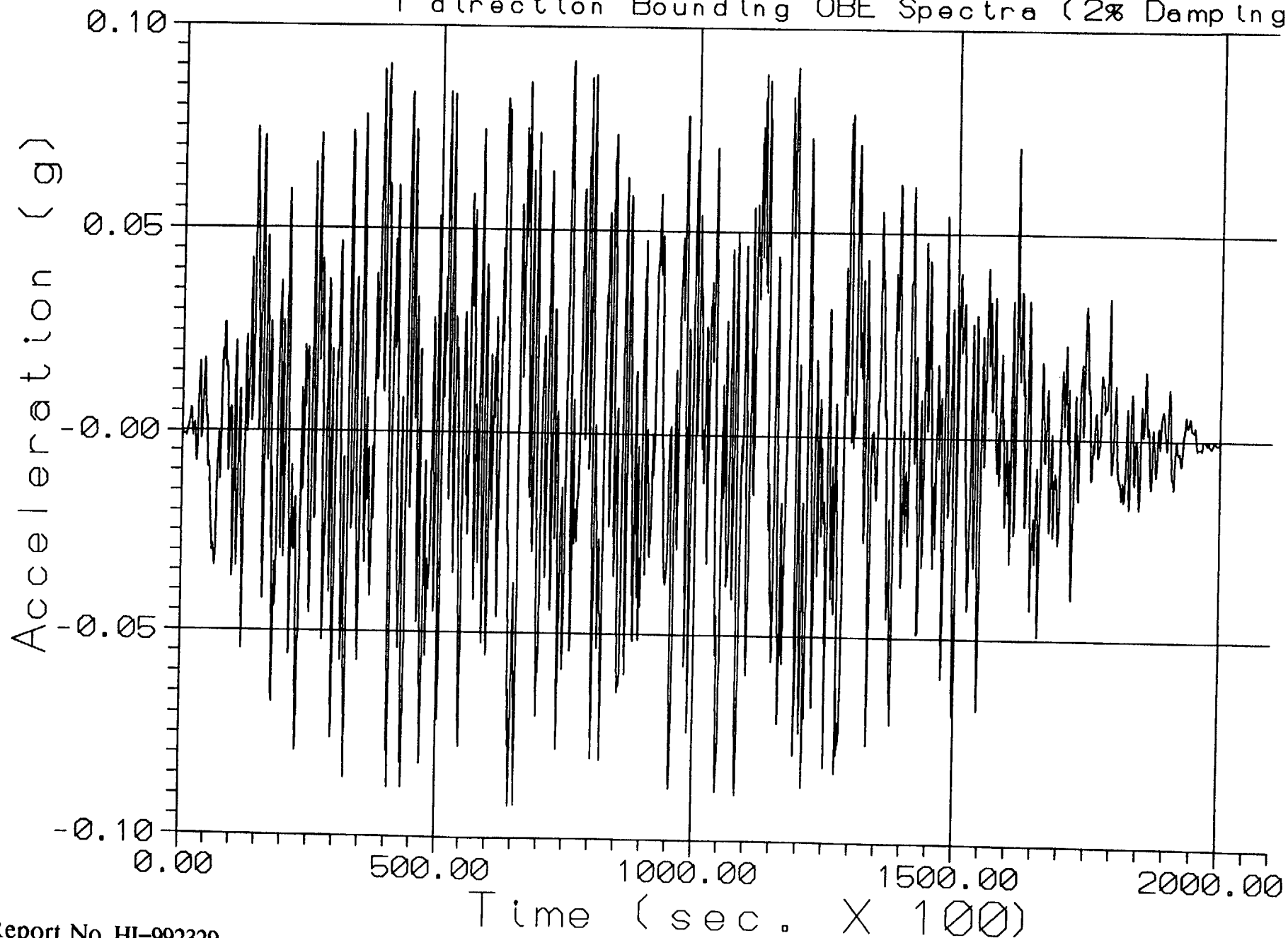
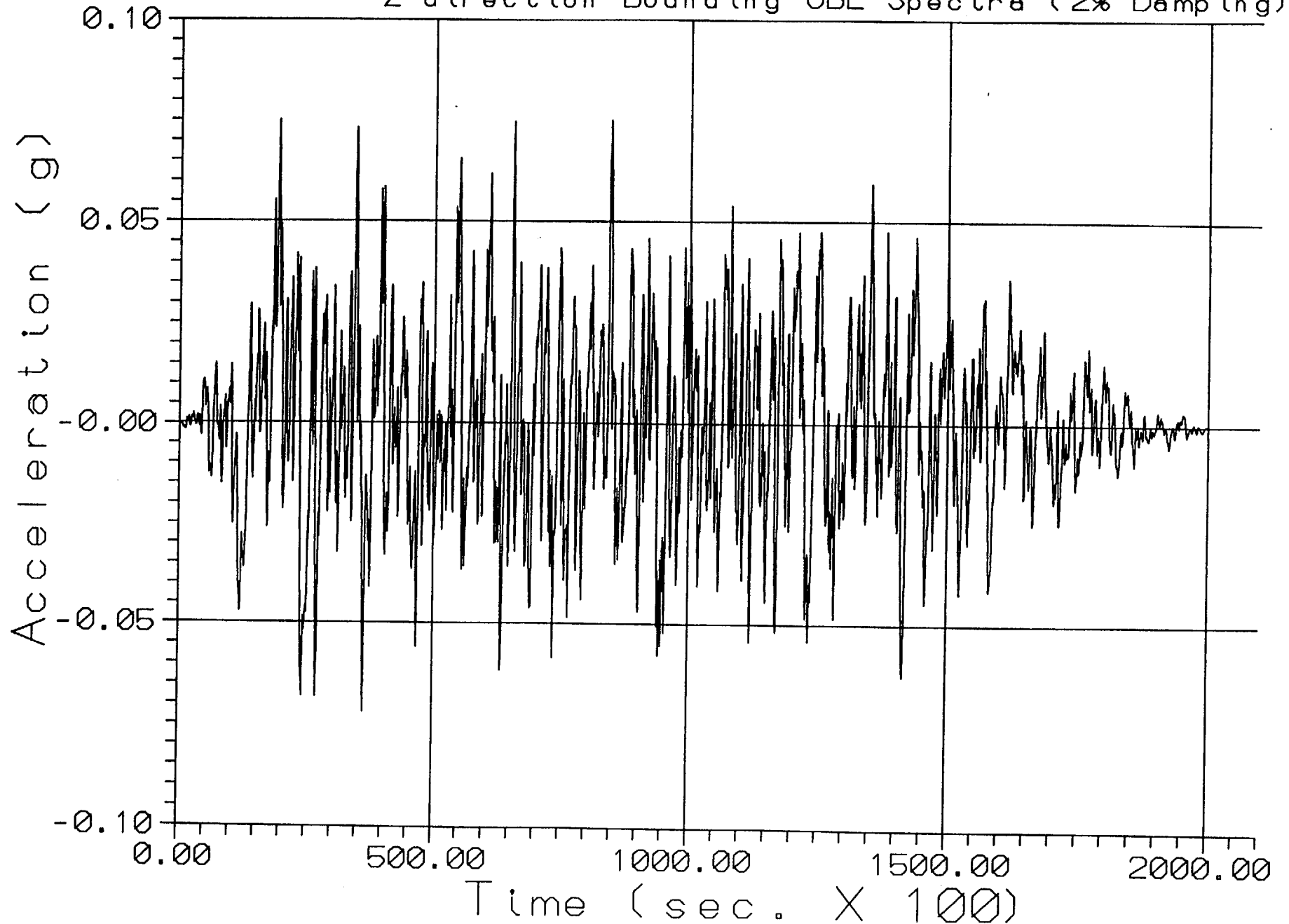


Figure 6.4.6: Davits-Besse SFP and Cask Plt  
Time History Accelerogram  
Z direction Bounding OBE Spectra (2% Damping)



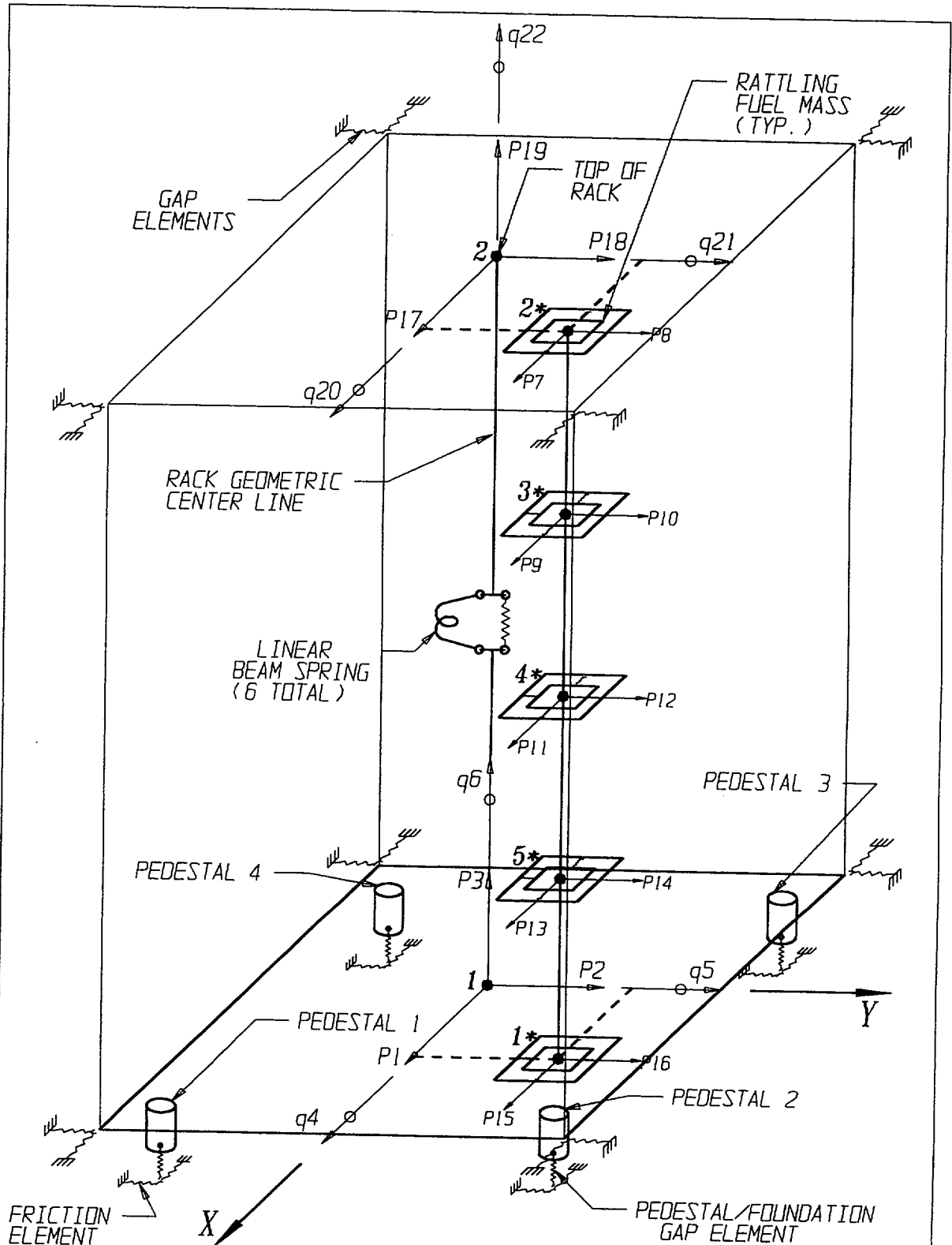


FIGURE 6.5.1; SCHEMATIC OF THE DYNAMIC MODEL OF A SINGLE RACK MODULE USED IN DYNARACK

Report No. HI-992329

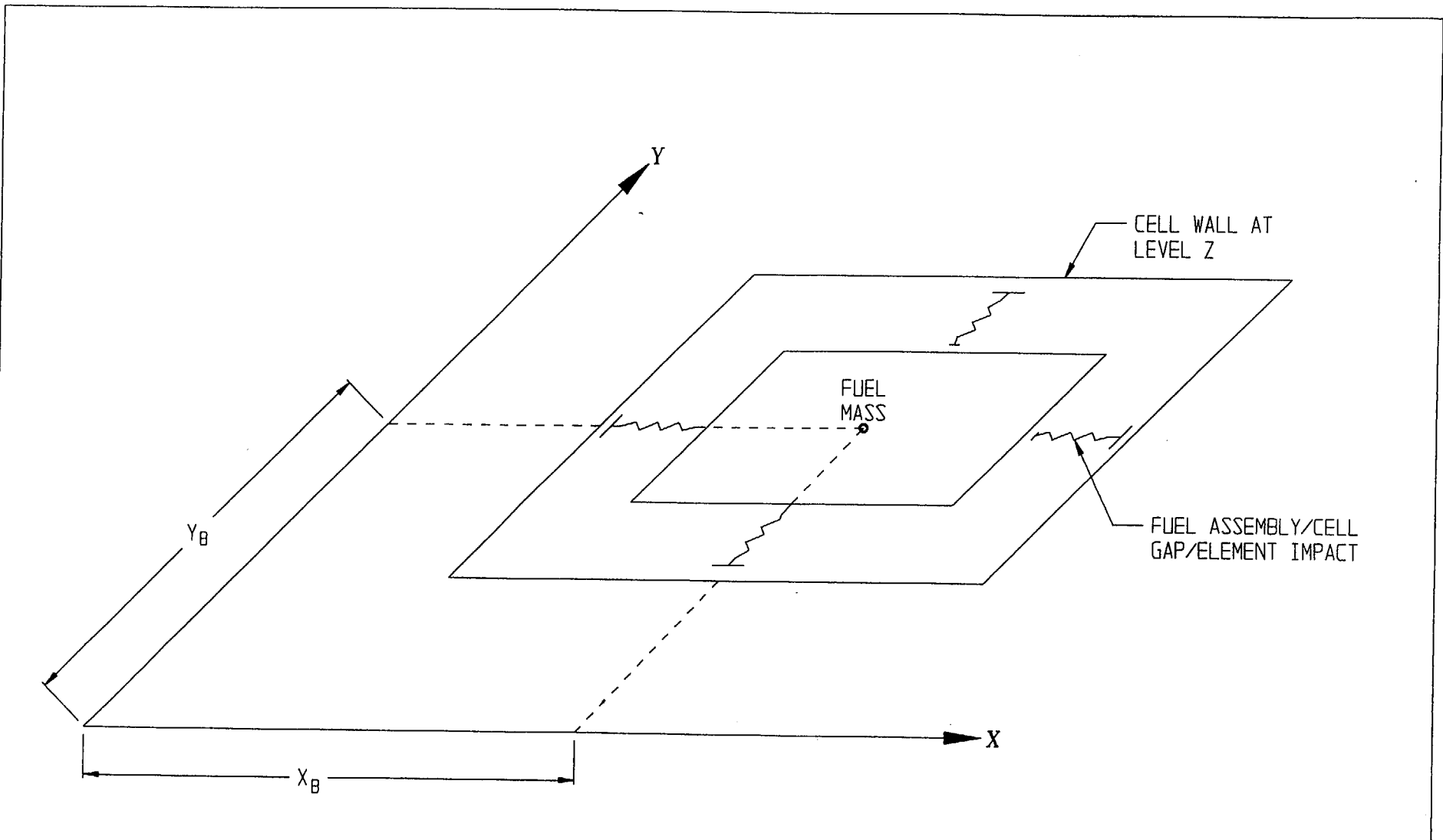


FIGURE 6.5.2 FUEL-TO-RACK GAP/IMPACT ELEMENTS AT LEVEL OF RATTLING MASS

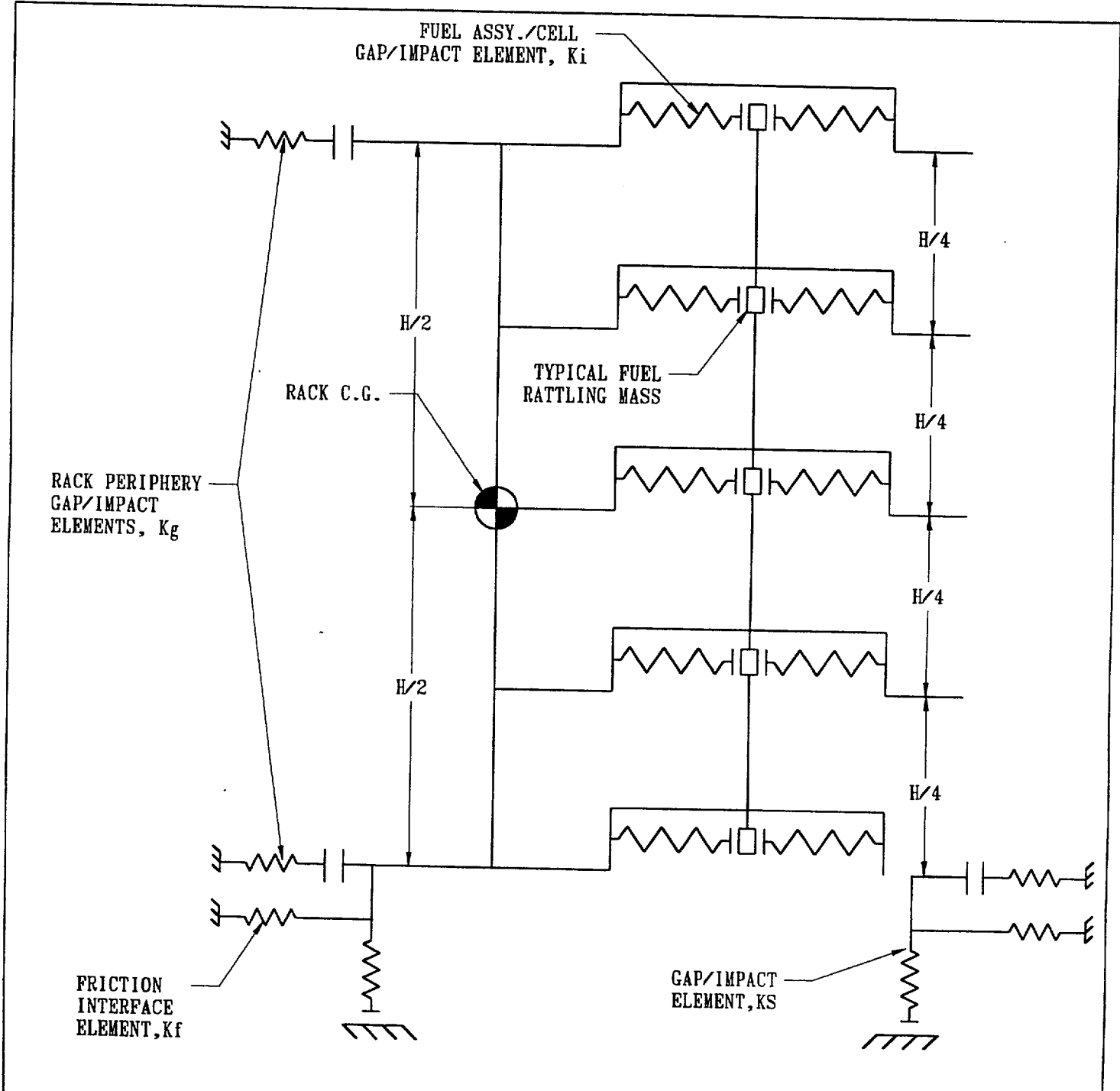
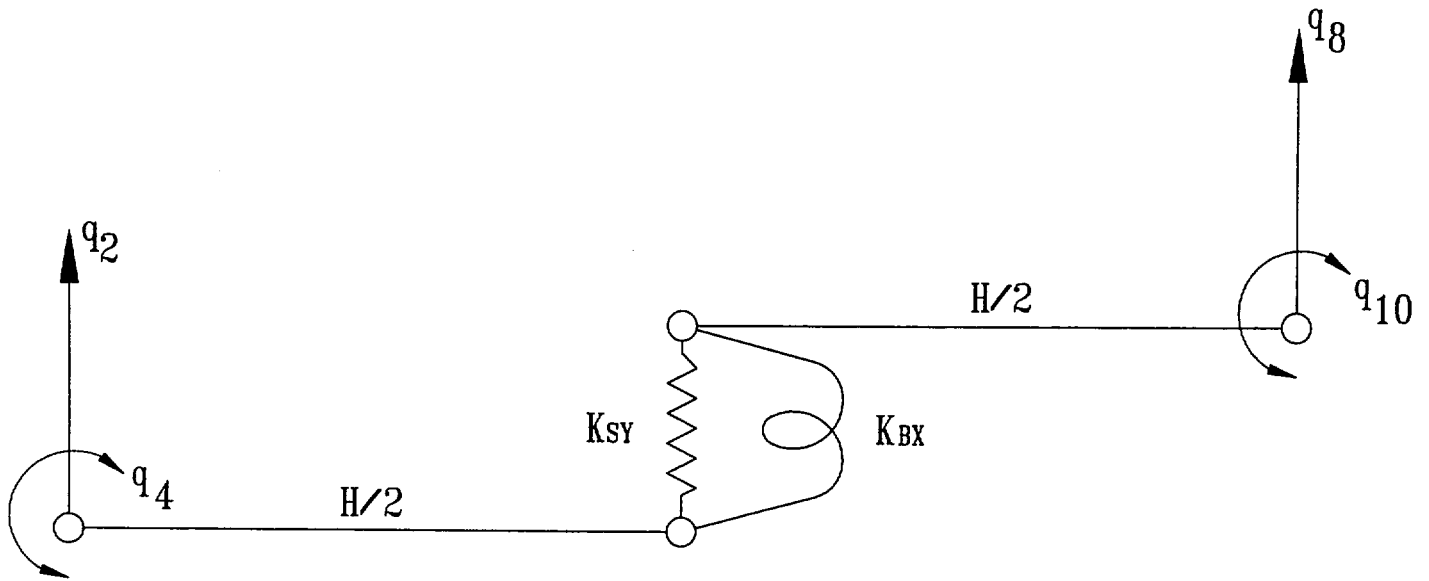
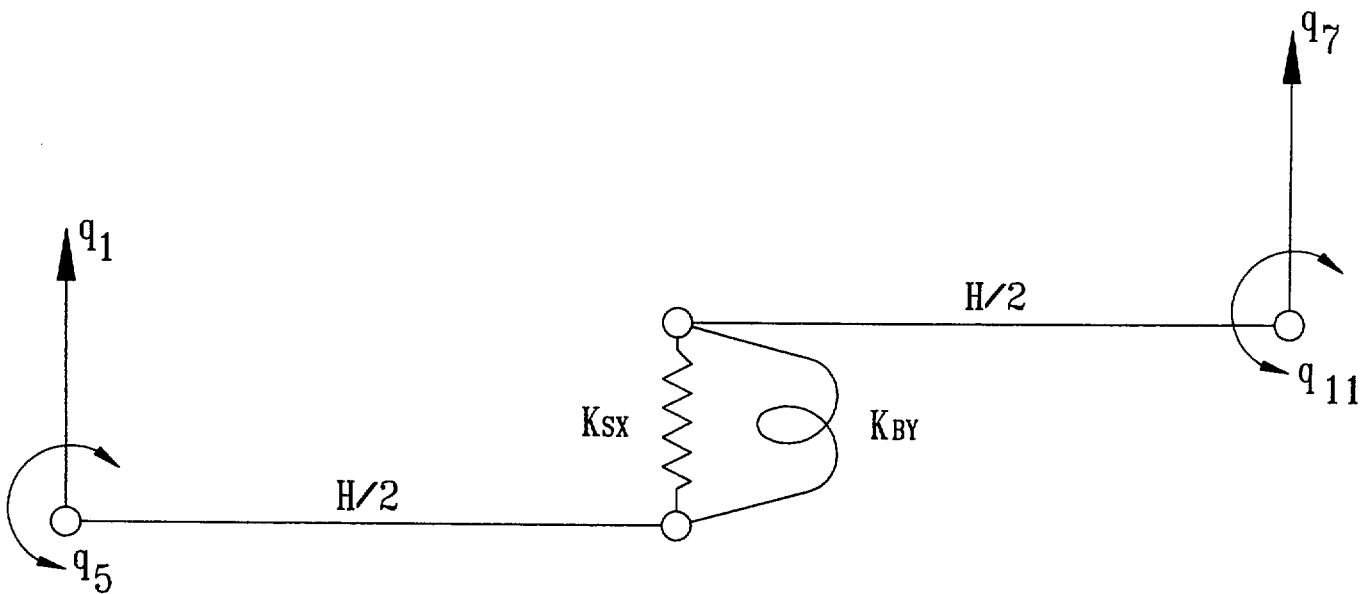


FIGURE 6.5.3; TWO DIMENSIONAL VIEW OF THE  
 SPRING-MASS SIMULATION

Report No. HI-992329



FOR Y-Z PLANE BENDING



FOR X-Z PLANE BENDING

FIGURE 6.5.4; RACK DEGREES-OF-FREEDOM WITH SHEAR AND BENDING SPRINGS

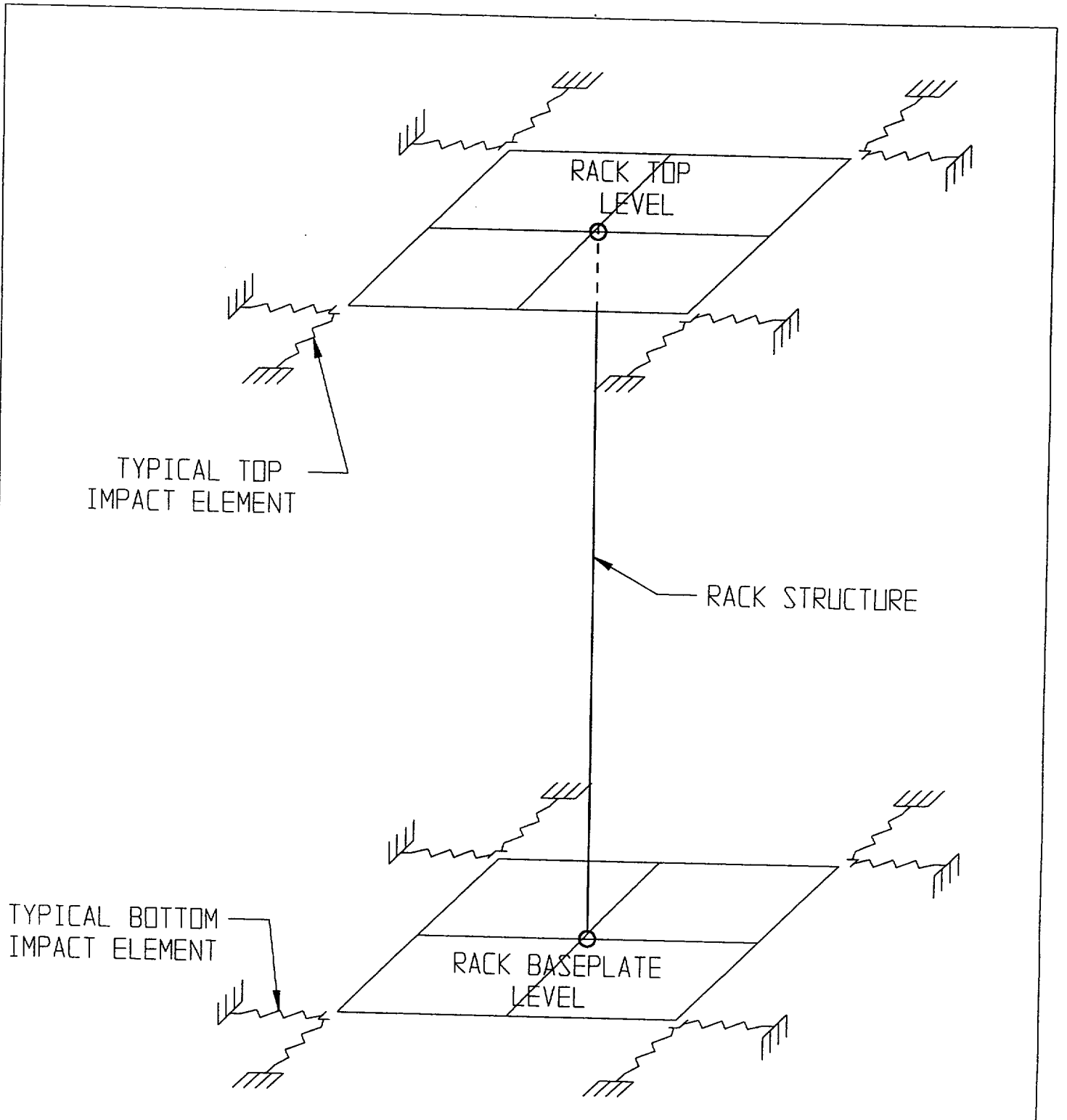
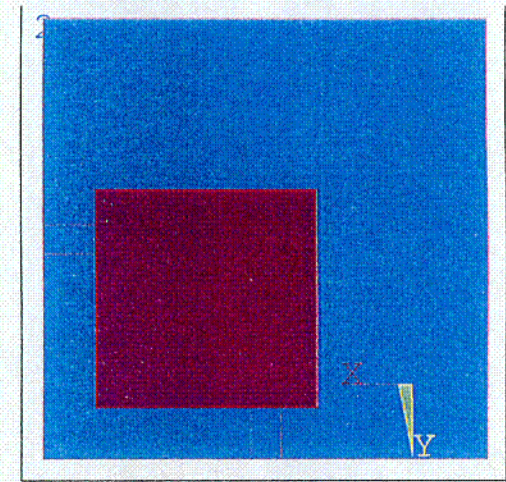
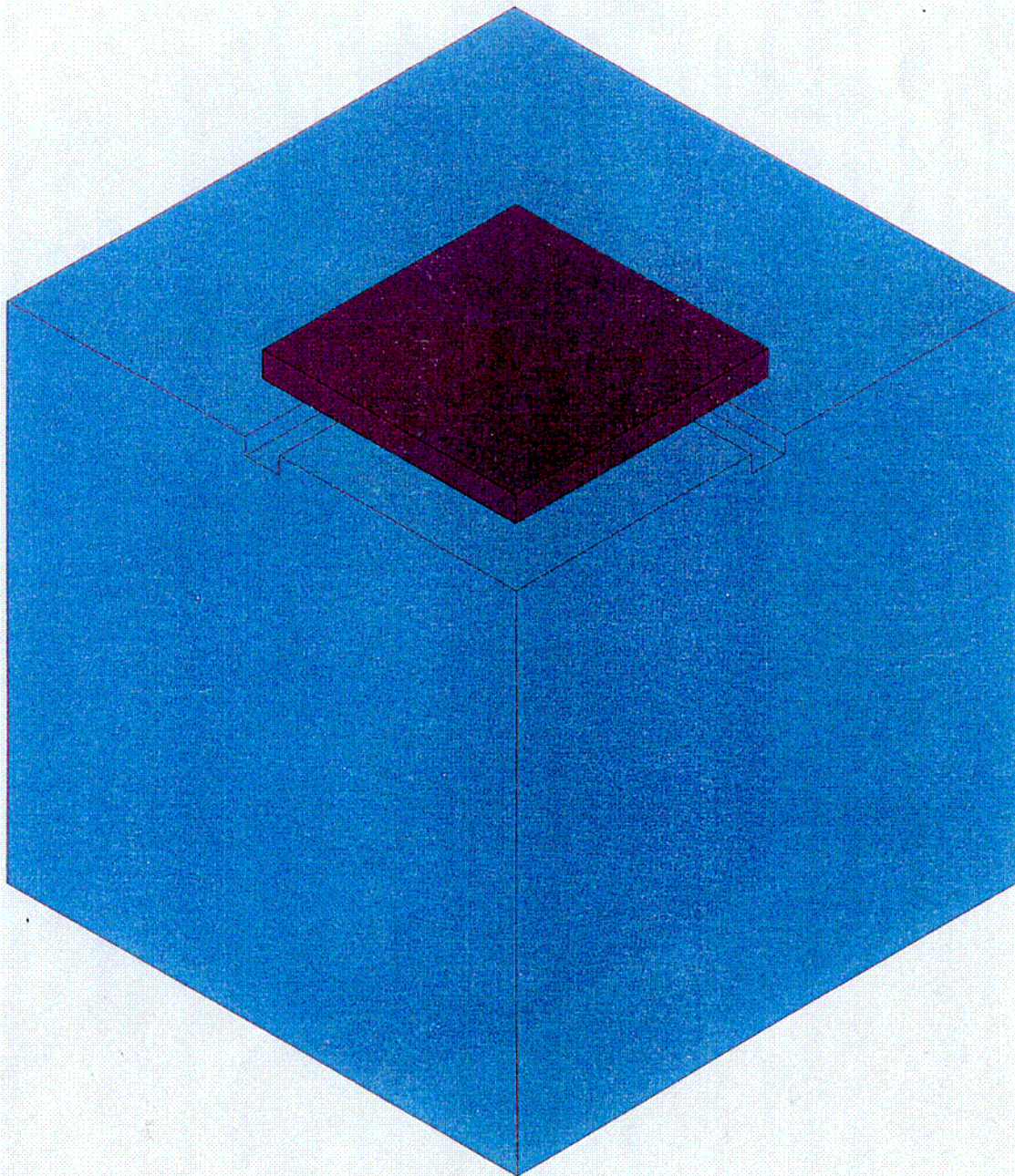
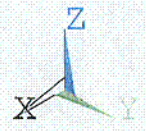


FIGURE 6.5.5; RACK PERIPHERY GAP/IMPACT ELEMENTS

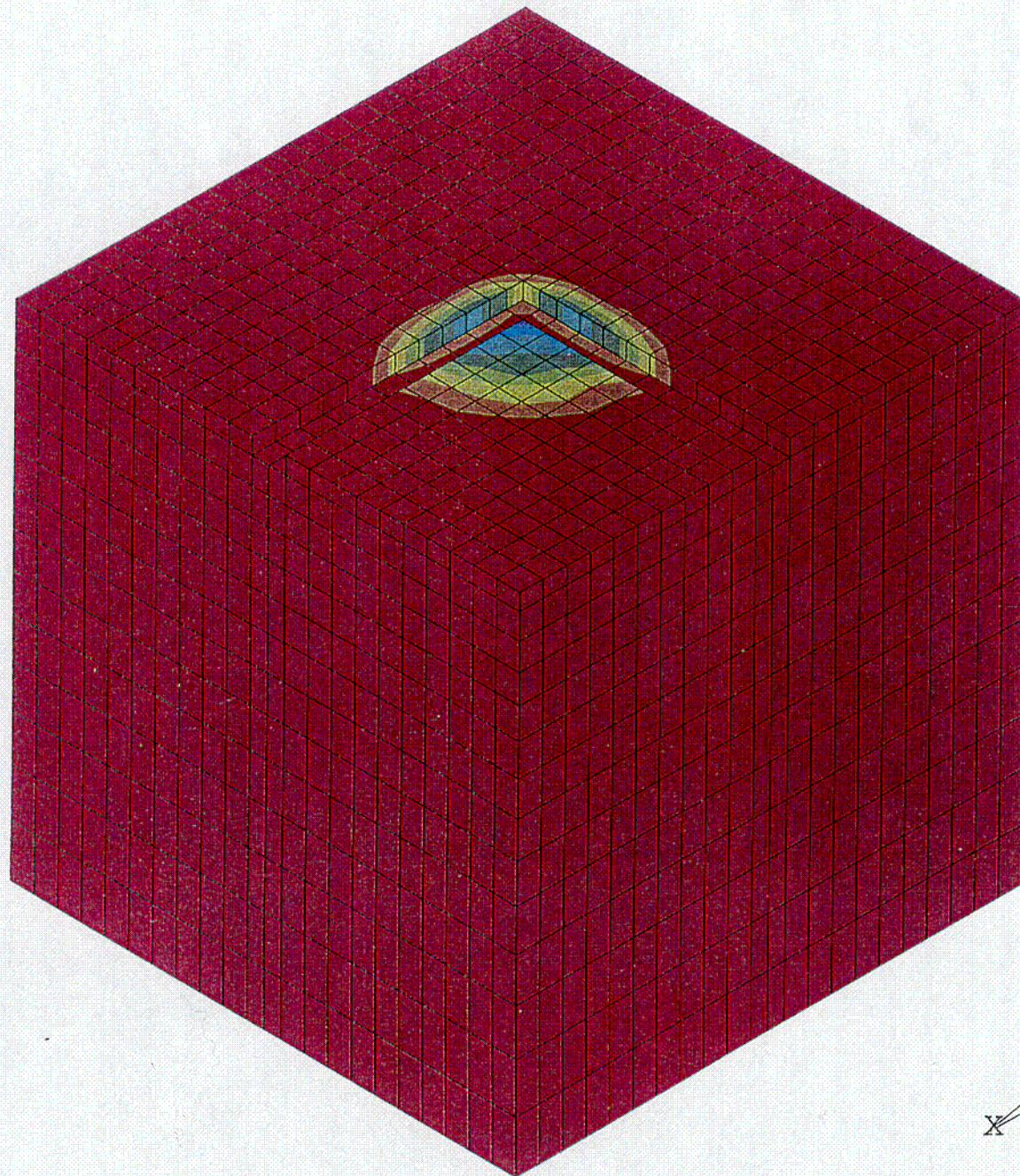
1



Davis Besse Spent Fuel Pool - Bearing Pad Analysis



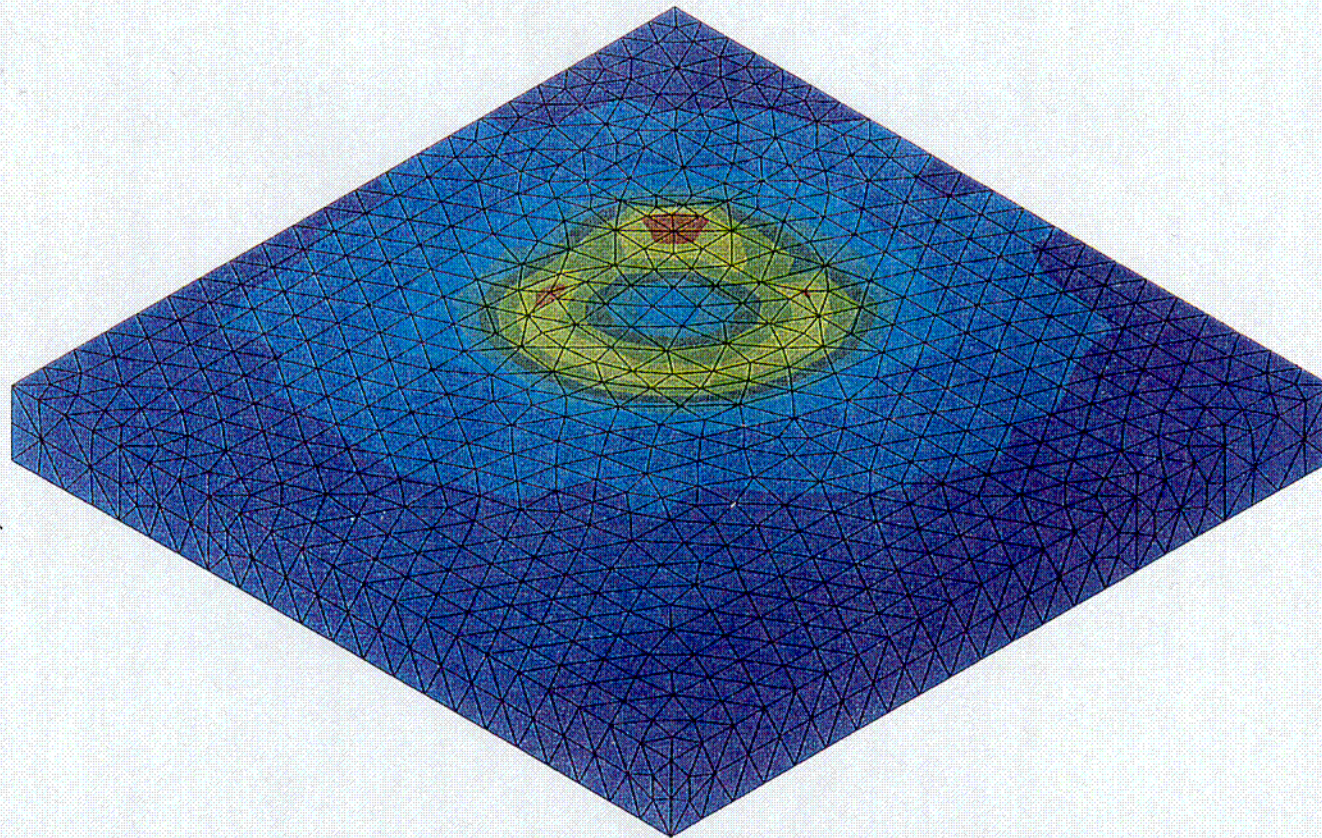
c-5



ANSYS 5.4  
 AUG 24 1999  
 15:18:38  
 NODAL SOLUTION  
 STEP=1  
 SUB =1  
 TIME=1  
 SZ (AVG)  
 RSYS=0  
 PowerGraphics  
 EFACET=1  
 AVRES=Mat  
 DMX =.006425  
 SMN =-6946  
 SMX =126.642

■	-6946
■	-6160
■	-5374
■	-4589
■	-3803
■	-3017
■	-2231
■	-1445
■	-659.227
■	126.642

Davis Besse Spent Fuel Pool - Bearing Pad Analysis



ANSYS 5.4  
AUG 24 1999  
15:30:02  
NODAL SOLUTION  
STEP=1  
SUB =1  
TIME=1  
SINT (AVG)  
PowerGraphics  
EFACET=1  
AVRES=Mat  
DMX =.008555  
SMN =8.92  
SMX =24170  
8.92  
2694  
5378  
8063  
10747  
13432  
16116  
18801  
21486  
24170

Davis Besse Spent Fuel Pool - Bearing Pad Analysis

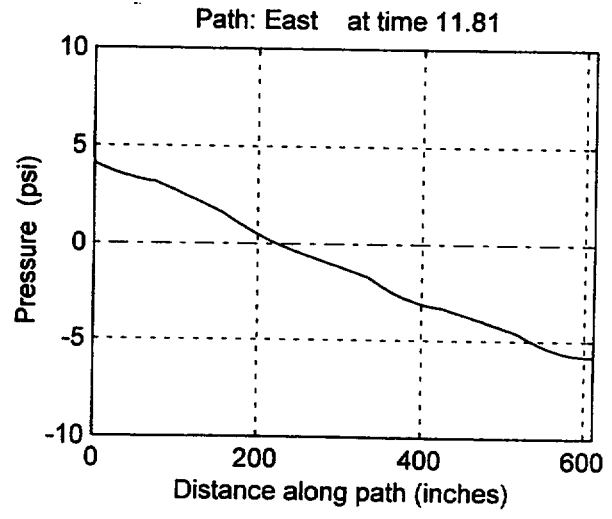
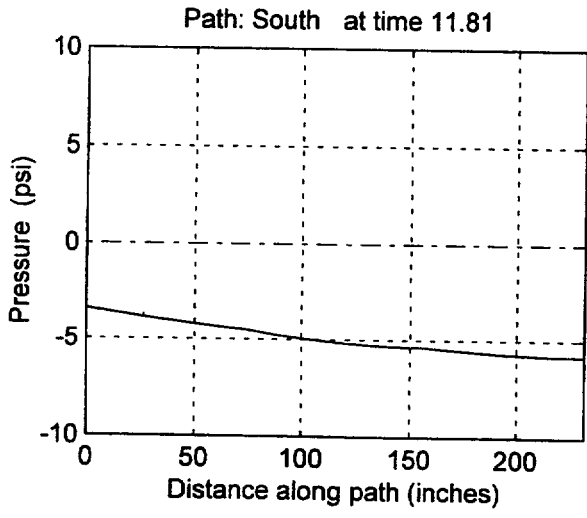
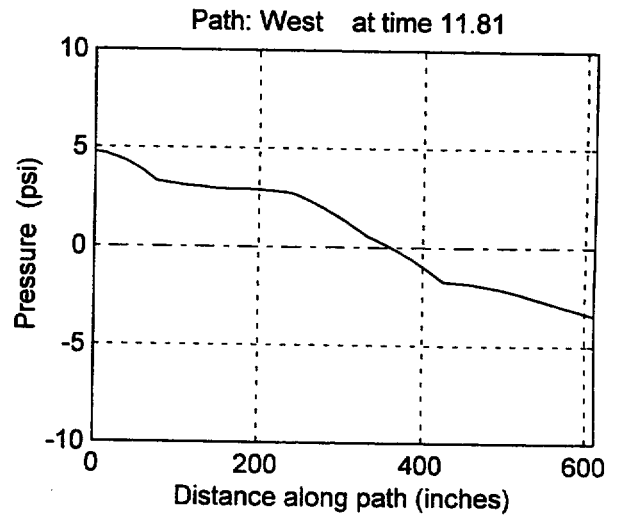
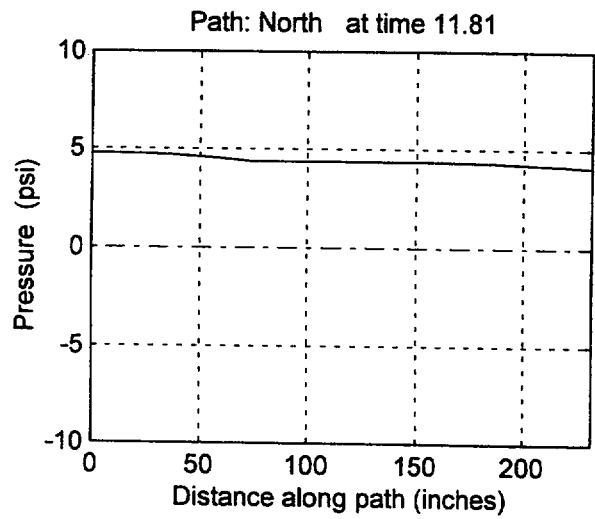


Figure 6.11.1; Rack Hydrodynamic Pressures

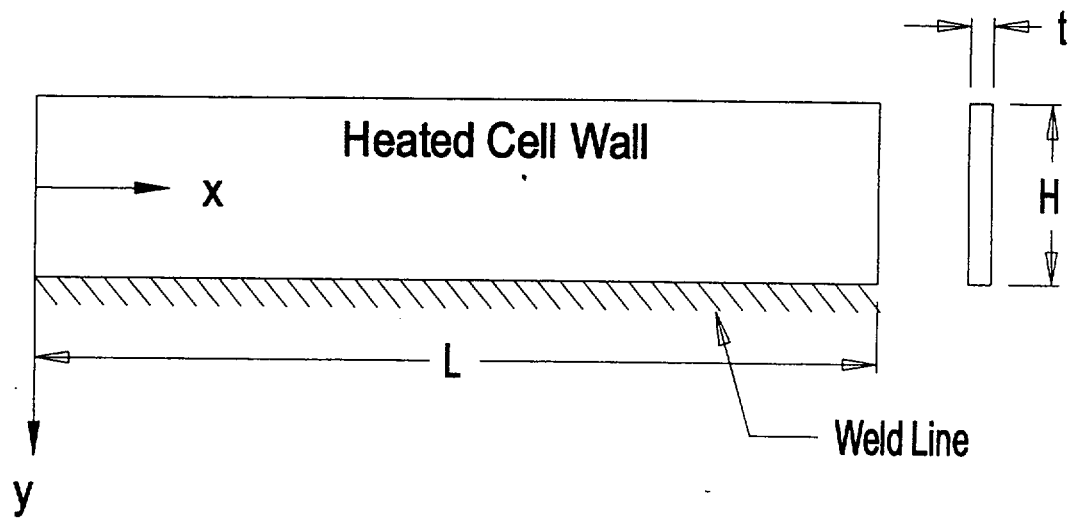


FIGURE 6.12.1; WELDED JOINT IN RACK

## 7.0 FUEL HANDLING AND MECHANICAL ACCIDENTS

### 7.1 Introduction

The USNRC OT position paper [7.1] specifies that the design of the rack must ensure the functional integrity of the spent fuel racks under the postulated load drop events. This section contains synopses of the analyses carried out to demonstrate the regulatory compliance of the proposed racks under postulated mechanical accidents germane to the Davis-Besse Nuclear Power Station (DBNPS).

If necessary for installation personnel (i.e., underwater diver) safety during the SFP re-racking, a rack will be placed in the Transfer Pit to allow temporary storage of fuel. The Transfer Pit is a flooded pit which is connected to the SFP by a three foot wide gate. The analyses described are applicable to both the Spent Fuel Pool (SFP) and the Transfer Pit.

### 7.2 Description of Accidents

In the evaluation of fuel handling accidents discussed herein, the concern is with the damage to the storage racks, and the Spent Fuel Pool (SFP) and Transfer Pit structures. The configuration of the rack cell size, spacing, and neutron absorber material must remain consistent with the configurations used in the criticality and thermal-hydraulic evaluations. Maintaining these designed configurations will ensure that the results of the criticality and thermal-hydraulic evaluations remain valid.

The top of the SFP and Transfer Pit floor liner is 6'-6" higher than the elevation of the Cask Pit floor liner. Except as noted below, all drop scenarios postulated to occur in the SFP and Transfer Pit are identical to the accidents postulated for the Cask Pit - which were presented to the NRC per LAR 98-0007 (Docket Number 50-346) and approved February 29, 2000. Based on the differences in floor elevations, the results for the Cask Pit will be conservative and valid for the SFP and Transfer Pit. The initial conditions for two of the Cask Pit scenarios were modified for the SFP and Transfer Pit analyses. As there will be a heavier rack installed in the SFP than was

installed in the Cask Pit, the weight of the dropped rack was changed. Also, shallow drop scenario 2 was re-run without the 6'-6" conservatism to give more realistic results.

Two categories of fuel assembly drop accidents are evaluated: a shallow drop and a deep drop, both of which are discussed in detail below. Each of the fuel handling accidents considers the drop of a fuel assembly, along with the portion of handling tool, which may be severed due to a single element failure. The total dropped weight is 2,482 pounds. The origin of the dropping trajectory is chosen as the highest elevation that the load can be lifted, by the Fuel Storage Handling Bridge, which is 98.13 inches above the upper elevation of the Cask Pit fuel storage racks. As explained above, a more realistic height of 18.875 inches was selected for shallow drop scenario 2.

Additional evaluations were also performed to consider the ability of the rack to withstand a 500 pound uplift force and the SFP and Transfer Pit to withstand a rack drop during installation. Material definitions are provided in Table 7.2.1.

These accident evaluations consider only the extent of rack and pool damage, and do not address fuel damage. As the new racks do not change the height of the stored fuel, and the design bases source term bounds the fuel to be stored in the racks, the design bases fuel handling accident in the Spent Fuel Pool Area remains the same.

#### 7.2.1 Shallow Drop Events

The first category of fuel handling accidents considers a fuel assembly striking either the top of stored fuel or the top of the storage rack and is referred to herein as a "shallow drop" event. The criticality evaluation described in section 4.6.4 limits the gross cell wall deformation of the impacted and 8 surrounding cells to 8.75 inches, (4.75 inches from the top of the cell to the top of the Boral, and 4 inches of Boral deformation). The thermal-hydraulic evaluation for the racks assumed a maximum flow blockage of 50% after a drop accident, (see section 5.6). Therefore, the acceptance criteria for the shallow drop events are, a) less than or equal to 8.75 inches of cell deformation, and b) less than or equal to 50% cell blockage.

The first shallow drop scenario considers a fuel assembly and a portion of the handling tool travelling vertically through the stratum of water before striking the top of a stored fuel assembly and subsequently impacting the top of the weakest module, which was determined to be an 8x8 cell rack. A portion of the kinetic energy of the impactor is absorbed by damage to the rack.

This first impact scenario determines the depth and extent of plastic deformation of the 0.075 inch thick cell wall after the impactor falls 98.13 inches before striking a fuel assembly stored in the cell. From the description of the rack modules in Section 3, the impact resistance of a single vertical cell wall at the rack corner is less than any other potential impact region represented by multiple cell walls or interior walls. Accordingly, the potential shallow drop scenario is postulated to occur at a rack corner cell in the manner shown in Figure 7.2.1. This impact region is chosen to minimize the cross sectional area. In order to maximize the penetration into the top of the rack by the falling assembly, the rack is considered empty, with the exception of the impacted corner cell, where an irradiated fuel assembly is stored.

The second shallow drop accident scenario considers a fuel assembly and a portion of the handling tool striking the top of an empty rack cell. This will maximize cell wall deformation and cell blockage. As noted in Section 7.2, to give more realistic results, the drop height for this scenario was reduced from the Cask Pit analyses of 98.13 inches to 18.875 inches for the SFP and Transfer Pit. All other elements of the impacting fuel assembly and the impacted rack assembly are identical to those used in the first shallow drop scenario.

### 7.2.2 Deep Drop Events

The second category of fuel assembly drop events postulate that the 2482 lb. impactor falls through an empty storage cell and impacts the rack base-plate. The origin of the dropping trajectory is again chosen as the highest elevation that the load can be lifted by the Fuel Storage Handling Bridge, which is 98.13 inches above the upper elevation of the fuel storage rack in the Cask Pit. (As noted in Section 7.2, this is conservative for the Spent Fuel Pool and the Transfer Pit.) This so-called deep drop scenario evaluates the structural integrity of the rack baseplate. If

the baseplate is pierced or deforms sufficiently, then the fuel assembly or base-plate might damage the pool liner and/or create an abnormal condition of the enriched zone of fuel assembly outside the poisoned space of the fuel rack.

The deep drop event is classified into two scenarios. The first scenario considers dropping an assembly and a portion of the handling tool through a cell located above a support pedestal, which is located directly above a leak chase, as shown in Figure 7.2.2. The relative location of the pedestal and leak chase are chosen to account for all possible occurrences of leak chases located beneath pedestals. The second scenario considers dropping the impactor at an interior cell near the center of the rack as shown in Figure 7.2.3.

In the first scenario, the base-plate is buttressed by the support pedestal and presents a hardened impact surface, resulting in a high impact load. The principal design objective is to ensure that the support pedestal does not cause catastrophic damage to the liner and underlying reinforced concrete pool slab such that rapid loss of pool water occurs.

For the second deep drop scenario, the base-plate is not as stiff at cell locations away from the support pedestal. This scenario is evaluated to determine the damage and deformation to the rack baseplate. Baseplate severing or large deflection of the base-plate, such that the liner would be impacted, would constitute an unacceptable result. The deformation must be shown to be less than the distance from the bottom of the baseplate to the pool floor liner, which is 5¾ inches, including tolerances. An additional criterion, based on the criticality evaluation, limits the displacement of the dropped assembly and the surrounding 8 stored assemblies to 4 inches, (see section 4.6.4).

### 7.2.3 Rack Drop Event

The rack drop event is analyzed to show that dropping a rack into the Spent Fuel Pool or Transfer Pit during installation will not result in catastrophic leakage. Damage must not lead to development of cracks through the entire floor section. Although this scenario is evaluated, implementation of the control of heavy loads should preclude this event from taking place.

#### 7.2.4 Uplift Force Evaluation

The 500 pound uplift force is evaluated to ensure the rack cell wall is able to withstand this load without deforming the rack cell such that it no longer satisfies dimensional requirements. The acceptance criterion for this evaluation is that local cell wall stress shall remain below the yield point.

#### 7.3 Mathematical Model

In the first step of the solution process, the velocity of the dropped object (impactor) is computed for the condition of underwater free fall. Table 7.3.1 summarizes the results for the fuel assembly drop events. In the second step of the solution, an elasto-plastic finite element model of the impacted region on Holtec's computer Code PLASTIPACT (Lawrence Livermore National Laboratory's DYNA3D implemented on Holtec's QA system) is prepared. PLASTIPACT simulates the transient collision event with full consideration of plastic, large deformation, wave propagation, and elastic/plastic buckling modes. The physical properties of material types undergoing deformation in the postulated impact events are summarized in Table 7.3.2.

#### 7.4 Results

##### 7.4.1 Shallow Drop Event Results

Figure 7.4.1 provides an isometric view of the finite element model utilized in the shallow drop impact analysis.

The first shallow drop scenario dynamic analysis shows that the top of the impacted region undergoes localized deformation. The impacting fuel assembly has an initial velocity of 249 in./sec. Figure 7.4.2 shows an isometric view of the post-impact geometry of the rack for this shallow drop scenario, as well as a plot of the Von-Mises stresses. The maximum Von Mises stress in the cell wall, recorded at maximum displacement time, is 38.39 ksi and the maximum

plastic strain is 0.106. Approximately 10% of the cell opening in the impacted cell is blocked. Therefore, the maximum cell blockage acceptance criterion of 50% is satisfied, The maximum gross deformation is limited to 3 inches, which is less than the acceptance criteria of 8.75 inches. Therefore, the penetration is determined to be acceptable from a criticality perspective and the racks will remain subcritical.

The study of residual plastic strain for the second shallow drop analysis shows that damage remains local to the impacted region of the rack, but is significantly more extensive than the first scenario. Figure 7.4.3 shows an isometric view of the post-impact geometry of the rack for this scenario as well as a plot of the Von-Mises stresses. Deformation of the impacted cell extends 5 inches downward from the top of the undeformed cells. Therefore, the acceptance criterion of less than or equal to 8.75 inches is satisfied. The maximum Von-Mises stress in the cell wall is 54.26 ksi and the maximum plastic strain is 0.238. The effective damaged area obstructs less than 50 percent of the cross section of the cell. Since the percentage of obstruction recorded is for an empty cell, it is concluded that this analysis would bound the damage sustained by a loaded cell. Therefore, the cell blockage acceptance criteria of 50 % based on the thermal-hydraulic analysis is not violated.

#### 7.4.2 Deep Drop Event Results

The first deep drop scenario considers the impacted area to be over a pedestal that is resting on the ¼ inch thick liner and located near the convergence of two leak chases. Figure 7.4.4 shows an isometric view of the finite element model for the impactor, pedestal, bearing pad, liner and underlying concrete. As shown in Figure 7.4.5, a Von-Mises stress of 106 ksi is observed in the pedestal cylinder at the contact surface with the bearing pad, which is below the failure stress of 140 ksi for the pedestal material. The bearing pad registers a Von-Mises stress of approximately 30 ksi, as shown in Figure 7.4.6.

The numerical analysis of this event shows that the liner is not pierced during the collision, since the maximum Von-Mises liner stress, as shown in Figure 7.4.7, is 27 ksi, which is less than the failure stress of 71 ksi. Therefore, the acceptance criteria is satisfied. The concrete stratum

directly below the pedestal sustains a very localized compressive stress of 21 ksi, as shown in Figure 7.4.8, which results in only localized damage to the concrete.

A plan view of the finite element model for the second deep drop scenario is shown in Figure 7.4.9. This scenario considers the dropped assembly to fall through an interior cell striking the base-plate at a point near the middle of the rack. This drop scenario produces some deformation of the base-plate and localized severing of the base-plate to cell wall welds. The collision between the 2482 lb. impactor and the 0.75 inch thick rack base-plate occurs at 406 in/sec initial velocity and results in an accentuated local deformation of the base-plate extending over a 26 inches square area around the impact zone. Due to the proximity of the fuel assembly lower end fitting, the shock of the initial impact is carried into the walls of the centrally located cell, and fails the connecting welds to the adjoining cells. The base-plate does not break during the impact, but the welds connecting the cells located in the vicinity of the collision area to the plate are severed.

The structural damage resulting from this scenario has no adverse effect on the coolant flow through the storage cells. The maximum calculated Von-Mises stress in the base-plate as shown in Figure 7.4.10 is 46.04 ksi and the maximum calculated plastic strain in the base-plate is 0.109, as shown in Figure 7.4.11. Figure 7.4.12 shows the deformed shape of the base-plate. The maximum displacement of the base-plate is 3.36 inches, which develops 0.0135 seconds after the initial collision and extends over less than 9 storage spaces. The maximum base-plate displacement is less than the distance to the liner plate (5¾ inches) and less than the 4 inches assumed in the criticality evaluation. Therefore, the liner integrity and criticality acceptance criteria, discussed in Section 7.2.2, are satisfied.

### 7.4.3 Rack Drop Event Results

Numerical analysis of the drop of a 14,030 pound rack into the SFP or Transfer Pit shows that the rack does not pierce the ¼ inch liner. (A 12,150 pound rack was appropriately assumed for the Cask Pit analysis.) The maximum calculated Von-Mises stress for the liner of about 26 ksi, as shown in Figure 7.4.13, is less than the failure stress of 71 ksi for the liner material. The

concrete stratum directly beneath the pedestal sustains a very localized compressive stress, as shown in Figure 7.4.14, with a maximum value of 10.3 ksi. This results in only localized damage to the concrete below the liner and does not compromise the global concrete integrity of the thick, heavily reinforced slab.

#### 7.4.4 Uplift Force Evaluation Results

This evaluation shows that the rack is able to withstand the uplift force of 500 pounds. For this scenario, the critical location for the load to be applied is at the top of a cell. For a load applied vertically anywhere along a cell wall, the resultant stress is only 1,100 psi, which is well below the yield stress of the material. For a load applied at a 45 degree angle to the top of a cell wall, tear out of the cell wall is evaluated. The damaged region extends no greater than 0.24 inches down the cell wall, which is well above the top edge of the neutron absorber material.

#### 7.5 Closure

The fuel assembly drop accident events postulated for the pools were analyzed and found to produce localized damage well within the design limits for the racks. The configuration of the fuel and poison (Boral) is not compromised from the configurations analyzed in the criticality evaluations discussed in Section 4.0. The base-plate deformation and corresponding fuel displacement is considered in the criticality evaluations. These evaluations concluded there are no criticality concerns for these accidents. The damage to the top of the racks reduces the cross sectional area available for coolant flow. However, the reduction of area is less than that considered in the thermal-hydraulic evaluations. Therefore, the accidents do not represent any thermal-hydraulic concerns. Analyses show that the pool liner will not be pierced by the pedestals, but the underlying concrete will experience local crushing. However, the pool structure will not suffer catastrophic damage. Therefore, there are no significant structural consequences.

The rack-drop evaluation determined the pool liner will not be pierced. The concrete damage is minimal and does not compromise the structural integrity of the Spent Fuel Pool or Transfer Pit.

The rack has been shown to be adequate to withstand the uplift load of 500 pounds with no permanent deformation.

## 7.6 References

[7.1] "OT Position for Review and Acceptance of Spent Fuel Storage and Handling Applications," dated April 14, 1978.

Table 7.2.1  
Material Definition

Material Name	Type	Density  (pcf)	Elastic Modulus	Stress		Strain	
				First Yield	Failure	Elastic	Failure
			(psi)	(psi)	(psi)		
Stainless Steel	ASME SA-240-304	490	2.760e+07	2.500e+04	7.100e+04	7.717e-04	3.800e-01
Stainless Steel	ASME SA-564-630	490	2.760e+07	1.063e+05	1.400E+05	3.851e-02	3.800e-01
Zircaloy	Irradiated	490	5.649e+06	5.649e+04	5.650e+04	1.000e-02	1.020e-02
Concrete	4000	150	3.605e+06	-	-	-	-

Table No. 7.3.1  
Impactor Weight and Impact Velocity Calculations

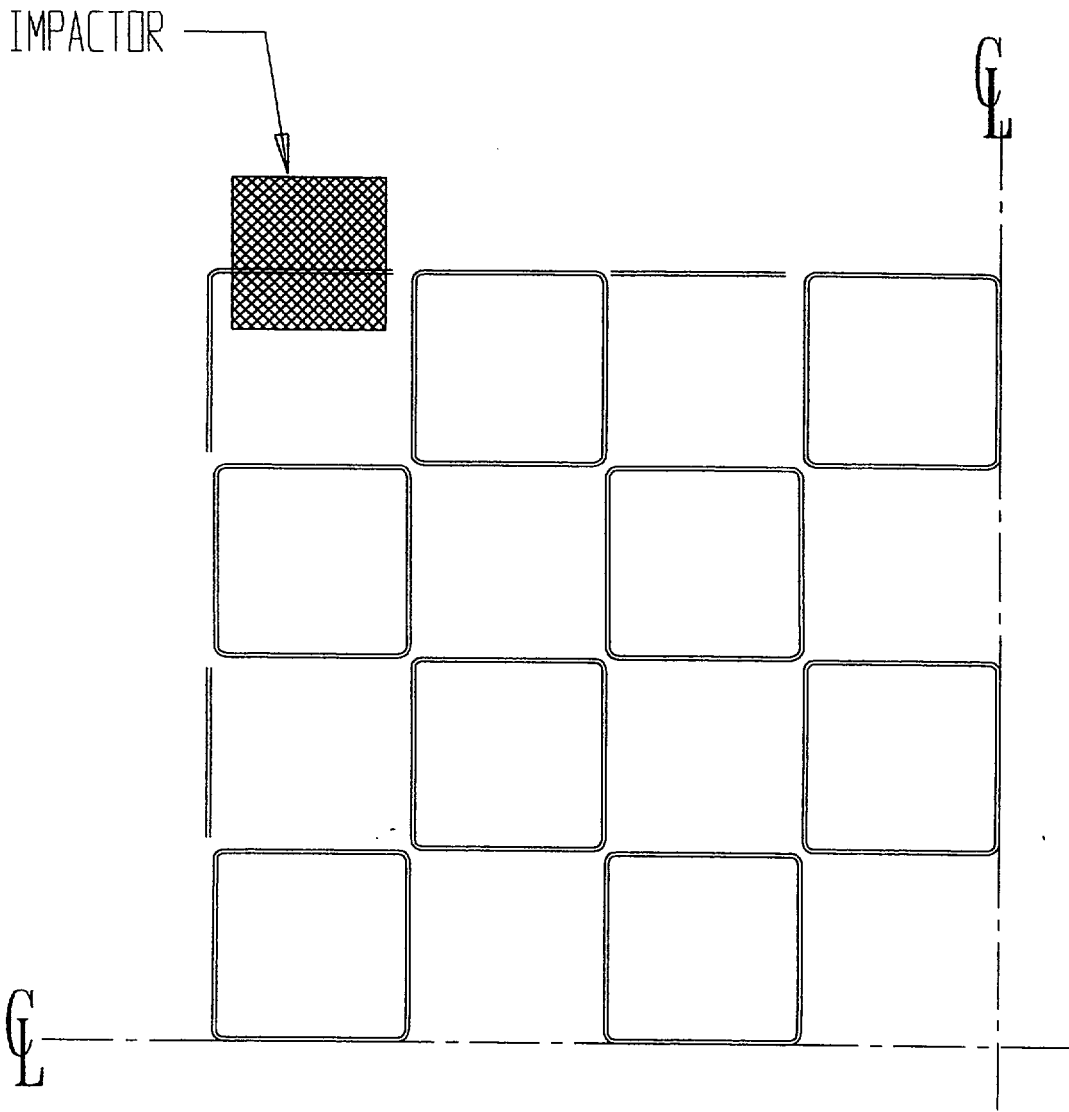
Drop Event	Impactor Type	Weight	Drop Height	Drag Surface	$\lambda$	$K_v$	$\theta$	$V_{\text{impact}}$
		W (lb)	H (in)	$A_c$ (in <sup>2</sup> )	(lb*sec <sup>2</sup> /in <sup>2</sup> )	(in <sup>2</sup> /sec <sup>2</sup> )		(in/sec)
"Shallow" Drop Scenario 1	Fuel Assembly & Tool	2482	98.13	61.78	0.001443	1.563e+06	4.042e-02	249
"Shallow" Drop Scenario 2	Fuel Assembly & Tool	2482	18.875	61.78	0.001443	1.563e+06	7.773e-03	110
"Deep" Drops	Fuel Assembly & Tool	2482	264.76	61.78	0.001443	1.563e+06	1.091e-01	403

Table No. 7.3.2

## Structural and Material Definition of Impactor and Target

Postulated Drop Event	Impactor Description		Target Description			
	Element	Structural Type	Element	Structural Type	Material †	
					Behavior	Type
Shallow	Fuel Assembly (2482 lb)	Elasto-Plastic	Corner Cell	Deformable	Elasto-Plastic	ASME SA-240-304
			Adjoining Cells	Deformable	Elasto-Plastic	ASME SA-240-304
Deep drop over rack	Fuel Assembly (2482 lb)	Rigid	Base Plate	Deformable	Elasto-Plastic	ASME SA-240-304
			Adjoining Cells	Deformable	Elasto-Plastic	ASME SA-240-304
Deep drop over rack pedestal	Fuel Assembly (2482 lb)	Rigid	Pedestal Block	Deformable	Elasto-Plastic	ASME SA-240-304
			Pedestal Cylinder	Deformable	Elasto-Plastic	ASME SA-564-630
			Pad	Deformable	Elasto-Plastic	ASME SA-240-304
			Liner	Deformable	Elasto-Plastic	ASME SA-240-304
			Concrete Stratum	Deformable	Elasto-Plastic	ASME SA-240-304 $f'_c=4000$

† The material properties are shown in Table 7.2.1.



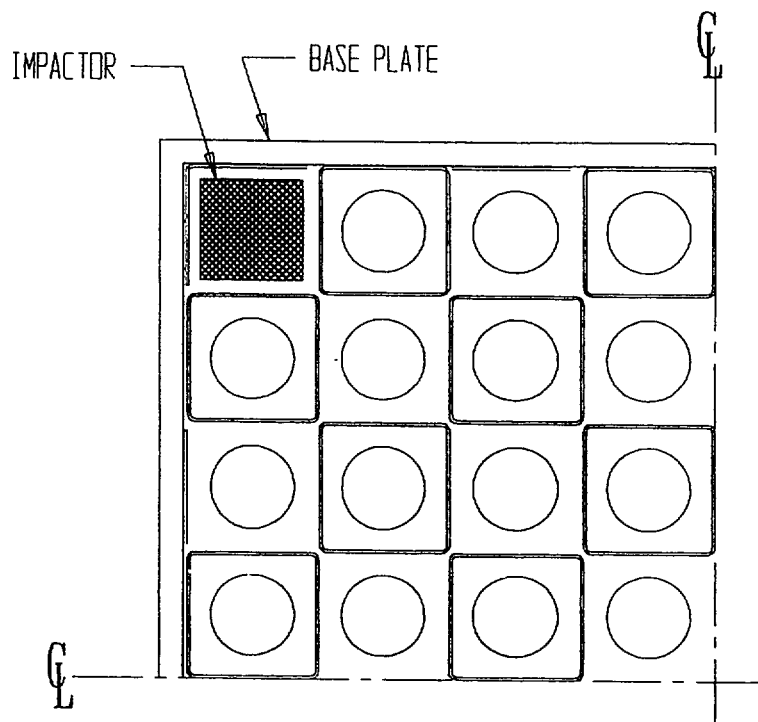


Figure 7.2.2; Plan View of "Deep Drop" Scenario 1

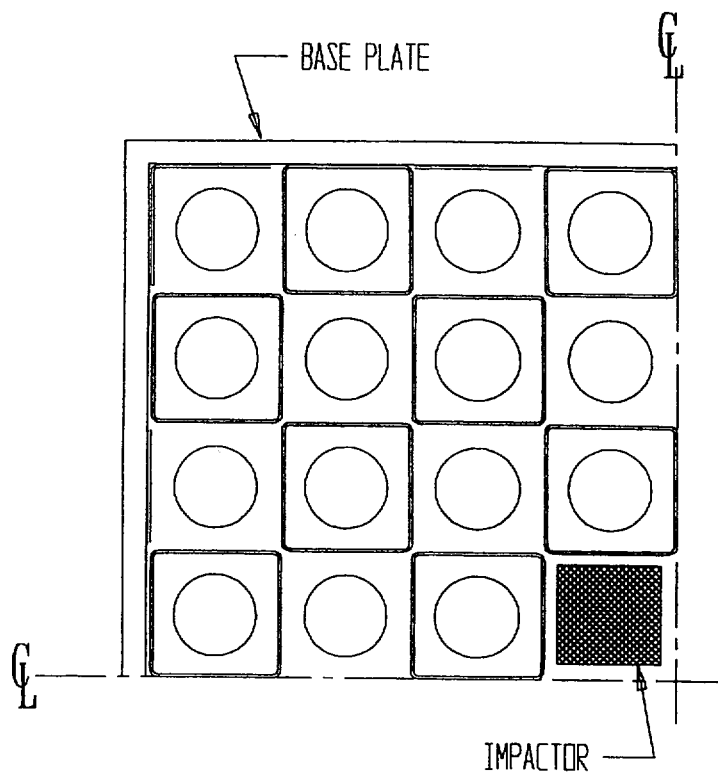


Figure 7.2.3; Plan View of "Deep Drop" Scenario 2

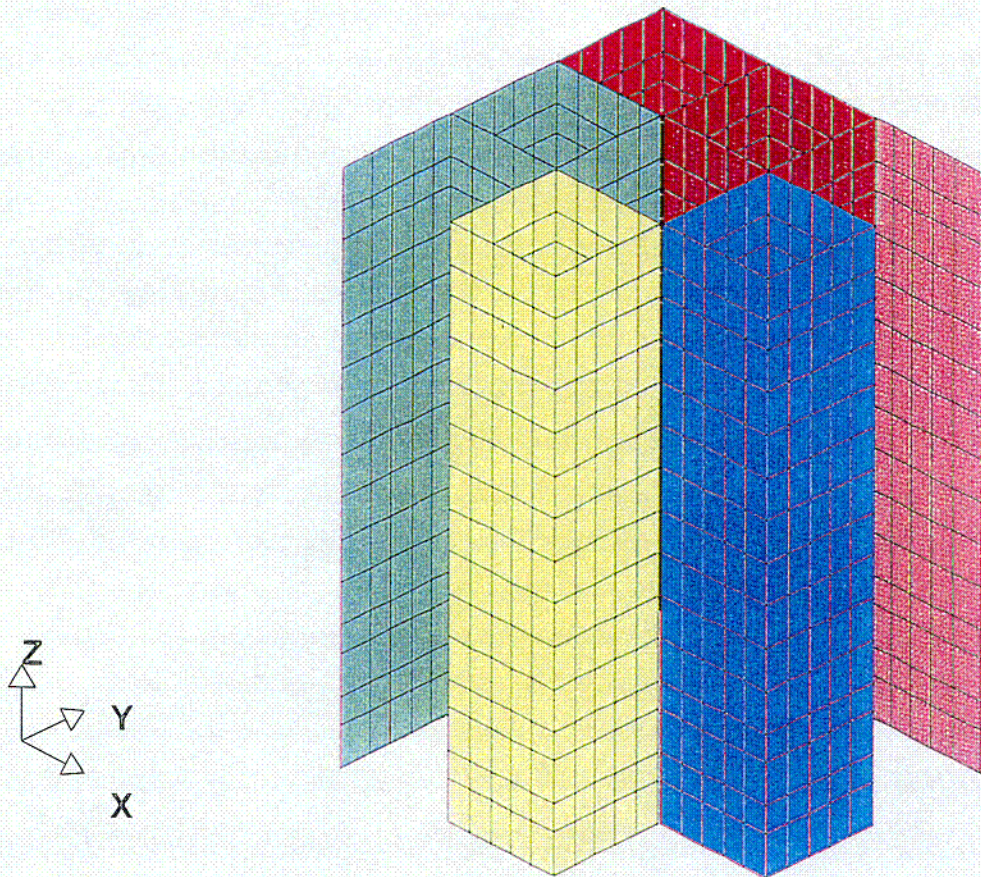
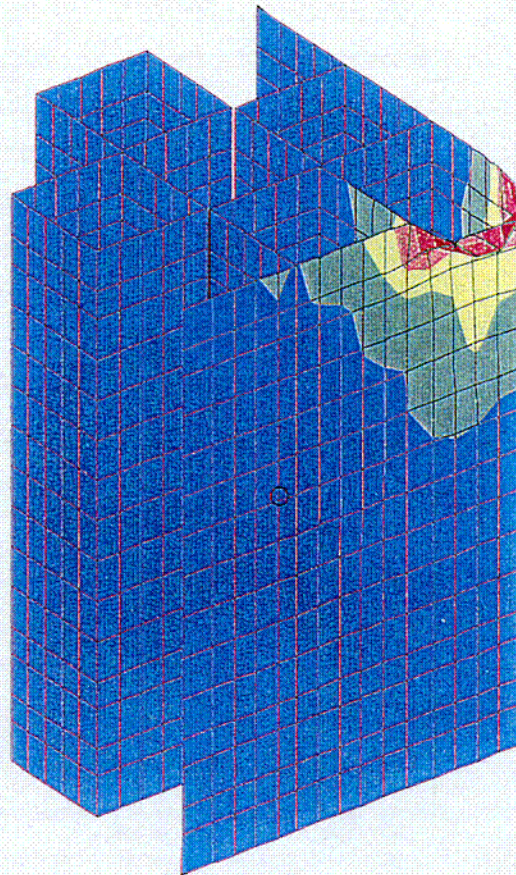
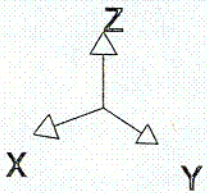


Figure 7.4.1; Isometric of "Shallow Drop" Finite Element Model

U-8

STEP 34 TIME = 8.4998824E-002  
MAX\_VONMISES



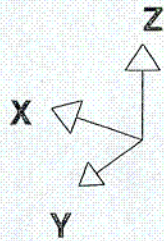
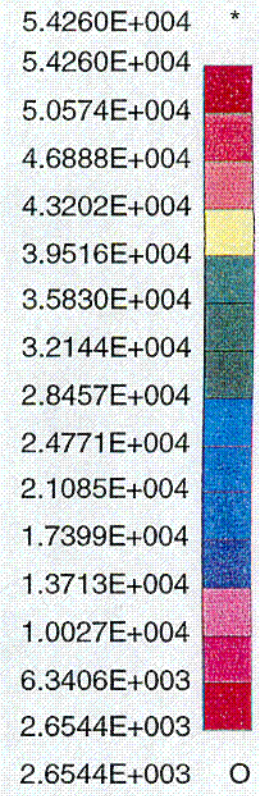
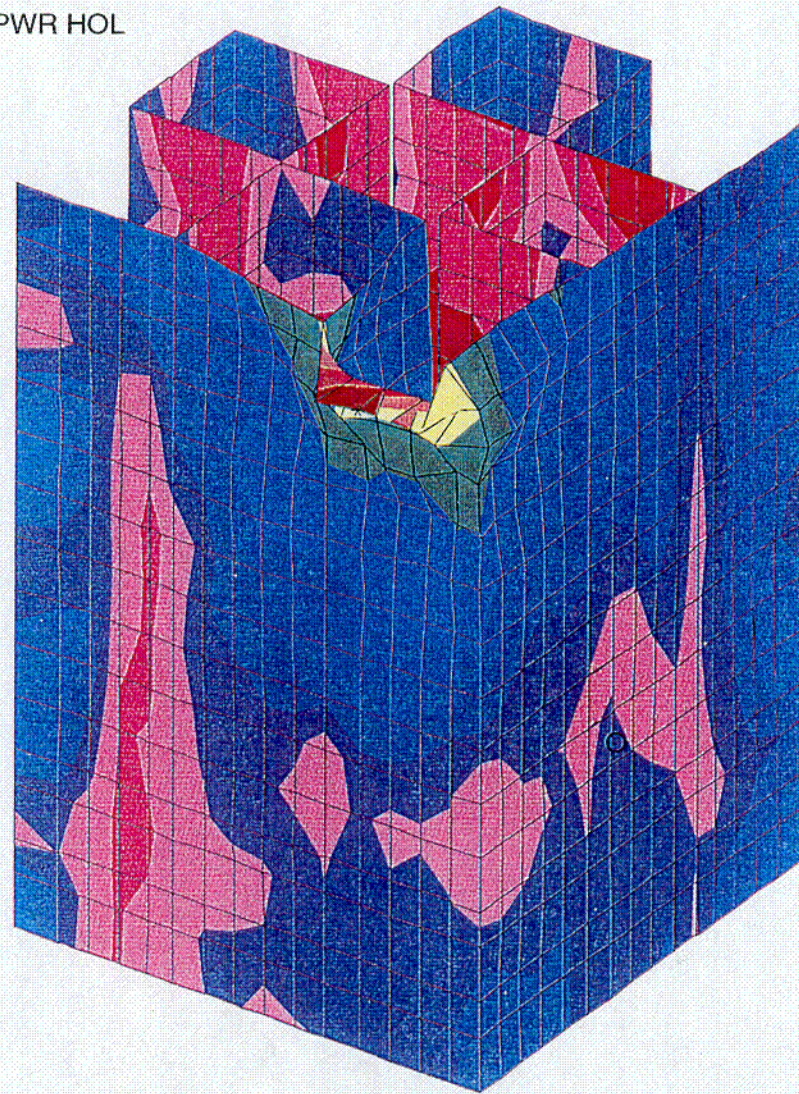
3.8385E+004  
3.8385E+004  
3.4595E+004  
3.0805E+004  
2.7016E+004  
2.3226E+004  
1.9436E+004  
1.5647E+004  
1.1857E+004  
8.0672E+003  
4.2775E+003  
4.8783E+002  
4.8783E+002

Figure 7.4.2; Isometric of Scenario 1

"Shallow Drop" Von Mises Stress

c-9

DAVIS-BESSE - IMPACT ON CELL 8X8 PWR HOL  
 STEP 26 TIME = 6.4999022E-002  
 MAX\_VONMISES



C-10

Figure 7.4.3; Isometric of Scenario 2

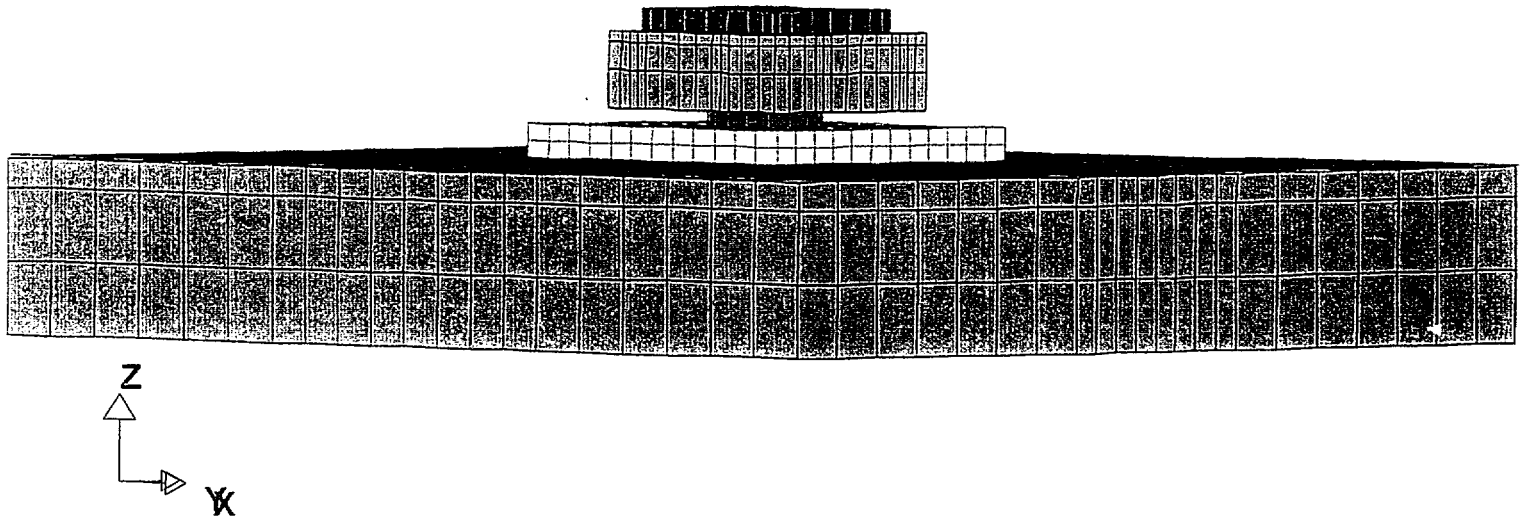


Figure 7.4.4; Isometric View of Over-Pedestal "Deep Drop"

Finite Element Model

STEP 7 TIME = 1.3997401E-003  
MAX\_VONMISES

1.0638E+008  
1.0638E+008  
9.5867E+007  
8.5352E+007  
7.4836E+007  
6.4321E+007  
5.3806E+007  
4.3291E+007  
3.2775E+007  
2.2260E+007  
1.1745E+007  
1.2295E+007  
1.2295E+007

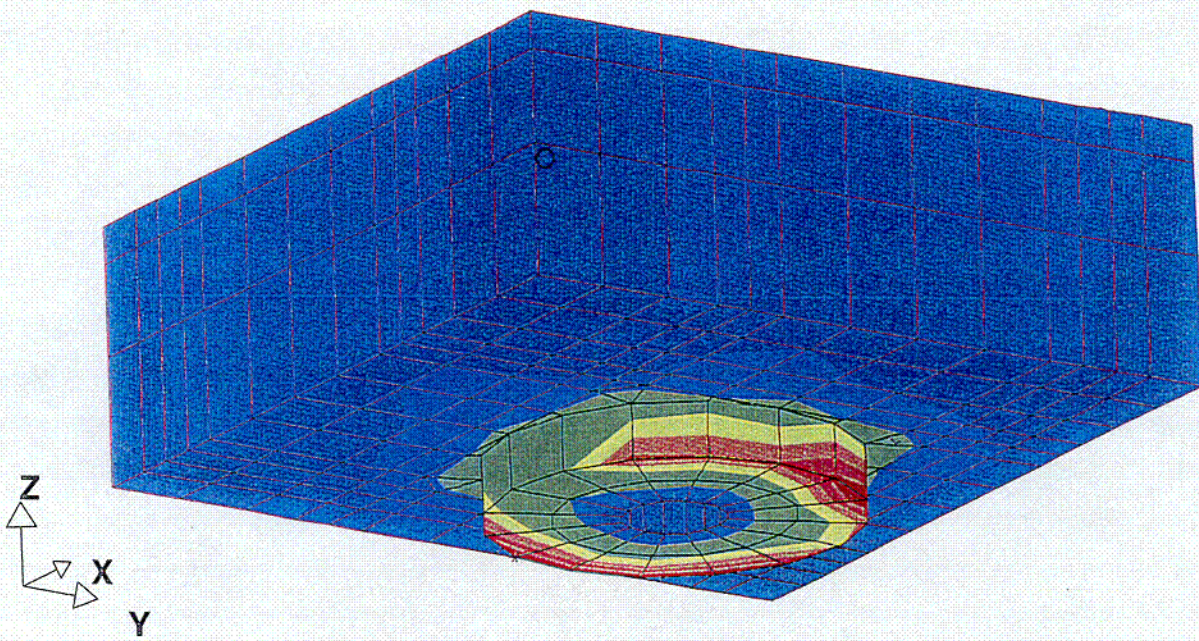


Figure 7.4.5; Over-Pedestal "Deep Drop" Pedestal Von Mises Stress

C-11

IMPACT ON RACK PLATE ABOVE  
STEP 7 TIME = 1.3997401E-003  
MAX\_VONMISES

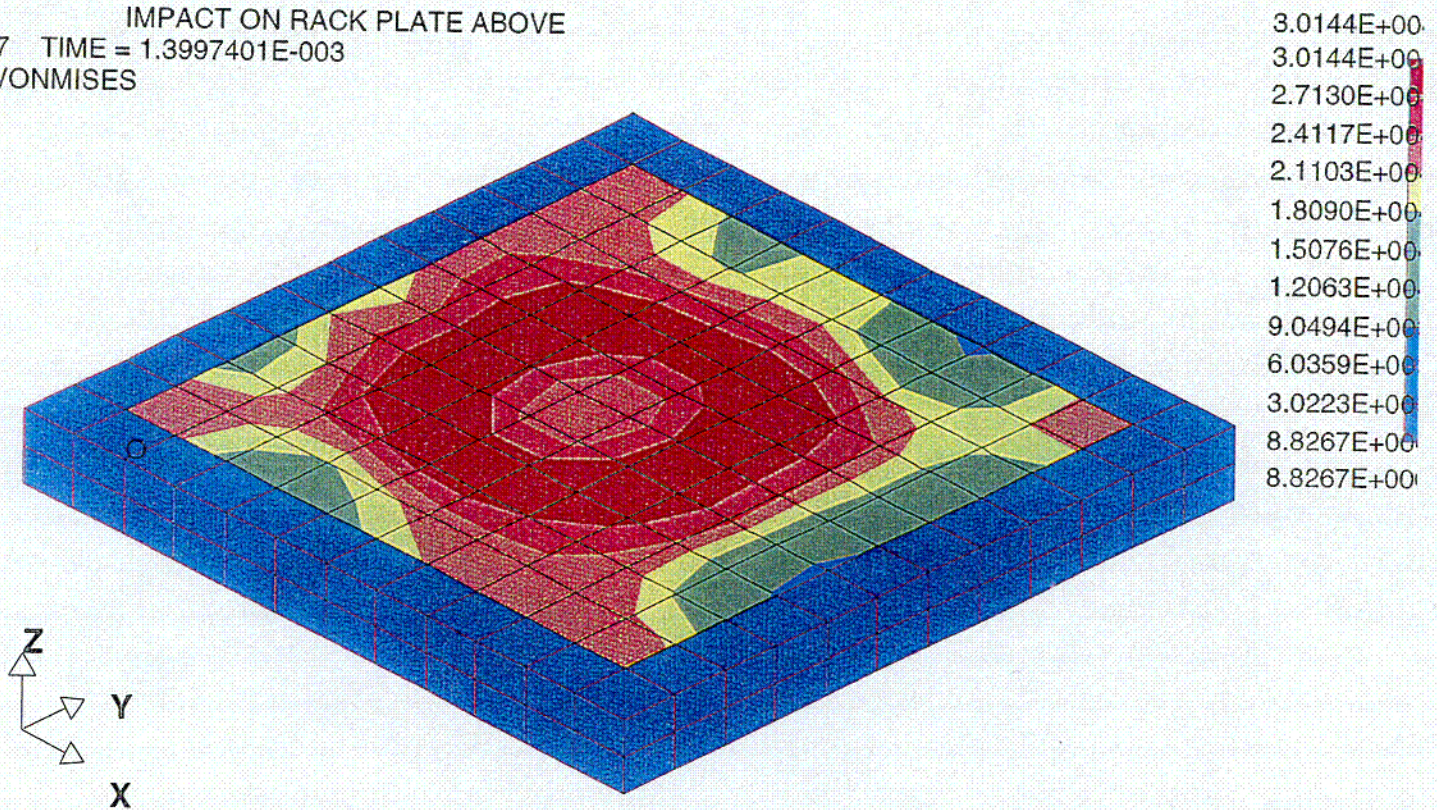


Figure 7.4.6; Over-Pedestal "Deep Drop" Bearing Pad Von Mises Stress

0-12

IMPACT ON RACK PLATE ABOVE  
STEP 9 TIME = 1.7998922E-003  
MAX\_VONMISES

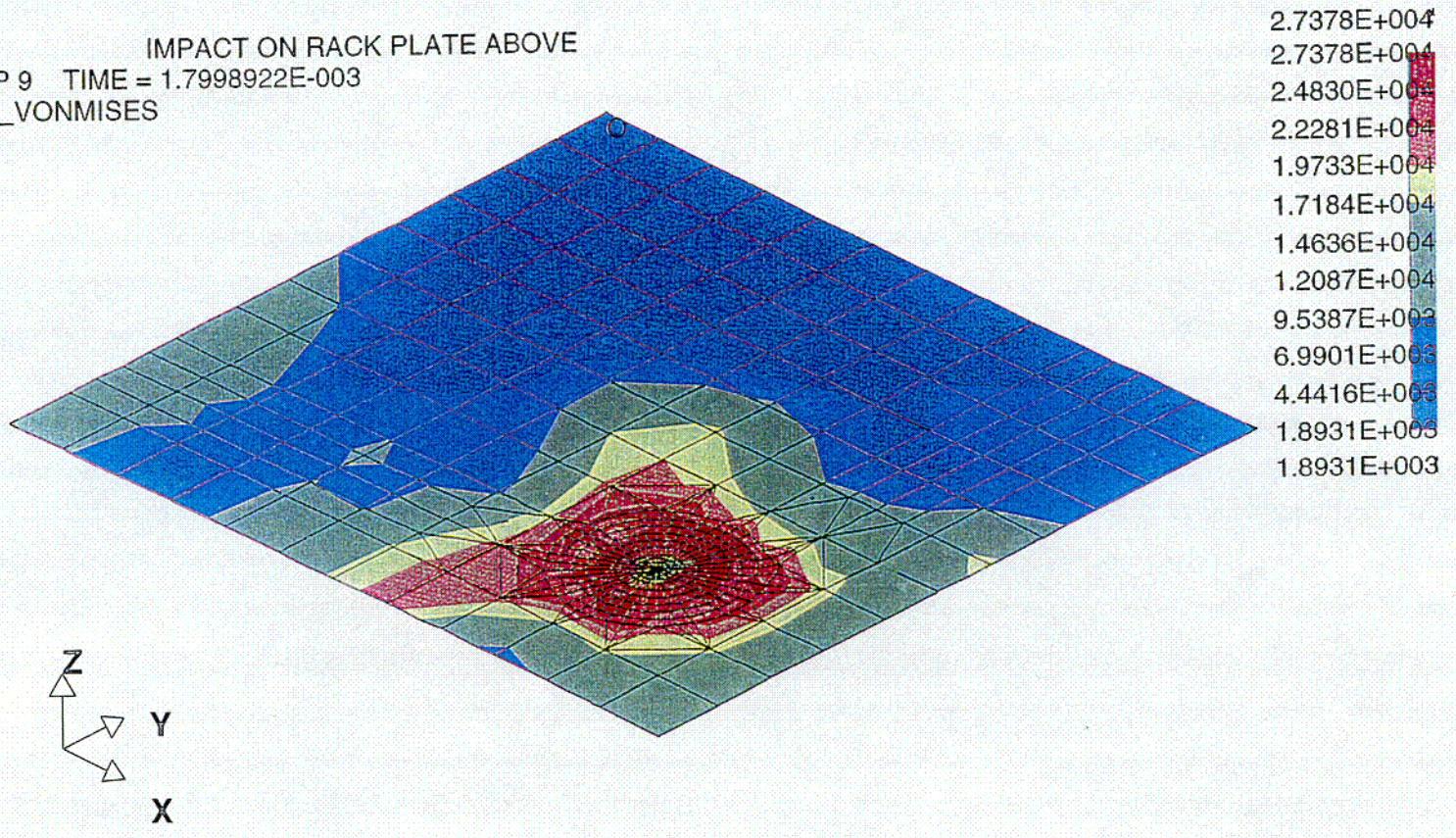


Figure 7.4.7; Over-Pedestal "Deep Drop" Liner Von Mises Stress

. IMPACT ON RACK PLATE ABOVE  
STEP 8 TIME = 1.5998161E-003  
SIGZZ(MID)

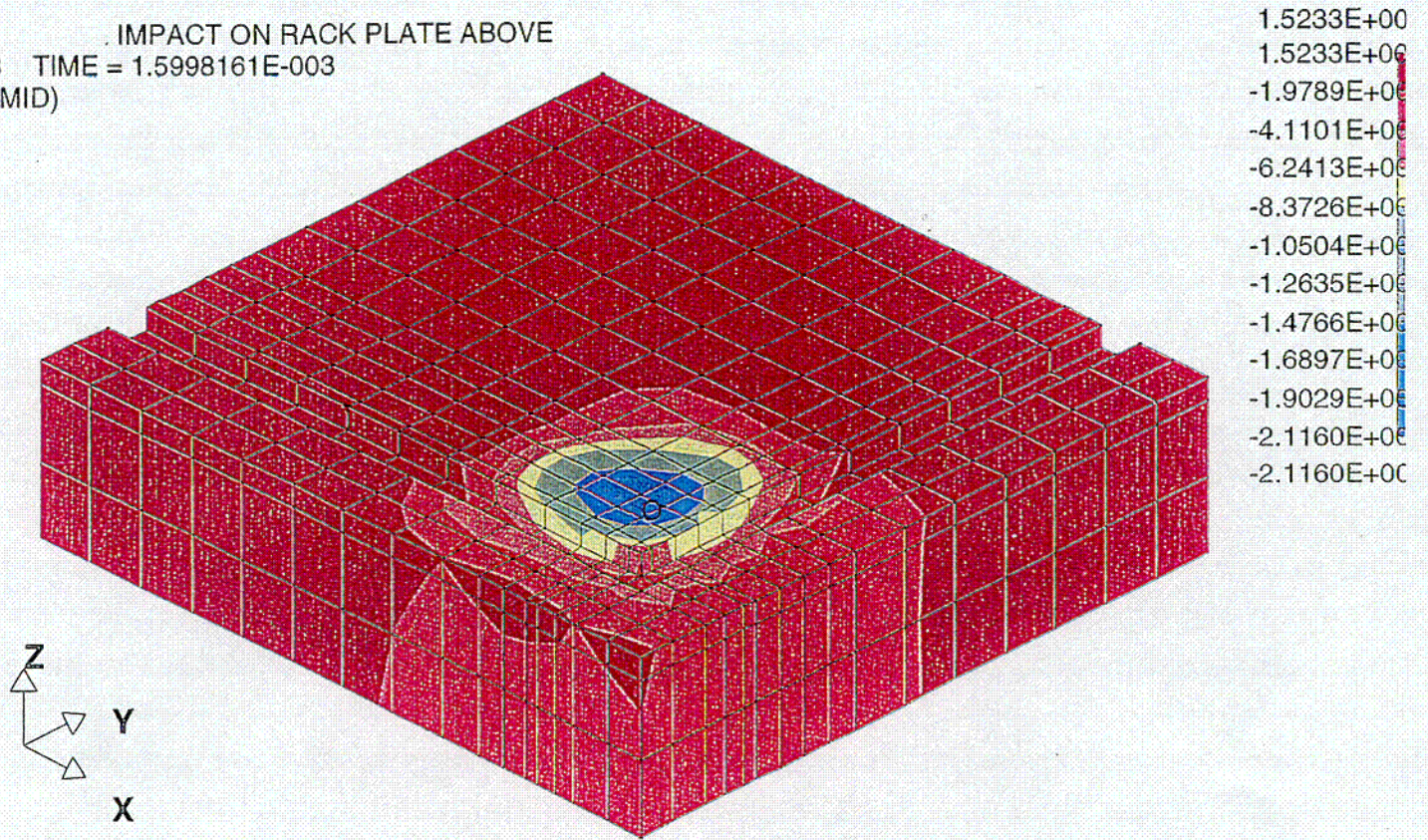


Figure 7.4.8; Over-Pedestal "Deep Drop" Concrete Von Mises Stress

c-14

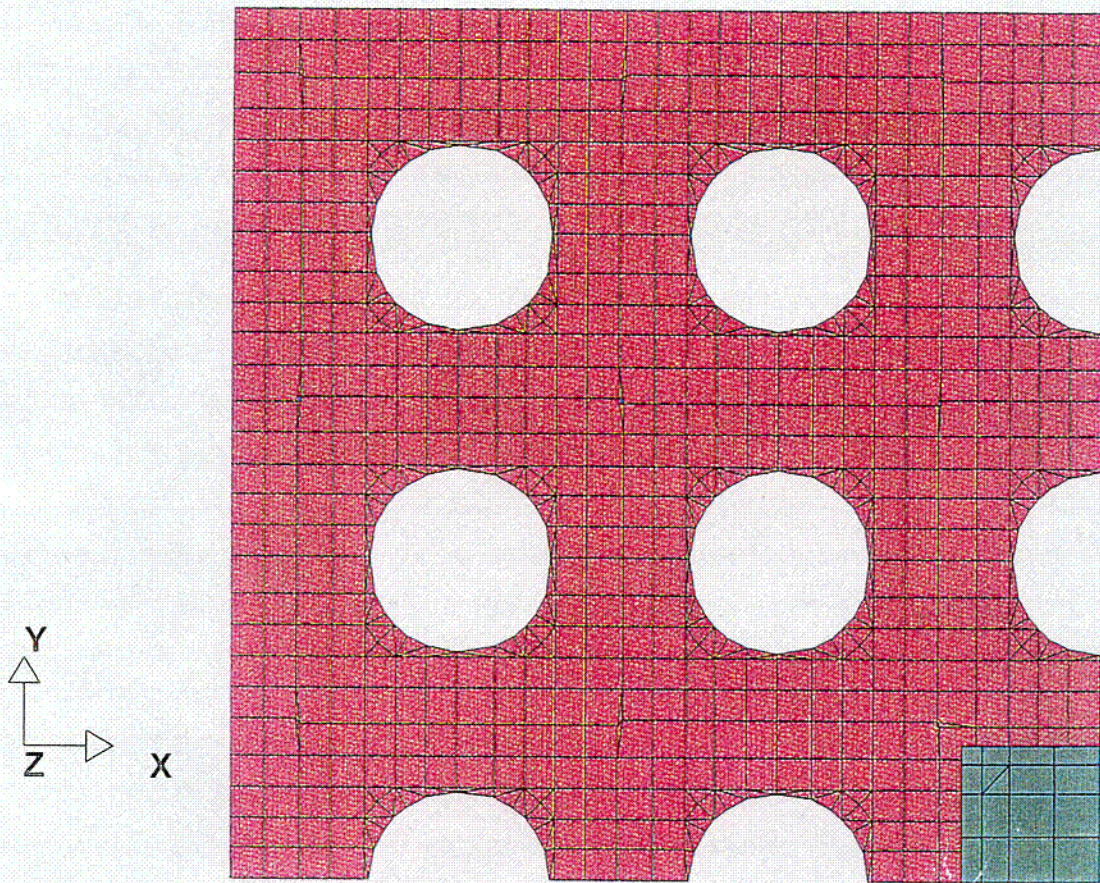


Figure 7.4.9; Plan of On-Center "Deep Drop" Finite Element Model

C-15

IMPACT ON PLATE 8X8 PWR H  
STEP 27 TIME = 1.3499969E-002  
MAX\_VONMISES

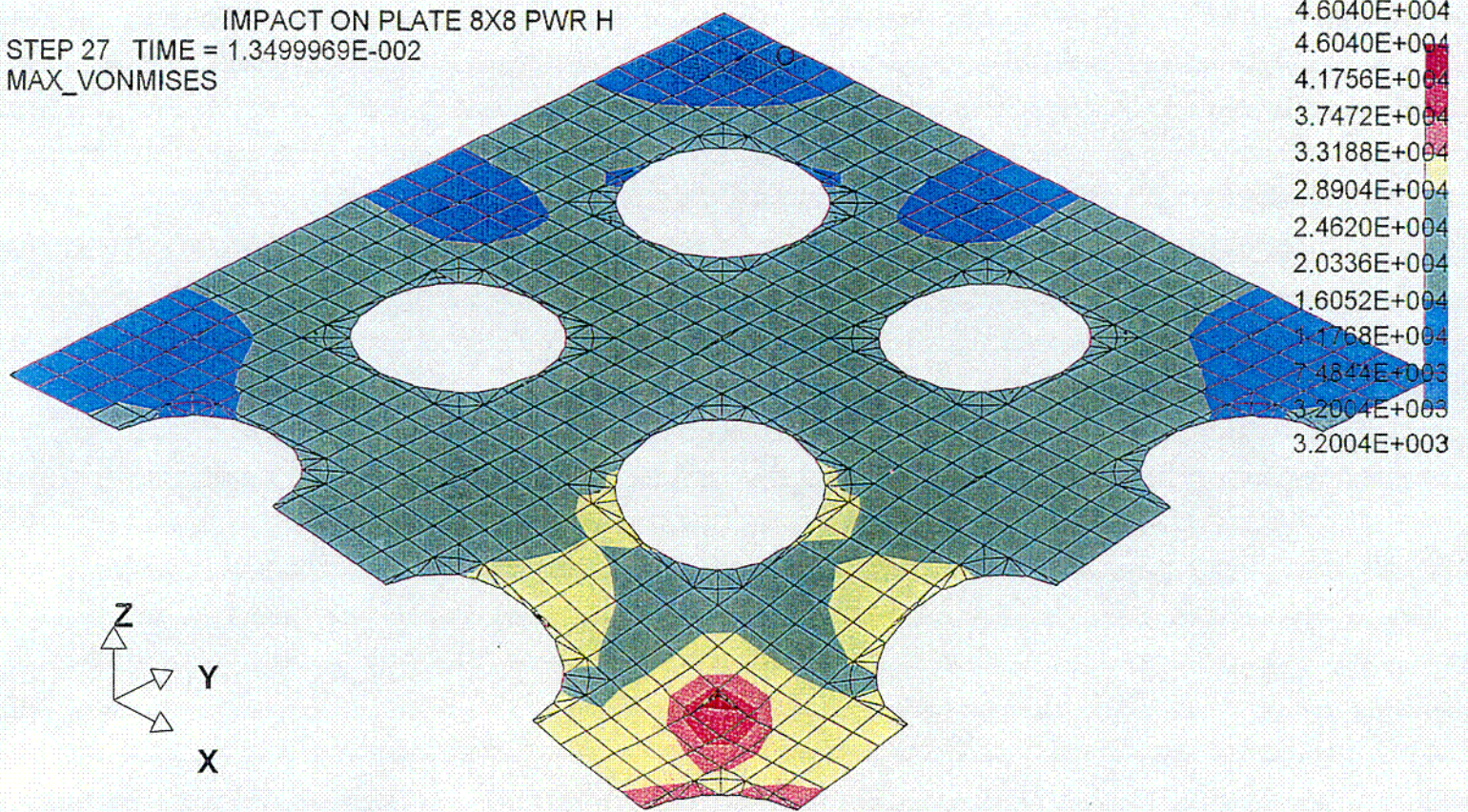


Figure 7.4.10; On-Center "Deep Drop" Baseplate Von Mises Stress

C-16

IMPACT ON PLATE 8X8 PWR H  
STEP 27 TIME = 1.3499969E-002  
PSTN(MID)

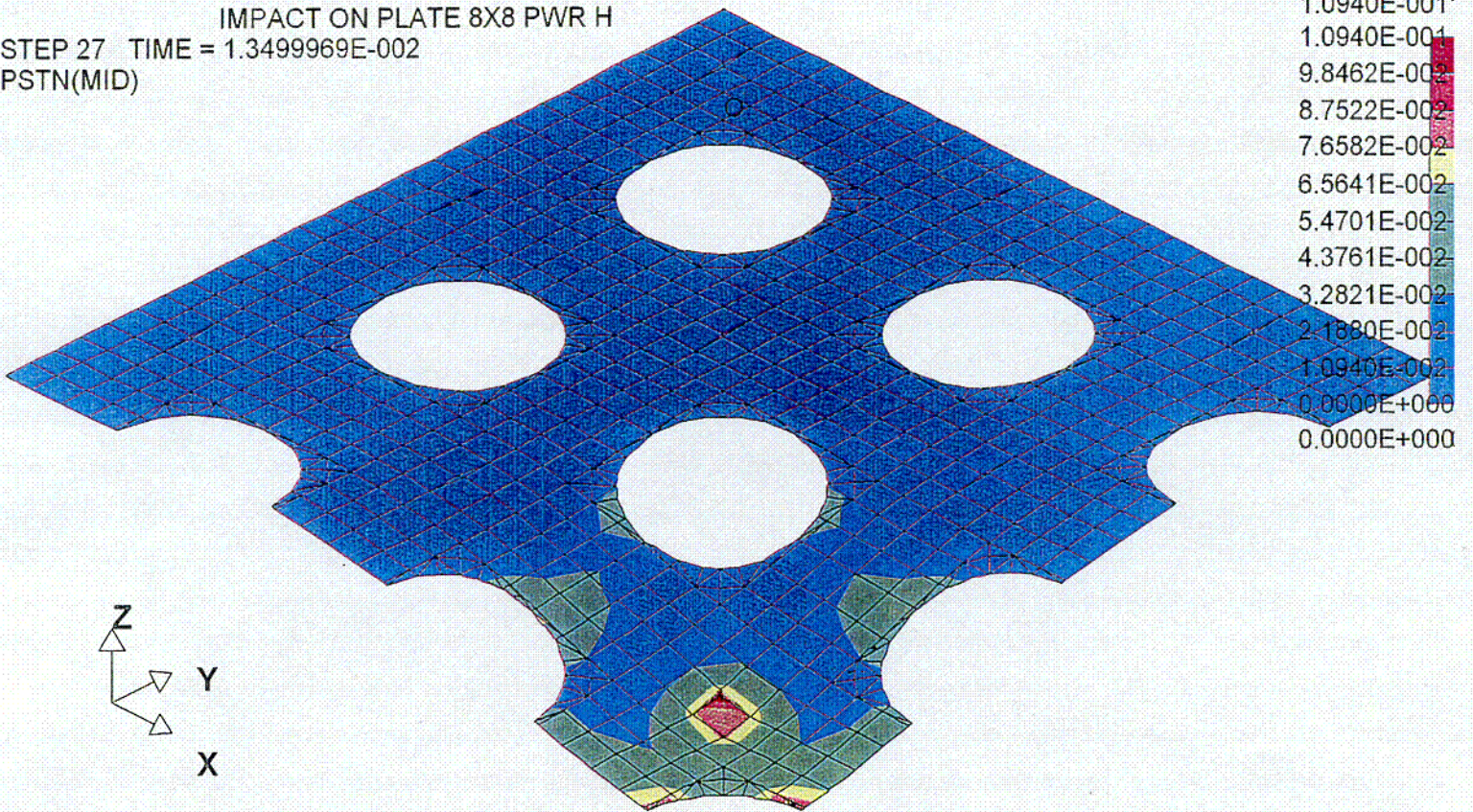


Figure 7.4.11; On-Center "Deep Drop" Baseplate Plastic Strain

C-17

STEP 27 TIME = 1.3499969E-002  
Z COORDINATE DISPLACEMENT

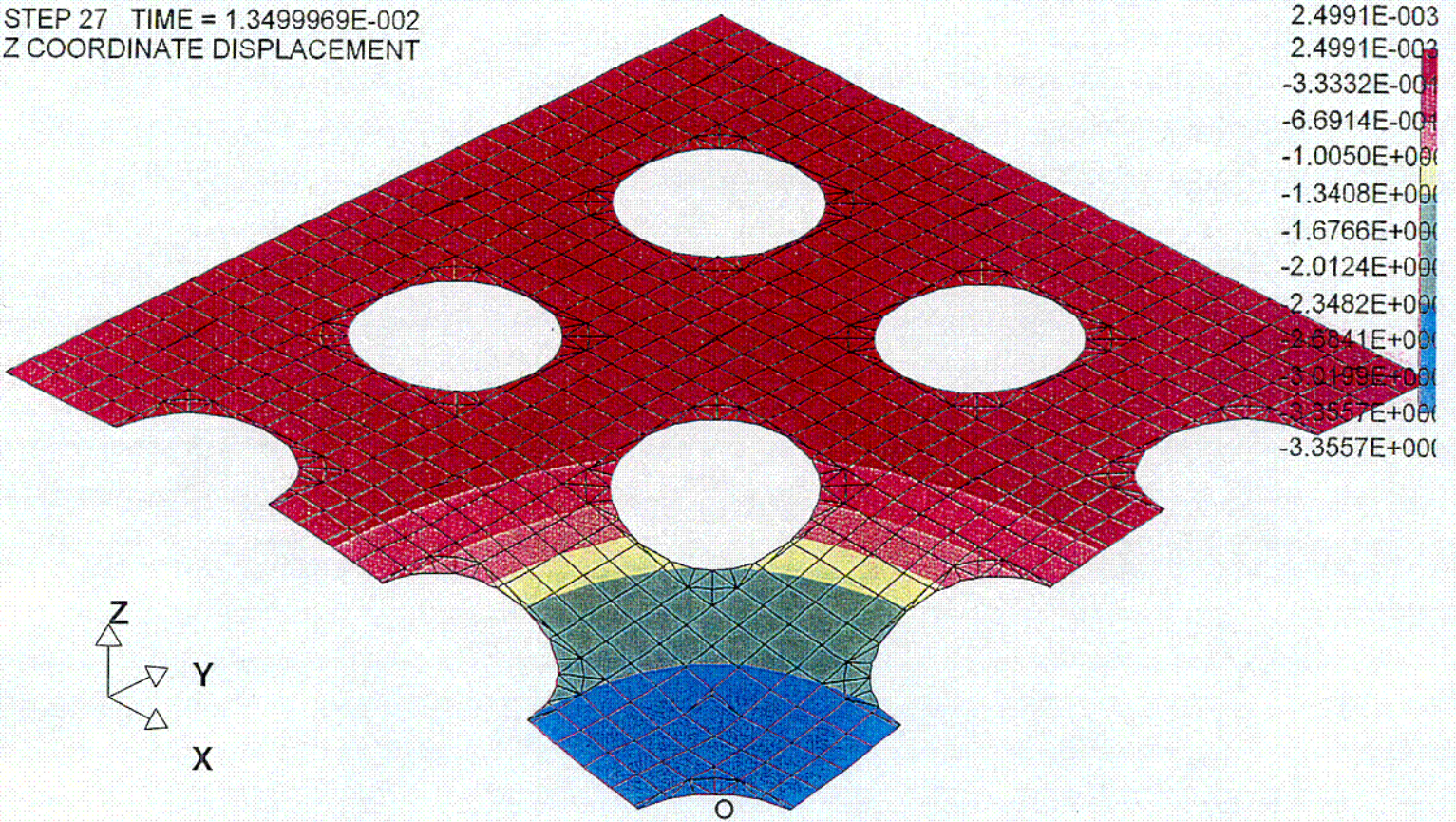


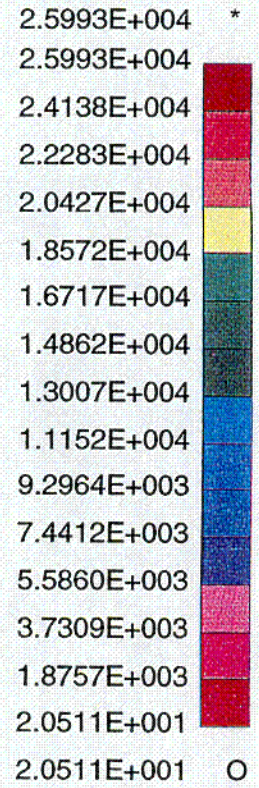
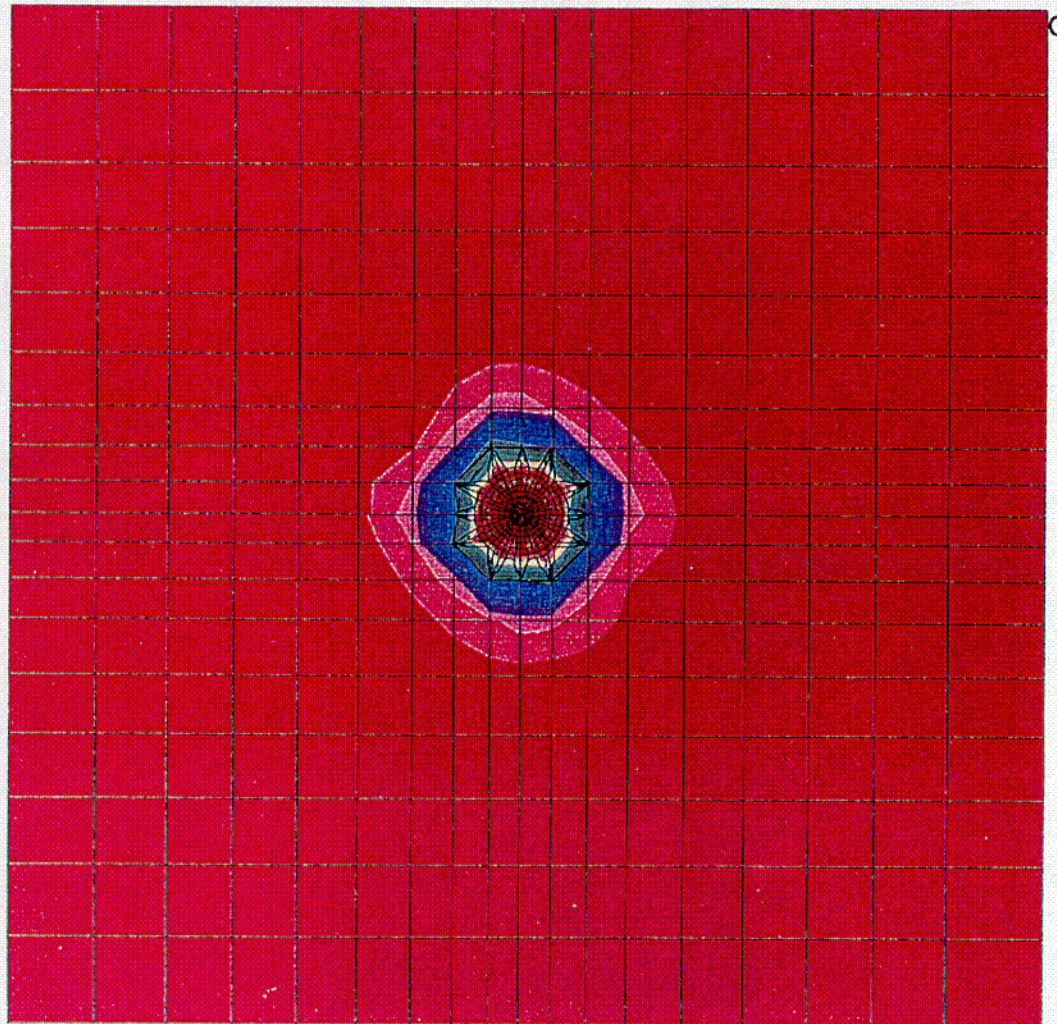
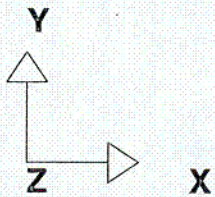
Figure 7.4.12; On-Center "Deep Drop" Baseplate Deformation

C-18

HEAVIEST RACK DROP ONTO POO

STEP 3 TIME = 5.9974566E-004

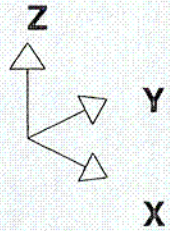
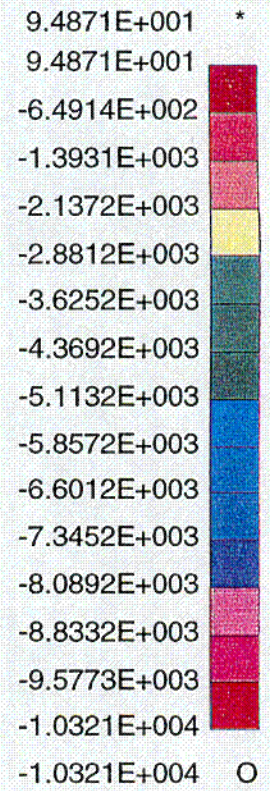
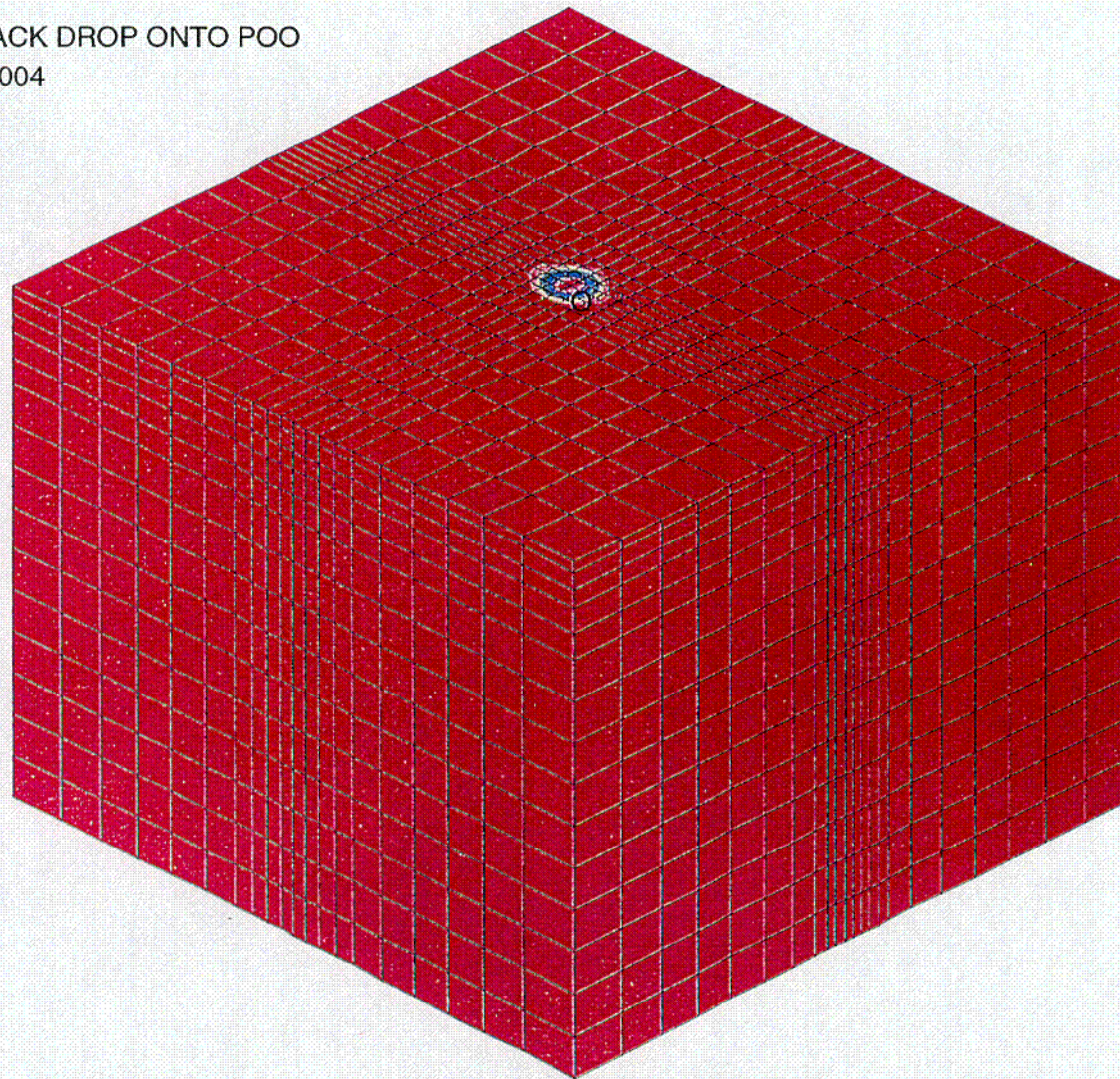
MAX\_VONMISES



13/10

Figure 7.4.13; "Heaviest Rack" Drop; Maximum Von Mises Stress - Liner

HEAVIEST RACK DROP ONTO POO  
STEP 3 TIME = 5.9974566E-004  
SIGZZ(MID)



## 8.0 SPENT FUEL POOL AREA STRUCTURE INTEGRITY CONSIDERATIONS

### 8.1 Introduction

The Davis-Besse Nuclear Power Station Spent Fuel Pool is an elevated reinforced concrete enclosure classified as safety related seismic category I. The pool walls and floor are monolithically integrated within the rest of the Auxiliary Building reinforced concrete structure.

The intent of this calculation is to assess the structural adequacy and determine the deformation and stress field of the all reinforced concrete structural elements pertinent to the Spent Fuel Pool (SFP) when subjected to the new loading conditions introduced by the proposed re-racking. The performance criteria, used to assess the structural performance and safety factors, is developed in accordance with the provisions stipulated in the USNRC OT Position Paper, Section IV [8.1.1], NUREG-0800 Standard Review Plan (SRP) [8.1.2], ACI-349 [8.1.3], ACI-318 [8.1.4], and the First Energy Corporation SFP Re-rack Specification [8.1.5].

### 8.2 Description of Spent Fuel Storage Pool Area Structure

The analyzed reinforced concrete structure, comprising the structural elements of the Spent Fuel Pool (SFP), Transfer Pit (TP) and Cask Pit (CP), is isolated from the remainder of the Auxiliary Building structure and is assumed to be a completely independent skeleton. The structural elements under investigation are shown on Figures 8.2.1 through 8.2.5. With the exception of the SFP West wall and CP North wall, which are 3' thick, all other reinforced concrete walls have a thickness of 5'-6". Additionally, the investigated structure also comprises three reinforced concrete walls located under the SFP slab, which are 2' thick, and the SFP and TP floor slabs are characterized by a uniform thickness of 5'. The upper face of the slabs is located at elevation 563'-6". The continuity of the SFP West wall is interrupted by the existence of two 3' wide gate openings, located between elevation 578' and elevation 603'. (These gate openings connect the SFP to the CP and TP.) The main reinforced concrete walls are spanning between elevation 545', the elevation of the general mat of the Auxiliary Building, and elevation 603', the elevation of the operation floor. The walls bounding the CP area are resting on the massive block of the reinforced concrete mat at elevation 557'. Although the CP reinforced concrete walls were previously investigated and declared qualified to sustain the new loads related to the installation of four racks inside the pit [8.2.1], they are

included in the present numerical investigation to obtain a more realistic behavior of the overall structure. There are four removable steel struts located in the TP, which span between the SFP West wall and the TP West wall. These struts are designed to support the wall between the TP and the SFP and must be installed prior to TP drainage below the depth of the bottom of the gates (578' el.).

### 8.3 Definition of the Individual Loads

Four of the load categories described in NUREG-0800 Standard Review Plan [8.1.2] are applicable. They are dead loads (D), live loads (L), thermal loads (operating - To and accident - Ta) and seismic induced loads (OBE - E and SSE - E').

#### 8.3.1 Static Loading (Dead and Live Loads)

(D1) - Dead weight of the modeled concrete structure.

(D2) - Dead weight of the fully loaded spent fuel racks. The weights pertinent to each rack pedestal are converted into concentrated forces.

(D3) - Dead load of the reinforced concrete Auxiliary Building upper structure resting on the modeled structure, which includes the weight of the Spent Fuel Cask Crane and fuel handling bridge.

(D4) - Hydro-static water pressures.

The total dead load (D) is obtained by the summation of the four individual load described above as follows:

$$D = D1 + D2 + D3 + D4$$

(L) - The live loads considered in this numerical investigation are the live loads induced by the Auxiliary Building upper structure. Additional live loads are induced by the Spent Fuel Cask Crane and by the fuel handling bridge.

### 8.3.2 Thermal Load - $T_o$ , $T_a$

Two thermal loading conditions, normal operating ( $T_o$ ) and accident ( $T_a$ ), are evaluated.

The steady state maximum normal bulk water temperature for partial discharge operating condition ( $T_o$ ) in the Spent Fuel Pool, Cask Pit, and Transfer Pit is taken to be 150°F (see additional discussion below). The accident condition considers the water temperature ( $T_a$ ) to be 170°F. The air temperature outside of the analyzed structure is conservatively considered to be -10°F under winter conditions. The soil temperature is taken to be 38°F. The temperature of the concrete casting, where the structure is supposed stress free, is established at 60°F. The temperature in the rooms of the Auxiliary Building outside of the space included in the 3-D finite-element model is also considered to be 60°F.

To accurately determine the temperatures existing at the faces of the concrete walls and slabs, the temperatures on each side of the wall or slab are determined using a one-dimensional steady-state heat transfer analysis. The temperatures determined from the heat transfer analysis are then used as inputs in the numerical analysis of the concrete structure elements.

The ACI-318 Code [8.1.4] limits the temperature under normal conditions to 150°F. The thermal-hydraulic evaluation of the pools (see Section 5.0) shows that the enclosed water may reach slightly greater bulk pool temperatures (actually 151.42°F is the calculated value) under the worst case conditions. Under these conditions it will conservatively be considered that the surface of the concrete reaches this temperature at some point. This is conservative because:

- The duration that the bulk pool temperature will exceed 150°F is short,
- The magnitude of the elevated temperature above 150°F is very small,
- The concrete has an associated thermal inertia, and
- The hottest water temperatures are found within the spent fuel storage racks, thus, the down comers along the wall will be slightly cooler than the bulk pool temperature.

A concrete temperature in excess of 150°F under the worst case conditions is acceptable, since it will be experienced for a short duration. Additionally, there will be no significant deterioration of the concrete material properties. Based on ACI Publication SP25 [8.3.1] and numerous other technical papers, concrete compressive strength decreases about 10% at temperature 200°F as compared with the design specified strength of 4,000 psi. However, based on an ASCE paper [8.3.2], the concrete compressive strength even at boiling conditions of 212°F is higher than the 28 day  $f_c'$ , if the strength margin from age is considered. At 212°F the concrete residual modulus of elasticity is about 96.5% of the concrete modulus of elasticity at ambient temperature ( $E_c$ ) and the rebar residual modulus of elasticity is about 95% of the rebar modulus of elasticity at ambient temperature ( $E_{rebar}$ ) according to ACI 216 [8.3.3]. In general, both thermal expansion in the cross-section and the water pressure tend to create moments which cause the tension side of the concrete in the structure to be on the side away from the elevated temperatures. The reinforcement and concrete on the outside face are not affected by temperature increases within the pool. Therefore, the short term elevated temperatures above the 150°F range do not significantly affect the material properties and evaluation of the cross-sections at 150°F for normal conditions is justified.

### 8.3.3 Seismic Induced Loads - (E, E')

Seismic induced loads consist of the following:

- 1) Vertical loads transmitted by the rack support pedestals to the slab during an OBE or SSE seismic event.
- 2) Hydrodynamic inertia loads due to the contained water mass and sloshing loads [8.3.4] which arise during a seismic event (OBE and SSE scenarios).
- 3) Hydrodynamic pressures between the rack and pool walls caused by the rack motion in the pool during a seismic event.
- 4) Seismic inertia forces of the entire structure.

Two levels of seismic events are considered in the analysis: the operating basis earthquake (OBE) and the safe shut down earthquake (SSE). The inertial loads generated for OBE and

SSE, noted as E and E', respectively, are obtained by an individual application of each one of the three-dimensional acceleration spectra (NS, EW, and Vertical) corresponding to this area of the Auxiliary Building. To determine the magnitude of the final deformation and stress fields the solution of all three orthogonal components of the seismic induced loads are summed using SRSS.

#### 8.4 Analysis Procedures

The structural region under investigation is comprised of six main reinforced concrete walls (SFP East wall, SFP West wall, TP and CP West wall, SFP and TP North wall, CP North wall, and SFP and CP South wall), two slabs (SFP floor slab, and TP floor slab) and three secondary walls located under the SFP slab. These building components are fictitiously considered isolated from the entire monolithic structure of the Auxiliary Building in order to prepare an analysis model. Due to the monolithic nature of the reinforced concrete Auxiliary Building, the artificial isolation of the structural region under investigation, as described above, requires that the interaction aspects, (rigidity and loading, with the remainder of the building) be accounted for in the numerical analysis. To keep the numerical evaluation in the conservative range, only the loads imposed by the surrounding reinforced concrete structure onto the analyzed model of the building are considered, while any additional rigidities (and associated load bearing pathways) which might participate from these portions of the Auxiliary Building structure are ignored.

The modeled structure is numerically investigated using the finite-element method. To account for the fact that the walls and slabs are very thick elements, a special shell finite-element, based on thick plate theory, is used to model those structural elements. The struts are modeled as beams with only axial rigidity.

The numerical results obtained for each individual load cases are combined using the load combinations required by the SRP [8.1.2] considering two scenarios. The loads considered for Scenario 1 depict the situation when the SFP is full of water and contains all fully loaded Holtec spent fuel racks, while the Cask Pit and Transfer Pit are empty and struts are in place. In Scenario 2 the loads are derived from the situation when the SFP is full of water and contains all fully loaded Holtec spent fuel racks, with the Transfer Pit is full of water up to elevation 578' (bottom of the gate), while the Cask Pit remain empty. The struts spanning the Transfer Pit are considered removed during Scenario 2.

#### 8.4.1 3-D Finite Element Model

The 3-D finite-element model encompasses the entire area of interest, around the SFP, described in the above section. The 3-D overview of the structural elements considered in the numerical investigation is shown in Figure 8.4.1.

The preprocessing capabilities of the STARDYNE computer code [8.4.1] are used to develop the 3-D finite element model. The STARDYNE finite element model contains 3425 nodes, 3393 thick shell type finite elements (QUADS), and for scenario 1 only, 4 beam type finite-elements (BEAMG). The plate type finite-element employed in the analysis has the capability to consider the shear deformation, which is essential for thick plates such as those representing the reinforced concrete slabs and walls.

#### 8.4.2 Boundary Conditions

In order to simplify the model, the monolithic joints between the modeled area of interest and the rest of the Auxiliary Building reinforced concrete structure are severed. To be conservative, no boundary conditions are imposed to simulate those connections.

The only boundary conditions imposed on the 3-D model are the total fixity of the nodes located at the junction between the lower walls and the Auxiliary Building mat and Cask Pit foundation block. Those nodes are completely restrained from movement or rotation. These restraints induce conservatism in the numerical evaluation.

#### 8.4.3 Material Properties

The behavior of the reinforced concrete existing in the structural elements (walls, slabs and beams) is considered elastic and isotropic. The elastic characteristics of the concrete are independent of the reinforcement contained in each structural element for the case when the uncracked cross-section is assumed. This assumption is valid for all load cases with the exception of the thermal loads, where the reinforced concrete cross section is assumed to be cracked. To simulate the variation and the degree of cracking patterns, the original elastic modulus of the concrete is modified.

The elastic characteristics for the concrete and reinforcement used in this calculation are summarized in Table 8.4.1. Table 8.4.2 contains the elastic isotropic material properties and the reduced elastic modulus ( $E_{\text{crack}}$ ) pertinent to each structural element present in the 3-D model.

#### 8.4.4 Load Combinations

##### 8.4.4.1 Concrete

The structural response is calculated for each of the thirty-four (34) individual load cases contained in Table 8.4.3. These various individual load cases are combined in accordance with the NUREG-0800 Standard Review Plan [8.1.1] requirements with the intent to obtain the most critical stress fields for the investigated reinforced concrete walls and slabs. The load combinations are repeated for Scenarios 1 and 2 defined in section 8.4.

For "Service Load Conditions" the following load combinations are:

- Load Combination No. 1 (LC1) =  $1.4 * D + 1.7 * L$
- Load Combination No. 2 (LC2) =  $1.4 * D + 1.7 * L + 1.9 * E$
- Load Combination No. 3 (LC3) =  $1.4 * D + 1.7 * L - 1.9 * E$
- Load Combination No. 4 (LC4) =  $0.75 * (1.4 * D + 1.7 * L + 1.9 * E + 1.7 * T_o)$
- Load Combination No. 5 (LC5) =  $0.75 * (1.4 * D + 1.7 * L - 1.9 * E + 1.7 * T_o)$
- Load Combination No. 6 (LC6) =  $1.2 * D + 1.9 * E$
- Load Combination No. 7 (LC7) =  $1.2 * D - 1.9 * E$

For "Factored Load Conditions" the following load combinations are:

- Load Combination No. 8 (LC8) =  $D + L + T_o + E'$

- Load Combination No. 9 (LC9) =  $D + L + T_o - E'$
- Load Combination No. 10 (LC10) =  $D + L + T_a + 1.25 * E$
- Load Combination No. 11 (LC11) =  $D + L + T_a - 1.25 * E$
- Load Combination No. 12 (LC12) =  $D + L + T_a + E'$
- Load Combination No. 13 (LC13) =  $D + L + T_a - E'$

where:

- D = dead load;
- L = live load;
- $T_o$  = thermal load during normal operation;
- $T_a$  = thermal load under accident condition;
- E = OBE earthquake induced loads;
- $E'$  = SSE earthquake induced loads.

#### 8.4.4.2 Steel (Struts)

The load combinations used in the evaluation of the four steel struts located inside the TP are prepared in accordance with NUREG-0800 Standard Review Plan [8.1.2] requirements. For "Service Load Conditions", in the presence of thermal stresses, the following load combinations are:

- Load Combination No. 1 (LC1) =  $D + L + T_o$
- Load Combination No. 2 (LC2) =  $D + L + T_o + E$
- Load Combination No. 3 (LC3) =  $D + L + T_o - E$

For "Factored Load Conditions" the following load combinations are:

- Load Combination No. 4 (LC4) =  $D + L + T_a$

- Load Combination No. 5 (LC5) =  $D + L + T_a + E$

- Load Combination No. 6 (LC6) =  $D + L + T_a - E$

- Load Combination No. 7 (LC7) =  $D + L + T_a + E'$

- Load Combination No. 8 (LC8) =  $D + L + T_a - E'$

where:

D = dead load;

L = live load;

$T_o$  = thermal load during normal operation;

$T_a$  = thermal load under accident condition;

E = OBE earthquake induced loads;

E' = SSE earthquake induced loads.

## 8.5 Results of Numerical Analyses and Safety Factor Calculations

The numerical investigation of the isolated portion of the Auxiliary Building reinforced concrete structure containing the SFP, TP, and CP walls and slabs, is conducted using a combination of the STARDYNE computer code [8.4.1] capabilities and spread sheet type calculations. The analysis is conducted as follows:

1. The disposition of the existing reinforcement located in the walls and slabs is studied considering that each individual steel bar has the capacity to fully carry tension. The walls and slabs are divided into two "capacity" zones, one longitudinal and the other vertical or transverse for each one of the structural components. For each "capacity" zone the axial-bending and axial-shear capacities are calculated in accordance with the requirements contained in ACI 349 [8.1.3].

2. The 3-D finite-element model of the region of interest (containing the SFP, TP, and CP walls and slabs) is created using the pre-processing capabilities of the STARDYNE computer code [8.4.1]. The “capacity” zones are reflected by the distribution of the finite-elements describing the walls and slab. This 3-D finite-element model, is used to simulate the structural behavior when subjected to the thirty-four individual load cases. The results can be plotted and inspected using the STARDYNE graphic pre-processor.
- 3.a The shear forces and bending moments, calculated for each finite-element contained in the 3-D finite-element model are extracted, segregated, and combined in the thirteen load combinations, as discussed in Section 8.4.4.1. The collected results can be plotted and inspected using the STARDYNE graphic pre-processor. Two types of safety factors, axial-bending and axial-shear, are calculated as the ratio of the reinforced concrete cross-sectional capacity to the corresponding calculated cross-sectional load.
- 3.b The strut axial forces and safety factors are calculated from the load combinations, as detailed in section 8.4.4.2.
4. At locations of discontinuities (such as re-entrant corners), it is appropriate to perform averaging of results for adjacent finite elements. However, in most cases the reported safety factors are not the results from averaging and are, therefore, conservative. In cases where the individual finite-elements show low axial-bending or axial-shear safety factors, the results are averaged together with the finite-elements located in the immediate vicinity.

A summary of the calculated minimum safety factors for the reinforced concrete cross-sections is provided in Tables 8.5.1 and 8.5.2 for Scenario 1 and Scenario 2, respectively (as described in Section 8.4). A summary of the calculated minimum safety factors for the steel struts is provided in Table 8.5.3.

## 8.6 Pool Liner

The pool liner is subject to in-plate strains due to movement of the rack support feet during the seismic event. Analyses are performed to establish that the liner will not tear or rupture under limiting loading conditions in the pool, and that there is no fatigue problem under the condition of 1 SSE event plus 20 OBE events. These analyses are based on loadings imparted from rack pedestals in the pool assumed to be positioned in the most unfavorable position. For pedestal locations near leak chases, liner integrity is shown to be maintained by conservatively analyzing the most highly loaded pedestal located in the worst configuration with respect to underlying leak chases.

## 8.7 CONCLUSIONS

The safety factors resulting from the numerical investigation of the reinforced concrete structural elements (walls and slabs) are contained in Tables 8.5.1 and 8.5.2 for Scenarios 1 and 2, respectively. The safety factors related to the struts are provided in Table 8.5.3. The tables show that the limiting safety factors have values greater than one (1.00). This fact demonstrates that the structural integrity of the Spent Fuel Pool area directly affected by the spent fuel capacity increase, is maintained under all load combinations required by NUREG-0800 [8.1.2].

The Transfer Pit is smaller than the Spent Fuel Pool, but the walls and slab are the same thickness. Therefore, temporary fuel storage during re-racking in a single rack placed in the Pit is bounded by the Pool analysis.

The calculated maximum pedestal force is not expected to tear the Cask Pit, Transfer Pit, or Spent Fuel Pool liner.

## 8.8 REFERENCES

- 8.1.1 U.S. NRC OT Position for Review and Acceptance of Spent Fuel Storage and Handling Applications, April 14, 1978, Revised January 18, 1979.
- 8.1.2 NUREG-0800, SRP 3.8.4, "Standard Review Plan, Section 3.8.4: Other Seismic Category I Structures," USNRC Office of Nuclear Reactor Regulation, Rev. 1, 7/81.
- 8.1.3 ACI 349-85 and ACI 349R-85, "Code Requirements for Nuclear Safety Related Concrete Structures and Commentary," American Concrete Institute, 1985.
- 8.1.4 ACI 318 and ACI 318R-95, "Building Code Requirements for Structural Concrete and Commentary," American Concrete Institute, 1995.
- 8.1.5 Specification C-063Q, "Technical Specification for Operational Phase for Engineering Activities, Fabrication and Delivery of High Density Spent Fuel Storage Racks for the Cask Pit and Spent Fuel Pool for the First Energy Corporation, Davis-Besse Nuclear Power Station Unit 1, Oak Harbor, Ohio", Revision 7, September 7, 1999.
- 8.2.1 Holtec Report HI-981933, Revision 2, "Design and Licensing Report Davis-Besse Nuclear Power Station 1 Cask Pit Rack Installation Project", submitted with First Energy License Amendment Application 98-007, dated May 21, 1999.
- 8.3.1 ACI Publication SP25, "Temperature and Concrete,"
- 8.3.2 ASCE Convention Paper, "Strength Properties of Concrete at Elevated Temperatures," Boston, Mass., April 1979.
- 8.3.3 ACI 216, R-81, "Guidelines for Determining the Fire Endurance of Concrete Elements"
- 8.3.4 TID-7024, "Nuclear Reactors and Earthquakes", US Atomic Energy Commission Division of Technical Information, Washington DC, August 1963.
- 8.4.1 Research Engineers Inc., "STARDYNE ", Version 4.55.

**Table No. 8.4.1 Concrete and Reinforcement Properties**

Parameter	Notation	Value
Concrete Compressive Strength (psi)	$f'_c$	4.000E+03
Un-Cracked Concrete Elastic Modulus (psi)	$E_c$	3.605E+06
Concrete Poisson's Ratio	$\nu$	0.167
Concrete Weight Density (lb/ft <sup>3</sup> )	$D_w$	150.0
Concrete Thermal Expansion Coefficient	$\alpha$	5.500E-06
Reinforcement Yield Strength (psi)	$F_y$	6.000E+04
Reinforcement Elastic Modulus (psi)	$E_{rebar}$	2.900E+07
Strut Steel Elastic Modulus (psi)	$E_{steel}$	2.900E+07
Strut Cross-Sectional Area (in <sup>2</sup> )	$A_{steel}$	16.10

**Table No. 8.4.2 Material Properties**

<b>Structural Element</b>	<b>Thickness (in)</b>	<b>Material Type</b>	<b><math>E_{crack}</math> (*) (psi)</b>
1. SFP East Wall Upper Zone	66	concrete	8.584E+05
2. SFP West Wall Upper Zone	36	concrete	1.293E+06
3. TP & CP West Wall Upper Zone	66	concrete	8.589E+05
4. SFP East Wall Lower Zone	66	concrete	-
5. SFP West Wall Lower Zone	36	concrete	-
6. TP & CP West Wall Lower Zone	66	concrete	-
7. SFP & TP North Wall Upper Zone	66	concrete	8.589E+05
8. SFP & CP South Wall Upper Zone	66	concrete	1.114E+06
9. SFP & TP North Wall Lower Zone	66	concrete	-
10. SFP & CP South Wall Lower Zone	66	concrete	-
11. Walls Under the SFP Slab	24	concrete	-
12. CP North Wall Upper Zone	36	concrete	1.293E+06
13. SFP Slab	60	concrete	1.331E+06
14. TP Slab	60	concrete	1.331E+06
15. CP North Wall Lower Zone	36	concrete	-
16. Struts	-	steel	-

Note: (\*)

- Upper Zone is located above the slab elevation 561'
- Lower Zone is located below the slab elevation 561'

**Table No. 8.4.3 Individual Load Cases**

Load No.	Type	Description
1	D1	Structural Concrete Weight
2	D2	Fully Loaded Racks
3	D3	Auxiliary Building Upper Structure
4	D4	Scenario 1 - SFP Hydro-Static Water Pressure Scenario 2 - SFP (full) and TP (up to gate only) Hydro-Static Water Pressure
5 (*)	D5	CP Hydro-Static Water Pressure (full)
6 (*)	D6	TP Hydro-Static Water Pressure (full)
7 (*)	D7	TP (up to gate only) Hydro-Static Water Pressure
8	L	Auxiliary Building Upper Structure
9	$E_{NS_s}$	OBE-NS- Structure Seismic Forces
10	$E_{NS_r}$	OBE-NS- Rack to Wall Coupling Pressure
11	$E_{NS_s}$	OBE-NS- Auxiliary Building Upper Structure Forces
12	$E_{NS_w}$	OBE-NS- Hydro-Dynamic Water Movement
13	$E_{EW_s}$	OBE-EW- Structure Seismic Forces
14	$E_{EW_r}$	OBE-EW- Rack to Wall Coupling Pressure
15	$E_{EW_s}$	OBE-EW- Auxiliary Building Upper Structure Forces
16	$E_{EW_w}$	OBE-EW- Hydro-Dynamic Water Movement
17	$E_{V_s}$	OBE-VERTICAL- Structure Seismic Forces
18	$E_{V_r}$	OBE-VERTICAL- Rack to Wall Coupling Pressure
19	$E_{V_s}$	OBE-VERTICAL- Auxiliary Building Upper Structure Forces
20	$E_{V_w}$	OBE-VERTICAL- Hydro-Dynamic Water Movement
21	$E_{NS_s}^c$	SSE-NS- Structure Seismic Forces
22	$E_{NS_r}^c$	SSE-NS- Rack to Wall Coupling Pressure
23	$E_{NS_s}^c$	SSE-NS- Auxiliary Building Upper Structure Forces
24	$E_{NS_w}^c$	SSE-NS- Hydro-Dynamic Water Movement
25	$E_{EW_s}^c$	SSE-EW- Structure Seismic Forces

26	$E_{EW_r}$	SSE-EW- Rack to Wall Coupling Pressure
27	$E_{EW_s}$	SSE-EW- Auxiliary Building Upper Structure Forces
28	$E_{EW_w}$	SSE-EW- Hydro-Dynamic Water Movement
29	$E_{V_s}$	SSE-VERTICAL- Structure Seismic Forces
30	$E_{V_r}$	SSE-VERTICAL- Rack to Wall Coupling Pressure
31	$E_{V_s}$	SSE-VERTICAL- Auxiliary Building Upper Structure Forces
32	$E_{V_w}$	SSE-VERTICAL- Hydro-Dynamic Water Movement
33	$T_o$	Temperature for Operating Condition
34	$T_a$	Temperature for Accident Condition

**Note: (\*) -load cases not used in the load combination cases.**

**Table No. 8.5.1 Scenario 1 (SFP full, CP & TP empty, Struts installed) Reinforced Concrete Minimum Safety Factors**

**8.5.1.1 SFP East Wall Above Elevation 561'**

Load Combination	Safety Factors			
	Horizontal		Vertical	
	Bending	Shear	Bending	Shear
1	2.80	2.75	3.89	3.17
2	1.97	5.82	2.43	2.24
3	2.91	1.80	7.56	2.24
4	1.57	11.12	4.42	2.80
5	1.63	2.64	4.68	2.58
6	2.66	7.69	2.61	2.53
7	3.33	1.95	9.54	2.56
8	2.14	15.44	5.39	2.77
9	1.93	2.51	5.85	2.63
10	1.79	10.08	4.76	3.06
11	1.76	2.84	4.94	2.79
12	1.80	16.71	4.35	2.74
13	1.74	2.55	4.94	2.58
Minimum	1.57	1.80	2.43	2.24

**8.5.1.2 SFP East Wall Below Elevation 561'**

Load Combination	Safety Factors			
	Horizontal		Vertical	
	Bending	Shear	Bending	Shear
1	82.73	17.15	15.23	14.85
2	28.58	10.94	5.09	7.59
3	51.10	4.82	14.70	14.30
4	1.29	2.40	1.09	2.39
5	1.07	2.02	3.33	3.00
6	29.38	10.15	4.75	8.65
7	50.47	4.99	12.92	16.52
8	2.71	3.27	1.29	3.02
9	3.07	2.49	4.91	4.12
10	1.54	2.59	1.33	2.70
11	1.83	2.20	3.51	3.35
12	1.49	2.69	1.34	2.60
13	1.87	2.14	3.94	3.49
Minimum	1.07	2.02	1.09	2.39

### 8.5.1.3 SFP West Wall Above Elevation 561'

Load Combination	Safety Factors			
	Horizontal		Vertical	
	Bending	Shear	Bending	Shear
1	4.20	2.04	4.88	3.10
2	2.78	1.17	2.96	2.10
3	2.96	3.21	3.57	2.26
4	2.14	2.23	2.90	2.91
5	2.95	6.59	5.24	2.36
6	3.14	1.25	3.24	2.34
7	3.28	4.13	3.93	2.51
8	2.32	1.86	2.67	2.84
9	3.41	8.09	6.77	2.39
10	2.15	2.47	3.09	3.16
11	2.84	6.58	5.18	2.58
12	2.05	1.97	2.46	2.86
13	3.03	9.33	5.72	2.35
Minimum	2.05	1.17	2.46	2.17

### 8.5.1.4 SFP West Wall Below Elevation 561'

Load Combination	Safety Factors			
	Horizontal		Vertical	
	Bending	Shear	Bending	Shear
1	62.60	31.33	11.89	10.46
2	15.73	5.75	6.00	3.16
3	16.15	9.09	9.46	2.33
4	2.56	3.62	5.75	6.57
5	2.40	4.13	4.07	2.41
6	15.79	5.92	5.87	2.98
7	16.26	8.69	8.90	2.38
8	3.47	3.63	7.43	3.64
9	3.06	4.39	4.51	2.30
10	2.93	4.04	6.27	9.20
11	2.73	4.54	4.29	2.59
12	2.98	3.30	6.29	4.03
13	2.70	3.97	3.92	2.18
Minimum	2.40	3.30	3.92	2.18

### 8.5.1.5 TP & CP West Wall Above Elevation 561'

Load Combination	Safety Factors			
	Horizontal		Vertical	
	Bending	Shear	Bending	Shear
1	6.89	10.75	12.63	14.39
2	5.00	4.11	6.98	6.07
3	4.39	66.59	9.61	20.41
4	1.90	8.92	3.07	4.42
5	2.45	13.49	5.93	12.41
6	6.05	4.26	7.74	6.59
7	5.17	35.61	10.10	18.74
8	2.22	6.33	3.38	4.70
9	3.04	12.47	7.75	22.27
10	2.35	9.60	4.26	4.92
11	2.91	17.82	7.18	13.13
12	2.11	6.45	3.41	4.44
13	2.73	12.13	7.75	17.88
Minimum	1.90	4.11	3.07	4.42

### 8.5.1.6 TP & CP West Wall Below Elevation 561'

Load Combination	Safety Factors			
	Horizontal		Vertical	
	Bending	Shear	Bending	Shear
1	100.00	100.00	30.44	32.62
2	7.44	7.66	2.00	4.72
3	14.69	8.22	5.42	6.16
4	1.06	11.12	1.36	1.92
5	1.12	5.28	1.79	1.78
6	7.63	7.34	2.14	4.81
7	14.37	8.27	5.37	6.02
8	1.07	8.09	1.40	2.45
9	2.06	5.48	3.02	2.40
10	1.42	11.94	2.28	2.60
11	1.91	6.67	2.91	2.42
12	1.06	7.46	1.48	2.43
13	1.99	5.70	3.03	2.28
Minimum	1.06	5.28	1.36	1.92

### 8.5.1.7 TP & SFP North Wall Above Elevation 561'

Load Combination	Safety Factors			
	Horizontal		Vertical	
	Bending	Shear	Bending	Shear
1	2.41	8.08	7.26	3.97
2	1.55	17.86	6.77	2.55
3	4.17	4.19	7.76	5.48
4	1.67	12.00	3.57	2.75
5	1.99	3.91	3.95	2.83
6	2.05	18.82	9.60	2.91
7	6.89	4.42	11.69	5.75
8	1.75	23.61	4.23	2.79
9	2.55	3.89	4.88	3.14
10	1.98	13.50	3.82	3.03
11	2.27	4.44	4.15	3.05
12	1.65	15.63	3.49	2.74
13	2.20	3.88	4.20	2.83
Minimum	1.55	3.88	3.49	2.55

### 8.5.1.8 TP & SFP North Wall Below Elevation 561'

Load Combination	Safety Factors			
	Horizontal		Vertical	
	Bending	Shear	Bending	Shear
1	100.00	16.67	42.70	20.13
2	32.49	6.26	6.90	11.66
3	57.99	4.09	15.51	8.85
4	1.39	2.32	2.94	2.98
5	1.86	2.03	5.60	4.36
6	33.27	5.47	6.37	12.47
7	56.59	4.27	13.98	10.10
8	3.72	3.10	3.04	3.57
9	4.27	2.50	8.78	5.08
10	2.10	2.50	3.25	3.28
11	2.50	2.20	5.93	4.99
12	1.99	2.57	2.70	3.01
13	2.60	2.15	6.98	5.12
Minimum	1.39	2.03	2.70	2.98

### 8.5.1.9 CP & SFP South Wall Above Elevation 561'

Load Combination	Safety Factors			
	Horizontal		Vertical	
	Bending	Shear	Bending	Shear
1	2.95	5.18	10.70	4.31
2	4.99	3.19	9.91	4.83
3	2.17	13.96	9.87	2.76
4	1.89	4.09	3.39	4.25
5	2.65	18.08	3.77	2.33
6	8.90	3.42	14.69	5.03
7	2.70	22.91	10.55	3.10
8	2.30	3.65	3.98	5.98
9	3.54	40.87	4.89	2.47
10	2.27	4.69	3.76	4.74
11	3.25	18.49	4.15	2.62
12	2.05	3.79	3.58	5.69
13	3.29	51.26	4.25	2.41
Minimum	1.89	3.19	3.39	2.33

### 8.5.1.10 CP & SFP South Wall Below Elevation 561'

Load Combination	Safety Factors			
	Horizontal		Vertical	
	Bending	Shear	Bending	Shear
1	64.74	16.00	30.18	34.14
2	20.25	4.99	6.72	6.83
3	11.57	10.43	6.92	13.09
4	1.63	1.23	2.84	1.25
5	2.33	1.87	3.92	1.35
6	19.68	5.14	6.92	6.96
7	11.84	9.83	6.63	12.44
8	2.75	1.38	2.93	1.76
9	3.84	2.66	4.44	1.81
10	2.35	1.37	3.60	1.79
11	3.14	1.92	3.98	1.64
12	2.21	1.20	3.02	1.49
13	3.29	2.09	3.70	1.60
Minimum	1.63	1.20	2.84	1.25

### 8.5.1.11 CP North Wall

Load Combination	Safety Factors			
	Horizontal		Vertical	
	Bending	Shear	Bending	Shear
1	5.50	27.87	38.19	8.42
2	3.64	9.64	22.35	5.28
3	8.82	55.66	45.84	20.67
4	4.80	23.67	19.54	5.11
5	6.36	8.27	43.29	13.23
6	4.02	9.79	23.95	5.83
7	9.76	44.65	49.00	32.70
8	4.62	100	18.41	5.22
9	6.79	9.18	43.50	21.33
10	5.22	58.86	23.22	5.90
11	7.17	11.59	44.54	15.50
12	4.67	100	17.75	5.28
13	6.58	9.85	39.36	22.36
Minimum	3.64	8.27	17.75	5.11

### 8.5.1.12 Walls Under the SFP Slab

Load Combination	Safety Factors			
	Horizontal		Vertical	
	Bending	Shear	Bending	Shear
1	29.98	14.76	18.57	37.97
2	17.44	11.28	9.03	12.33
3	15.28	7.63	11.28	10.76
4	1.60	5.43	2.31	8.12
5	1.35	3.96	6.62	12.35
6	18.83	11.50	8.77	12.79
7	16.70	8.35	11.87	11.34
8	1.39	7.99	2.74	9.45
9	1.32	4.68	7.88	12.28
10	1.35	5.95	3.03	9.17
11	1.17	4.35	7.22	14.23
12	1.13	6.17	1.78	8.20
13	1.30	4.09	6.86	11.79
Minimum	1.13	3.96	1.78	8.12

### 8.5.1.13 SFP Slab

Load Combination	Safety Factors			
	N-S		E-W	
	Bending	Shear	Bending	Shear
1	8.89	1.81	6.32	8.01
2	6.38	1.38	4.75	5.30
3	10.54	1.51	5.53	8.11
4	4.39	1.82	3.69	4.92
5	4.00	2.00	3.26	3.33
6	7.35	1.55	5.43	5.85
7	12.03	1.72	6.32	7.95
8	5.45	1.84	4.51	6.17
9	4.69	1.97	3.70	3.76
10	4.61	1.95	3.88	5.29
11	4.23	2.10	3.45	3.65
12	4.71	1.80	4.00	5.79
13	4.15	1.93	3.36	3.44
Minimum	4.00	1.38	3.26	3.33

### 8.5.1.14 TP Slab

Load Combination	Safety Factors			
	N-S		E-W	
	Bending	Shear	Bending	Shear
1	39.11	9.61	10.02	16.68
2	11.80	5.37	7.82	5.15
3	34.49	4.26	13.48	6.05
4	11.26	6.86	7.95	2.78
5	10.05	3.52	5.95	2.58
6	12.21	5.92	9.09	5.41
7	34.14	4.53	17.11	6.15
8	14.52	13.24	10.91	3.04
9	11.99	4.13	6.95	2.84
10	13.93	7.39	9.14	3.14
11	12.19	3.89	6.82	2.86
12	14.19	8.84	9.80	2.85
13	11.70	3.58	6.49	2.61
Minimum	10.05	3.52	5.95	2.58

**Table No. 8.5.2 Scenario 2 (SFP full, CP empty, TP @578' el., Struts removed)  
Reinforced Concrete Minimum Safety Factors**

**8.5.2.1 SFP East Wall Above Elevation 561'**

Load Combination	Safety Factors			
	Horizontal		Vertical	
	Bending	Shear	Bending	Shear
1	2.81	2.75	3.90	3.17
2	1.97	5.82	2.44	2.23
3	2.9	1.80	7.59	2.25
4	1.54	12.67	4.55	2.74
5	1.62	2.72	4.73	2.51
6	2.66	7.69	2.61	2.52
7	3.32	1.95	9.53	2.56
8	2.12	17.89	5.55	2.72
9	1.92	2.57	5.89	2.57
10	1.77	11.48	4.87	2.98
11	1.76	2.94	4.96	2.70
12	1.78	21.11	4.49	2.68
13	1.74	2.63	4.9	2.51
Minimum	1.54	1.80	2.44	2.23

**8.5.2.2 SFP East Wall Below Elevation 561'**

Load Combination	Safety Factors			
	Horizontal		Vertical	
	Bending	Shear	Bending	Shear
1	81.8	14.74	15.15	25.36
2	28.16	7.54	5.02	11.02
3	51.06	100.00	14.6	14.36
4	1.18	4.64	1.42	2.26
5	1.07	3.31	3.09	1.93
6	28.95	8.59	4.67	13.03
7	50.07	72.65	12.83	16.58
8	2.42	7.48	1.21	2.94
9	2.77	4.06	4.54	2.38
10	1.25	5.00	1.23	2.42
11	1.52	3.61	3.22	2.08
12	1.2	5.50	1.25	2.50
13	1.57	3.42	3.6	2.02
Minimum	1.07	3.31	1.21	1.93

### 8.5.2.3 SFP West Wall Above Elevation 561'

Load Combination	Safety Factors			
	Bending	Horizontal	Vertical	
		Shear	Bending	Shear
1	3.14	2.13	3.6	2.65
2	2.06	1.15	1.6	1.78
3	2.5	3.83	2.64	1.89
4	2.43	2.21	2.79	2.66
5	3.15	7.09	3.33	2.26
6	2.32	1.23	1.76	1.98
7	2.77	5.11	2.91	2.10
8	2.45	1.84	2.36	2.53
9	3.09	10.17	3.27	2.36
10	2.47	2.35	2.95	2.87
11	3.35	6.58	3.54	2.46
12	2.28	1.94	2.36	2.56
13	3.04	10.57	3.23	2.22
Minimum	2.06	1.15	1.6	1.78

### 8.5.2.4 SFP West Wall Below Elevation 561'

Load Combination	Safety Factors			
	Bending	Horizontal	Vertical	
		Shear	Bending	Shear
1	60.68	36.66	11.92	13.35
2	14.8	5.87	5.85	2.90
3	17.06	7.84	9.55	2.45
4	2.64	3.44	5.83	2.79
5	2.47	4.16	4.88	3.24
6	14.75	6.03	5.75	2.78
7	17.04	8.14	8.95	2.49
8	3.58	3.52	5.46	2.22
9	3.14	4.39	5.26	2.86
10	3.04	3.91	6.38	3.34
11	2.82	4.56	5.3	3.80
12	3.09	3.17	5.42	1.97
13	2.78	3.97	4.74	2.96
Minimum	2.47	3.17	4.74	1.97

### 8.5.2.5 TP West Wall Above Elevation 561'

Load Combination	Safety Factors			
	Horizontal		Vertical	
	Bending	Shear	Bending	Shear
1	6.1	9.48	26.2	19.66
2	4.39	3.79	15.72	7.67
3	4.59	100.00	11.56	22.08
4	1.53	19.73	1.54	4.04
5	2.26	7.85	3.13	9.34
6	5.28	3.95	16.49	8.22
7	5.25	48.32	11.99	18.88
8	1.82	9.01	1.76	4.45
9	2.88	8.13	4.3	15.89
10	1.87	28.99	1.86	4.38
11	2.65	8.47	3.42	9.49
12	1.66	12.82	1.54	4.01
13	2.55	6.80	3.73	11.69
Minimum	1.53	3.79	1.54	4.01

### 8.5.2.6 TP West Wall Below Elevation 561'

Load Combination	Safety Factors			
	Horizontal		Vertical	
	Bending	Shear	Bending	Shear
1	100	72.54	32.69	44.46
2	7.52	6.61	2.01	4.92
3	13.86	9.14	5.38	5.60
4	1.07	4.86	1.37	1.28
5	1.07	6.92	1.83	1.13
6	7.66	6.44	2.14	4.96
7	13.65	9.01	5.32	5.54
8	1.07	4.45	1.38	1.69
9	1.08	6.83	3.15	1.60
10	1.12	4.90	2.05	1.58
11	1.1	9.95	3.08	1.39
12	1.06	3.62	1.44	1.50
13	1.12	7.85	3.22	1.37
Minimum	1.06	3.62	1.37	1.13

### 8.5.2.7 TP & SFP North Wall Above Elevation 561'

Load Combination	Safety Factors			
	Bending	Horizontal	Vertical	
		Shear	Bending	Shear
1	2.40	8.42	7.26	4.07
2	1.55	43.91	6.77	2.58
3	4.15	4.28	7.76	5.22
4	1.66	5.64	2.48	2.55
5	1.66	2.86	3.01	2.56
6	2.05	39.46	9.59	2.96
7	6.65	4.50	11.68	5.50
8	1.75	8.05	2.98	2.63
9	2.20	3.02	3.75	2.85
10	1.96	5.68	2.64	2.79
11	1.84	3.05	3.13	2.71
12	1.64	6.35	2.4	2.53
13	1.81	2.78	3.17	2.53
Minimum	1.55	2.78	2.4	2.53

### 8.5.2.8 TP & SFP North Wall Below Elevation 561'

Load Combination	Safety Factors			
	Bending	Horizontal	Vertical	
		Shear	Bending	Shear
1	100.00	15.76	42.32	20.00
2	32.25	6.51	6.72	11.85
3	58.41	4.01	15.5	8.82
4	1.54	1.97	2.61	2.97
5	1.34	1.75	4.66	2.48
6	33.03	5.65	6.22	12.69
7	56.53	4.19	13.96	10.05
8	3.13	2.42	2.73	3.67
9	3.67	2.16	7.04	3.08
10	1.83	2.11	2.83	3.34
11	2.22	1.89	4.82	2.78
12	1.71	9.14	2.38	3.11
13	2.31	1.85	5.53	2.68
Minimum	1.34	1.75	2.38	2.48

### 8.5.2.9 CP & SFP South Wall Above Elevation 561'

Load Combination	Safety Factors			
	Horizontal		Vertical	
	Bending	Shear	Bending	Shear
1	2.950	5.19	10.70	4.31
2	4.99	3.18	9.90	4.83
3	2.17	14.15	9.87	2.76
4	1.92	3.67	3.23	3.96
5	2.58	12.50	3.64	2.24
6	8.89	3.41	14.69	5.04
7	2.69	23.41	10.55	3.09
8	2.32	3.36	3.74	5.55
9	3.45	22.94	4.75	2.39
10	2.28	4.16	3.61	4.39
11	3.09	12.51	4.00	2.50
12	2.07	3.40	3.34	5.19
13	3.12	22.22	4.1	2.32
Minimum	1.92	3.18	3.23	2.24

### 8.5.2.10 CP & SFP South Wall Below Elevation 561'

Load Combination	Safety Factors			
	Horizontal		Vertical	
	Bending	Shear	Bending	Shear
1	65.47	15.98	30.12	34.58
2	20.01	4.98	6.64	6.82
3	11.53	10.16	6.93	12.85
4	1.53	1.19	3.33	1.15
5	2.22	1.78	3.56	1.32
6	19.45	5.11	6.84	6.92
7	11.79	9.60	6.63	12.28
8	2.64	1.34	3.24	1.66
9	3.68	2.54	4.08	1.78
10	2.21	1.32	4.45	1.67
11	2.98	1.83	3.59	1.60
12	2.07	1.16	3.47	1.38
13	3.15	1.98	3.37	1.57
Minimum	1.53	1.16	3.24	1.15

### 8.5.2.11 CP North Wall

Load Combination	Safety Factors			
	Horizontal		Vertical	
	Bending	Shear	Bending	Shear
1	4.34	9.31	28.7	6.84
2	2.93	4.77	16.95	4.12
3	7.95	30.24	26.82	20.34
4	4.24	13.48	5.1	3.62
5	5.67	5.39	6.11	7.63
6	3.24	5.01	18.29	4.53
7	9.31	54.21	29.2	36.61
8	4.01	53.06	6.18	3.75
9	6.12	6.30	8.31	11.20
10	4.35	16.63	5.02	3.98
11	5.62	6.34	5.87	8.08
12	4.08	24.15	4.52	3.62
13	5.68	5.57	6.11	10.11
Minimum	2.93	4.77	4.52	3.62

### 8.5.2.12 Walls Under the SFP Slab

Load Combination	Safety Factors			
	Horizontal		Vertical	
	Bending	Shear	Bending	Shear
1	30.04	14.70	18.58	39.14
2	18.57	11.25	8.75	12.53
3	15.42	7.58	11.24	10.79
4	1.68	4.57	2.03	7.47
5	1.41	3.44	5.9	9.90
6	19.93	11.46	8.52	12.93
7	16.81	8.25	11.83	11.36
8	1.11	6.28	2.47	8.74
9	1.35	4.11	7.09	10.28
10	1.14	4.90	2.63	8.29
11	1.39	3.71	6.31	10.99
12	1.51	4.99	1.53	7.49
13	1.19	3.52	6.05	9.43
Minimum	1.11	3.44	1.53	7.47

### 8.5.2.13 SFP Slab

Load Combination	Safety Factors			
	Horizontal		Vertical	
	Bending	Shear	Bending	Shear
1	8.89	1.77	6.37	7.98
2	6.37	1.38	4.71	5.27
3	10.54	1.48	5.57	8.43
4	4.28	1.78	3.6	3.88
5	3.94	2.27	3.2	2.81
6	7.35	1.56	5.38	5.83
7	12.03	1.68	6.36	8.21
8	5.33	1.81	4.41	5.29
9	4.63	2.16	3.64	3.24
10	4.49	1.90	3.78	4.05
11	4.16	2.43	3.38	3.00
12	4.59	1.56	3.89	4.35
13	4.08	2.20	3.29	2.86
Minimum	3.94	1.38	3.2	2.81

### 8.5.2.14 TP Slab

Load Combination	Safety Factors			
	Horizontal		Vertical	
	Bending	Shear	Bending	Shear
1	30.39	5.50	9.76	7.63
2	10.15	3.59	7.59	3.52
3	41.38	3.07	13.22	4.16
4	4.81	9.73	4.3	1.93
5	4.65	3.35	3.6	1.93
6	10.63	4.04	8.81	3.79
7	39.28	3.33	16.81	4.37
8	6.11	25.89	5.73	2.14
9	5.75	3.28	4.3	2.14
10	5.07	10.20	4.5	2.07
11	4.91	3.66	3.81	2.07
12	5.11	13.48	4.68	1.93
13	4.87	3.22	3.69	1.92
Minimum	4.65	3.07	3.6	1.92

**Table No. 8.5.3 Scenario 1 (SFP full, CP & TP empty, Struts installed) Steel Strut  
Minimum Safety Factors**

Load Combination	Safety Factors
	Axial
1	1.94
2	1.64
3	1.64
4	1.79
5	1.53
6	1.53
7	1.37
8	1.37
Minimum	1.37

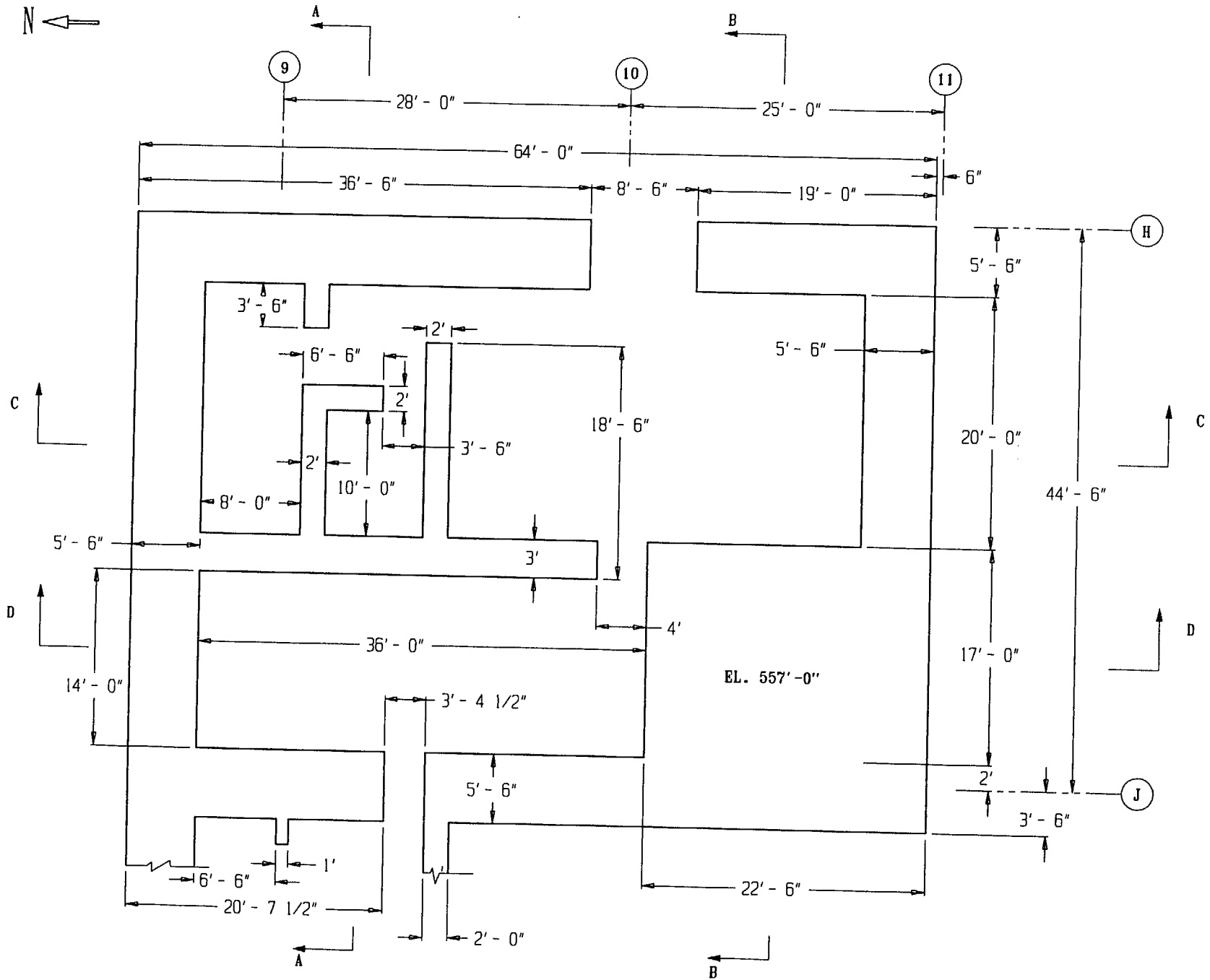


Figure 8.2.1; Plan View of Auxiliary Bldg. Below SFP

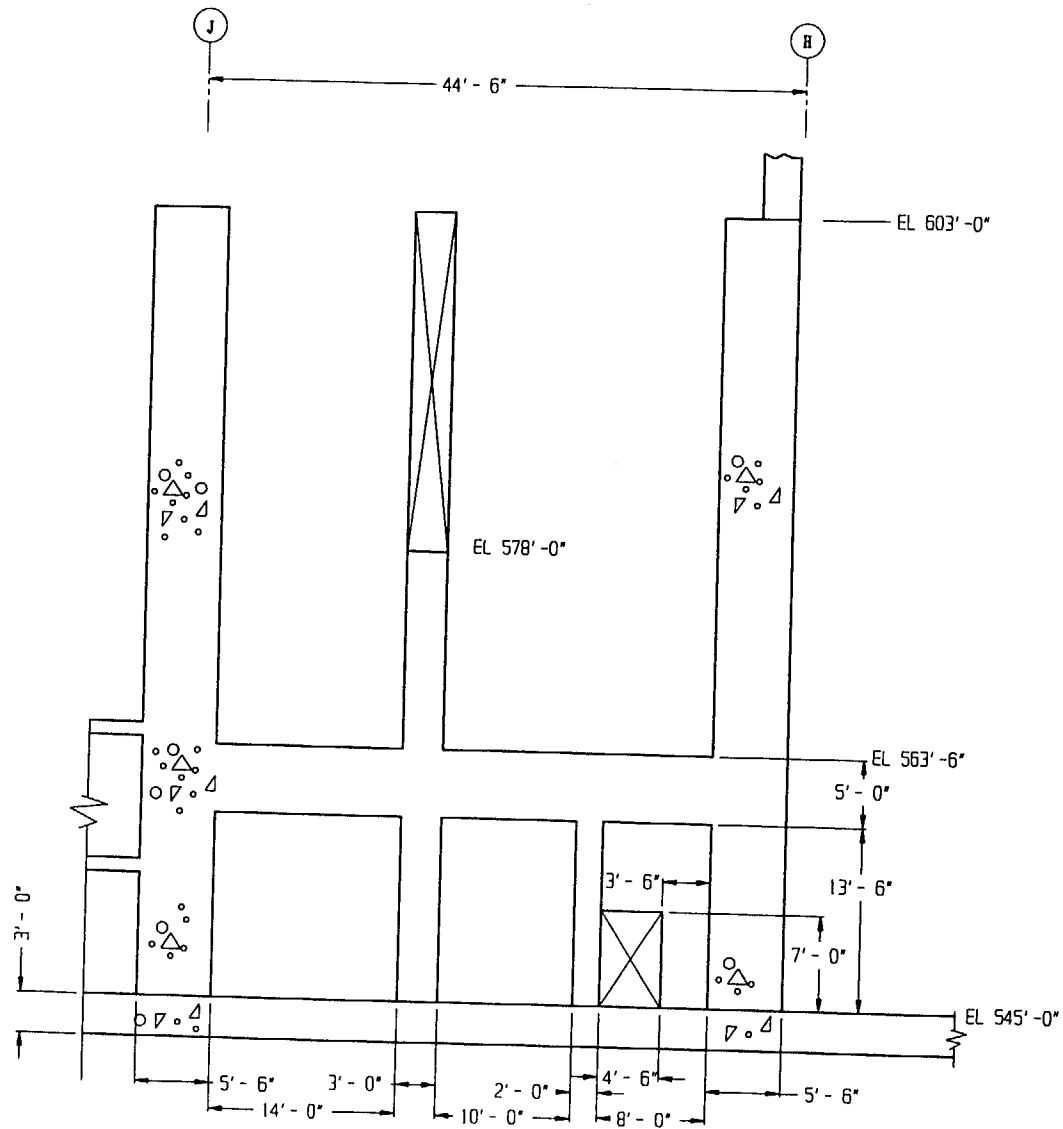


Figure 8.2.2; Sectional View A-A of Auxiliary Building

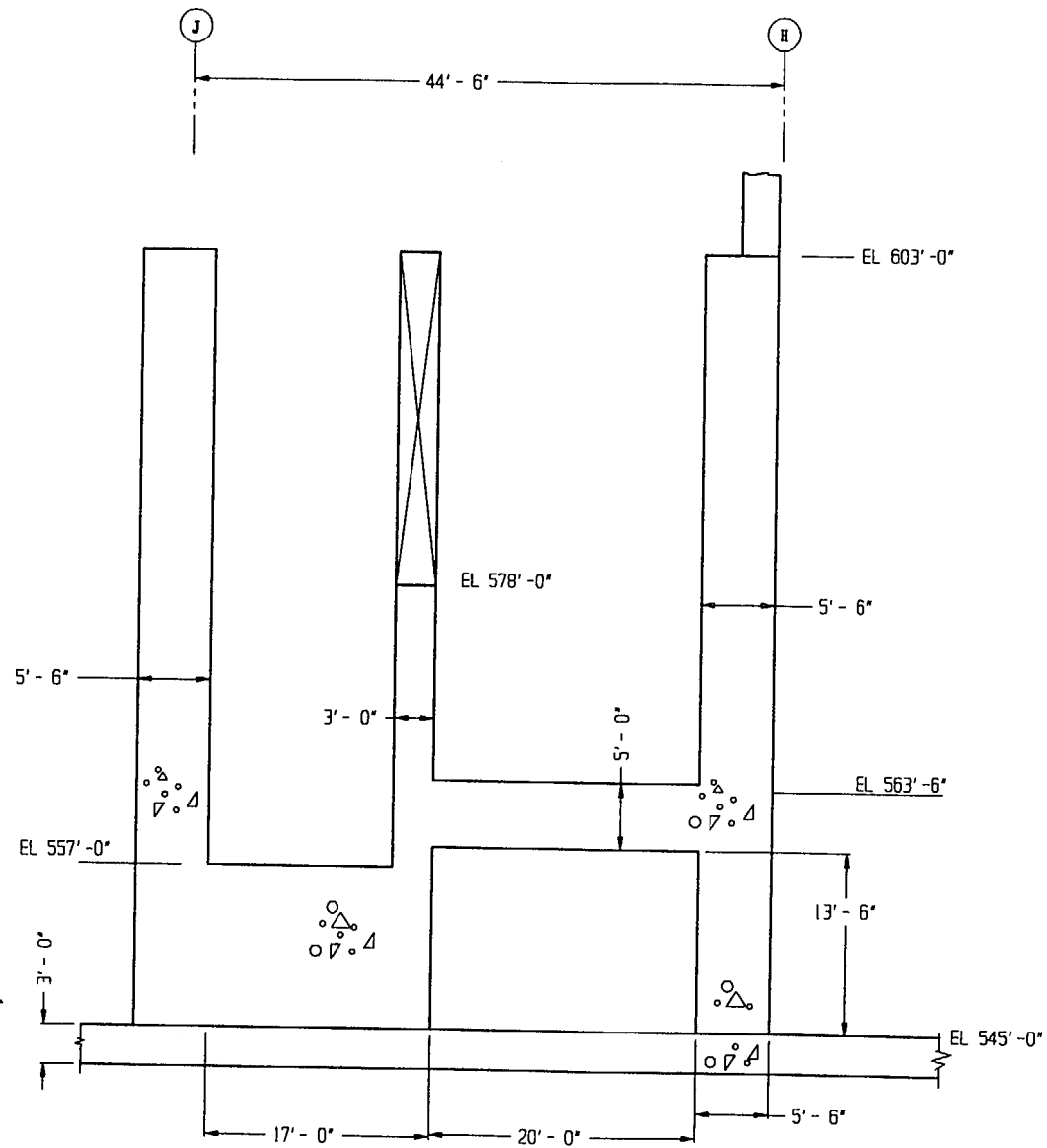


Figure 8.2.3; Sectional View B-B of Auxiliary Building

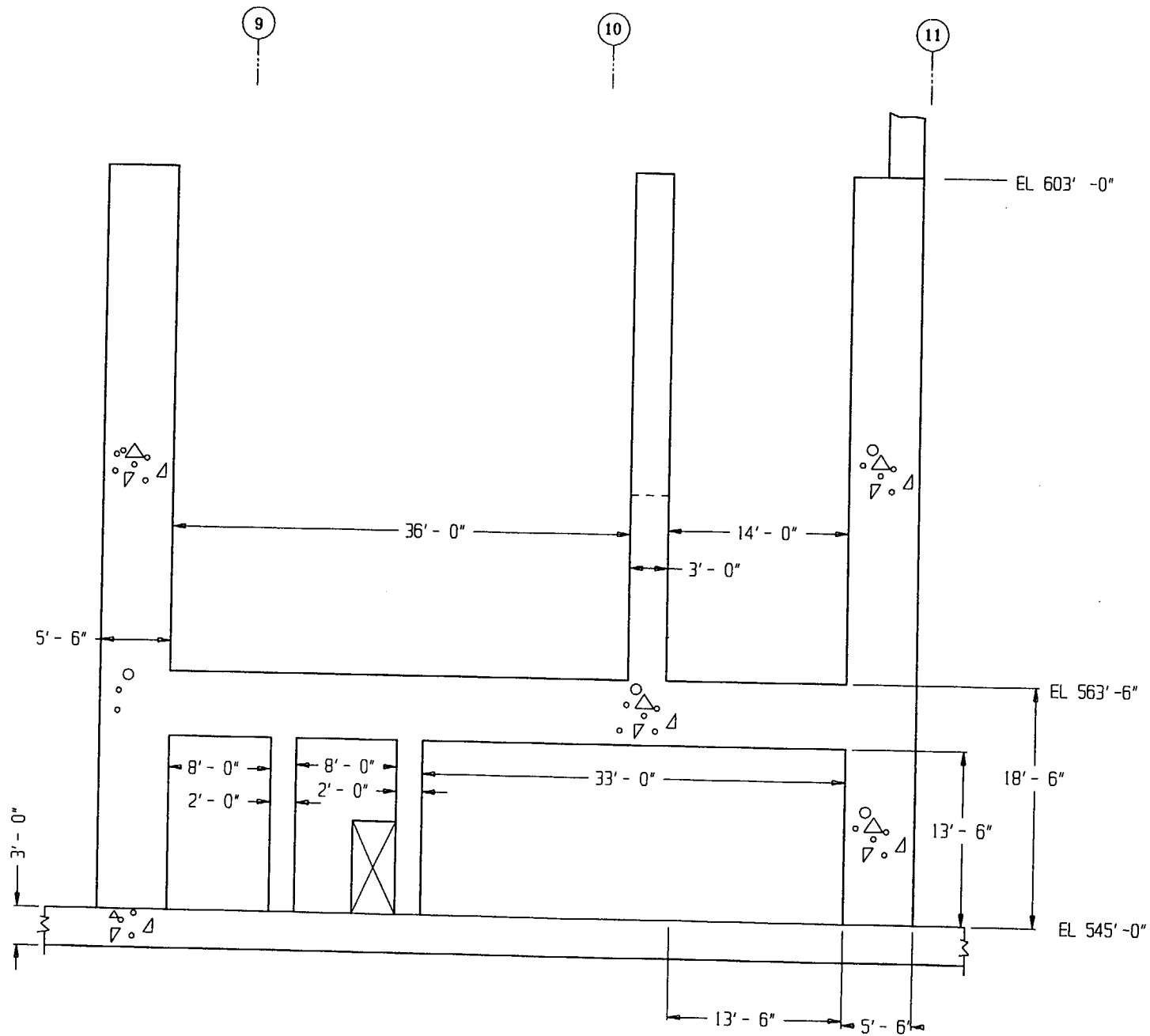
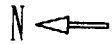


Figure 8.2.4; Sectional View C-C of Auxiliary Building

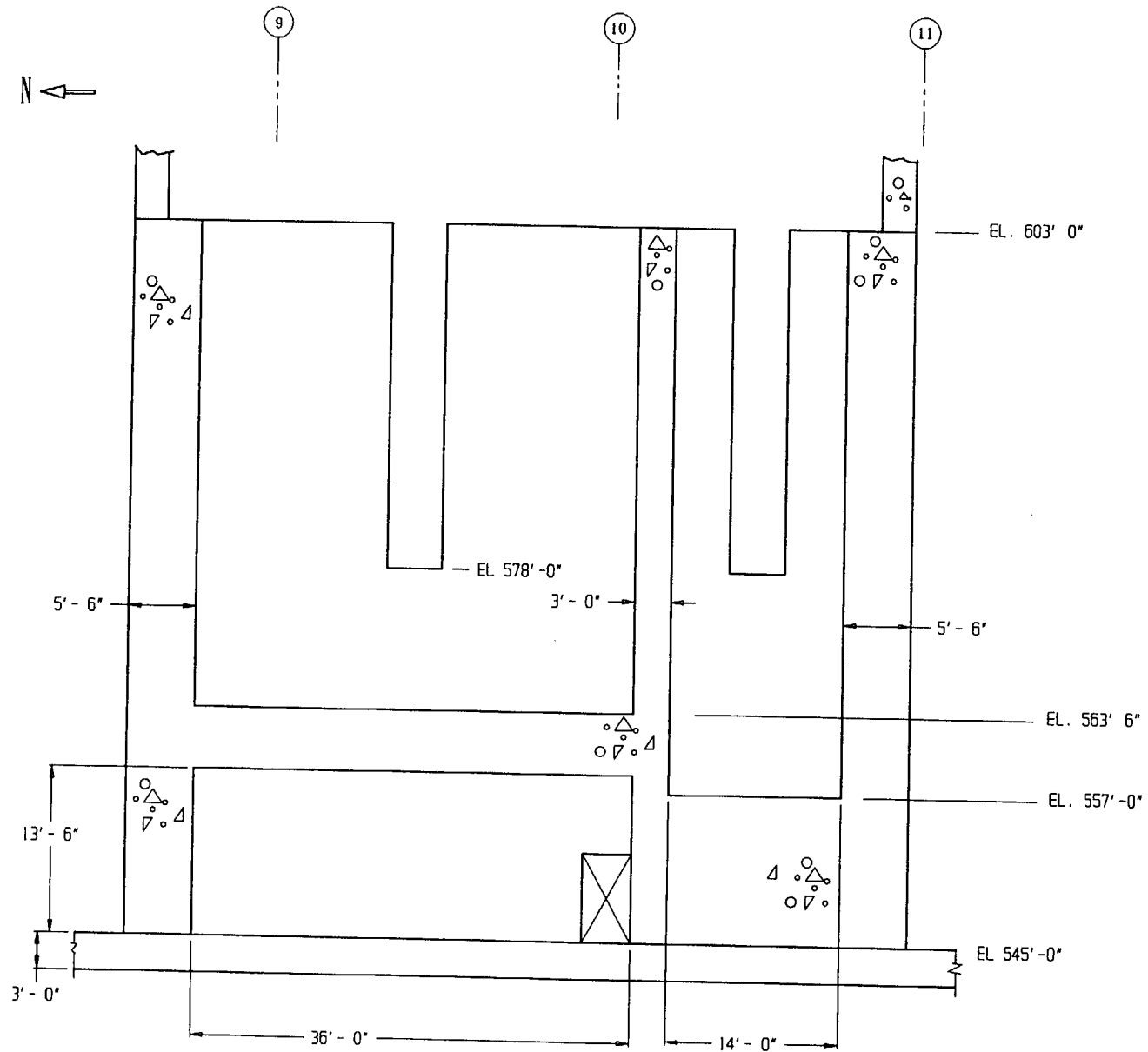
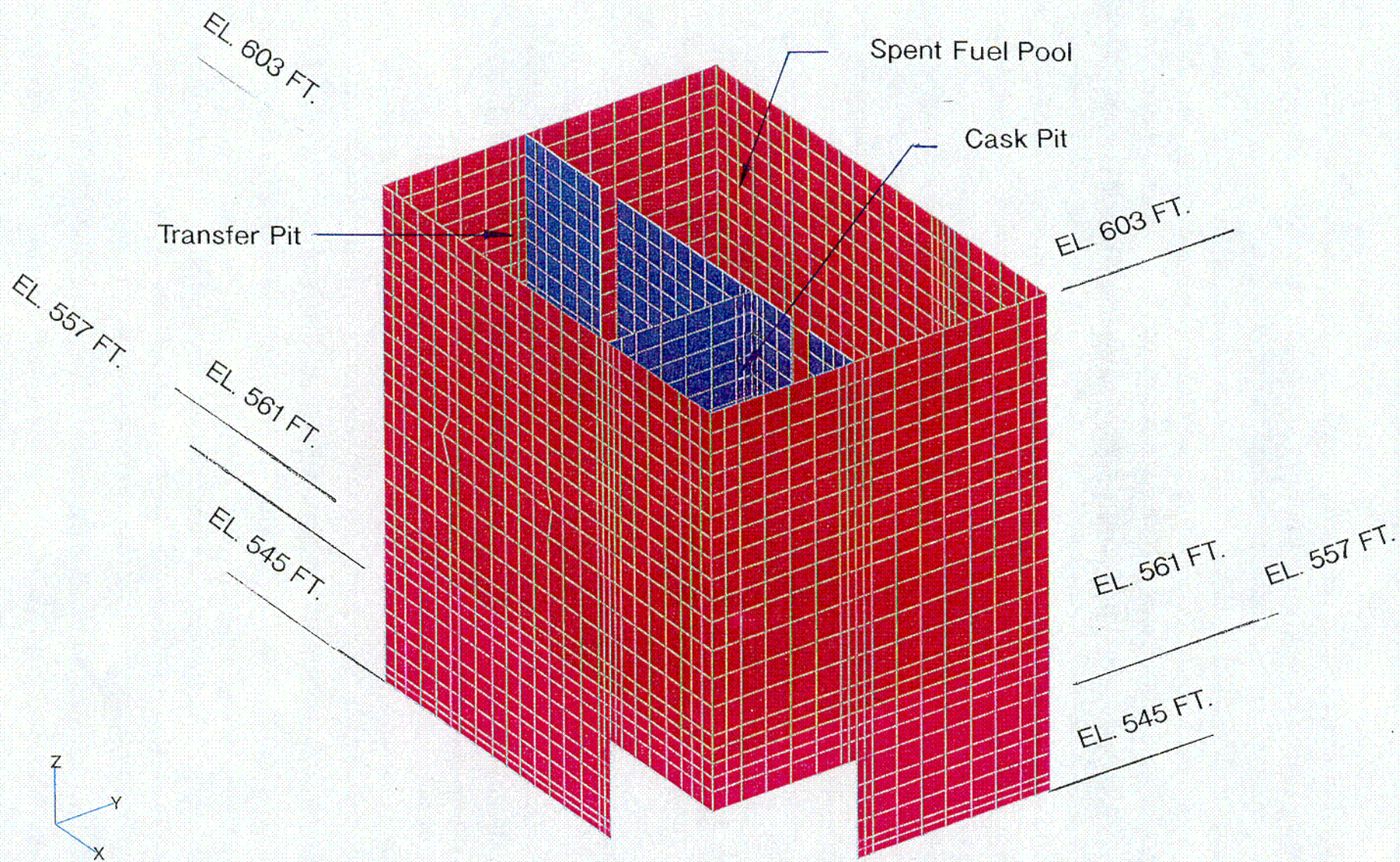


Figure 8.2.5; Sectional View D-D of Auxiliary Building

V1  
L5



## 9.0 RADIOLOGICAL EVALUATION

### 9.1 Solid Radwaste

The Spent Fuel Pool (SFP) Purification System currently generates approximately 50 cubic feet of solid radioactive waste annually at the Davis-Besse Nuclear Power Station (DBNPS). The necessity for pool filtration resin replacement is determined primarily by the requirement for water clarity, and the resin is normally changed about once every 18 months. Re-racking activities may result in a one-time shortening of the resin change-out interval, however, the long-term normal resin replacement frequency is not expected to be significantly affected by the additional number of fuel assemblies in storage.

Although no significant increase in the annual volume of solid radioactive waste is expected from operating with expanded spent fuel storage capacity, there are 12 fuel storage rack modules and the module for 15 "failed fuel" storage locations currently installed in the SFP that are being replaced with the new rack modules. There are also other miscellaneous items in the SFP, such as portions of piping, that will be removed to accommodate the new racks. There will be a one-time increase in solid waste generation due to the need to dispose of these components, however this represents an insignificant incremental increase in the total quantity of solid waste generated as a result of plant operation. The old racks and other miscellaneous items will be decontaminated via pressure washing or other acceptable cleaning mechanisms, prior to removal from the pool. The rack modules will be disassembled as required to facilitate their removal from the pool. The components will be removed from the pool under Health Physics dose rate surveillance, and transported to a designated location for any needed wrapping or placement into anti-contamination bags. An appropriate shipping container will be used to remove the existing rack components for eventual processing.

## 9.2 Liquid Releases

The number of spent fuel assemblies in storage does not affect the release of radioactive liquids from the plant. The contribution of radioactive materials in the SFP water from the stored assemblies is insignificant relative to other sources of activity, such as the reactor coolant system. The volume of SFP water processed for discharge is independent of the number of fuel assemblies stored.

## 9.3 Gaseous Releases

Gaseous releases from the fuel storage area are combined with other plant exhausts. Currently there is no detectable contribution from the fuel storage area, and no significant increases are expected as a result of the expanded storage capacity.

Release of radioactive gases by the DBNPS will remain a small fraction of the limits of 10 CFR 20.1301 and the design objectives of Appendix I to 10 CFR 50 following the implementation of the proposed modification to increase spent fuel storage capacity. This conclusion is based on the following supporting statements:

- a) The half-lives of short-lived nuclides such as I-131 are short in comparison to fuel cycle length; therefore, short-lived nuclides are present only in freshly offloaded fuel. The quantity of freshly offloaded fuel placed in storage each refueling outage is independent of the number of spent fuel assemblies being stored. Therefore, the inventory of I-131 will not be affected by the increased fuel storage capacity.
- b) Inventories of long-lived fission products (e.g. Kr-85 and ternary tritium) in spent fuel assemblies will decrease slowly within individual fuel assemblies over years in storage. Therefore, an increase in the number of stored spent fuel assemblies would increase the total inventory of these radionuclides. However, these radionuclides are not released in significant amounts from the stored fuel to the pool water, even for failed fuel, since the fuel pellet

temperature of stored fuel is not high enough to create sufficient gas pressure in the gap to overcome the static pressure of the pool water.

- c) The radioactivity in the pool water is independent of the number of stored assemblies. The water activity is primarily dependent on the amount of fuel assembly movement within the pool. The number of fuel assembly movements required for a refueling outage is generally limited to the movements required to complete the outage. The number of plant refueling outages should not change. Typical pool activities are listed in Table 9.3.1.
- d) The increased number of spent fuel assemblies in storage will raise the heat load on the pool and could result in an increase in the evaporation rate. Other than a small amount of tritiated water released by evaporation, the radionuclides are non-volatile and consequently are not released from the pool water. The increased evaporation rate of tritiated water would result in an increase in gaseous tritium released in the plant's effluents. However, the discharge of gaseous radioactive effluents will continue to be a small fraction of the limits of 10 CFR 20.1301 and the design objectives of Appendix I to 10 CFR 50.

#### 9.4 Personnel Doses

During normal operations, personnel working in the fuel storage area are exposed to radiation from the SFP. Operating experience has shown that area radiation dose rates originate primarily from radionuclides in the pool water.

During refueling and other fuel-movement operations, pool water concentrations might be expected to increase somewhat due to crud deposits spalling from spent fuel assemblies and due to activities carried into the pool from the primary system. With respect to the rack installation, fuel movements will be required in support of this project to reduce the possible dose to divers during the rack installation. For this reason, although dose rates above and around the Transfer Pit, Cask Pit, and SFP perimeter may increase marginally, the dose fields will still approximate

conditions seen during normal operating conditions. Routine radiation surveys would identify any change to dose rates, and the appropriate radiological controls would be revised as required.

Relative to the present racks, the new racks will give a higher density of fuel next to the Spent Fuel Pool (SFP) walls. The new racks will also be positioned closer to the walls than the present racks. Dose rates were conservatively calculated for the Auxiliary Building rooms (elevation 565 ft.) which are adjacent to the SFP and at the elevation of the racks. The maximum calculated dose rate for various fuel cooling times is given below.

Fuel Cooling Time	Dose Rate (mR/hr)
72 hours	12.2
1 year	0.19
5 years	0.01

If fuel is temporarily stored in the Transfer Pit (TP) during re-racking, the above results would be bounding. The SFP and TP walls are the same thickness, but the TP rack would set much farther from the walls than the SFP racks, ( $\approx 5$  feet vs.  $\approx 5$  inches).

USAR Figure 12.1-2 provides Radiation Zones for normal operation at elevation 565 ft. in the Auxiliary Building. Per this figure, the rooms with walls adjacent to the SFP and TP are designated C ( $\leq 15$  m<sup>r</sup>/hr) and E1 ( $\leq 1000$  m<sup>r</sup>/hr). It is expected dose rates experienced in actual practice will be significantly lower than calculated for the re-racked SFP, as the calculated results are based on conservative assumptions. Therefore, no changes to these Radiation Zone designations in the USAR are anticipated. During the re-racking, routine radiation surveys will be conducted to determine the actual dose rates in the rooms.

USAR Figure 12.1-1 provides Radiation Zones for normal operation at elevation 545 ft. in the Auxiliary Building. Per this figure, the rooms below the SFP and TP are designated D ( $\leq 100$  m<sup>r</sup>/hr) and E1 ( $\leq 1000$  m<sup>r</sup>/hr).

The dose rates at the ceilings of the rooms below the SFP and TP, from the fuel stored in the new racks, will be marginally (probably undetectable) greater than the dose rates from the fuel stored

in the present racks, as the source will have a higher density due to the closer spacing of the fuel. The amount of water, distance, and rack structural metal between active fuel and the floor slabs is greater than between the active fuel and the walls. Therefore, even with the floor slabs being thinner than the walls (5 feet vs. 5.5 feet), the dose rates at the ceilings from the fuel should be no greater than the dose rates through the walls. Based on this, no changes to these Radiation Zone designations in the USAR are anticipated. During the re-racking, routine radiation surveys will be conducted to determine the actual dose rates in the rooms.

Operating experience at the DBNPS has also shown that there are no detectable concentrations of airborne radioactivity in the SFP area except tritium, at approximately  $3E-3$  Derived Air Concentration (DAC). No increase in airborne radioactivity is expected as a result of the expanded storage capacity.

#### 9.5 Anticipated Dose During Rack Installation

All of the operations involved in the rack installation will utilize detailed procedures prepared with full consideration of ALARA principles. Similar operations have been performed in a number of facilities in the past, and there is every reason to believe that re-racking can be safely and efficiently accomplished at the DBNPS, with low radiation exposure to personnel.

Based on Holtec International's experience with re-racking similar spent fuel pools, the total dose for the re-racking operation is estimated to be between 6 and 12 person-rem, as indicated in Table 9.5.1. While individual task efforts and doses may differ from those in Table 9.5.1, the total is believed to be a reasonable estimate for planning purposes. The estimated person-rem burden for rack installation takes into consideration the use of divers.

The existing radiation protection program at the DBNPS is adequate for the rack installation operations. Where there is a potential for significant airborne activity, continuous air monitors will be in operation. Personnel will wear protective clothing as required and, if necessary,

respiratory protective equipment. Activities will be governed by a Radiation Work Permit, and personnel monitoring equipment will be issued to each individual.

Divers will be used for the removal of the existing SFP racks, installation of the new racks, and removal of rack interferences in the SFP. Each diver will be equipped with whole body and extremity dosimetry with remote, above surface, readouts which will be continuously monitored by Radiation Protection (RP) personnel. Divers will also be equipped with underwater survey instrumentation with remote readout capabilities. Divers will be in continuous communication with RP personnel. Radiation surveys of the dive area will be conducted prior to each dive operation and following movement of radioactive components in the SFP. Either visual or physical barriers will be used to ensure divers maintain a safe distance from radiation sources. A safety line attached to the diver will be manned by a dive tender at all times. This line will be used as necessary to limit diver movement.

Personnel traffic and equipment movement in the SFP area will be controlled to minimize contamination and to assure exposures are maintained ALARA. Cleanup of source material, which could contribute to an excessive dose for the divers, will be performed, as necessary, in accordance with good practices to limit dose ALARA. The existing SFP filtration system, or a temporary filtration system, will be used to maintain water clarity in the SFP.

After the rack installations, the lifting device will be washed with demineralized water and wrapped as necessary for contamination controls. The lift rig will be stored at the DBNPS site.

Table 9.3.1

AVERAGE ACTIVITY OF WEEKLY SFP SAMPLES  
(From February, 1999)

<u>Nuclide</u>	<u>Average Microcuries / cc</u>
Co-57	4.40 E-07
Co-58	1.57E-05
Co-60	8.65E-06
Ag-110M	3.66E-06
Sb-125	2.66E-05
Cs-134	9.88E-06
Cs-137	4.71E-05
Total	1.12E-04

Table 9.5.1

ESTIMATE OF PERSON-REM DOSE  
DURING RERACKING

Step	Number of Personnel	Hours	Estimated Person-Rem Dose †
Remove empty racks	5	40	0.5 to 1.0
Wash racks	3	10	0.08 to 0.2
Clean and vacuum pool	3	25	0.3 to 0.6
Remove underwater appurtenances	4	80	0.4 to 0.8
Partial installation of new rack modules	5	20	0.25 to 0.5
Move fuel to new racks	2	150	0.8 to 1.5
Remove remaining racks	5	120	1.5 to 3.0
Install remaining new rack modules	5	35	0.4 to 0.8
Decon and prepare old racks for shipment	4	80	1.0 to 2.0 ††
Total Dose, person-rem			6 to 12

† Based on Holtec's re-racking experience, assumes minimum dose rate of 2-1/2 mrem/hr (expected) to a maximum of 5 mrem/hr except for pool vacuuming operations, which assume 4 to 8 mrem/hr, and diving operations, which assume 20 to 40 mrem/hr.

†† Maximum expected dose, although details of preparation and packaging of old racks for shipment have not yet been determined.

10.0            INSTALLATION

10.1            Introduction

The installation phase of the Davis-Besse Nuclear Power Station (DBNPS) Unit 1 Spent Fuel Pool (SFP) re-rack project will be executed by Holtec International's Field Services Division. Holtec, serving as the installer, is responsible for performance of specialized services, such as underwater diving and welding operations, as necessary. All installation work at the DBNPS is performed in compliance with NUREG-0612 (refer to Section 3.0), Holtec Quality Assurance Procedure 19.2, DBNPS project specific procedures, and applicable DBNPS procedures.

A Cask Pit cover is necessary as the load path of some heavy loads will traverse the Cask Pit when it is loaded with fuel. The cover will be designed to ASME B & PV Code, Division 1, Subsection NF. The cover will be qualified to withstand the drop of an object of 17,530 lbs. from a height dictated by the cover design. The height will be administratively controlled by procedures.

The Cask Pit cover will be a heavy load. The activities associated with the installation and removal of the cover, including the rigging, will meet the requirements of NUREG-0612

Crane operators are trained in the operation of overhead cranes per the requirements of ANSI/ASME B30.2, and the plant's specific training program. Consistent with the installer's past practices, a videotape aided training session is presented to the installation team, all of whom are required to successfully complete a written examination prior to the commencement of work. Fuel handling bridge operations are performed by the DBNPS personnel, who are trained in accordance with DBNPS procedures.

A temporary crane will be used, as necessary, to position existing racks for removal and the final positioning of the new racks. The crane will be designed using CMAA-70 and the AISC manual, to meet the intent of NUREG 0612 through a defense-in-depth approach, (see Section 3.6).

The lifting device designed for handling and installation of the new racks at the DBNPS is engaged and disengaged on lift points at the bottom of the rack. The lifting device complies with the provisions of ANSI N14.6-1978 and NUREG-0612, including compliance with the design stress criteria, load testing at a multiplier of maximum working load, and nondestructive examination of critical welds.

Slings used for removal of the existing racks will be selected, inspected, and maintained in accordance with ANSI B30.9-1971.

A surveillance and inspection program shall be maintained as part of the installation of the racks. A set of inspection points, which have been proven to eliminate any incidence of rework or erroneous installation in previous rack projects, is implemented by the installer.

Underwater diving operations are required to remove underwater obstructions and the existing racks, to aid in the rack installation by assisting in the positioning of new rack modules, and to verify installation per design. The DBNPS procedures for control of diving and radiological controls for diving operations are utilized. The DBNPS procedures are supplemented by the safe-practices guidance provided by the diving company. These documents describe the precautions and controls for dive operations and were developed utilizing OSHA Standard 29CFR-1910, Subpart T.

Holtec International developed procedures, to be used in conjunction with the DBNPS procedures, which cover the scope of activities for the rack installation effort. Similar procedures have been utilized and successfully implemented by Holtec on previous rack installation projects. These procedures are written to include ALARA practices and provide requirements to assure equipment, personnel, and plant safety. These procedures are reviewed and approved in accordance with DBNPS administrative procedures prior to use on site. The following is a list of the Holtec procedures, used in addition to the DBNPS procedures to implement the installation phase of the project.

A. Installation/Handling/Removal Procedure:

This procedure provides direction for the disassembly and removal of the 12 existing rack modules and the module for 15 failed fuel storage locations, and the handling/installation of the 21 new high density modules in the Spent Fuel Pool. This procedure delineates the steps necessary to decontaminate an existing fuel rack, engage the existing rack with the lift frame, and remove the rack from the Spent Fuel Pool. It also provides overall direction for the handling and installation of the new maximum density fuel storage rack modules in the SFP. This procedure delineates the steps necessary to receive the new maximum density racks on site, the proper method for unloading and uprighting the racks, staging the racks prior to installation, and installation of the racks. The procedure provides for the installation of rack bearing pads, adjustment of the rack pedestals and verification of the as-built field configuration to ensure compliance with design documents. The procedure will provide guidance for rack removal and final placement of the four racks in the Cask Pit. If temporary use of a rack in the Transfer Pit is required, this procedure will provide guidance for rack installation and removal, and final placement in the SFP. The procedure also delineates the steps for installation and removal of the Cask Pit cover.

B. Receipt Inspection Procedure:

This procedure delineates the steps necessary to perform a thorough receipt inspection of a new rack module after its arrival on site. The receipt inspection includes dimensional measurements, cleanliness inspection, visual weld examination, and verticality measurements.

C. Cleaning Procedure:

This procedure provides for the cleaning of a new rack module, if required. The modules are to meet the requirements of ANSI N45.2.1, Level B, prior to placement in the SFP. Methods and limitations on cleaning materials to be utilized are provided.

D. Pre- and Post-Installation Drag Test Procedure:

These two procedures stipulate the requirements for performing a functional test on a new rack module prior to and following installation. The procedures provide direction for inserting and withdrawing an insertion gage into designated cell locations, and establishes an acceptance criteria in terms of maximum drag force.

E. ALARA Procedure:

Consistent with Holtec International's ALARA Program, this procedure provides guidance to minimize the total man-rem received during the rack installation project, by accounting for time, distance, and shielding. This procedure will be used in conjunction with the DBNPS ALARA program.

F. Liner Inspection Procedure:

In the event that a visual inspection of any submerged portion of the pool liner is deemed necessary, this procedure describes the method to perform such an inspection using an underwater camera and describes the requirements for documenting any observations.

G. Leak Detection Procedure:

This procedure describes the method to test the pool liner for potential leakage using a vacuum box. This procedure may be applied to any suspect area of the liner.

H. Liner Repair and Underwater Welding Procedure:

In the event of a positive leak test result, underwater welding procedures may be implemented which provide for a weld repair, or placement of a stainless steel repair patch, over the area in question. The procedures contain appropriate qualification records documenting relevant

variables, parameters, and limiting conditions. The weld procedure is qualified in accordance with AWS D3.6-93, Specification for Underwater Welding or may be qualified to an alternate code accepted by the DBNPS and Holtec International.

## 10.2 Rack Arrangement

The final rack arrangement allows for a total of 21 freestanding Holtec racks in the SFP, which provides a total of 1624 storage locations. A schematic plan view depicting the completed configuration of the SFP is shown in Figure 1.1.

The DBNPS Cask Pit is licensed (Amendment No. 237 to Facility Operating License No. NPF-3) to contain four freestanding Holtec racks, providing 289 storage locations. Two of the racks were installed in April, 1999 to add 153 storage locations. After licensing approval, these storage locations provided sufficient storage to regain full core offload capability (FCOC) for fuel Cycle 12 and allowed for core offload at the end of Cycle 12 (April, 2000), as required for the reactor vessel 10 year in-service-inspection. The installed Cask Pit racks also provide FCOC during Cycle 13 (May, 2000 to April, 2002). Prior to starting the SFP re-racking, the final two racks will be installed in the Cask Pit, (see also Section 11.2). Movement of the fuel into these racks will allow diver access to the SFP for removal of the existing racks. If necessary for diver safety, a rack may be placed in the Transfer Pit to allow for temporary storage of fuel. In the latter stages of the re-racking the fuel in the Cask Pit and Transfer Pit racks will be moved into the new racks, and the racks will permanently installed in the SFP.

## 10.3 Pool Obstructions

A survey was conducted to identify any objects which would interfere with rack installation or prevent usage of any storage locations. This survey determined unused light pole support brackets on the SFP walls must be removed. These brackets are mounted on one-half inch mounting plates attached to the liner. Each bracket will be removed from the mounting plate, leaving the plate intact, without effecting the liner.

At the north end of the SFP there is a sump in the floor to allow the Pool to be drained. The drain line enters the Pool through the north wall, takes a 90 degree bend downward, and extends into this sump. To install rack N4, this drain line and the associated supports must be removed. The line will be cut off close to the north wall. This line will not be re-installed as, 1) it serves no safety function, 2) it is rarely used, and a temporary alternate means of draining the pool can be made available, and 3) it would interfere with storage of fuel in the rack. In the south-east corner of the SFP, the cooling system return line enters the Pool through the east wall. This piping turns downward and extends to the bottom of the Pool where it discharges parallel to the floor. This line and its supports interfere with the installation and use of rack A1. Based on the SFP Computational Fluid Dynamics analysis, this line may be cut off close to the east wall.

In addition, it was identified the SFP floor liner restraint blocks may interfere with the bearing pad for the new racks. The design analysis allows for specific modifications to the bearing pads to accommodate the restraint blocks.

#### 10.4 SFP Cooling and Purification

##### 10.4.1 SFP Cooling

The pool cooling system shall be operated in order to maintain the pool water temperature at an acceptable level. It is anticipated that specific activities, such as bearing pad elevation measurements, may require the temporary shutdown of the Spent Fuel Pool cooling system.

Prior to any shutdown of the Spent Fuel Pool cooling system, the duration to raise the pool bulk coolant temperature to a selected value of  $\leq 120$  °F will be determined. A temperature of  $\leq 120$  °F is chosen such that cooling may be restored to ensure the pool bulk temperature will not exceed 150 °F.

#### 10.4.2 Purification

A portable vacuum system may be employed to remove extraneous debris, reduce general contamination levels prior to diving operations, and to assist in the restoration of SFP clarity following any installation processes.

#### 10.5 Fuel Shuffling

As new high density racks are installed in the SFP, fuel shuffles will be performed in independent phases in order to transfer irradiated assemblies from existing racks into the new racks. This will be completed in a sequence to allow diver access to the next set of racks while maintaining diver exposure ALARA. Fuel movement operations shall be conducted in accordance with DBNPS procedures.

#### 10.6 Removal and Decontamination of Existing Racks and Associated Structures

There are 12 rack modules and a module for 15 failed fuel storage locations in the Spent Fuel Pool, all of which are to be removed. Additionally, portions of the coolant discharge pipe and the pool drain line, as well as other miscellaneous items in the fuel pool, which will inhibit installation of new rack modules, will be removed from the pool through the use of a diver and underwater cutting tools. (See Section 10.3.)

Prior to removal of any existing structure from the Spent Fuel Pool, a pressure washer or other acceptable cleaning mechanism shall be employed to reduce general contamination levels and to eliminate to the best extent possible any "hot particles" which may be detected. A stainless steel wire brush, or equivalent abrasive tool may be utilized to supplement the removal of discrete high-source particles. These items shall be removed from the pool under dose rate surveillance and placed in an interim storage location to await processing.

Prior to pressure washing and removal of an existing rack, a quality verification shall be performed in order to ensure that no fuel assemblies remain in the module. The interior of each storage location shall be subjected to pressure washing. Upon completion of pressure washing rack internals, the rack will be disassembled as required for removal.

The individual storage cells will be disconnected from the rack frame and removed. After being cut into appropriate size parts, the remaining rack skeletal frame and the associated rack-to-wall braces will be hoisted from the pool. After rigging, the rack components shall be lifted a short distance and held stationary for a procedure-defined duration. The components will be removed from the pool using the Spent Fuel Cask Crane, Temporary Crane, and/or fuel handling bridge mono-rails (based on load restrictions).

The cells and/or rack skeletal frame will then be lifted slowly to a point just below the pool water surface to allow for any additional pressure washing of the exteriors. Upon completion of pressure washing, the existing rack components shall be removed from the fuel pool under Health Physics dose rate surveillance. The components shall remain over the pool until all significant dripping has abated. If required, additional volume reduction shall take place. The components shall then be transported along the safe load path to a designated location for any needed wrapping or placement into anti-contamination bags. An appropriate shipping container will arrive on site to remove the existing rack components for eventual processing.

#### 10.7 Installation of New Racks

Installation of the new high density racks, supplied by Holtec International, involves the following activities. The racks are delivered in the horizontal position. A new rack module is removed from the shipping trailer using a suitably rated crane, while maintaining the horizontal configuration. The rack is placed on the up-ender and secured. Using two independent overhead hooks, or a single overhead hook and a spreader beam, the module is up-righted into a vertical position.

The new rack lifting device is engaged in the lift points at the bottom of the rack. The rack is then transported to a pre-leveled surface where, after leveling the rack, the appropriate quality control receipt inspection is performed. (See 10.1B & D.)

The SFP floor is inspected and any debris, which may inhibit the installation of bearing pads, is removed.

After SFP floor preparation, new rack bearing pads are positioned on the floor before the module is lowered into the pool. The new rack module is lifted with the Spent Fuel Cask Crane (SFCC) and transported along the pre-established safe load path. The rack module is carefully lowered into the SFP. A temporary hoist, with an appropriate capacity, is attached to the SFCC in order to eliminate contamination of the hook during lifting operations in the SFP. For some racks, a temporary crane (see Section 3.6) may be necessary to move racks along the pool floor to their final position on the bearing pads.

Elevation readings are taken to confirm that the module is level. In addition, rack-to-rack and rack-to-wall off-set distances are also measured. Adjustments are made as necessary to ensure compliance with design documents. The lifting device is then disengaged and removed from the SFP under Health Physics direction. As directed by procedure, post-installation free path verification is performed using an inspection gage.

A Cask Pit cover, designed to withstand a rack load drop from an appropriate height above the operating deck shall be used to protect the fuel loaded in the Cask Pit racks. This Cask Pit cover is necessary because the load path of some racks will traverse the Cask Pit as they are moved into the Spent Fuel Pool.

10.8            Safety, Health Physics, and ALARA Methods

10.8.1        Safety

During the installation phase of the SFP re-rack project, personnel safety is of paramount importance, outweighing all other concerns. All work shall be carried out in compliance with applicable approved procedures.

10.8.2        Health Physics

Health Physics is carried out per the requirements of the DBNPS Radiation Protection Program.

10.8.3        ALARA

The key factors in maintaining project dose As Low As Reasonably Achievable (ALARA) are time, distance, and shielding. These factors are addressed by utilizing many mechanisms with respect to project planning and execution.

Time

Each member of the project team is trained and provided appropriate education and understanding of critical evolutions. Additionally, daily pre-job briefings are employed to acquaint each team member with the scope of work to be performed and the proper means of executing such tasks. Such pre-planning devices reduce worker time within the radiological controlled area and, therefore, project dose.

## Distance

Remote tooling such as lift fixtures, pneumatic grippers, a support leveling device and a lift rod disengagement device have been developed to execute numerous activities from the SFP surface, where dose rates are relatively low. For those evolutions requiring diving operations, diver movements shall be restricted by an umbilical, which will assist in maintaining a safe distance from irradiated sources. Additional restricting devices may be used as determined necessary by Davis-Besse. By maximizing the distance between a radioactive sources and project personnel, project dose is reduced. Fuel will be shuffled as necessary to ensure safe distances are maintained to satisfy ALARA principles.

## Shielding

During the course of the re-rack project, primary shielding is provided by the water in the Spent Fuel Pool. The amount of water between an individual at the surface (or a diver in the pool) and an irradiated fuel assembly is an essential shield that reduces dose. Additionally, other shielding, may be employed to mitigate dose when work is performed around high dose rate sources. If necessary, additional shielding may be utilized to meet ALARA principles.

### 10.9 Radwaste Material Control

Radioactive waste generated from the rack installation will be controlled in accordance with established DBNPS procedures.

## 11.0 ENVIRONMENTAL COST / BENEFIT ASSESSMENT

### 11.1 Introduction

Article V of the USNRC OT Position Paper [11.1] requires the submittal of a cost/benefit analysis for a fuel storage capacity enhancement. This section provides justification for selecting replacement of the racks in the Davis-Besse Nuclear Power Station (DBNPS) Spent Fuel Pool (SFP) as the most viable alternative.

### 11.2 Imperative for SFP Rack Replacement

In January of 1996, the DBNPS completed storage of 72 spent fuel assemblies in the certified NUHOMS® dry spent fuel storage system in accordance with the requirements of 10CFR72 Subpart K. After production of the NUHOMS® system was temporarily stopped and the technology was sold to another vendor, a decision was made to provide additional fuel storage by temporarily installing fuel racks in the Cask Pit, and then completely re-rack the SFP. Prior to installing the Cask Pit fuel racks, the DBNPS lost full core offload capability (FCOC) in April 1998, during the refueling outage conducted after Fuel Cycle 11. (The Davis-Besse reactor core contains 177 fuel assemblies.) Although FCOC is neither a license condition nor commitment for the DBNPS, it is considered a prudent operating practice.

In March of 2000, DBNPS received NRC approval (License Amendment No. 237 to Facility Operating License NPF-3) to utilize four racks modules (289 storage locations) in the Cask Pit. Two of the new fuel rack modules have been temporarily placed in the Cask Pit adding 153 fuel assembly storage locations. These two racks regained FCOC during Fuel Cycle 12 and maintain FCOC in Cycle 13 (May, 2000 to April, 2002).

A sufficient amount of fuel must be removed from the SFP to allow divers to safely take out the existing racks and install the new racks. This additional storage space will be provided by installing the two remaining Cask Pit racks prior to starting the SFP re-racking. If necessary, a

rack may be temporarily installed in the Transfer Pit. Near the end of the re-racking sequence, the four Cask Pit racks, and any placed in the Transfer Pit, will be relocated in the SFP.

Re-racking of the Spent Fuel Pool is scheduled to take place during Fuel Cycle 13. If the re-racking is not completed during Cycle 13, the two remaining Cask Pit racks may be installed in Cycle 13 to provide full core offload capability until the re-racking is initialized in Cycle 14. During Cycle 15 there will not be sufficient storage locations for safe diver access to the SFP, even with a rack in the Transfer Pit. Therefore, re-racking must take place prior to the end of Cycle 14 (April, 2004).

### 11.3 Appraisal of Alternative Options

Adding fuel storage space to the DBNPS SFP is the most viable option for increasing spent fuel storage capacity.

The key considerations in evaluating the alternative options included:

- Safety: Minimize the risk to the public.
- Economy: Minimize capital and O&M expenditures.
- Security: Protection from potential saboteurs, natural phenomena.
- Non-intrusiveness: Minimize required modifications to existing plant systems.
- Maturity: Extent of industry experience with the technology.
- ALARA: Minimize cumulative dose.
- Schedule: Minimize time to implement a plan which will maintain full-core offload capability for the distant future.
- Risk Management: Maximize probability of completing the expansion to support fuel storage needs.

### Rod Consolidation

Rod consolidation involves disassembly of spent fuel, followed by the storage of the fuel rods from two assemblies into the volume of one, and the disposal of the fuel assembly skeleton outside of the pool (this is considered a 2:1 compaction ratio). The rods are stored in a stainless steel can that has the outer dimensions of a fuel assembly. The can is stored in the spent fuel racks. This technology is still in its developmental infancy and thus, based on the aforementioned DBNPS schedule, is not a viable option based on the time frame.

### On-Site Dry Cask Storage

Dry cask storage is a method of storing spent nuclear fuel in a high capacity container. The cask provides radiation shielding and passive heat dissipation. Typical storage system capacities for PWR fuel range from 21 to 37 assemblies that have been removed from the reactor for at least five years.

In the early 1990s, Toledo Edison made the decision to reclaim some of the DBNPS SFP storage using a dry fuel storage system. In January 1996, seventy-two spent fuel assemblies were loaded into three Dry Shielded Canisters and were placed in dry fuel storage utilizing the certified NUHOMS<sup>®</sup> system, in accordance with 10CFR72.214, Certificate Number 1004. Changes within the dry spent fuel storage industry have caused cost increases. The contracted supplier of the NUHOMS system voluntarily stopped fabrication activities and was unable to provide additional storage systems within an acceptable schedule. Further use of this technology was re-evaluated and determined not to be the best choice for future storage expansion at the DBNPS. This decision was based on economics, schedule, and risk management.

## Other Storage Options

Other options such as Modular Vault Dry Storage, Horizontal Silo Storage, and a new Fuel Storage Pool are overly expensive as compared to placing new racks in the SFP. Due to the complexity of implementation, these options could not meet the required schedule for regaining and maintaining full-core offload capability.

### 11.3.1 Alternative Option Summary

An estimate of relative costs in 1998 dollars for the aforementioned options is provided in the following:

SFP Rack Expansion:	\$6-8 million
Horizontal Silo:	\$35-45 million
Rod consolidation:	\$25 million
Metal cask (MPC):	\$68-100 million
Modular vault:	\$56 million
New fuel pool:	\$150 million

The above estimates are consistent with estimates by EPRI and others [11.2, 11.3].

To summarize, based on the required short time schedule, the status of the dry spent fuel storage industry, and the storage expansion costs, the most acceptable alternative for increasing the on-site spent fuel storage capacity at the DBNPS is expansion of the wet storage capacity. First, there are no commercial independent spent fuel storage facilities operating in the United States. Second, the adoption of the Nuclear Waste Policy Act (NWPA) created a de facto throw-away nuclear fuel cycle. Since the cost of spent fuel reprocessing is not offset by the salvage value of the residual uranium, reprocessing represents an added cost for the nuclear fuel cycle which already includes the NWPA Nuclear Waste Fund fees. In any event, there are no domestic reprocessing facilities. Third, at over \$½ million per day replacement power cost, shutting down

the DBNPS is many times more expensive than addition of high density racks to the existing SFP.

#### 11.4 Cost Estimate

The plant modification proposed for the DBNPS fuel storage expansion utilizes freestanding, high density, poisoned spent fuel racks in the SFP. The engineering and design is completed for full re-racking of the SFP.

The total capital cost is estimated to be approximately \$7 million as detailed below.

Engineering, design, project management:	\$1/2 million
Rack fabrication:	\$5 1/2 million
Rack installation:	\$1 million

As described in the preceding section, other fuel storage expansion technologies were evaluated prior to deciding on the use of SFP racks. Storage rack capacity expansion provides a cost advantage over other technologies.

#### 11.5 Resource Commitment

The expansion of the DBNPS Spent Fuel Pool capacity via the SFP, using the four racks already slated for the Cask Pit, is expected to require the following primary resources:

Stainless steel:	72 tons
Boral neutron absorber:	8 tons, of which 6 tons is Boron Carbide powder and 4 tons are aluminum.

The requirements for stainless steel and aluminum represent a small fraction of total world output of these metals (less than 0.001%). Although the fraction of world production of Boron Carbide required for the fabrication is somewhat higher than that of stainless steel or aluminum, it is

unlikely that the commitment of Boron Carbide to this project will affect other alternatives. Experience has shown that the production of Boron Carbide is highly variable, depends upon need, and can easily be expanded to accommodate worldwide needs.

#### 11.6 Environmental Considerations

Due to the additional heat-load arising from increased Spent Fuel Pool inventory, the anticipated maximum bulk pool temperature will increase by about 4°F. † at the time when the pool's capacity is exhausted. The increased bulk pool temperature will result in an increase in the pool water evaporation rate. This increase has been determined to increase the relative humidity of the Fuel Building atmosphere by less than 25 percent relative humidity †. This increase is within the capacity of both normal and the ESF Ventilation System. The net result of the increased heat loss and water vapor emission to the environment is negligible.

#### 11.7 References

- [11.1] OT Position Paper for Review and Acceptance of Spent Fuel Storage and Handling Applications, USNRC (April 1978).
- [11.2] Electric Power Research Institute, Report No. NF-3580, May 1984.
- [11.3] "Spent Fuel Storage Options: A Critical Appraisal", Power Generation Technology, Sterling Publishers, pp. 137-140, U.K. (November 1990).

---

† These numbers are based on more than doubling the amount of fuel in the Spent Fuel Pool by re-racking the entire pool.

Docket Number 50-346  
License Number NPF-3  
Serial Number 2640  
Enclosure 2

**PROPOSED TECHNICAL SPECIFICATIONS AND BASES CHANGES  
REVISION BAR FORMAT**

(12 pages follow)

## REFUELING OPERATIONS

### CRANE TRAVEL - FUEL HANDLING BUILDING

#### LIMITING CONDITION FOR OPERATION

---

3.9.7 Loads in excess of 2430 pounds shall be prohibited from travel over fuel assemblies in the spent fuel pool, cask pit\*, or transfer pit.

APPLICABILITY: With fuel assemblies and water in the spent fuel pool, cask pit, or transfer pit.

#### ACTION:

With the requirements of the above specification not satisfied, place the crane load in a safe condition. The provisions of Specification 3.0.3 are not applicable.

#### SURVEILLANCE REQUIREMENTS

---

4.9.7 The weight of each load, other than a fuel assembly, shall be verified to be  $\leq 2430$  pounds prior to moving it over fuel assemblies in the spent fuel pool, cask pit\*, or transfer pit.

---

\* An impact cover weighing in excess of 2430 pounds may be moved over fuel assemblies in the cask pit provided that administrative controls are established. Other loads in excess of 2430 pounds may be moved over fuel assemblies in the cask pit provided: 1) an impact cover is installed, and 2) administrative controls are established to limit the load to 17,530 pounds and to limit the height that the load may travel over the impact cover.

## REFUELING OPERATIONS

### STORAGE POOL WATER LEVEL

#### LIMITING CONDITION FOR OPERATION

---

3.9.11 As a minimum, 23 feet of water shall be maintained over the top of irradiated fuel assemblies seated in the storage racks in the spent fuel pool, cask pit, or transfer pit.

APPLICABILITY: Whenever irradiated fuel assemblies are in the spent fuel pool, cask pit, or transfer pit.

#### ACTION:

With the requirement of the specification not satisfied, suspend all movement of fuel and crane operations with loads in the fuel storage area and restore the water level to within its limit within 4 hours. The provisions of Specification 3.0.3 are not applicable.

#### SURVEILLANCE REQUIREMENTS

---

4.9.11 The water level in the spent fuel pool, cask pit, and transfer pit shall be determined to be at least its minimum required depth at least once per 7 days when irradiated fuel assemblies are in these locations.

## REFUELING OPERATIONS

### STORAGE POOL VENTILATION

#### LIMITING CONDITION FOR OPERATION

---

3.9.12 Two independent emergency ventilation systems servicing the storage pool area shall be OPERABLE.

APPLICABILITY: Whenever irradiated fuel is in the spent fuel pool, cask pit, or transfer pit.

ACTION:

- a. With one emergency ventilation system servicing the storage pool area inoperable, fuel movement within the spent fuel pool, cask pit, or transfer pit, or crane operation with loads over the spent fuel pool, cask pit, or transfer pit, may proceed provided the OPERABLE emergency ventilation system servicing the storage pool area is in operation and discharging through at least one train of HEPA filters and charcoal adsorbers.
- b. With no emergency ventilation system servicing the storage pool area OPERABLE, suspend all operations involving movement of fuel within the spent fuel pool, cask pit, or transfer pit, or crane operation with loads over the spent fuel pool, cask pit, or transfer pit, until at least one system is restored to OPERABLE status.
- c. The provisions of Specifications 3.0.3 and 3.0.4 are not applicable.

#### SURVEILLANCE REQUIREMENTS

---

4.9.12.1 The above required emergency ventilation system servicing the storage pool area shall be demonstrated OPERABLE per the applicable Surveillance Requirements of 4.6.5.1, and at least once each REFUELING INTERVAL by verifying that the emergency ventilation system servicing the storage pool area maintains the storage pool area at a negative pressure of  $\geq 1/8$  inches Water Gauge relative to the outside atmosphere during system operation.

4.9.12.2 The normal storage pool ventilation system shall be demonstrated OPERABLE at least once each REFUELING INTERVAL by verifying that the system fans stop automatically and that dampers automatically divert flow into the emergency ventilation system on a fuel storage area high radiation test signal.

## REFUELING OPERATIONS

### SPENT FUEL ASSEMBLY STORAGE

#### LIMITING CONDITION FOR OPERATION

---

3.9.13 Fuel assemblies shall be placed in the spent fuel storage racks in accordance with the following criteria:

- a. Fuel assemblies stored in the spent fuel pool shall meet the criteria shown in Figure 3.9-1, when located in the low density spent fuel storage racks.
- b. Fuel assemblies stored in the cask pit shall meet the criteria shown in Figure 3.9-2, when located in the high density spent fuel storage racks.
- c. Fuel assemblies stored in the spent fuel pool or transfer pit shall meet the criteria shown in Figure 3.9-3, when located in the high density spent fuel storage racks.

**APPLICABILITY:** Whenever fuel assemblies are in the spent fuel pool, cask pit, or transfer pit.

#### **ACTION:**

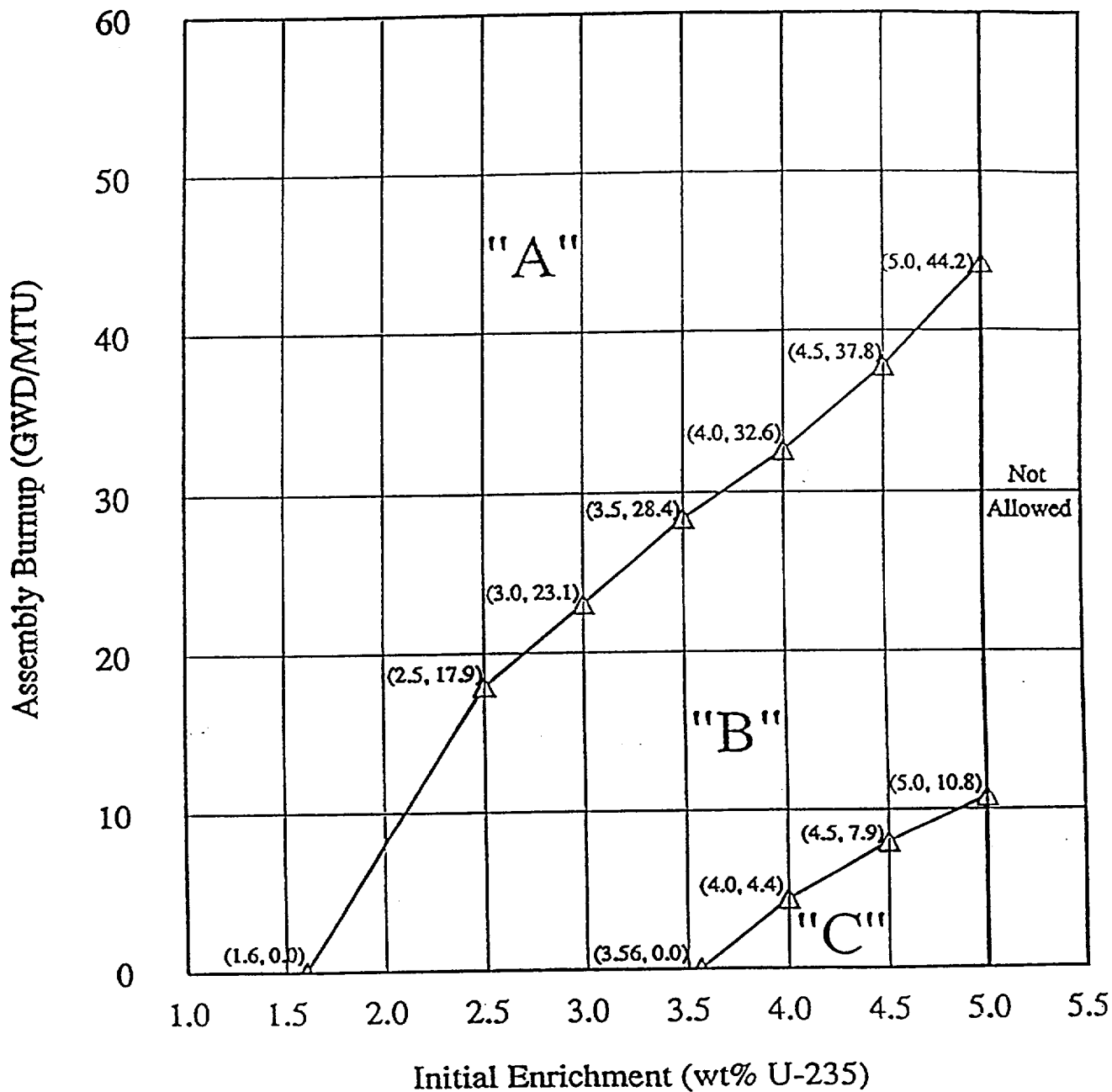
With the requirements of the above specification not satisfied, suspend all other fuel movement within the spent fuel pool, cask pit, or transfer pit and move the non-complying fuel assemblies to allowable locations in accordance with Figure 3.9-1, Figure 3.9-2, or Figure 3.9-3, as appropriate. The provisions of Specifications 3.0.3 and 3.0.4 are not applicable.

#### **SURVEILLANCE REQUIREMENTS**

---

4.9.13.1 Prior to storing a fuel assembly in the spent fuel pool, cask pit, or transfer pit, verify by administrative means that the initial enrichment and burnup of the fuel assembly are in accordance with Figure 3.9-1, Figure 3.9-2, or Figure 3.9-3, as appropriate.

Figure 3.9-1  
 Burnup vs. Enrichment Curves  
 For the Davis-Besse Low Density  
 Spent Fuel Pool Storage Racks

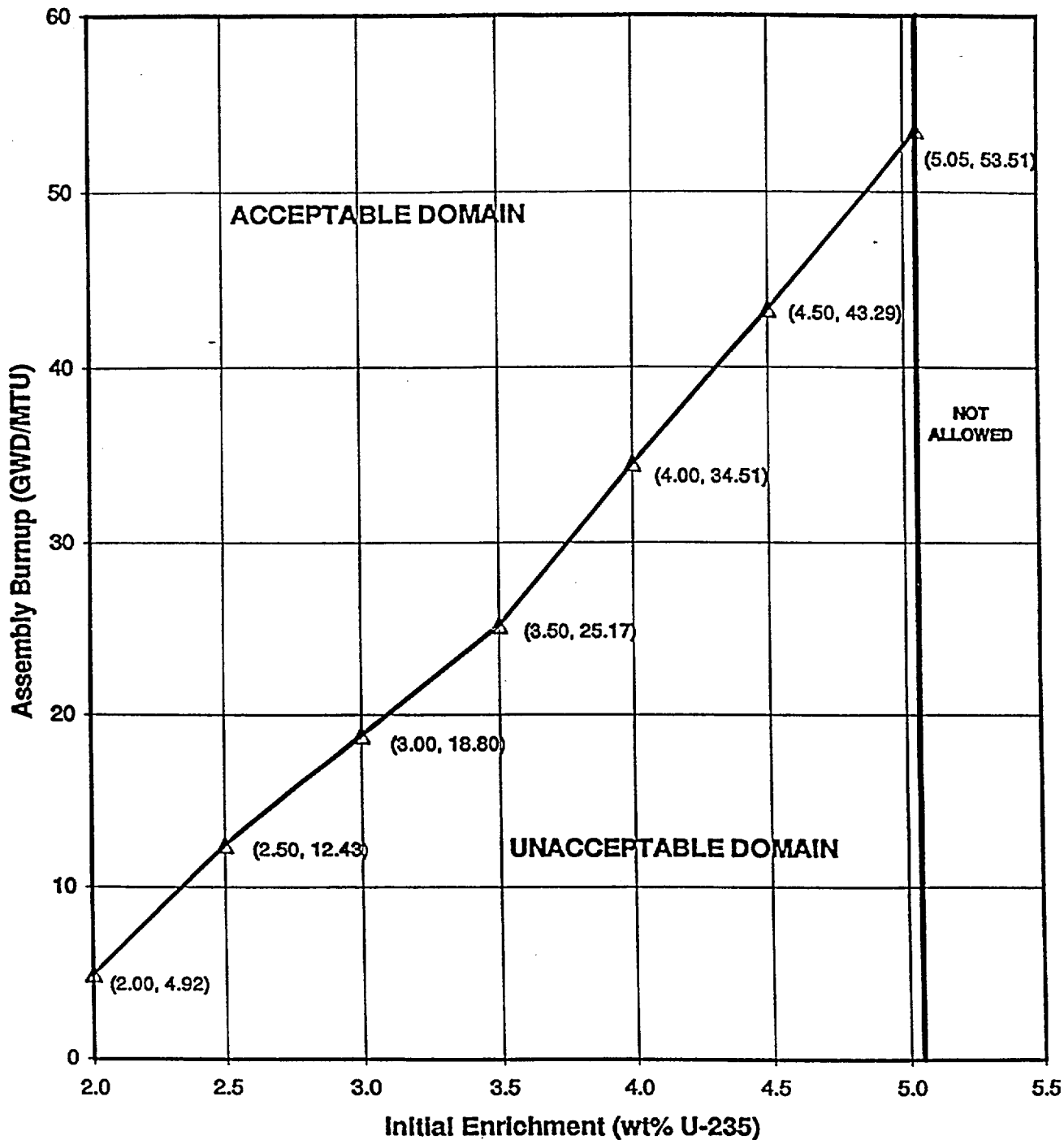


Category "A": May be placed in any rack location

Category "B": Must not be placed directly adjacent to Category "C" assemblies

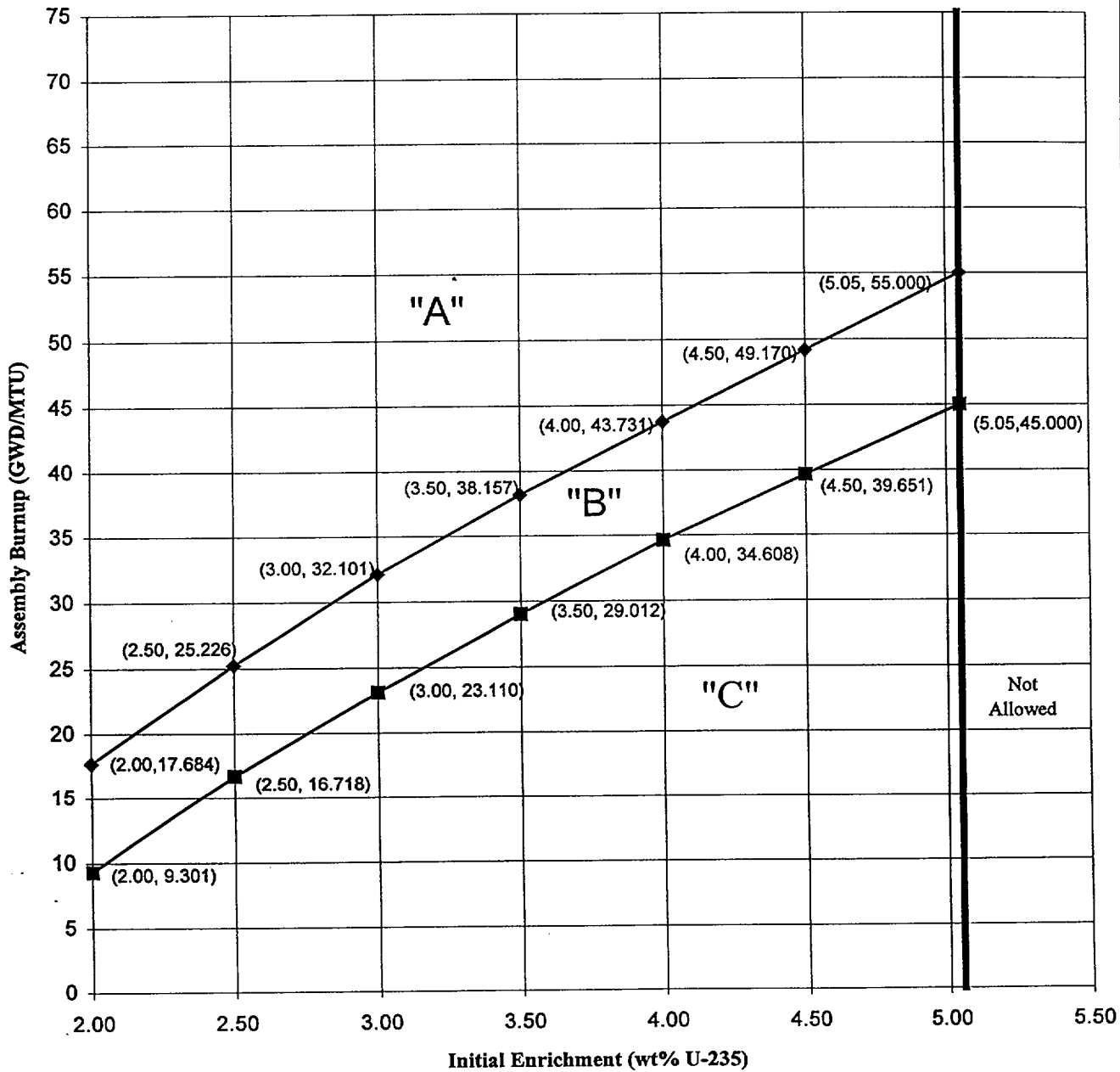
Category "C": May only be placed directly adjacent to Category "A" assemblies or non-fuel locations

Figure 3.9-2  
 Burnup vs. Enrichment Curve  
 For the Davis-Besse High Density  
 Cask Pit Storage Racks



Note: Fuel assemblies with initial enrichments less than 2.0 wt% <sup>235</sup>U will conservatively be required to meet the burnup requirements of 2.0 wt% <sup>235</sup>U assemblies).

**Figure 3.9-3  
Burnup vs. Enrichment Curves  
For the Davis-Besse High Density  
Spent Fuel Pool and Transfer Pit Storage Racks**



Notes: Fuel assemblies with initial enrichments less than 2 wt% U-235 will conservatively be required to meet the burnup requirements of 2.0 wt% U-235 assemblies.  
Loading pattern considerations applicable to Category "A", "B", and "C" assemblies are described in the Bases.

## REFUELING OPERATIONS

### BASES

---

#### 3/4.9.6 FUEL HANDLING BRIDGE OPERABILITY

The OPERABILITY requirements of the hoist bridges used for movement of fuel assemblies ensures that: 1) fuel handling bridges will be used for movement of control rods and fuel assemblies, 2) each hoist has sufficient load capacity to lift a fuel element, and 3) the core internals and pressure vessel are protected from excessive lifting force in the event they are inadvertently engaged during lifting operations.

#### 3/4.9.7 CRANE TRAVEL – FUEL HANDLING BUILDING

The restriction on movement of loads in excess of the nominal weight of a fuel assembly in a failed fuel container over other fuel assemblies in the spent fuel pool, cask pit, or transfer pit ensures that in the event this load is dropped (1) the activity release will not exceed the source term assumed in the design basis fuel handling accident for outside containment, and (2) any possible distortion of fuel in the storage racks will not result in a critical array.

During spent fuel pool re-racking activities, if it is necessary to move a storage rack over fuel assemblies stored in the cask pit, the 2430 pound weight limitation may be exceeded in order to install or remove an impact cover over the cask pit. The physical design of the impact cover, together with administrative controls established while the cover is being moved, ensure that it can not fall into the cask pit in the unlikely event that it is dropped. Once installed over the cask pit, the impact cover is capable of withstanding a dropped load of up to 17,530 pounds (the heaviest rack, including rigging). The height that such loads may travel over the cover is established by calculation based on the design of the cover. Administrative controls ensure that maximum height and weight restrictions are not exceeded.

#### 3/4.9.8 COOLANT CIRCULATION

The requirement that at least one decay heat removal loop be in operation ensures that (1) sufficient cooling capacity is available to remove decay heat and maintain the water in the reactor pressure vessel below 140°F as required during the REFUELING MODE, and (2) sufficient coolant circulation is maintained through the reactor core to minimize the effect of a boron dilution incident and prevent boron stratification.

The requirement to have two DHR loops OPERABLE when there is less than 23 feet of water above the core ensures that a single failure of the operating DHR loop will not result in a complete loss of decay heat removal capability. With the reactor vessel head removed and 23 feet of water above the core, a large heat sink is available for core cooling. Thus, in the event of a failure of the operating DHR loop, adequate time is provided to initiate emergency procedures to cool the core.

In MODE 6, the RCS boron concentration is typically somewhat higher than the boron concentration required by Specification 3.9.1, and could be higher than the boron concentration of normal sources of water addition. The flowrate through the decay heat system may at times be reduced to somewhat less than 2800 gpm. In this situation, if water with a boron concentration equal to or greater than the boron concentration required by Specification 3.9.1 is added to the RCS, the RCS is assured to remain above the Specification 3.9.1 requirement, and a flowrate of less than 2800 gpm is not of concern.

## REFUELING OPERATIONS

### BASES

---

#### 3/4.9.9 CONTAINMENT PURGE AND EXHAUST ISOLATION SYSTEM

Deleted

#### 3/4.9.10 and 3/4.9.11 WATER LEVEL - REACTOR VESSEL AND STORAGE POOL

The restrictions on minimum water level ensure that sufficient water depth is available to remove 99% of the iodine gas activity released from the rupture of an irradiated fuel assembly. The minimum water depth is consistent with the assumptions of the safety analysis.

#### 3/4.9.12 STORAGE POOL VENTILATION

The requirements on the emergency ventilation system servicing the storage pool area to be operating or OPERABLE ensure that all radioactive material released from an irradiated fuel assembly will be filtered through the HEPA filters and charcoal adsorber prior to discharge to the atmosphere. The OPERABILITY of this system and the resulting iodine removal capacity are consistent with the assumptions of the safety analyses.

#### 3/4.9.13 SPENT FUEL ASSEMBLY STORAGE

The restrictions on the placement of fuel assemblies within the spent fuel pool, cask pit, and transfer pit, as dictated by Figure 3.9-1, Figure 3.9-2, and Figure 3.9-3, ensure that the k-effective of the spent fuel pool, cask pit, and transfer pit will always remain less than 0.95 assuming the spent fuel pool, cask pit, and transfer pit to be flooded with non-borated water. The restrictions delineated in Figure 3.9-1, Figure 3.9-2, and Figure 3.9-3, and the action statement, are consistent with the criticality safety analyses performed for the spent fuel pool, cask pit, and transfer pit. The term "directly adjacent" as used in Figure 3.9-1 refers to fuel assemblies stored face-to-face.

The criticality analyses qualify the high density rack modules for storage of fuel assemblies in one of three different loading patterns, subject to certain restrictions: Mixed Zone Three Region, Checkerboard, and Homogeneous Loading. Figure 3.9-3 provides the Category-specific burnup/enrichment limitations. Different loading patterns may be used in different rack modules, provided each rack module contains only one loading pattern. Two different loading patterns may be used in a single rack module, subject to certain additional restrictions. The loading pattern restrictions are maintained in fuel handling administrative procedures.

The design features of the low density spent fuel storage racks are described in Specification 5.6.1.1. The design features of the high density spent fuel storage racks are described in Specification 5.6.1.3.

---

## 5.0 DESIGN FEATURES

---

### 5.1 Site Location

The Davis-Besse Nuclear Power Station, Unit Number 1, site is located on Lake Erie in Ottawa County, Ohio, approximately six miles northeast from Oak Harbor, Ohio and 21 miles east from Toledo, Ohio. The exclusion area boundary has a minimum radius of 2400 feet from the center of the plant.

---

### 5.2 (Deleted)

---

### 5.3 Reactor Core

#### 5.3.1 Fuel Assemblies

The reactor core shall contain 177 fuel assemblies. Each assembly shall consist of a matrix of zircaloy, M5, or ZIRLO clad fuel rods with an initial composition of natural or slightly enriched uranium dioxide ( $UO_2$ ) as fuel material. Limited substitutions of zirconium alloy or stainless steel filler rods for fuel rods, in accordance with approved applications of fuel rod configurations, may be used. Fuel assemblies shall be limited to those fuel designs that have been analyzed with applicable NRC staff approved codes and methods and shown by tests or analyses to comply with all fuel safety design bases. A limited number of lead test assemblies that have not completed representative testing may be placed in non-limiting core regions.

#### 5.3.2 Control Rods

The reactor core shall contain 53 safety and regulating control rod assemblies and 8 axial power shaping rod (APSR) assemblies. The nominal values of absorber material for the safety and regulating control rods shall be 80 percent silver, 15 percent indium and 5 percent cadmium. The absorber material for the APSRs shall be 100 percent Inconel.

---

### 5.4 (Deleted)

---

### 5.5 (Deleted)

---

### 5.6 Fuel Storage

#### 5.6.1 Criticality

5.6.1.1 The low density spent fuel pool storage racks are designed and shall be maintained with:

- a. A  $K_{eff}$  equivalent to less than or equal to 0.95 when flooded with unborated water, which includes a conservative allowance of 1% delta k/k for calculation uncertainty.  
(continued)

## 5.0 DESIGN FEATURES

---

### 5.6 Fuel Storage (continued)

- b. A rectangular array of stainless steel cells spaced 12 31/32 inches on centers in one direction and 13 3/16 inches on centers in the other direction. Fuel assemblies stored in the spent fuel pool shall be placed in a stainless steel cell of 0.125 inches nominal thickness or in a failed fuel container.
- c. Fuel assemblies stored in the spent fuel pool in accordance with Technical Specification 3.9.13.

#### 5.6.1.2 The new fuel storage racks are designed and shall be maintained with:

- a. A  $K_{\text{eff}}$  equivalent to less than or equal to 0.95 when flooded with unborated water, which includes a conservative allowance of 1% delta k/k for uncertainties as described in Section 9.1 of the USAR.
- b. A  $K_{\text{eff}}$  equivalent to less than or equal to 0.98 when immersed in a hydrogenous "mist" of such a density that provides optimum moderation (i.e., highest value of  $K_{\text{eff}}$ ), which includes a conservative allowance of 1% delta k/k for uncertainties as described in Section 9.1 of the USAR.
- c. A nominal 21 inch center-to-center distance between fuel assemblies placed in the storage racks.
- d. Fuel assemblies having a maximum initial enrichment of 5.0 weight percent uranium-235.

#### 5.6.1.3 The high density spent fuel pool storage racks, cask pit storage racks, and transfer pit rack are designed and shall be maintained with:

- a. A  $K_{\text{eff}}$  equivalent to less than or equal to 0.95 when flooded with unborated water, which includes a conservative allowance for manufacturing tolerances and calculation uncertainty.
- b. A rectangular array of stainless steel cells with walls of 0.075 inches nominal thickness, spaced a nominal 9.22 inches on center in both directions. Boral neutron absorber material is utilized between each cell for criticality considerations.
- c. Fuel assemblies stored in the spent fuel pool, cask pit, or transfer pit in accordance with Technical Specification 3.9.13.

DESIGN FEATURES

---

5.6 Fuel Storage (continued)

5.6.2 Drainage

The spent fuel storage pool, cask pit, and transfer pit are designed and shall be maintained to prevent inadvertent draining below 9 feet above the top of the fuel storage racks.

5.6.3 Capacity

- a. The spent fuel storage pool is designed and shall be maintained with a storage capacity limited to no more than 1624 fuel assemblies, less the number of fuel assemblies stored in racks located in the cask pit and transfer pit.
- b. The cask pit is designed and shall be maintained with a storage capacity limited to no more than 289 fuel assemblies.
- c. The transfer pit is designed and shall be maintained with a storage capacity limited to no more than 90 fuel assemblies.

---

5.7 (Deleted)

### **COMMITMENT LIST**

THE FOLLOWING LIST IDENTIFIES THOSE ACTIONS COMMITTED TO BY THE DAVIS-BESSE NUCLEAR POWER STATION (DBNPS) IN THIS DOCUMENT. ANY OTHER ACTIONS DISCUSSED IN THE SUBMITTAL REPRESENT INTENDED OR PLANNED ACTIONS BY THE DBNPS. THEY ARE DESCRIBED ONLY FOR INFORMATION AND ARE NOT REGULATORY COMMITMENTS. PLEASE NOTIFY THE MANAGER – REGULATORY AFFAIRS (419-321-8450) AT THE DBNPS OF ANY QUESTIONS REGARDING THIS DOCUMENT OR ANY ASSOCIATED REGULATORY COMMITMENTS.

#### **COMMITMENTS**

#### **DUE DATE**

- |   |   |
|---|---|
| 1. The four cask pit high density rack modules (289 total storage locations) currently approved for use will be utilized to provide temporary storage of fuel assemblies during the re-racking, however they will be eventually emptied and relocated to the SFP as part of the modification...Like the cask pit rack modules, the transfer pit rack module will eventually be emptied and relocated to the SFP as part of the modification.  | 1. Upon completion of the implementation of the SFP re-rack plant modification.             |
| 2. The criticality analyses qualify the high density rack modules for storage of fuel assemblies in one of three different loading patterns, subject to certain restrictions...different loading patterns may be used in different rack modules, provided each rack module contains only one loading pattern. With additional restrictions, two different loading patterns may be used in a single rack module. The loading pattern restrictions will be maintained in fuel handling administrative procedures. | 2. Upon implementation of the amendment associated with this license amendment application. |

**COMMITMENTS**

3. Administrative controls have been established to ensure that the SFP boron concentration is maintained at  $\geq 1800$  ppm during and following fuel movement, until completion of verification that no misloading has occurred.
4. Based on a conservative evaluation of the projected spent fuel discharge schedule for the DBNPS, the analyses determined the maximum bulk and local temperatures that would result from a worst case SFP heat load of  $30.15 \times 10^6$  BTU/hr. This heat load value is based on the SFP filled to capacity. Consistent with the evaluation, the maximum total heat generation rate of a single fuel assembly stored in the SFP is limited to 80,209 watts (273,870 BTU/hr). In addition, the maximum heat generation rate per heat transfer surface area of assembly cladding is limited to  $445 \text{ watts/ft}^2$  ( $1520 \text{ BTU/hr-ft}^2$ ). These limits will be included in the USAR Technical Requirements Manual (TRM). Future changes to the USAR TRM will be evaluated under the requirements of 10 CFR 50.59, and the NRC will be informed of these changes in accordance with the USAR update requirements of 10 CFR 50.71(e).
5. In conclusion, fuel may be stored in the transfer pit with the transfer pit-to-SFP gate either closed or open. The analysis limits the transfer pit total heat load to 88,110 watts. This limit will be included in the USAR Technical Requirements Manual (TRM). Future changes to the USAR TRM will be evaluated under the requirements of 10 CFR 50.59, and the NRC will be informed of these changes in accordance with the USAR update requirements of 10 CFR 50.71(e).

**DUE DATE**

3. Upon implementation of the amendment associated with this license amendment application.
4. Upon implementation of the amendment associated with this license amendment application.
5. Upon implementation of the amendment associated with this license amendment application.

### **COMMITMENTS**

6. As described in Section 3.6 of Reference 4, due to the limited travel of the spent fuel cask crane, a temporary crane will be used, as necessary, to position existing racks for removal, and for final positioning of the new racks. The crane will be designed to meet the intent of NUREG-0612 through a defense-in-depth approach. The temporary crane will only lift the racks several inches above the pool floor to move them horizontally. It will not be used to lift any heavy loads out of the pool, will not be used to lift any heavy loads over fuel assemblies or safety-related equipment, and will not be used to move fuel assemblies.
7. The load path of some racks during the re-racking activities may traverse fuel assemblies stored in the cask pit. If it is necessary to move racks over fuel assemblies in the cask pit, an impact cover will be required. The physical design of the impact cover, together with administrative controls established while the cover is being moved, ensure that it can not fall into the cask pit in the unlikely event it is dropped. The activities associated with installation and removal of the cover will meet the requirements of NUREG-0612.
8. The cask pit impact cover will be qualified to withstand the drop of the heaviest rack, including rigging. The height that such loads may travel over the cover will be established by calculation based on the design of the cover. Administrative controls will ensure that maximum height and weight restrictions are not exceeded.
9. Underwater diving operations are required in the SFP to remove underwater obstructions, position the new rack modules, and verify installation per design. Fuel in the SFP will be shuffled, as necessary, to reduce the exposure to the divers.

### **DUE DATE**

6. Prior to use of the temporary crane during the SFP re-rack plant modification.
7. Prior to movement of the impact cover over fuel assemblies stored in the cask pit during implementation of the SFP re-rack plant modification.
8. Prior to movement of loads in excess of 2430 pounds over the installed cask pit impact cover during implementation of the SFP re-rack plant modification.
9. Prior to underwater diving operations in the SFP during implementation of the SFP re-rack plant modification.

**COMMITMENTS**

10. Each diver will be equipped with whole body dosimetry with remote, above surface, readouts that will be continuously monitored by Radiation Protection personnel. Contingency measures will be implemented in the case of signal loss with remote reading dosimeters. Divers will be equipped with extremity dosimetry, and will be equipped with underwater survey instrumentation with remote readout capabilities. Divers will also be in continuous communication with Radiation Protection personnel via a dive master. The DBNPS will conduct radiation surveys of the diving area prior to each diving operation and following the movement of any radioactive components in the SFP. The DBNPS will use either visual or physical barriers to ensure that divers maintain a safe distance from spent fuel assemblies or other high radiation sources stored in the SFP. The DBNPS will also use a safety line attached to the diver and manned by a dive tender at all times.
11. The DBNPS will monitor and control personnel traffic and equipment movement in the SFP area to minimize contamination and to assure that exposures are maintained as low as reasonably achievable (ALARA).
12. Cleanup of source material will be performed, as necessary, in accordance with good ALARA practices. The DBNPS will take appropriate action to maintain water clarity during rack module installation.

**DUE DATE**

10. Prior to underwater diving operations in the SFP during implementation of the SFP re-rack plant modification.
11. During implementation of the SFP re-rack plant modification.
12. During implementation of the SFP re-rack plant modification.

**COMMITMENTS**

13. The same rigorous controls presently applied to fuel movements in the spent fuel pool and cask pit will also be applied to fuel movements in the transfer pit, to ensure that the basis for TS 3.9.13 will be preserved. These controls include:

- Preparation and independent review of all fuel movement sheets for compliance with TS 3.9.13 by the Nuclear Engineering Unit.
- Reactor Engineering oversight of Operations during all fuel movements.
- Independent verification of refueling device (bridge, crane, etc.) location prior to fuel assembly placement or retrieval in the spent fuel storage racks.
- Visual verification that the spent fuel storage rack loading pattern for those assemblies moved complies with TS 3.9.13 within 30 days of any fuel movement in the spent fuel storage racks.
- Chemistry verification every 72 hours that the SFP/cask pit/transfer pit boron concentration is at least 1800 ppm during fuel movements in the SFP, cask pit, and transfer pit, and until the spent fuel storage rack loading pattern verification is performed.

**DUE DATE**

13. Upon implementation of the amendment associated with this license amendment application.

**COMMITMENTS**

14. The old racks and other miscellaneous items will be decontaminated via underwater pressure washing or other acceptable cleaning mechanisms, prior to removal from the pool area. The rack modules will be disassembled as required to facilitate their removal from the pool. The components will be removed from the pool under Radiation Protection dose rate surveillance, and transported to a designated location for any needed wrapping or placement into anti-contamination bags. An appropriate shipping container will be used to remove the existing rack components for eventual processing.
15. During the re-racking, routine radiation surveys will be conducted to determine the actual dose rates in the rooms. Should dose rates above and around the SFP area increase, this change would be identified by routine radiation surveys, and the appropriate radiological controls would be revised as required.

**DUE DATE**

14. During implementation of the SFP re-rack plant modification.
15. During implementation of the SFP re-rack plant modification.